

Stony Brook University



OFFICIAL COPY

The official electronic file of this thesis or dissertation is maintained by the University Libraries on behalf of The Graduate School at Stony Brook University.

© All Rights Reserved by Author.

**Inhibition and Mechanism of the 1,4-Dihydroxy-2-naphthoyl-CoA Synthase (MenB)
from *Mycobacterium tuberculosis***

A Dissertation Presented

by

Xiaokai Li

to

The Graduate School

in Partial Fulfillment of the

Requirements

for the Degree of

Doctor of Philosophy

in

Chemistry

Stony Brook University

August 2011

Stony Brook University
The Graduate School

Xiaokai Li

We, the dissertation committee for the above candidate for the
Doctor of Philosophy degree, hereby recommend
acceptance of this dissertation.

Peter J. Tonge – Dissertation Advisor
Professor, Department of Chemistry

Dale G. Drueckhammer - Chairperson of Defense
Professor, Department of Chemistry

Elizabeth M. Boon – Third Committee Member of Defense
Assistant Professor, Department of Chemistry

Derek S. Tan – Outside Committee Member of Defense
Tri-Institutional Associate Professor, Sloan-Kettering Institute for Cancer
Research, Cornell University, and The Rockefeller University

This dissertation is accepted by the Graduate School

Lawrence Martin
Dean of the Graduate School

Abstract of the Dissertation

**Inhibition and Mechanism of the 1,4-Dihydroxy-2-naphthoyl-CoA Synthase (MenB)
from *Mycobacterium tuberculosis***

by

Xiaokai Li

Doctor of Philosophy

in

Chemistry

Stony Brook University

2011

Tuberculosis is a common, deadly, and contagious disease that is caused by the Gram positive bacterium *Mycobacterium tuberculosis*. In order to better treat TB, novel antibiotics with shorter treatment periods and improved activity against drug-resistant and latent TB infections are urgently needed. The redox cofactor menaquinone is an essential component of the electron transport chain in *M. tuberculosis* and enzymes in the biosynthetic pathway for this cofactor are promising targets for anti-TB drug discovery.

1,4-Dihydroxy-2-naphthoyl-CoA synthase (MenB), is the sixth enzyme in the menaquinone biosynthesis pathway, and catalyzes the formation of DHNA-CoA from o-succinylbenzoate-CoA via Claisen condensation. In order to develop novel inhibitors of MenB, a high-throughput screen was performed at Harvard Medical School and a series

of 2-amino-4-aryl-4-oxo-butanoic acids were identified as a promising scaffold for subsequent structure-activity relationship studies. However, further research revealed that these compounds were not stable in aqueous buffer and degraded to (*E*)-4-aryl-4-oxo-but-2-enoic acids, which subsequently reacted with coenzyme A in situ to form the corresponding 4-aryl-2-CoA-4-oxo-butanoic acids adducts. These coenzyme A adducts are potent inhibitors of MenB, with K_i values as low as 49 nM. Further experiments have subsequently been performed to decrease the polarity and increase the in vitro antibacterial activity of the CoA adducts. Target validation experiments performed with *S. aureus* demonstrate that these compounds inhibit bacterial growth through a direct effect on menaquinone biosynthesis.

In separate studies, a series of OSB-CoA analogues were rationally designed and successfully synthesized in order to probe the mechanism of the MenB catalyzed reaction. In particular, an OSB-*N*-CoA has been successfully used as a ligand for structural studies, leading to the first X-ray structure of MenB in which the entire active site can be visualized. A new MenB reaction mechanism has been proposed based on the structural data together with site-directed mutagenesis.

Dedication

Xiaokai Li dedicates this dissertation to:

Xinhua Guo & Zhong Li: my parents, I am infinitely indebted to you.

Sichen Liu: my wife, for your love and support.

Ashley Li: my daughter, I am proud of you.

Table of Contents

List of Figures.....	xi
List of Tables.....	xiii
List of Schemes.....	xv
List of Equations.....	xvii
List of Abbreviations.....	xviii
Acknowledgement.....	xxiii
Publication.....	xxv
Chapter 1 : Tuberculosis and Menaquinone Biosynthesis Pathway.....	1
Overview of tuberculosis (TB).....	2
Overview of <i>Mycobacterium tuberculosis</i>	3
TB diagnosis and treatment.....	4
Drug discovery for latent TB infection.....	8
Electron transport chain in <i>M. tuberculosis</i>	10
Menaquinone biosynthesis pathway – a potential drug target.....	12
Overview of research presented in the dissertation.....	20
Chapter 2 : Synthesis of OSB-CoA analogues as a 1,4-dihydroxy-2-naphthoyl-CoA synthase (MenB) reaction mechanism probe.....	22
Introduction.....	23
Result and Discussion.....	30
<i>Preliminary OSB-N-CoA synthesis</i>	30
<i>Modified OSB-N-CoA synthesis</i>	33
<i>DeCOOH-OSB-COOH Synthesis</i>	36

<i>2-Br-CoA:mtMenB</i> cocrystallography	37
<i>OSB-N-CoA:ecMenB</i> cocrystallography	38
<i>ecMenB Y97F</i> mutation	40
<i>New Proposed MenB</i> reaction mechanism.....	42
<i>Inhibition studies of DeCOOH-OSB-CoA</i>	43
Conclusion.....	44
Experimental section	45
<i>General</i>	45
<i>Synthesis of OSB-N-CoA</i>	46
<i>General method for the synthesis of compounds 10-12</i>	57
<i>General method for the synthesis of compounds 13-15</i>	59
<i>General method for the synthesis of compound 16-18</i>	60
<i>Expression and purification of mtMenB</i>	63
<i>Expression and purification of ecMenB</i>	64
<i>Expression and purification of ecMenE</i>	65
<i>Expression and purification of ecMenB Y97F mutant</i>	66
<i>IC₅₀ measurement of mtMenB</i>	67
Chapter 3 : Identification of <i>mtMenB</i> inhibitors by high-throughput screen and structure-activity relationship studies on 4-aryl-2-CoA-4-oxo-butanoic Acid.....	68
Introduction.....	69
Result and discussion.....	71
<i>Pilot screen</i>	71
<i>High-throughput Screen</i>	75

<i>2-Amino-4-aryl-4-oxo-butanoic acid as a potent scaffold to inhibit mtMenB</i>	81
<i>Synthesis of 2-amino-4-aryl-4-oxo-butanoic acids</i>	82
<i>Inhibitors were broken down by retro-Michael addition</i>	86
<i>Stable 2-amino-4-aryl-4-oxo-butanoic acid analogues</i>	88
<i>In situ formation of CoA adduct inhibitors</i>	90
<i>SAR of CoA adduct inhibitors</i>	92
<i>Preliminary CoA surrogates library synthesis</i>	99
<i>Antibacterial activity of (E)-4-aryl-4-oxo-but-2-enoic acid as a prodrug</i>	102
<i>Non-replicating M. tuberculosis inhibition evaluation</i>	106
Conclusion.....	107
Experimental section	108
<i>General</i>	108
<i>Z'-factor determination</i>	109
<i>High-throughput screen</i>	110
<i>General procedure for the synthesis of (E)-4-aryl-4-oxo-but-2-enoic acids 19-37</i>	110
<i>General procedure for the synthesis of the 2-amino-4-aryl-4-oxo-butanoic acids</i> <i>(38-69)</i>	120
<i>Synthesis of compound 70</i>	139
<i>Synthesis of compound 71</i>	140
<i>Synthesis of compound 72</i>	142
<i>Synthesis of Stable 2-amino-4-aryl-4-oxo-butanoic acid analogues</i>	143
<i>Synthesis of the 4-aryl-2-CoA-4-oxo-butanoic acids (80-89)</i>	151

<i>Synthesis of compounds 91-93</i>	159
<i>Synthesis of CoA surrogates 94-99</i>	160
<i>General procedure for the synthesis of methyl (E)-4-aryl-4-oxo-but-2-enoate 100, 101, and 103</i>	164
<i>IC₅₀ measurement of mtMenB</i>	166
<i>K_i and K_i' determination of compound 80</i>	166
<i>K_i and K_i' determination of compound 89</i>	166
<i>MIC determination against M. tuberculosis</i>	168
<i>MIC determination against S. aureus</i>	168
<i>Menadione rescue</i>	169
 Chapter 4 : Synthesis and SAR studies of 1,4-benzoxazine MenB inhibitors as novel antibacterial reagents against M. tuberculosis	 170
Introduction.....	171
Result and discussion.....	173
<i>Hits from HTS</i>	173
<i>Synthesis of (Z)-methyl 2-(2-oxo-2H-substituted benzo[b][1,4]oxazin-3(4H)ylidene)acetates 105-115</i>	175
<i>In vitro inhibition of mtMenB and antibacterial activity against M. tuberculosis and M. smegmatis</i>	175
<i>Menadione rescue experiment with S. aureus</i>	178
<i>Non-replicating M. tuberculosis inhibition evaluation</i>	179
<i>Synthesis of (Z)-3-(2-(2-chlorophenyl)-2-oxo-ethylidene)-3,4-dihydro-2H-substitutedbenzo[b][1,4]oxazin-2-one 118-128</i>	180

<i>In vitro</i> antibacterial activity of compound 118-124	181
Conclusion.....	182
Experimental section	183
<i>General</i>	183
<i>Synthesis of compound 105-115</i>	183
<i>Synthesis of compound 116</i>	188
<i>Synthesis of compound 117</i>	188
<i>Synthesis of (Z)-3-(2-(2-chlorophenyl)-2-oxo-ethylidene)-3,4-dihydro-2H-</i> <i>substitutedbenzo[b][1,4]oxazin-2-one compound 118-128</i>	189
<i>MIC determination against M. tuberculosis</i>	193
<i>MIC determination against S. aureus</i>	193
<i>MIC determination against M. Smegmatis</i>	193
Bibliography	194

List of Figures

Figure 1.1 Current ten FDA approved first and second-line anti-tuberculosis drugs	6
Figure 1.2 Novel chemical scaffolds as non-replicating <i>M. tuberculosis</i> inhibitors	10
Figure 1.3 Proposed pathway of aerobic electron flow in mycobacteria (65)	11
Figure 1.4 Structures of benzoquinone and naphthoquinone redox cofactors	12
Figure 1.5 Proposed menaquinone biosynthesis pathway in <i>E. coli</i>	14
Figure 1.6 An alternative menaquinone biosynthesis pathway in microorganisms.....	15
Figure 1.7 Representative structures targeting electron transport chain and ATP synthesis	17
Figure 1.8 Representatives menaquinone biosynthesis inhibitors.....	19
Figure 2.1 Solved MenB crystal structures.....	24
Figure 2.2 The chemical structure of CoA	25
Figure 2.3 Examples of coenzyme A analogues	26
Figure 2.4 Design of OSB-CoA analogues.....	29
Figure 2.5 Retrosynthesis of OSB-N-CoA	30
Figure 2.6 2-Br-CoA: <i>mt</i> MenB cocrystallography structure	38
Figure 2.7 OSB-N-CoA: <i>ec</i> MenB crystal structure	40

Figure 2.8 <i>ecMenB</i> Y97F mutant structure.....	41
Figure 2.9 New Proposed <i>ecMenB</i> reaction mechanism.....	42
Figure 3.1 Plate design in the high-throughput screen.....	74
Figure 3.2 Chemical structure of hexachlorophene.....	75
Figure 3.3 HTS hits containing OSB backbone.....	81
Figure 3.4 Correlation between enzymatic and bacterial growth inhibition.....	87
Figure 3.5 Stable 2-amino-4-aryl-4-oxo-butanoic acid analogues.....	88
Figure 3.6 CoA adduct binding mode.....	95
Figure 3.7 Potential hydrogen bond interactions between <i>mtMenB</i> and AcAc-CoA.....	98
Figure 3.8 Menaquinone production in <i>S. aureus</i>	106
Figure 4.1 1,4-Benzoxazine scaffolds with various biological activities.....	172
Figure 4.2 Chemical structures of hits from the HTS.....	174

List of Tables

Table 1.1 Action mechanisms of second-line anti-TB drugs.....	7
Table 1.2 Quinone usage in different species	13
Table 2.1 DeCOOH-OSB-CoA analogues inhibition against <i>mtMenB</i>	44
Table 3.1 Compounds information for pilot screen	73
Table 3.2 Compound library information for the high-throughput screen.....	76
Table 3.3 Hits with strong and medium inhibition against <i>mtMenB</i> activity	80
Table 3.4 2-Amino-4-aryl-4-oxo-butanoic acid as <i>mtMenB</i> inhibitor and whole cell inhibition	85
Table 3.5 Stability test on randomly selected compounds.....	87
Table 3.6 Inhibition and stability test of 2-amino-4-aryl-4-oxo-butanoic acid analogues	90
Table 3.7 Analysis of 2-amino-4-aryl-4-oxo-butanoic acid enzyme inhibition	92
Table 3.8 SAR of CoA adducts	94
Table 3.9 Inhibition comparison among compound 89-93.....	97
Table 3.10 CoA surrogates inhibition against <i>mtMenB</i>	101
Table 3.11 Antibacterial activities of (<i>E</i>)-4-aryl-4-oxo-but-2-enoic acid and its methyl esters	103

Table 3.12 Menadione supplementary MIC testing	105
Table 4.1 Inhibition data from hits of the HTS	174
Table 4.2 Inhibition studies for 1,4-benzoxazine analogues (compound 105-117).....	177
Table 4.3 Whole-cell inhibition against <i>S. aureus</i> RN4220 with or without menadione	179
Table 4.4 Inhibition studies for 1,4-benzoxazine analogues (compound 118-124).....	182

List of Schemes

Scheme 2.1 The reaction catalyzed by MenB	23
Scheme 2.2 Instability of acyl-CoA.....	26
Scheme 2.3 OSB-CoA degradation.....	28
Scheme 2.4 MenE-MenB coupled assay	28
Scheme 2.5 Tentative OSB- <i>N</i> -CoA synthesis route.....	32
Scheme 2.6 Modified OSB- <i>N</i> -CoA synthetic route	35
Scheme 2.7 Synthesis of DeCOOH-OSB-CoA	37
Scheme 3.1 Synthesis of 2-amino-4-aryl-4-oxo-butanoic acid	82
Scheme 3.2 <i>retro</i> -Michael addition.....	87
Scheme 3.3 CoA adduct formation in situ	92
Scheme 3.4 Synthesis of 4-aryl-2-CoA-4-oxo-butanoic acids	93
Scheme 3.5 Synthesis of compound 91-93.....	96
Scheme 3.6 Synthesis of CoA surrogates 94-99.....	100
Scheme 3.7 Synthesis of compound 70.....	140
Scheme 3.8 Synthesis of compound 71	141
Scheme 3.9 Synthesis of compound 72.....	142

Scheme 3.10 Synthesis of compound 73	144
Scheme 3.11 Synthesis of compound 74	145
Scheme 3.12 Synthesis of compound 75	146
Scheme 3.13 Synthesis of compound 76	147
Scheme 3.14 Synthesis of compound 77	148
Scheme 3.15 Synthesis of compound 78	149
Scheme 3.16 Synthesis of compound 79	150
Scheme 3.17 Synthesis of compound 90	158
Scheme 3.18 Synthesis of methyl (<i>E</i>)-4-aryl-4-oxo-but-2-enoate.....	164
Scheme 4.1 Synthesis of compounds 105-115	175
Scheme 4.2 Synthesis of compounds 118-124	181
Scheme 4.3 Synthesis of compounds 116 and 117	188

List of Equations

Equation 2.1	67
Equation 3.1	72
Equation 3.2	73
Equation 3.3	166
Equation 3.4	167
Equation 3.5	167
Equation 3.6	167
Equation 3.7	167

List of Abbreviations

9-BBN	9-borabicyclo(3.3.1)nonane
AcAc-CoA	Acetoacetyl-CoA
AcOH	acetic acid
ACP	acyl carrier protein
ATP	adenosine triphosphate
Ave	average
BCG	Bacille Calmette-Guérin
<i>B. anthracis</i>	<i>Bacillus anthracis</i>
BSL	biosafety level
<i>B. subtilis</i>	<i>Bacillus subtilis</i>
CDI	carbonyldiimidazole
CFU	colony-forming unit
CoA	Coenzyme A
DCC	<i>N,N</i> -dicyclohexylcarbodiimide
DCI	deuterium chloride
DHNA	1,4-dihydroxy-2-naphthoic acid
DHNA-CoA	1,4-dihydroxy-2-naphthoyl-CoA
DIPEA	<i>N,N</i> -diisopropylethylamine
DiAT	dihydrolipoamide acyl transferase
DMAP	4-dimethylaminopyridine
DMF	dimethylformamide

DMSO	dimethyl sulfoxide
DNA	deoxyribonucleic acid
DPCK	dephospho-CoA kinase
ECF	ethyl chloroformate
<i>E. coli</i>	<i>Escherichia coli</i>
EDC-HCl	1-ethyl-3-(3-dimethylaminopropyl)carbodiimide hydrochloride
ESI-MS	electrospray ionization mass spectrometry
EtOAc	ethyl acetate
FDA	Food and Drug Administration
<i>G. kaustophilus</i>	<i>Geobacillus kaustophilus</i>
HCl	hydrochloric acid
HIV	human immunodeficiency virus
HPLC	high-performance liquid chromatography
HTS	high-throughput screen
IC ₅₀	half maximal inhibitory concentration
InhA	enoyl-ACP reductase
IPTG	isopropyl-1-thio-β-D-galactopyranoside
KatG	catalase-peroxidase
KOH	potassium hydroxide
LB	lysogeny broth
LC-MS	liquid chromatography – mass spectrometry
LORA	low oxygen recovery assay
<i>M. bovis</i>	<i>Mycobacterium bovis</i>

MDR-TB	multiple drug-resistant tuberculosis
MenA	1,4-dihydroxy-2-naphthoate prenyltransferase
MenB	1,4-dihydroxy-2-naphthoyl-CoA synthase
MenC	<i>o</i> -succinylbenzoic acid synthase
MenD	SEPHCHC synthase
MenE	<i>o</i> -succinylbenzoyl-CoA synthase
MenF	isochorismate synthase
MenH	SHCHC synthase
MeOH	methanol
MIC	minimum inhibitory concentration
<i>M. phlei</i>	<i>Mycobacterium phlei</i>
MRSA	methicillin-resistant <i>Staphylococcus aureus</i>
MRSE	methicillin-resistant <i>Staphylococcus epidermidis</i>
<i>M. smegmatis</i>	<i>Mycobacterium smegmatis</i>
<i>M. spp</i>	<i>Mycobacterium spp</i>
<i>M. tuberculosis</i>	<i>Mycobacterium tuberculosis</i>
NADH	nicotinamide adenine dinucleotide
NADPH	nicotinamide adenine dinucleotide phosphate
NaOH	sodium hydroxide
NMR	nuclear magnetic resonance
NTZ	nitazoxanide
OD	optical density
OSB	<i>o</i> -succinylbenzoic acid

OSB-CoA	<i>o</i> -succinylbenzoyl-CoA
PanK	pantetheine kinase
PFOR	pyruvate-ferredoxin oxidoreductase
PK	pharmacokinetics
PPAT	phosphopantetheine adenylyltransferase
PT70	5-hexyl-2-(<i>o</i> -tolylloxy)phenol
RMSD	root mean square deviation
RNA	ribonucleic acid
SAM	<i>S</i> -adenosylmethionine
SAR	structure-activity relationship
<i>S. aureus</i>	<i>Staphylococcus aureus</i>
SCV	small colony variants
SD	standard deviation
SEPHCHC	2-succinyl-5-enolpyruvyl-6-hydroxy-3-cyclohexene-1-carboxylate
SHCHC	2-succinyl-6-hydroxy-2,4-cyclohexadiene-1-carboxylate
TB	tuberculosis
TEA	triethylamine
THF	tetrahydrofuran
TLC	thin layer chromatography
TMS	trimethylsilyl
TraSH	transposon site hybridization

Trt	triphenylmethyl
TSB	tryptic soy broth
TsOH	<i>p</i> -toluenesulfonic acid
UbiE	SAM-dependent methyl transferase
WHO	World Health Organization
XDR-TB	extensively drug-resistant tuberculosis

Acknowledgement

Foremost, I would like to express my sincere gratitude to my Ph.D. advisor Dr. Peter J. Tonge, who continuously showed his patience, motivation, enthusiasm, and immense knowledge during my way to reach the highest academic education level. In addition, he was always accessible and willing to help his students with their research. His perpetual guidance and great ideas motivate me all the time during my own research in drug discovery, especially the toughest times. He spent tremendous time on changing grammar mistakes after I drafted this dissertation. Without his dedicated assistance, I could not make this far on my Ph.D. pursuit.

In addition, I would like give many thanks to my dissertation chairperson Dr. Dale G. Drueckhammer. His great ideas about the CoA analogue synthesis are the solid foundations of the Chapter 2 in this dissertation. I got valuable illuminations in every talk about my research projects.

Furthermore, I am heartily thankful to my dissertation committee member Dr. Elizabeth M. Boon, who attended most of my presentations during my Ph.D. life. She patiently filled out most of the evaluation forms, which told me how to make successful and brilliant presentations. She also sent strong recommendation letter for me to support me to get a postdoctoral position in my next career life.

I would also like to thank my dissertation outside member, Dr. Derek S. Tan, who traveled 2 hours to reach Stony Brook and evaluated my dissertation. His great

research on MenE inhibitors design and synthesis also gave me inspirations for my own research.

Special thanks go to Dr. Huaning Zhang, who brought me into the MenB project and made my first year Ph.D. life easier. I would also like to give many thanks to Dr. Nina Liu, who evaluated most of my inhibitors against MenB.

It is an honor to join a cheerful group of fellow students in Stony Brook University. I thank my labmates: Dr. Carl A. Machutta, Dr. Jim Truglio, Dr. Xujie Zhang, Dr. Hua Xu, Dr. Hao Lu, Dr. Janine Borgaro, Dr. Gopal Reddy Bommineni, Huei-jiun Li, Christopher am Ende, Kanishk Kapilashrami, Pan Pan, Li Liu, Allison Haigney Richard Brust, Yang Lu, Cheng-Tsung Lai, Andrew Chang, Carla Neckles , Sonam Shah, Hui Wang, Weixuan Yu, for the stimulating discussion, for the sleepless night working together, and for all the fun we have had with each other in last five years.

I would also express my thanks to Dr. Caroline Kisker and Shambhavi Mishra, who dedicated a lot on MenB crystallography.

I would also express my thanks to Dr. Richard A. Slayden, Susan E. Knudson, and Kathleen England, who spent lots of times on evaluation my inhibitors against *M. tuberculosis*.

Last but not least, I sincerely express my thanks to my family. Zhong Li and Xinhua Guo, my parents, born me, raised me, taught me, supported me, and loved me. Sichen Liu, my dear wife, dropped her decent job in China, companied with me on my Ph.D. life, and gave birth to my darling daughter – Ashley Li. To them, I dedicate my dissertation.

Publication

1. Synthesis and SAR studies of 1,4-benzoxazine MenB inhibitors: Novel antibacterial agents against *Mycobacterium tuberculosis*. Li, X., Liu, N., Zhang, H., Knudson, S. E., Slayden, R. A., Tonge, P. J.. *Bioorg. Med. Chem. Lett.*, 2010, 20, 6306-6309.

Chapter 1 : Tuberculosis and Menaquinone Biosynthesis Pathway

Tuberculosis (TB) is a common, deadly, and contagious disease mainly caused by *Mycobacterium tuberculosis*. Current statistics data from the World Health Organization (WHO) showed that there were an estimated 9.4 million incident cases of tuberculosis in 2008 globally. Currently, active TB can be treated by taking several first-line drugs for 6-12 months. However, if the patients stop taking the drugs too soon or take the drugs incorrectly, the bacteria could become drug-resistant. Most of the tuberculosis patients are involved with its latent form, which shows no clinical symptoms due to the dormancy stage of the bacilli. Most of the current FDA-approved first and second line drugs are only effective against active TB. In order to better treat tuberculosis, novel antibiotics with shorter treatment period and higher effectiveness to drug-resistant and latent TB infection are urgently needed. The redox cofactor menaquinone is an essential component of the electron transport chain and enzymes in the menaquinone biosynthesis pathway are promising targets for anti-tuberculosis drug discovery.

Overview of tuberculosis (TB)

The existence of tuberculosis can be dated back to 2000 - 4000 B.C. as historians found the traces of *M. tuberculosis* in mummies (1). Tuberculosis is also certainly the leading cause of death in Europe (2) and the United States (3) in recorded history (4). Currently, it is estimated that one third of the world's population is infected with *M. tuberculosis* and the high-burden countries are mostly localized in Asia and Africa (5).

Tuberculosis is an airborne and in some cases deadly infectious disease. Since *M. tuberculosis* is an aerobic bacterium, tuberculosis normally attacks the patients' upper air sacs of the lungs, while it can also affect the central nervous system, the lymphatic system, the circulatory system, the genitourinary system, the gastrointestinal system, bones and joints, and even the skin (6-7).

There are two forms of tuberculosis, TB infection (latent TB) and TB disease (active TB) (8). Most patients are involved with TB infection, which is asymptomatic and non-infectious. However, without treatment, the dormant bacilli can reproduce active TB in 2-23% per lifetime, often many years after infection (9-10). This occurs even more frequently in immunosuppressed people and young children (11-12). The typical symptoms of active tuberculosis include a chronic cough with blood-tinged sputum, fever, night sweats, and weight loss (8). If active TB is left untreated, it kills more than 50% of its victims.

Overview of *Mycobacterium tuberculosis*

TB-causing mycobacteria include *M. tuberculosis* (the major cause), *Mycobacterium bovis*, *Mycobacterium canetti*, and *Mycobacterium microti* (13). *M. tuberculosis* is an aerobic rod-shaped bacillus, which was discovered by Dr. Robert Koch in 1882. *M. tuberculosis* divides every 16-20 hours, an extremely slow rate compared with other bacteria such as *Escherichia coli* (14). It is classified as Gram-positive bacterium because it has a cell wall but lacks the phospholipid outer membrane. However, if a Gram stain is performed, *M. tuberculosis* either stains very weakly or does not retain dye due to the high lipid and mycolic acid content of its cell wall (15). The genome of *M. tuberculosis* H37Rv strain was published in 1998 (16).

The infectious bacilli are transmitted by inhaling droplet nuclei in the air into the human body and the minimum infection dosage is a single bacterium. After the bacterium reaches the lung, it will be taken up by alveolar macrophages. However, the macrophage cannot digest the bacterium due to its high lipid and mycolic acid content cell wall (17-18). The invasion of the infected cells into the subtending epithelium leads the recruitment of monocytes from blood circulation and vascularization of the infected sites and this is the early stage of the granuloma formation. The formed granuloma can become further stratified and an outer layer is formed by the extracellular matrix material. Most of the granulomas persist in this balanced state, while disease progression will happen if the vascularization is lost. The accumulation of caseum in the granulomas center will result a hypoxic environment (19), which will induce the latent TB infection. Ultimately, infectious bacilli are released into the airway when the granuloma

cavitory collapses into the lungs, which is the lead of active TB infection. The life cycle of *M. tuberculosis* was well summarized in a recent published review (20).

TB diagnosis and treatment

Tuberculosis can be definitively diagnosed by identifying *M. tuberculosis* from a patient's clinical sample, such as sputum or pus. However, the major problem for this method is the difficulties in culturing the slow growing bacteria in the laboratory, which may take weeks. In a time-deficient situation, the replacement diagnostic methods are Mantoux tuberculin skin test and interferon-gamma release assay (21-23).

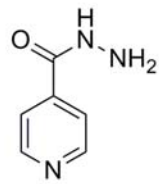
Bacille Calmette-Guérin, or BCG, is a vaccine for TB prevention (24-25), which is often given to infants and young children in many countries with high prevalence of TB, while it is rarely used in the United States. BCG is prepared from a strain of the attenuated live bovine tuberculosis bacillus, *M. bovis*, that has lost its virulence in humans by being specially cultured in an artificial medium for years. At best, the BCG vaccine is 80% effective in preventing tuberculosis for duration of 15 years. However, the protective effect varies under different circumstances.

Currently there are 10 drugs approved by U.S. Food and Drug Administration that can be used to treat tuberculosis, including 5 first-line drugs (isoniazid, rifampin, pyrazinamide, ethambutol, and rifapentine) and 5 second-line drugs (streptomycin, cycloserine, *p*-aminosalicylic acid, ethionamide, and capreomycin) (**Figure 1.1**). Current

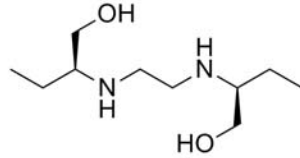
U.S. standard regimen consists of 4 first-line drugs, while second-line drugs would be used when the infection is caused by a drug-sensitive strain.

Isoniazid was first discovered in 1912 and it was found to be effective against tuberculosis in 1952. It is never used alone to treat TB because the drug resistant develops quickly. Isoniazid inhibits the fatty acid biosynthesis pathway in *M. tuberculosis* (26). It acts as a prodrug that must be activated by KatG, a bacterial catalase-peroxidase enzyme in *M. tuberculosis* (27).

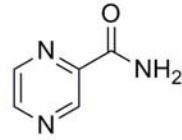
First-line Drugs



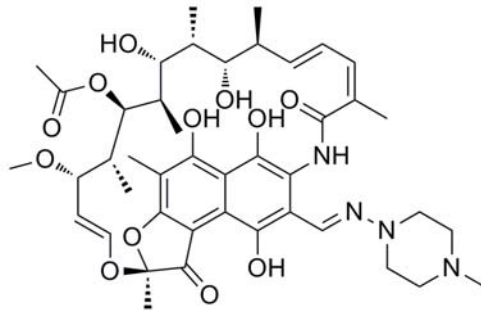
isoniazid



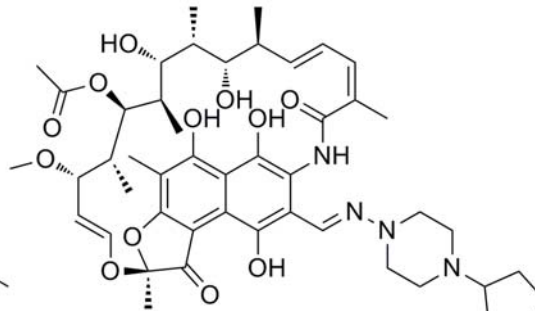
ethambutol



pyrazinamide

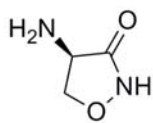


rifampin

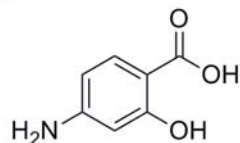


rifapentine

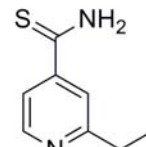
Second-line Drugs



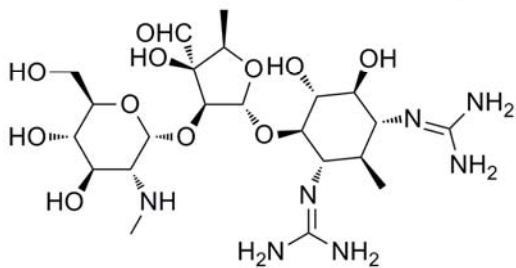
cycloserine



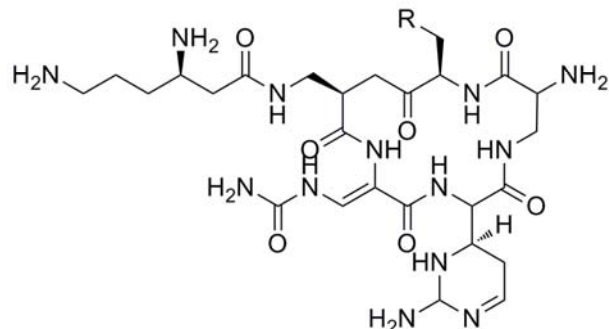
p-aminosalicylic acid



ethionamide



streptomycin



R=OH, capreomycin IA

R=H, capreomycin IB

Figure 1.1 Current ten FDA approved first and second-line anti-tuberculosis drugs

Pyrazinamide was also brought into clinical use for TB treatment in 1952 (28-29). The mechanism is still not conclusive. However, it is thought to inhibit the enzyme fatty acid synthase (30-31), disrupt plasma membrane potential(32), and disrupt energy

(ATP) production (33). Current research showed that mutations of *pncA* gene encoding for pyrazinamidase are responsible for pyrazinamide resistance in *M. tuberculosis* (34).

Ethambutol is a bacteriostatic antimycobacterial drug developed in 1961. It disrupts arabinogalactan synthesis by inhibiting the arabinosyl transferase (35-36). It inhibits the polymerization of cell wall arabinan, resulting in the accumulation of the lipid carrier decaprenol phosphoarabinose. Resistance to ethambutol has been described in up to 4% of clinical isolates of *M. tuberculosis*, and it results from the overexpression of the Emb protein(s), structural mutation in EmbB, or both (37).

Rifampin and rifapentine were introduced to market in 1967 and 1998 separately. Rifampin inhibits the DNA-dependent RNA polymerase, thus preventing transcription to RNA (38). Resistance to rifampin involves alterations of RNA polymerase (39).

The mechanism of second-line anti-TB drugs are summarized in **Table 1.1**.

Name	Mechanism
Cycloserine	Inhibiting alanine racemase (40) and D-alanine ligase (41)
<i>p</i> -Aminosalicylic acid	Inhibiting biosynthesis of the iron-chelating mycobactins (42)
Ethionamide	Inhibiting InhA, enzyme in fatty acid synthesis (26)
Streptomycin	Inhibiting protein synthesis (43-44)
Capreomycin	Inhibition protein synthesis (44)

Table 1.1 Action mechanisms of second-line anti-TB drugs

There are several other drugs that have not been approved by FDA but are widely used in other countries, such as rifabutin, amikacin, kanamycin, levofloxacin, mexifloxacin, and gatifloxacin. At present, challenge for new discovery falls into 5 preferences: reduced treatment duration, acceptable toxicity profile, improved activity

against multi-drug resistant and extensively-drug resistant tuberculosis (MDR/XDR-TB), low drug-drug interaction with HIV regimen, and activity against latent TB (45-46). At present, MDR-TB is treated by a combination of eight to ten different drugs with therapies lasting up to 18-24 months. These drugs also can cause severe side effects including nephrotoxicity, ototoxicity, hepatotoxicity, and dysglycaemia. TB accounts for one in four of deaths that occur among HIV-positive patient. In order to better to treat this old, but still challenging bacterium, new chemical scaffolds are needed.

Drug discovery for latent TB infection

Current anti-tuberculosis drugs are most effective against active tuberculosis disease. However, only rifampin has shown activity against latent tuberculosis (47-48). There is great interest in identifying new antimycobacterial chemical scaffolds with activity against non-replicating tuberculosis. **Figure 1.2** shows several recently developed novel organic entities that can eliminate non-replicating tuberculosis infection.

Metronidazole is the first molecule that was identified sensitive to non-replicating tuberculosis *in vitro* (49-50). However, recent discovery demonstrates that metronidazole lacks *in vivo* antibacterial activity in infectious guinea pigs (51-52). The nitroimidazoles, such as (S)-2-nitro-6-(4-(trifluoromethoxy) benzyloxy)-6,7-dihydro-5H-imidazo[2,1-b][1,3]oxazine (PA-824) are promising compounds that show activity against non-replicating tuberculosis and are now under clinical evaluation (53-54).

Further studies showed that PA-824 produced accumulation of hydroxymycolic acid and reduction in ketomycolate (54), thus the authors concluded that PA-824 inhibited or depleted a cofactor responsible for the catalysis of hydroxymycolate to ketomycolate. Recent research showed that nitazoxanide (NTZ) and its active metabolite (TIZ) kill replicating and non-replicating *M. tuberculosis* at low µg/mL level (55). It is believed that after TIZ entered into the bacteria, it behaves as an inhibitor against pyruvate-ferredoxin oxidoreductase (PFOR) (56) and perhaps also against nitroreductases and peptide disulfide isomerases (57-59). The D155931 was developed as an inhibitor against dihydrolipoamide acyl transferase (DlaT), an enzyme that is required by *M. tuberculosis* to cause the disease in guinea pigs, which is used by the bacterium to resist nitric oxide-derived reactive nitrogen intermediates, a stress encountered in the host (60-61). To ensure the compound successfully penetrate the phagosome, D157070, the propanolic ester of D155931 was synthesized and evaluated as a prodrug. These two molecules are only sensitive to non-replicating tuberculosis. The authors proposed that either the inhibition of DlaT would interfere with metabolic processes that the pathogen needs to sustain viability, or it would impair pathways of detoxification or repair that the pathogen uses to protect itself from sterilization by the host chemistry that prevents it from replicating (60). TMC207 (formerly R207910) is an investigational diarylquinoline compound that offers a new mechanism of anti-tuberculosis action by specific inhibition of mycobacterial ATP synthase (62-64).

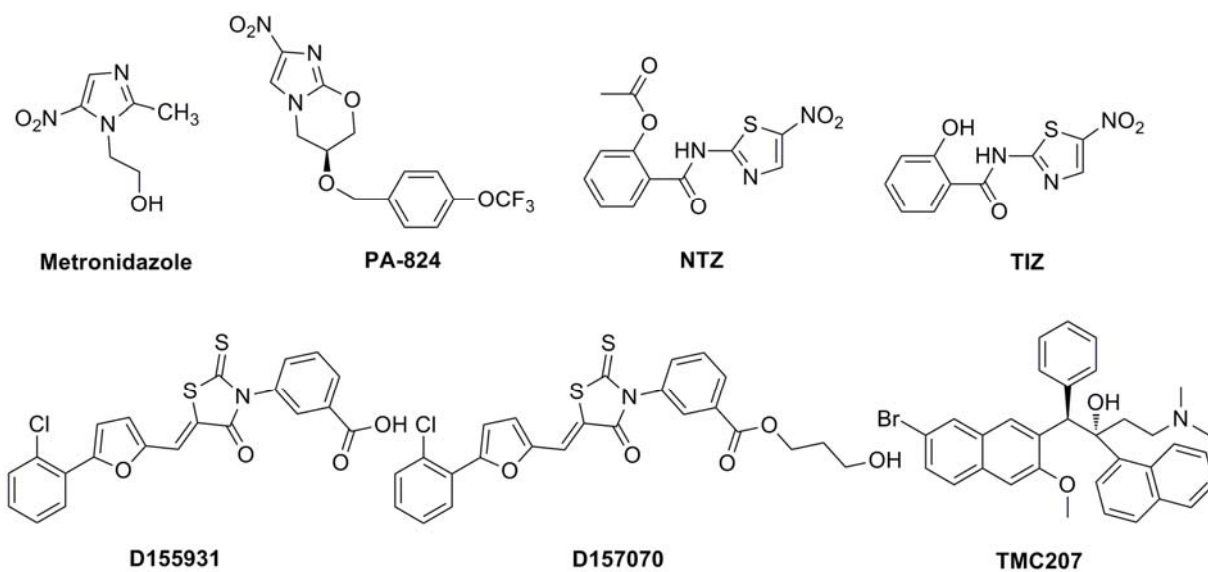


Figure 1.2 Novel chemical scaffolds as non-replicating *M. tuberculosis* inhibitors

Electron transport chain in *M. tuberculosis*

An electron transport chain couples electron transfer between an electron donor (such as NADH and succinate) and an electron acceptor to transfer H⁺ cations across the cell membrane. In **Figure 1.3**, the electron transport chain is proposed for mycobacteria.

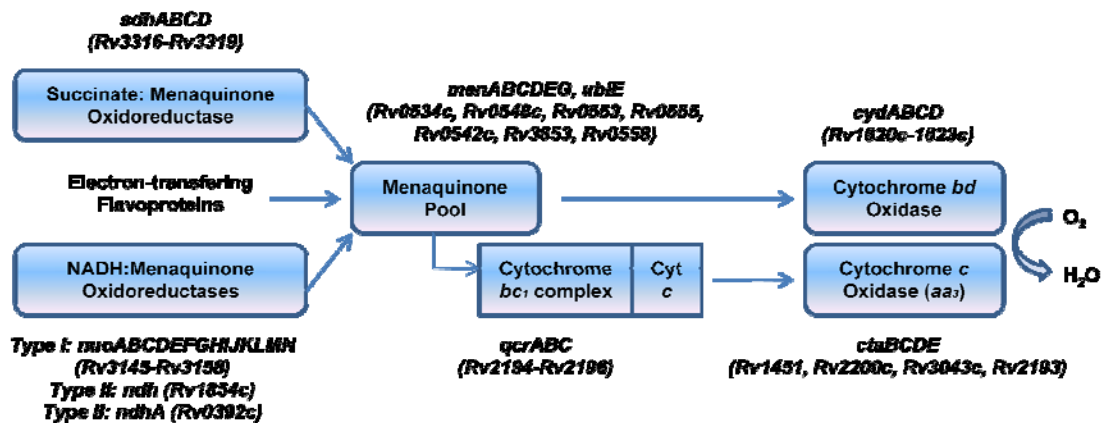


Figure 1.3 Proposed pathway of aerobic electron flow in mycobacteria (65)

M. tuberculosis mostly uses succinate (FADH₂) or NADH as electron donor. For example, two electrons are removed from the electron donor NADH and NADH is oxidized to NAD⁺ by NADH:Menaquinone oxidoreductases and protons are pumped outside bacteria membrane simultaneously. The generated electrons are transferred to a mobile lipid-soluble carrier – menaquinone, which is subsequently reduced to menaquinol. In cytochrome bc₁ complex, menaquinol is oxidized back to menaquinone and the two electrons will be sequentially transferred to two molecules of cytochrome c, a mobile water-soluble electron carrier located within the intermembrane space. Four electrons will be removed from four cytochrome c molecules in cytochrome c oxidase and transferred to an oxygen molecule, producing two water molecules. At the same time, four protons are translocated across the membrane, contributing to the proton gradient.

The transmembrane electrochemical potential gradient may enable transport of molecules across the membrane. It may also enable ATP production, the main energy intermediate in the living organism. If the electrochemical potential gradient is disturbed,

the normal function of the bacteria will be significantly impacted, which will lead to its mortality. As its importance, the electron transport chain is crucial for the bacteria's survival and a potential target for antibacterial development.

Menaquinone biosynthesis pathway – a potential drug target

In the electron transport chain, quinones are used to shuttle electrons between the membrane-bound protein complexes. Quinones can be divided into two major groups by structure difference, the benzoquinone and naphthoquinone (**Figure 1.4**). The difference within the quinone pool also lies on the length of the repeated isoprenoid units.

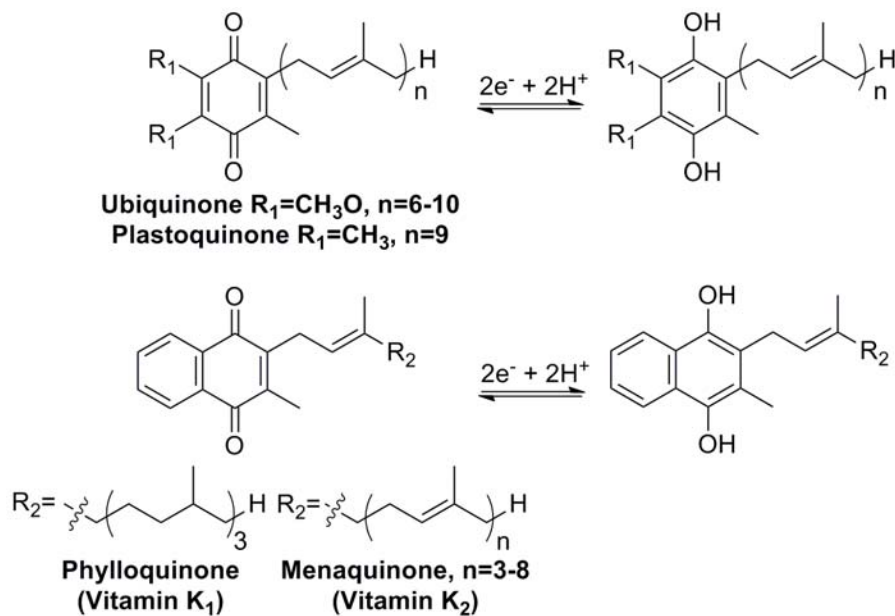


Figure 1.4 Structures of benzoquinone and naphthoquinone redox cofactors

Species	Quinone type
Mammals	Ubiquinone-10
<i>E. coli</i>	Ubiquinone-8 – aerobic condition
	Menaquinone-8 – anaerobic condition
<i>B. subtilis</i>	Menaquinone-7
<i>S. aureus</i>	Menaquinone-8
<i>M. tuberculosis</i>	Menaquinone-9

Table 1.2 Quinone usage in different species

The quinones in mammals are ubiquinones (coenzyme Q) (66). It is located in the inner mitochondrial membrane and participates in the electron transport process. By contrast, prokaryotes employ either ubiquinone or menaquinone in the electron transport system. In different bacteria or different condition, such as oxygen concentration, the participating quinones differ in the chain length or type. The quinone usage is summarized in **Table 1.2**.

Eukaryotes and aerobic Gram-negative bacteria use only ubiquinone in the electron transport chain. Facultative anaerobic bacteria, such as *E. coli*, use ubiquinone under aerobic condition and menaquinone under anaerobic condition (66-67). Most Gram-positive bacteria use only menaquinone for electron transfer (67).

The biosynthesis of menaquinone in *M. tuberculosis* is thought to mirror the pathway found in organisms such as *E. coli*, *B. subtilis* and *M. phlei* (68-70), where it is studied in depth. The proposed menaquinone biosynthesis pathway for *E. coli* is shown in **Figure 1.5**.

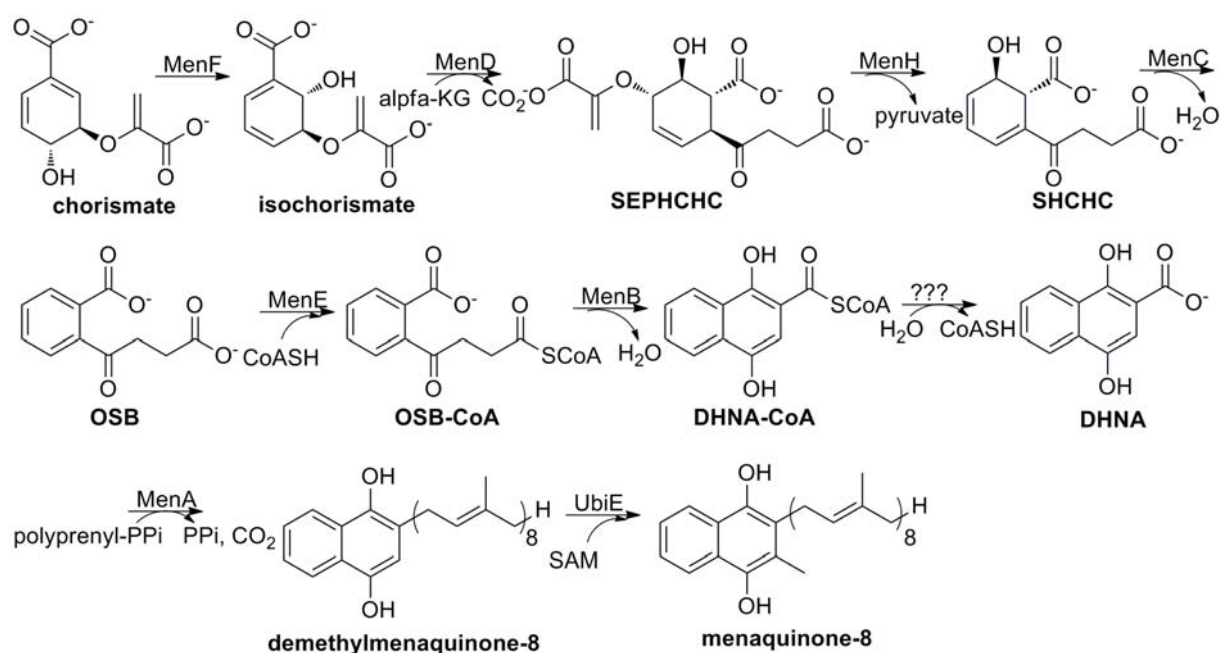


Figure 1.5 Proposed menaquinone biosynthesis pathway in *E. coli*

Chorismate, derived from the shikimate pathway (71), is converted into isochorismate, catalyzed by MenF (72). The condensation of isochorismate with α -ketoglutarate is catalyzed by MenD and this procedure also requires thiamine pyrophosphate as a cofactor to form 2-succinyl-5-enolpyruvyl-6-hydroxy-3-cyclohexene-1-carboxylate (SEPHCHC) (73-74), which is transformed to 2-succinyl-6-hydroxy-2,4-cyclohexadiene-1-carboxylate (SHCHC) under MenH catalyzation (75). SHCHC is dehydrated by MenC to form the aromatic product *o*-succinylbenzoate (OSB) (76), which is subsequently couples with coenzyme A and forms OSB-CoA accomplished by the coenzyme A ligase MenE (77-78). Afterwards, MenB catalyzes the cyclization to form the naphthalenoid aromatic compound (DHNA-CoA) (79) and the thioester bond in DHNA-CoA is hydrolyzed by an unknown thioester hydrolase to form the free DHNA. The prenyl side chain is then attached to the aromatic ring by MenA, resulting the loss

of the carboxylate (79). The last step in the pathway is methylation, catalyzed by UbiE, an S-adenosylmethionine (SAM)-dependent methyl transferase (80).

Recent studies showed that there is an alternative menaquinone biosynthesis pathway in some other microorganisms, such as *Streptomyces coelicolor* A3(2) (81), *Streptomyces avermitilis* (81), *Helicobacter pylori* (82), and *Campylobacter jejuni* (82). These bacteria lack the *men* genes, although they could individually synthesize menaquinone. An alternative menaquinone biosynthesis pathway via futasoline is proposed, which is shown in **Figure 1.6** (83).

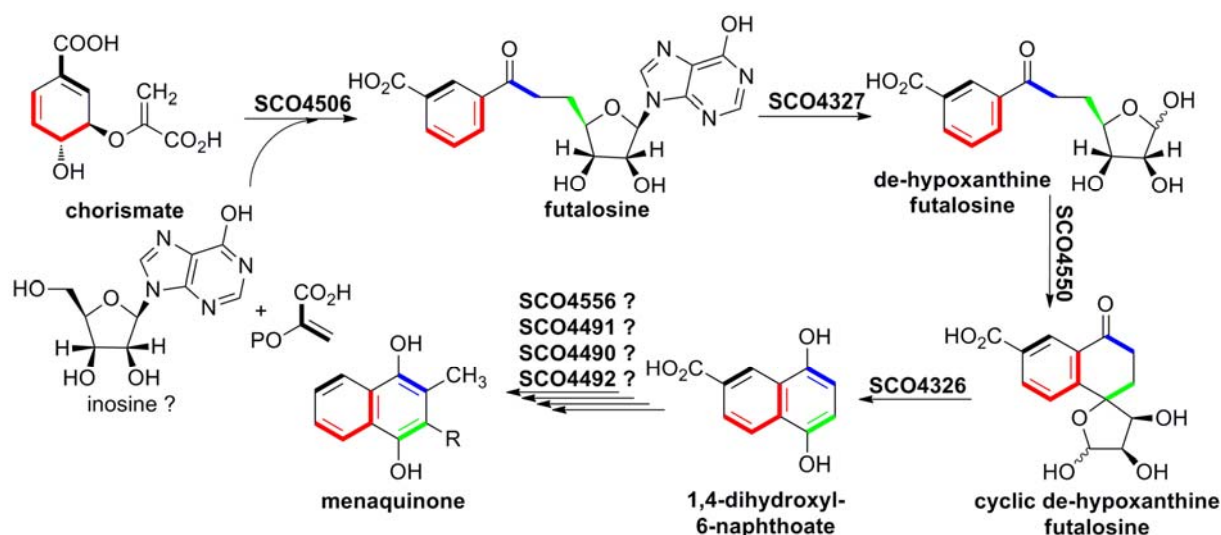


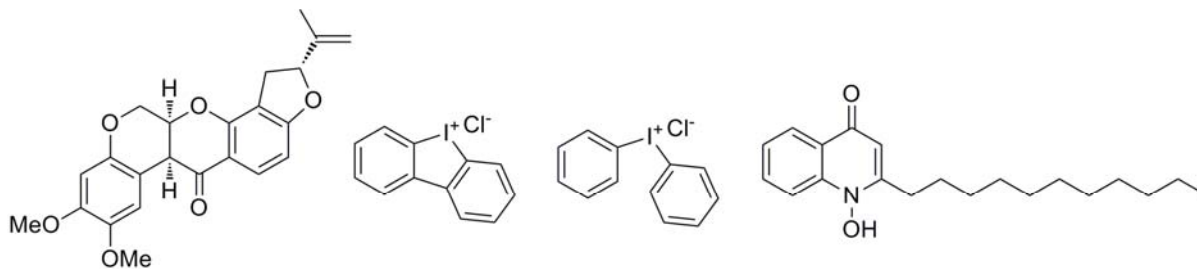
Figure 1.6 An alternative menaquinone biosynthesis pathway in microorganisms

As discussed above, maintenance of the mitochondrial membrane potential is essential for cellular energy production. In recent years, the mitochondrial electron transport chain has been extensively explored for the development of new antimalarial molecules (84). Most of this research was focused on the inhibition of Type II NADH:quinone oxidoreductase (*pf*NDH2) (85-86), succinate:ubiquinone oxidoreductase

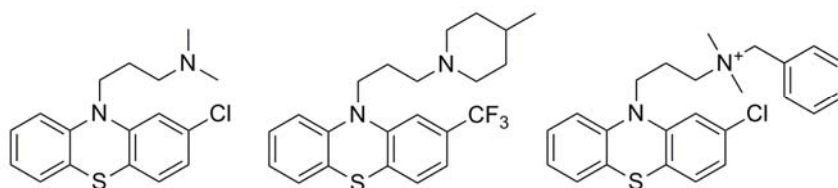
(SDH) (87-89) and cytochrome *c* oxidoreductase (cytochrome *bc*₁ complex) (90). These promising chemical scaffolds are summarized in **Figure 1.7**.

Although structures targeting electron transport system of malaria parasites are known, there are very few investigations about the electron transport chain inhibition in antibacterial drug development. Recently, phenothiazine analogues were synthesized and they specifically inhibit NADH:menaquinone oxidoreductase. The analogues can also kill *M. tuberculosis in vitro* and suppress the bacteria growth in mouse models of acute infection (65).

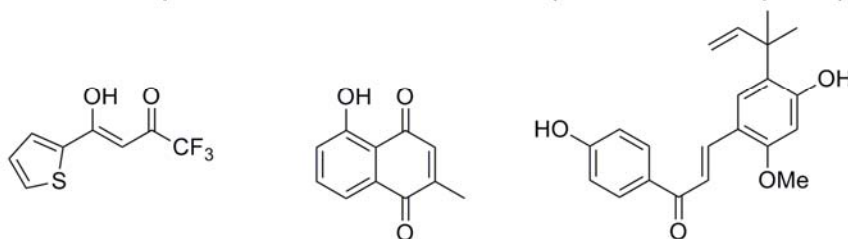
Type II NADH:ubiquinone oxidoreductase inhibitors (*Plasmodium falciparum*)



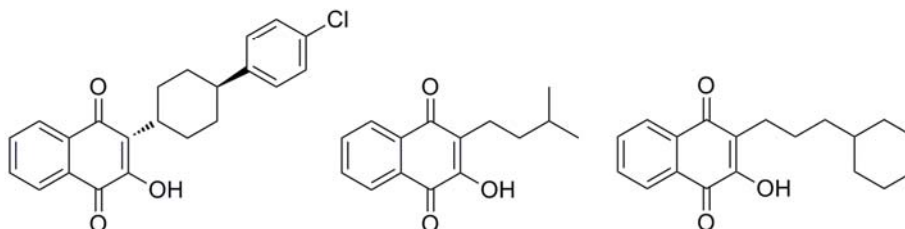
Type II NADH:menaquinone oxidoreductase inhibitors (*Mycobacterium tuberculosis*)



Succinate:ubiquinone oxidoreductase inhibitors (*Plasmodium falciparum*)



Cytochrome c oxidoreductase inhibitors (*Plasmodium falciparum*)



ATP synthase inhibitors (*Mycobacterium tuberculosis*)

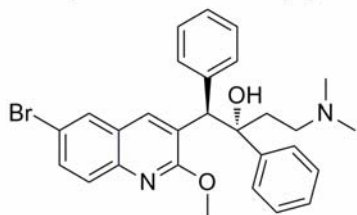


Figure 1.7 Representative structures targeting electron transport chain and ATP synthesis

Another example is TMC207, an ATP synthase inhibitor (91) developed by Johnson & Johnson, with a MIC as low as 0.06 µg/mL. This study demonstrated that the bacteria cannot survive after the ATP production is compromised.

Menaquinone, the sole quinone found in most of the Gram-positive bacteria, plays an important role in electron transport (92), oxidative phosphorylation (93), active transport (92), and endospore formation (94). Inhibition of the menaquinone biosynthesis would disturb the hydrogen gradient, which is essential for the ATP production, thus killing the bacteria. Since the pathway leading to the menaquinone biosynthesis is absent in humans, the bacterial enzyme catalyzing menaquinone biosynthesis are novel potential drug targets leading to antibacterial drug discovery. Moreover, the non-replicating bacilli still rely on the ATP for survival. Thus inhibition of menaquinone biosynthesis pathway could have a profound effects on treating non-replicating tuberculosis (95).

Currently, several chemical structures have been developed to target menaquinone biosynthesis pathway, which are summarized in **Figure 1.8**. The MenA inhibitors were first introduced by Dr. Dean C. Crick and his co-workers (96-97). They generated a small compound library possessing the shown scaffold. These compounds act as selective antibacterial agents against Gram-positive organisms including methicillin-resistant *S. aureus* (MRSA), *S. epidermidis* (MRSE), and *M. spp.* MenE inhibitors were also synthesized and their activity was evaluated against *M. tuberculosis* (98) and *B. anthracis* (99). On these scaffolds, the inhibitors were designed as reaction intermediate or mechanism-based. They inhibit MenE activity at micromolar concentration. However, it is surprising that these molecules did not inhibit the growth of

bacteria, suggesting additional pharmacological issues that may need to be addressed. Acylphosphonate ester analogues of α -ketoglutarate have been designed and synthesized recently as menD substrate analogue inhibitors (100). The best inhibitor was shown in **Figure 1.8**, with a K_i value of 0.7 μM . However, this scaffold showed no significant inhibition of *M. tuberculosis* growth either. Furthermore, plumbagin derivatives were synthesized and their inhibitory activity was evaluated against *M. tuberculosis* and *M. smegmatis* (101).

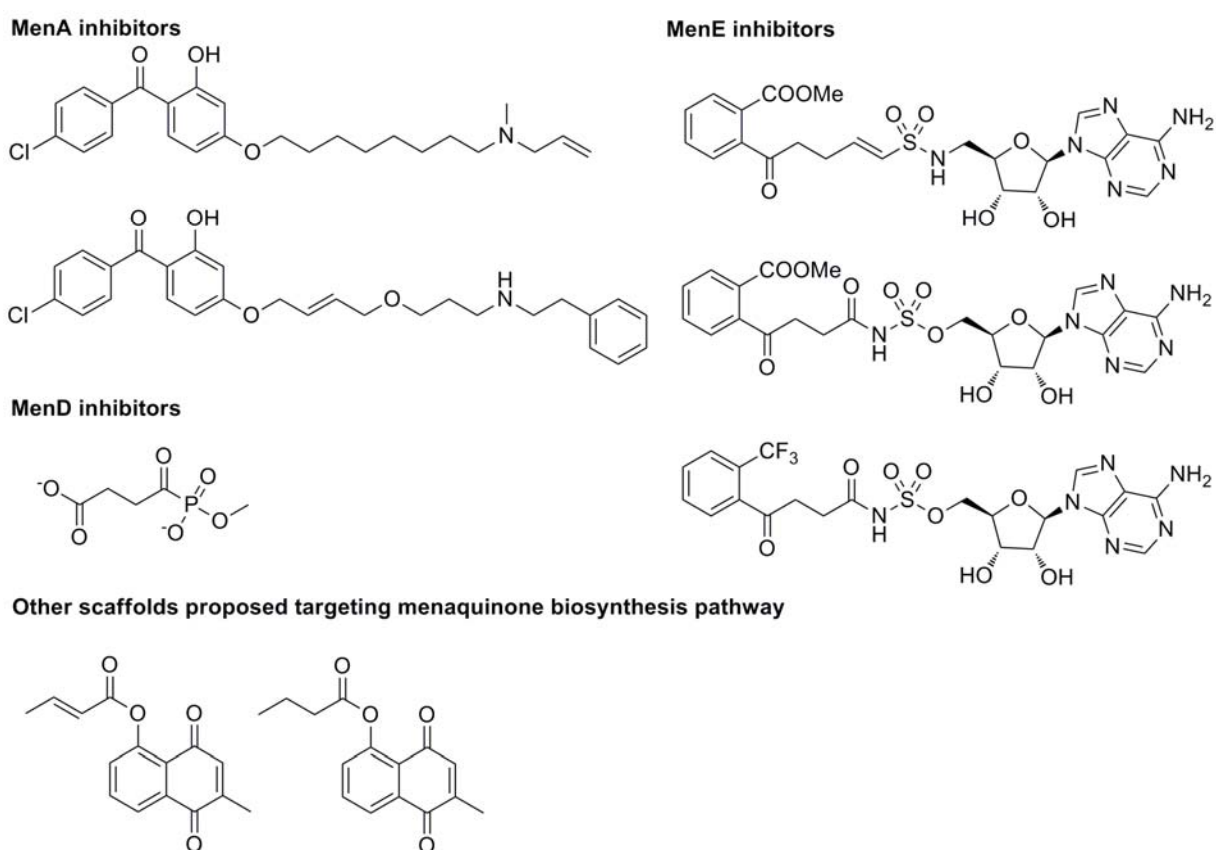


Figure 1.8 Representatives menaquinone biosynthesis inhibitors

Overview of research presented in the dissertation

My research is mainly focused on the design, synthesis, purification, and characterization of novel organic small molecules that can inhibit the 1,4-dihydroxynaphthoyl-CoA synthase in the menaquinone biosynthesis pathway from *M. tuberculosis*. The long term goal of this research is to understand the enzymatic reaction mechanism, to discover potent inhibitors against this enzyme, and to validate this pathway as a novel target for development of broad spectrum antibiotics for Gram-positive bacteria.

In Chapter 2, several OSB-CoA analogues were rationally designed and successfully synthesized, which were used as probes to investigate the MenB reaction mechanism. X-ray crystallography was used to determine the interaction structure between the enzyme, MenB and the OSB-CoA analogues. In this research, an intact ecMenB active site was first revealed and the substrate-residue interactions can help to understand the MenB reaction mechanism.

In Chapter 3, a high-throughput screen (HTS) was performed on *mt*MenB inhibitor discovery, which yielded several promising hits, which are MenB substrate analogues. Structure-activity relationship (SAR) studies have led to the development of several low μM inhibitors, some of which inhibit *M. tuberculosis* growth with MIC values of 1-2 $\mu\text{g/ml}$. However, there is no/low correlation between the enzymatic assay and whole cell growth inhibitions. Further research found that these compounds are relatively unstable in aqueous solution and the degraded product reacts with coenzyme A and forms a new series of inhibitors against MenB *in situ*. SAR studies, together with data from X-ray

crystallography, are being utilized to optimize the potency and antibacterial activity of these compounds and to make them more drug-like. Currently, the most potent compounds have MIC values of 0.65 and 0.5 $\mu\text{g/ml}$ against *M. tuberculosis* and *S. aureus*, respectively. Target validation experiments demonstrate that these compounds can compromise the menaquinone biosynthesis in *S. aureus*.

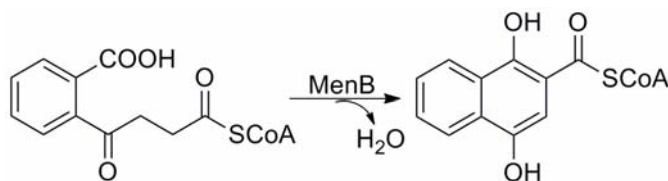
In Chapter 4, several 1,4-benzoxazines were also identified from HTS. The scaffold is a MenB product analogue. Subsequent SAR studies resulted in the discovery of compounds with excellent antibacterial activity against *M. tuberculosis* H37Rv with MIC values as low as 0.6 $\mu\text{g/mL}$. Therefore, the 1,4-benzoxazine scaffold is a promising foundation for the development of antitubercular agents.

Chapter 2 : Synthesis of OSB-CoA analogues as a 1,4-dihydroxy-2-naphthoyl-CoA synthase (MenB) reaction mechanism probe

1,4-Dihydroxy-2-naphthoyl-CoA synthase (MenB), is the sixth enzyme in the menaquinone biosynthesis pathway and belongs to the crotonase superfamily. It catalyzes the naphthalene ring formation of 1,4-dihydroxy-2-naphthoyl-CoA (DHNA-CoA) from *o*-succinylbenzoate-CoA (OSB-CoA). In this research, several substrate analogues were rationally designed and successfully synthesized. Cocrystallization structures with *ec*MenB and *mt*MenB were obtained. These structures offered a clear overview of MenB active site geometry and interactions between substrate and protein residues.

Introduction

The *M. tuberculosis* 1,4-dihydroxy-2-naphthoyl-CoA (DHNA-CoA) synthase, *mtMenB*, is the sixth enzyme in the biosynthetic pathway leading from chorismate to menaquinone, and catalyzes the conversion of *o*-succinylbenzoyl-CoA (OSB-CoA) to DHNA-CoA (**Scheme 2.1**).



Scheme 2.1 The reaction catalyzed by MenB

MenB structures have been heavily studied in *M. tuberculosis* (102), *S. aureus* (103), *G. kaustophilus* (104), *B. subtilis* (105-106), and *E. coli* (107). The *mtMenB* crystal structure was first solved in 2003 (102), in which it forms a 208kDa (α_3)₂ hexamer (a dimer of trimers) with two hexamers in the asymmetric unit (**Figure 2.1A and 2.1B**). The MenB structures from different species are well overlaid due to their highly conserved sequences (**Figure 2.1C**). The overall fold of MenB is characterized as the enoyl-CoA hydratase/isomerase (crotonase) superfamily. The other members of this family have been structurally well characterized, including enoyl-CoA hydratase (108), methylmalonyl-CoA decarboxylase (109), dienoyl-CoA isomerase (110), Δ^3 - Δ^2 -enoyl-CoA isomerase (111), 4-chlorobenzoyl-CoA dehalogenase (112), 6-oxo-camphor hydrolase (113), and the human AUH protein (114).

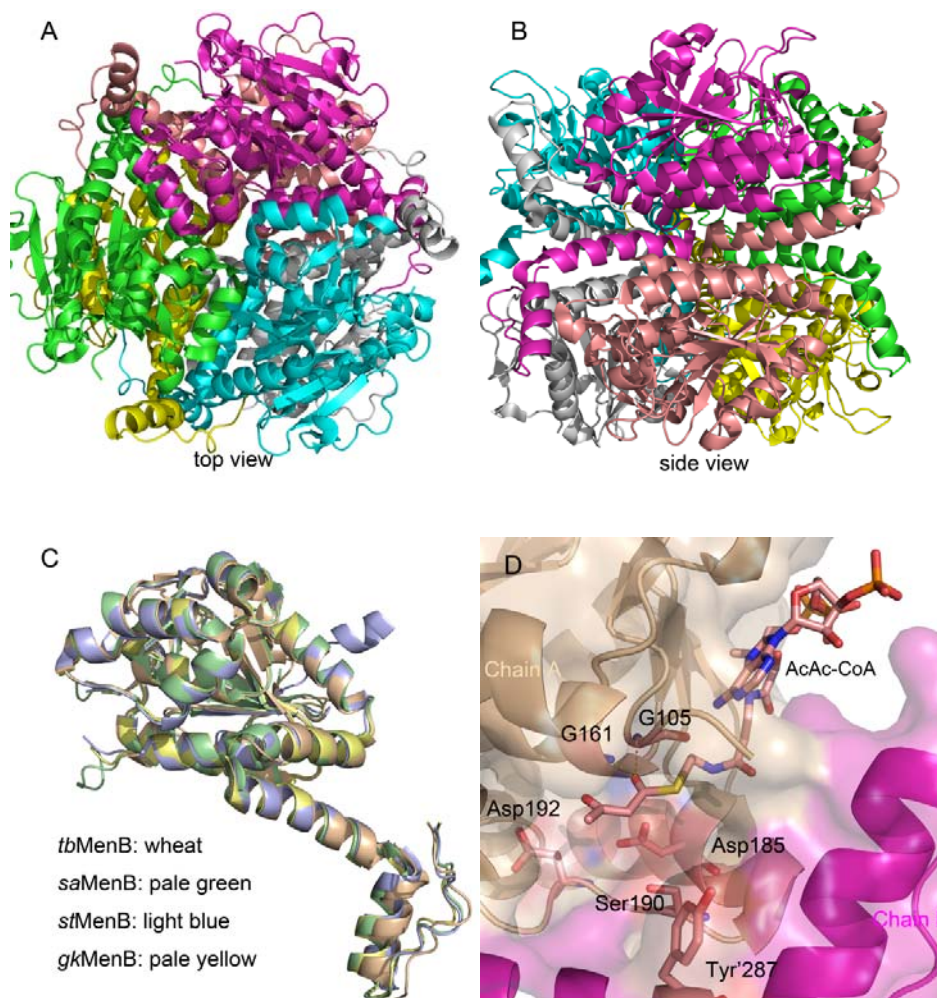


Figure 2.1 Solved MenB crystal structures

A: top view of *mt*MenB (PDB ID#: 1Q51); B: side view of *mt*MenB; C: overlay MenB monomers from *M. tuberculosis*, *S. aureus* (PDB ID#: 2UZf), *S. typhimurium* (PDB ID#: 3H02), and *G. kaustophilus* (PDB ID#: 2lEX); D: *mt*MenB active site.

*mt*MenB crystals soaked with acetoacetyl-CoA (AcAc-CoA) was successfully solved to 2.3 Å resolution (**Figure 2.1D**). In this structure, conserved residues in the active site are clearly identified (102). Gly105 and Gly161 form the oxyanion hole, which is a common characteristic in the crotonase superfamily (115). They interact with the carbonyl group in the thioester, and the formation of hydrogen bonds stabilizes the enolate intermediate. Ser190 and Tyr'287 are hydrogen bonded with the OSB ketone carbonyl group adjacent to the aromatic ring in order to position the OSB in the active

site. Asp185 and Asp192 are in close proximity to the OSB aromatic carboxylate, thereby raising the pK_a of this group to promote proton abstraction from the OSB α -carbon of the thioester. However, this structure also has several deficiencies. Due to its high flexibility, residues 107 – 134 are disordered, which gives an incomplete active site. Furthermore, AcAc-CoA lacks the aromatic ring as in the OSB-CoA and DHNA-CoA, and would not offer a direct substrate-enzyme interaction.

Coenzyme A (CoA) (**Figure 2.2**) is a cofactor that aids in the activation and transfer of acyl groups in many enzyme catalyzed reactions. It is estimated that CoA is used by 4% of all known enzymes and it plays a crucial role in a wide range of biological pathways (116). CoA consists of a 3'-phosphoadenosine moiety and pantetheine, linked by a pyrophosphate group. Although CoA structure is complex, the enzymatic reactions of CoA involve only the free thiol group. The remaining of the CoA molecule serves as a recognition element for enzyme binding.

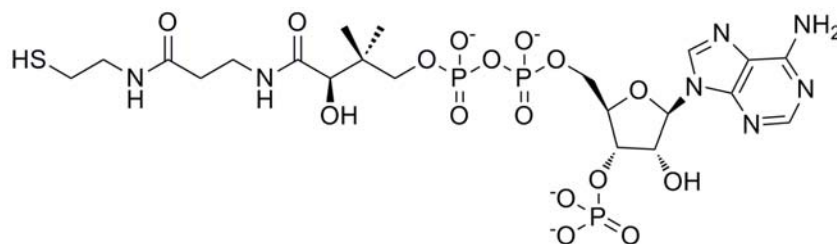
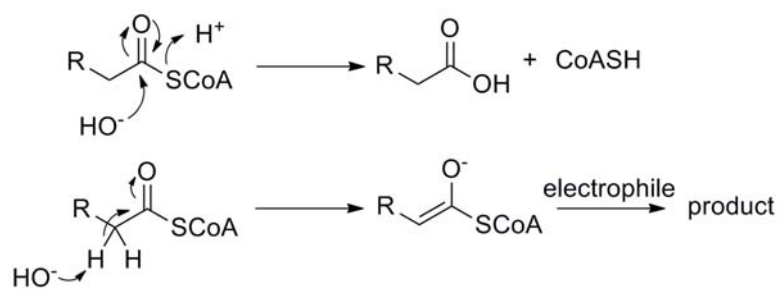


Figure 2.2 The chemical structure of CoA

CoA thioesters are easily subject to hydrolysis, which directly leads to the instability of acyl-CoA molecules. Furthermore, deprotonation of α -carbon forms a nucleophile, which can react with an electrophile through Claisen reaction and form a new product (**Scheme 2.2**).



Scheme 2.2 Instability of acyl-CoA

Some strategies are widely used to overcome the degradation issue, which are summarized in **Figure 2.3**. Methylene-substituted CoA analogues differ from the natural acyl-CoA by insertion of a methylene group between the carbonyl and sulfur atom. S-(2-oxopentadecyl-CoA) was synthesized as a nonhydrolyzable analogue of myristoyl-CoA, which was used as a potent inhibitor of *N*-myristoyltransferase (117). Another group of CoA analogues are the keto-replaced CoA (thioether). In this case, the carbonyl group in the thioester is replaced with methylene group, which is chemically stable and cannot undergo any reactions that involve hydrolysis or deprotonation. This chemical scaffold is always synthesized as a protein inhibitor or cocrystallography ligand, for example in the methylmalonyl-CoA decarboxylase (109), 3-hydroxy-3-methylglutaryl-CoA reductase, and citrate synthase (118).

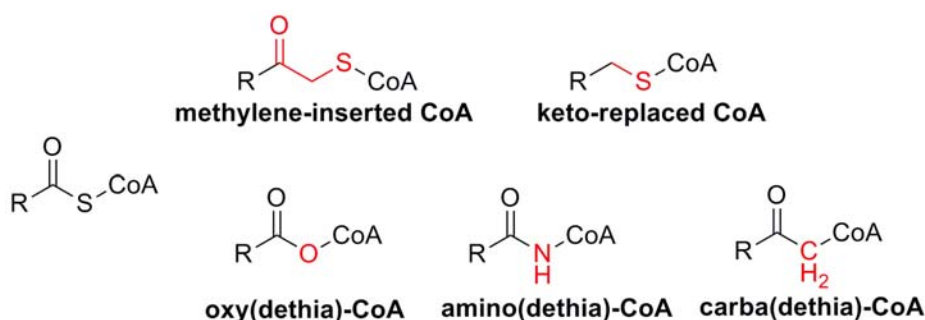
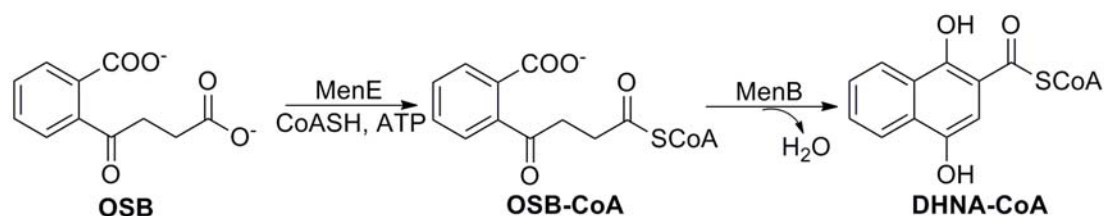
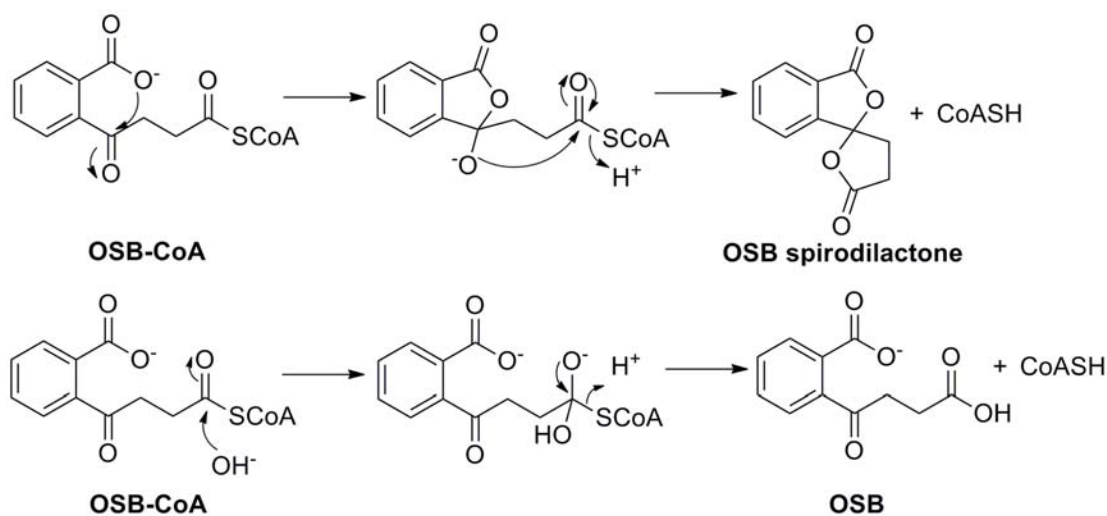


Figure 2.3 Examples of coenzyme A analogues

Another analogue modification strategy is the replacement of the sulfur atom with an oxygen, a nitrogen, or a methylene, making the ester, amide or ketone instead of thioester, respectively. Oxy(dethia)-CoA was first synthesized in 2001, and it was used as a enoyl-CoA hydratase substrate analogue (119), while carba(dethia)-CoA was synthesized as a tool for trapping polyketide intermediates (120). In this strategy, amide and ketone analogues are nonhydrolyzable. Furthermore, the α -protons of these analogues are less acidic than the thioester (121), which can prevent deprotonation.

OSB-CoA, the substrate of MenB, rapidly decomposes to OSB spirodilactone (122) and can be easily hydrolyzed to OSB under basic condition (**Scheme 2.3**). Consequently, it cannot be synthesized, purified, and stored as a substrate for enzymatic assay. In order to perform MenB enzyme kinetic assay, a coupled assay with MenE, the preceding enzyme, needs to be performed (**Scheme 2.4**) (102). However, this assay is based on two assumptions. First, OSB-CoA generation *in situ* under the catalysis of MenE with OSB, ATP, and CoA is rapid and complete and second, OSB-CoA fully turns into DHNA-CoA. However, as it is discussed above, the two ideal scenarios cannot be guaranteed due to the instability of OSB-CoA.



In this chapter, two questions will be addressed.

1). Is it possible to synthesize OSB-CoA analogues that can be solely utilized in the MenB activity assay?

2). Is it possible to synthesize stable OSB-CoA analogues that can be utilized in crystallography?

To answer question 1, the designed compounds should not undergo spirodilactone formation and should be active under MenB catalysis. OSB-*N*-CoA was subsequently designed, in which the thioester is replaced by amide. In this molecule, the amide is nonhydrolyzable at pH 7.0 in aqueous solution and it is a poor leaving group under nucleophile attack, thus prevents the second step in the spirodilactone

formation. However, the risk for this molecule is the α -proton of an amide is approximately 25,000,000-fold less acidic than the α -proton of a thioester (119, 121), which suggests that the enolate formation will be significantly impaired, thus it might not be an active substrate.

To answer question 2, several thioesters are designed, in which the aromatic carboxylate is replaced with several substitutes with similar size of carboxylate. The functional groups are added onto the aromatic ring to preserve the ligand binding affinity. In this case, the first step of the spirodilactone formation is prevented. Moreover, they have the aromatic ring, which is always missing in previous cocrystallography studies. However, these molecules may still be hydrolyzed during the cocrystallography process.

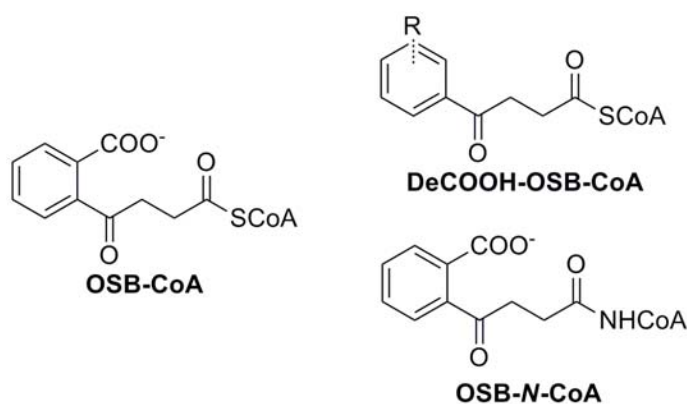


Figure 2.4 Design of OSB-CoA analogues

Result and Discussion

Preliminary OSB-N-CoA synthesis

The retrosynthesis of OSB-N-CoA is shown in **Figure 2.5**. The synthetic route can be divided into two major parts – organic and enzymatic. The organic synthesis mainly focuses on the OSB-N-Pantetheine synthesis, and the enzymatic synthesis focuses on the biosynthesis of the CoA scaffold.

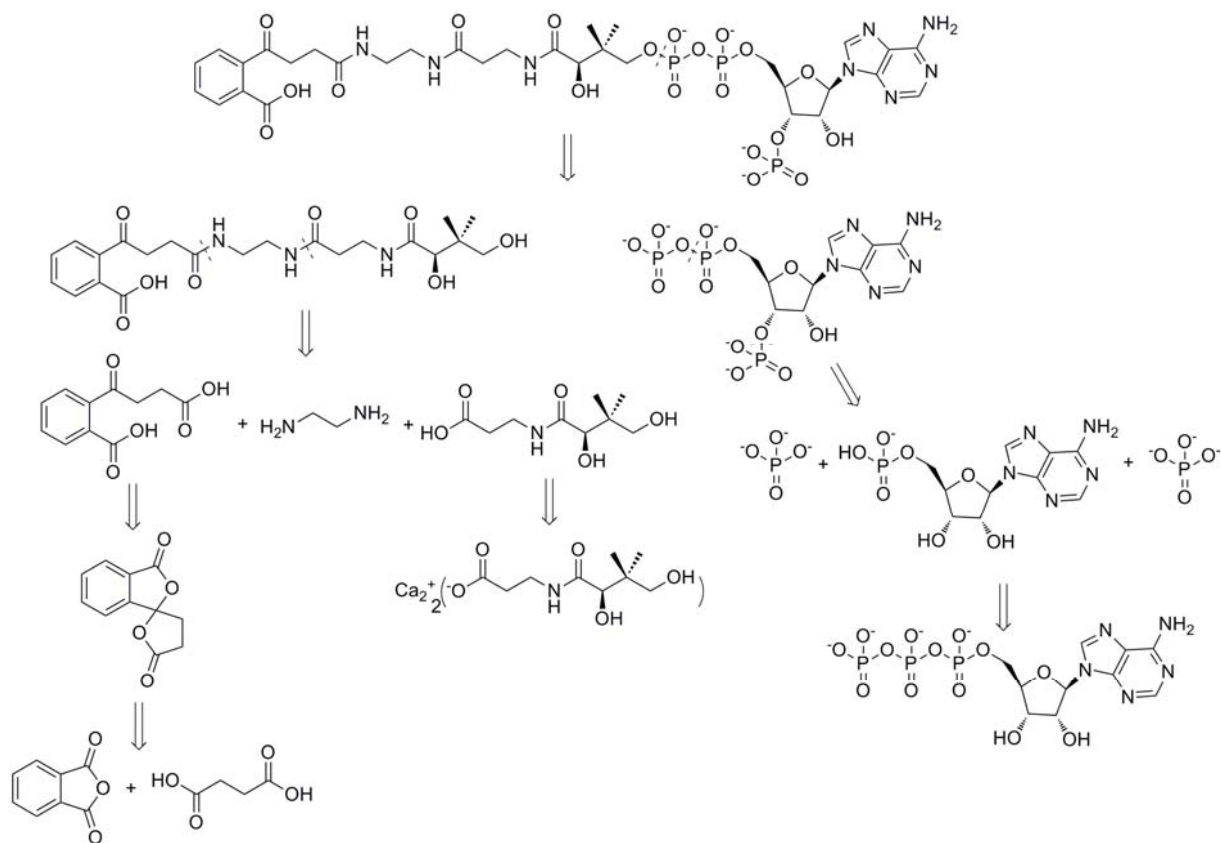
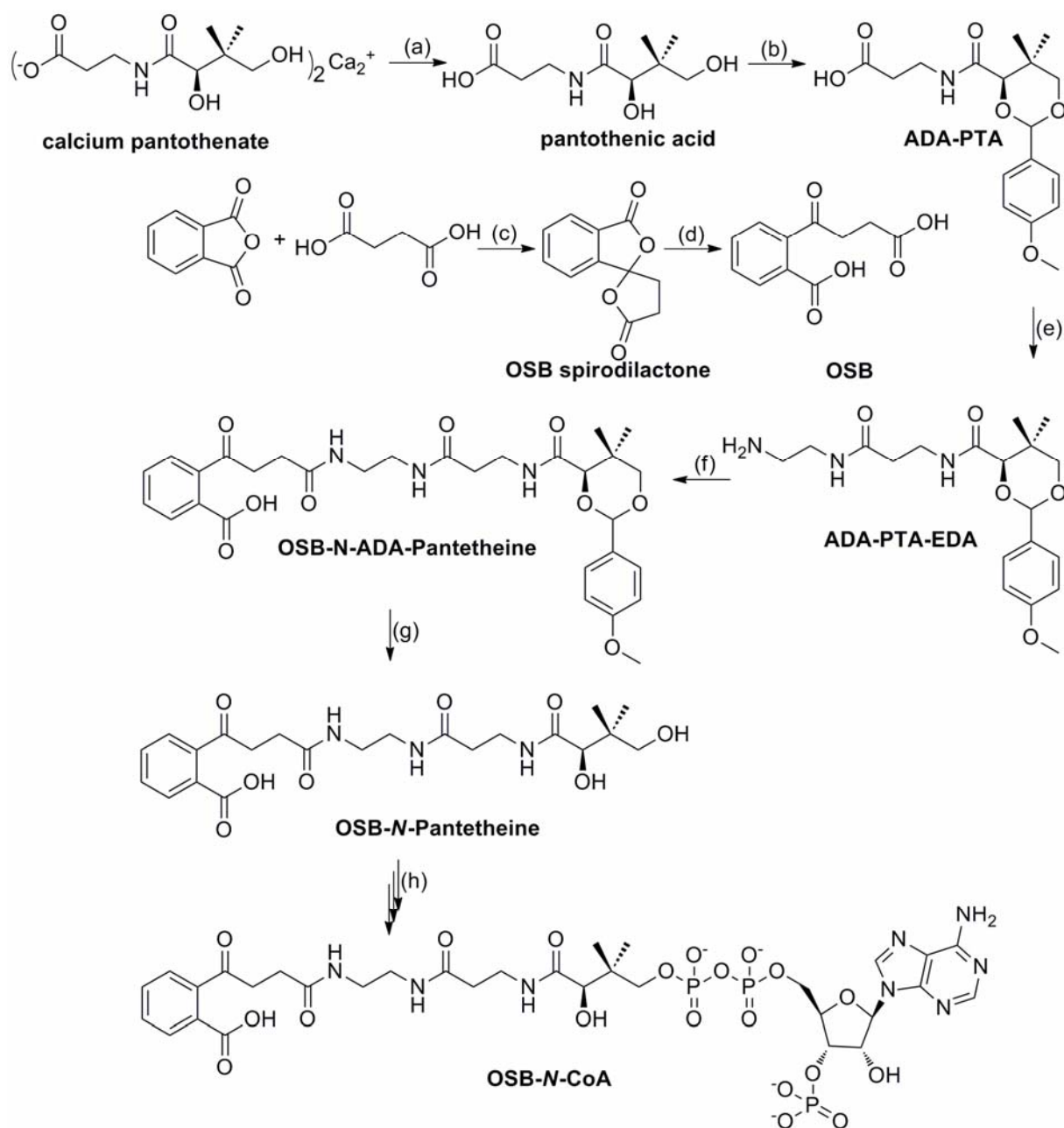


Figure 2.5 Retrosynthesis of OSB-N-CoA

Based on the retrosynthesis, the synthetic route is designed as **Scheme 2.5**. Commercially available calcium pantothenate is easily converted to pantothenic acid by eluting through cation exchange column and subsequently the two free hydroxyl groups

in pantothenic acid are protected by the reaction with *p*-anisaldehyde dimethyl acetal (123). Symmetric ethylenediamine can be selectively monoacylated with the protected pantothenic acid (ADA-PTA) via prior complexation with 9-borabicyclo(3.3.1)nonane (9-BBN) (124). OSB spirodilactone can be generated by heating phthalic anhydride, succinic acid, and sodium carbonate to 210°C, which can be subsequently hydrolyzed to OSB by refluxing in 1 M NaOH aqueous solution (125). The free amine in ADA-PTA-EDA and the aliphatic carboxylic acid in OSB can be selectively coupled due to the higher reactivity of the aliphatic carboxylic acid (125). The ADA protection group is removed under 1 M HCl condition, giving OSB-*N*-Pantetheine as a product. OSB-*N*-Pantetheine is subsequently converted to OSB-*N*-CoA using the catalysis of pantothenate kinase, phosphopantetheine adenylyltransferase, and 3'-dephosphoCoA kinase with ATP.



Scheme 2.5 Tentative OSB-N-CoA synthesis route

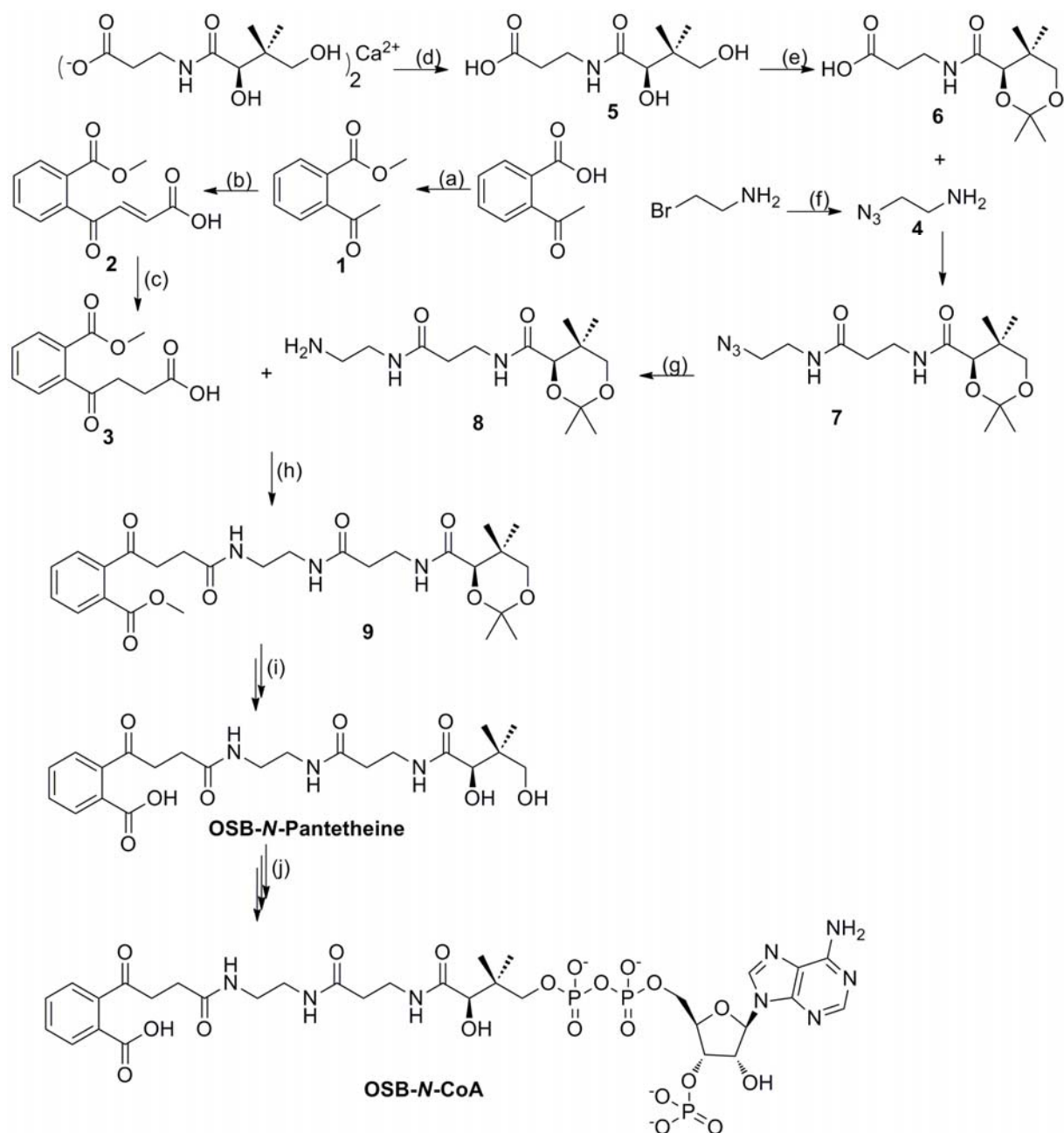
Reagents and conditions: (a) Dowex 50W-X8 hydrogen form cation exchange resin; (b) *p*-anisaldehyde dimethyl acetal, TsOH (cat.), anhydrous THF, 25°C, 18 hours; (c) Na₂CO₃, 210-220°C, 30 minutes; (d) 1M NaOH, reflux, 2 hours; (e) ECF, 9-BBN, TEA, anhydrous CH₂Cl₂, 25°C, 18 hours; (f) CDI, DMAP, anhydrous CH₂Cl₂, 25°C, 18 hours; (g) 1M HCl, THF, 25°C, 1 hour; (h) PanK, PPAT, DPCK, ATP, pH 7.5 buffer, 25°C, 4 hours.

However, this synthetic route is problematic when it was put into practice. First, during the synthesis of ADA-PTA-EDA, the reaction yield is as low as 30-40%. Moreover, the product is a free amine, which has a high polarity and is difficult to purify by silica-gel chromatography. Secondly, the OSB spirodilactone synthesis yield is extremely low, even lower than 5%. The greatest concern is the coupling reaction between OSB and ADA-PTA-EDA. There are two different carboxylates in OSB: aromatic and aliphatic one. The selectivity of the coupling reaction is crucial for the final product. It is reported that the aromatic carboxylic acid is less reactive because of the steric hindrance and the conjugation of benzene ring (125). However, the experiment has not been repeated for more than 30 years and no other similar reactions were reported in recent years. Furthermore, it is difficult to confirm which carboxylic acid reacts because the products have similar NMR spectra and the same molecular weight. Due to its low feasibility, a new OSB-*N*-CoA synthetic route was carefully designed (**Scheme 2.6**).

Modified OSB-*N*-CoA synthesis

After careful design, OSB-*N*-CoA can be synthesized by route shown in **Scheme 2.6**. Generally, 2-acetylbenzoic acid is protected by its methyl ester, and the methyl 2-acetylbenzoate subsequently reacted with glyoxylic acid monohydrate to synthesize (*E*)-4-(2-(methoxycarbonyl)phenyl)-4-oxo-but-2-enoic acid (compound **2**) by refluxing in acetic acid (126). The resulting double bond is easily reduced under hydrogen

atmosphere with catalytical amount of Pd/C (127). Commercially available calcium pantothenate is converted to pantothenic acid by washing through cation exchange column (128), after which the two free hydroxyl groups in the pantothenic acid are subsequently protected by reaction with acetone in the presence of catalytical amount of *p*-toluenesulfonic acid (TsOH) (129). Compared with the tentative *p*-anisaldehyde dimethyl acetal protection method, acetone can be easily removed under reduced pressure and TsOH is quite soluble in aqueous phase, which indicates the product from this method needs no further purification. 2-Azidoethylamine is generated by heating 2-bromoethylamine with NaN₃ in aqueous solution (130), which is coupled with protected pantothenic acid in the next step. The azido group is reduced to the free amine under hydrogen atmosphere in the presence of catalytical amount of Pd/C (131). The resulting free amine can be coupled with mono-methyl-protected OSB. The methyl ester (protection for the aromatic carboxylate) can be removed by 1 M NaOH solution and the acetal (protection for the two hydroxyl groups) can be removed by 1 M HCl solution, giving the OSB-*N*-Pantetheine as the product, which is converted to OSB-*N*-CoA by three individual CoA synthase enzymes (132).



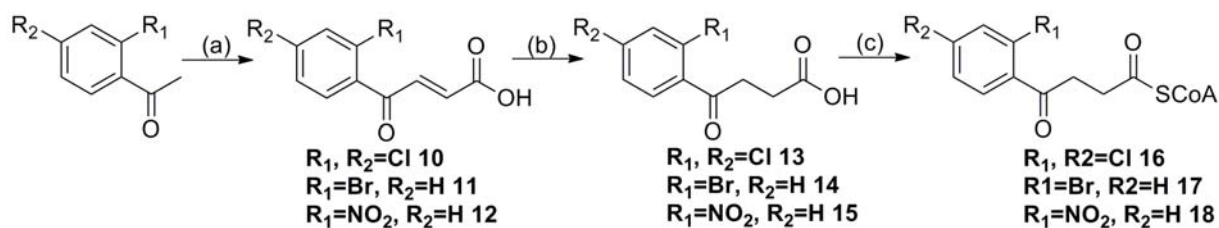
Scheme 2.6 Modified OSB-N-CoA synthetic route

Reagents and conditions: (a) DCC, DMAP, MeOH, anhydrous CH_2Cl_2 , 25°C , 18 hours; (b) glyoxylic acid monohydrate, AcOH, reflux, 18 hours; (c) Pd/C (cat.), EtOAc, 25°C , 3 hours; (d) Dowex 50W-X8 hydrogen form cation exchange resin; (e) anhydrous acetone, *p*-toluenesulfonic acid (cat.), 25°C , 18 hours; (f) NaN_3 , H_2O , 80°C , 18 hours; (g) EDC·HCl, DIPEA, anhydrous CH_2Cl_2 , 25°C , 18 hours; (h) EDC·HCl, DIPEA, anhydrous CH_2Cl_2 , 25°C , 18 hours; (i) (1) 1M NaOH, H_2O , 25°C , 1 hour, (2) 1M HCl, THF, 25°C , 1 hour; (j) PanK, PPAT, DPCK, ATP, pH 7.5 buffer, 25°C , 4 hours.

Compared with the tentative synthetic scheme, this method has several advantages. Although the synthetic route has more steps than the initial one, several steps do not need purification, which might be the most time-consuming process in organic synthesis. The designed reactions for several high polarity compounds, such as free amine and free acid, are clean with high yields. The new synthetic route yields mono-methylated OSB, which can then be coupled with pantetheine. This strategy excludes the possible coupling of the amino-pantetheine with the aromatic carboxylate in OSB.

DeCOOH-OSB-COOH Synthesis

The first step in the breakdown of OSB-CoA involves the attack of the aromatic carboxylate on the ketone group adjacent to the aromatic ring (**Scheme 2.3**). Thus if the carboxylate is removed, then the molecule should be more stable. However, in order to preserve the binding affinity, functional groups which share similar size of carboxylate, can be added on the aromatic ring. For preliminary research, two molecules were synthesized as shown in **Scheme 2.7**. Commercially available substituted acetophenone first reacted with glyoxylic acid monohydrate in acetic acid at 110°C for 12 h to generate the substituted (*E*)-4-aryl-4-oxo-but-2-enoic acid. Subsequently the double bond was reduced to single bond under hydrogen atmosphere catalyzed by catalytical amount of 5% Pd/C. The resulting substituted 4-aryl-4-oxo-butanoic acid coupled with CoASH after ECF activation.



Scheme 2.7 Synthesis of DeCOOH-OSB-CoA

Reagents and conditions: (a) glyoxylic acid monohydrate, AcOH, reflux, 18 hours; (b) Pd/C (cat.), EtOAc, 25°C, 2 hours; (c) (1) ECF, TEA, anhydrous THF, 25°C, 2 hours; (2) CoA, H₂O, 25°C, 30 minutes.

2-Br-CoA:mtMenB cocrystallography

In compound **17**, the aromatic carboxylate in OSB-CoA was replaced by bromine atom, which prevents the first step in the OSB spirodilactone formation. Moreover, in previous crystallography study, the ligand (AcAc-CoA) lacks the aromatic ring in the original substrate (102-103), while compound **17** do have a similar aromatic ring, thus it may be a good ligand for crystallography study. Then compound **17** was sent to Dr. Kisker's group in Germany to cocrystallize with MenB from different organism.

In the 2-Br-CoA:mtMenB cocrystallography structure, the overall fold of the protein is well overlaid with the previous mtMenB structure (PDB ID#: 1Q51) with a RMSD value of 0.252 Å (**Figure 2.6A**). It is surprising that the electron density for the aromatic ring in the ligand is still missing, which might be due to the flexibility of the aromatic ring or the hydrolysis of the ligand. However, the active site residues are similar with the structure found in previous structure.

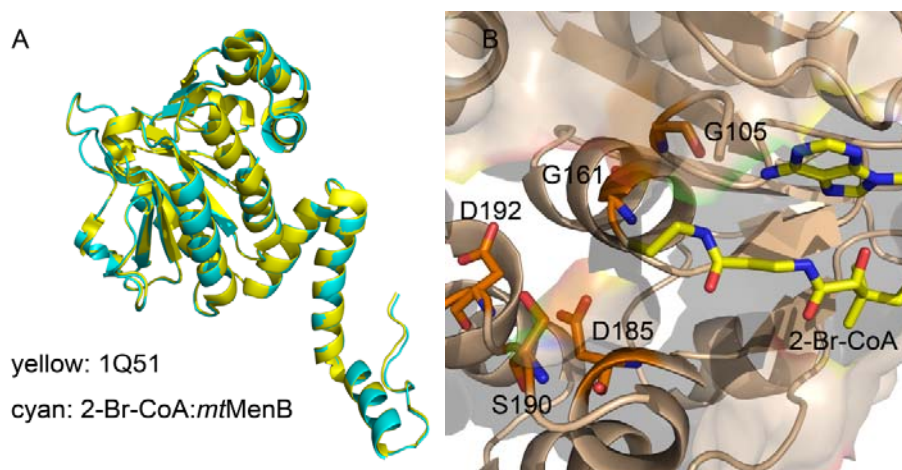


Figure 2.6 2-Br-CoA:*mtMenB* cocrystallography structure

A: overlay with 1Q51; B: active site view.

***OSB-N-CoA:ecMenB* cocrystallography**

The single-atom substitution of nitrogen with sulfur is expected to have a minimal effect on the geometry of the ligand. Enzyme activity assay first confirmed that OSB-*N*-CoA is not a substrate for MenB, probably due to the increased pK_a of the α -proton of the amide and the enolate formation is prevented, which is the first step in the MenB catalytic reaction. However, the increased stability and similar geometry make the OSB-*N*-CoA an ideal ligand to be crystallized with MenB.

The best crystal structure is the OSB-*N*-CoA:*ecMenB* cocrystallography structure. **Figure 2.7A** shows the hexameric structure of *ecMenB*. The C-terminal domain (C-terminal to D241) of one subunit folds across the trimer-trimer interface and covers the active site in the opposite trimer, which is a character of all published MenB hexamers structures. Moreover, the *ecMenB* and *mtMenB* monomer (1Q51) overlay with each other very well (**Figure 2.7B**) with a RMSD value of 0.965 Å. Compared with

previous crystal structures, OSB-*N*-CoA is the first ligand to give a clear electron density of the benzoate in the active site, which was always missing due to its flexibility. More importantly, an intact ordered loop (Q88 – L106) covering the active site is first revealed, which was always invisible in other published crystal structures (**Figure 2.7C**). The ordered loop forms an additional α coil, followed by a loop leading to a β turn and a short β hairpin. The catalytical residues in the active site are highly conserved (**Figure 2.7D**). L106, V108, and L109 provide favorable hydrophobic interaction with the aromatic ring. G86 and G133 form the oxyanion hole, which form hydrogen bonds with the carbonyl oxygen to stabilize the enolate reaction intermediate. Y'258 from the opposite chain interacts with α -proton, which might be the potential base required for the reaction. D163 forms a hydrogen bond with the ketone group in OSB.

In previous crystal structure, electron density for Q88 – L106 was always missing due to their flexibility. In our OSB-*N*-CoA:ecMenB structure, Y97 is first shown adjacent to the substrate analogue. Moreover, Y97 is a conserved residue by alignment of MenB from different organism. Based on the hypothesis that Y97 plays an essential role in the catalytic process, Y97F mutant was expressed and purified.

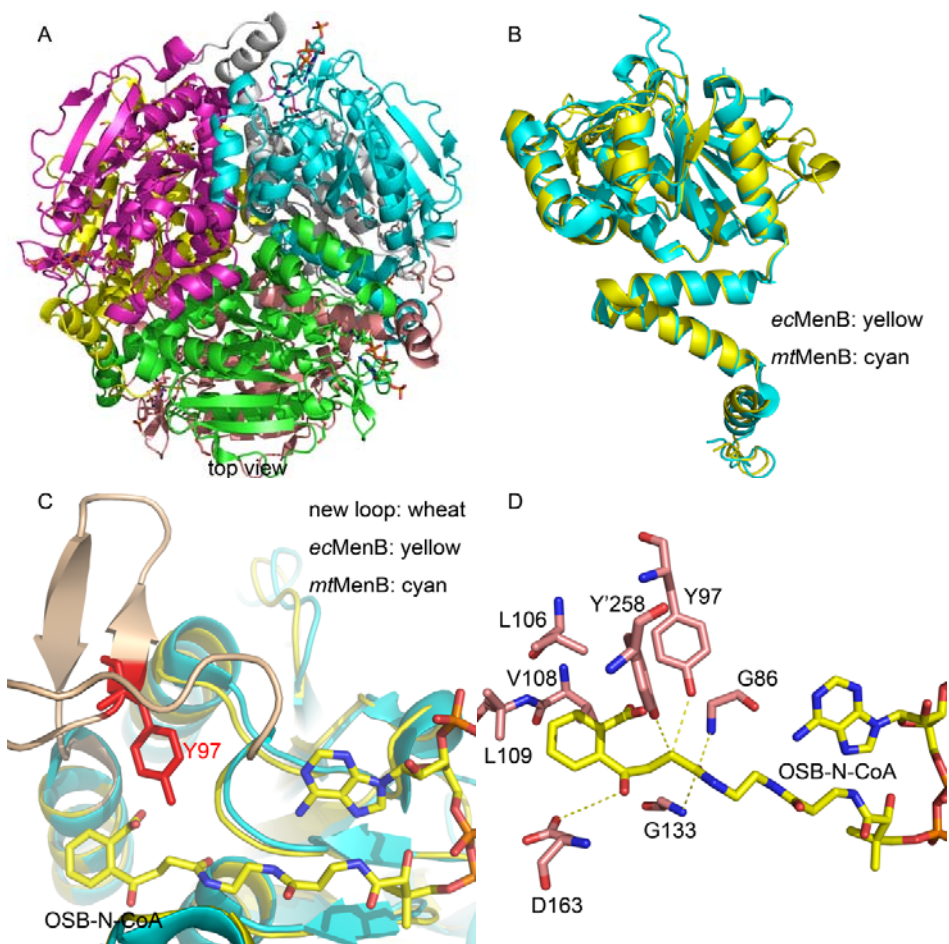


Figure 2.7 OSB-N-CoA:ecMenB crystal structure

A: overall crystal structure of ecMenB; B: overlay ecMenB with *mtMenB* (PDB ID#: 1Q51); C: ordered loop in ecMenB and catalytic residue Y97; D: ecMenB active site

***ecMenB* Y97F mutation**

After Y97F mutant was obtained, enzyme activity assay was performed. The mutant totally lost its catalytic activity, which offers direct evidence that Y97 is a catalytic residue. To avoid the possibility that the single amino acid mutant might cause the disorder of active site or protein misfolding, a preliminary fluorescence titration was performed. Wild-type *ecMenB* and its Y97F mutant were both titrated with acetoacetyl-

CoA. The binding affinity of AcAc-CoA towards wild-type ecMenB ($K_d=61.4\mu\text{M}$) is 2-fold tighter than Y87F mutant ($K_d=118.8\mu\text{M}$). The difference might suggest a disordered active site formation during the mutation. However, crystal structure of Y97F mutant shows that its overall folding is well overlaid with wild-type with a RMSD value of 0.251\AA (**Figure 2.8A**). More importantly, the active site structure is not disturbed (**Figure 2.8B**).

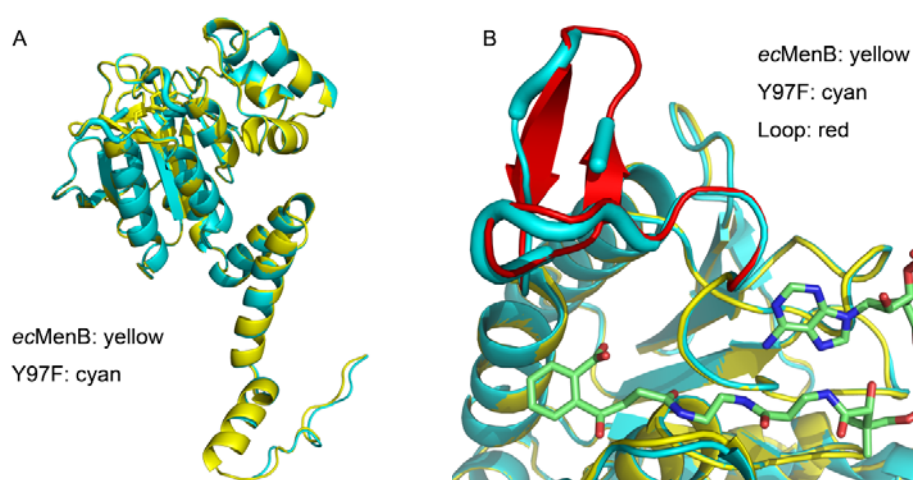


Figure 2.8 ecMenB Y97F mutant structure

A: overall overlay structure of ecMenB and its Y97F mutant; B: overlay structure of active site, and the ordered loop is featured in red.

In summary, ecMenB Y97F mutant proves that tyrosine 97 serves as a catalytic residue. The single amino acid mutant did not disturb the shape of the active site. However, the removal of hydroxyl group on the tyrosine ring blocks the enzyme activity, which indicates that the hydroxyl group is essential in the acid-base catalysis.

New Proposed MenB reaction mechanism

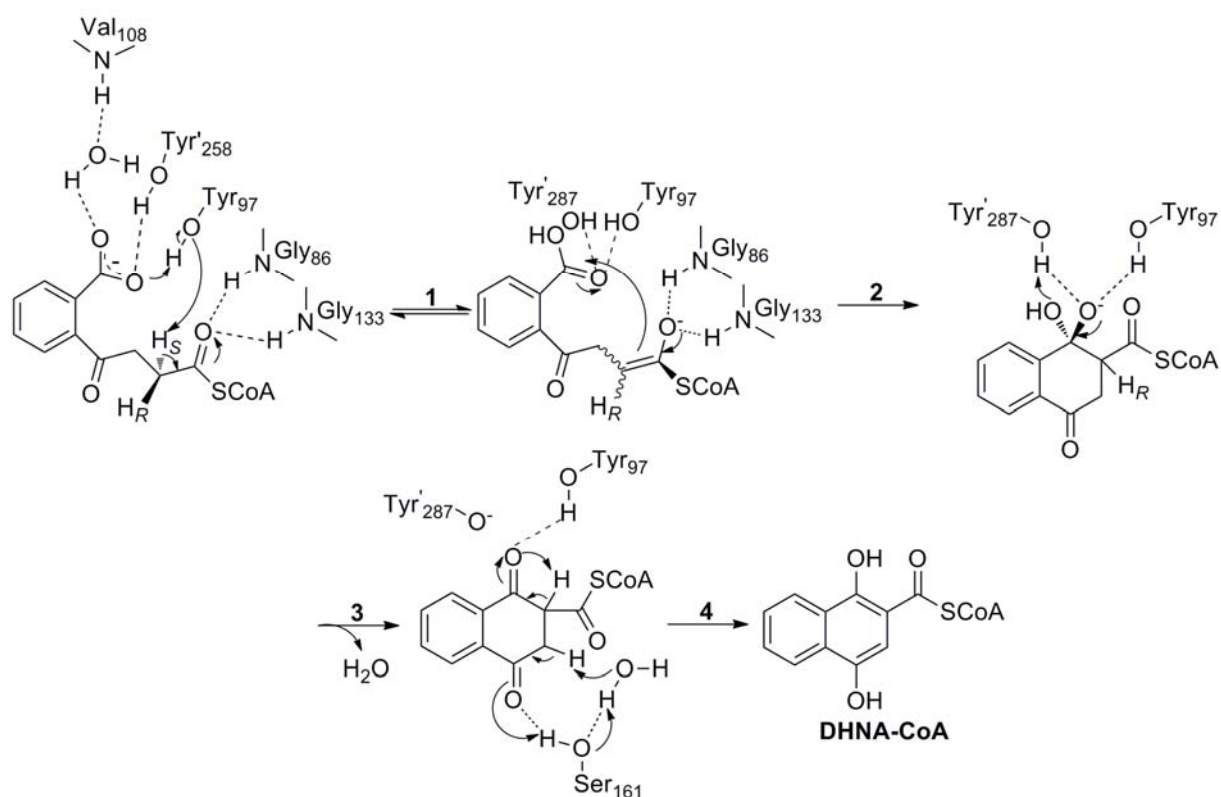


Figure 2.9 New Proposed *ecMenB* reaction mechanism

Based on the well-defined active site structure of *ecMenB*, a new MenB reaction mechanism is proposed (**Figure 2.9**). Tyr97, Tyr258 and Val108 forms hydrogen bonds with the aromatic carboxylate and make the substrate stay at the right position in the active site, and subsequently the pro-2S proton is taken by Tyr97 to form the important reaction intermediate enolate, which is stabilized by the oxyanion hole formed by Gly86 and Gly133. The resulting nucleophile attacks the inactivated aromatic carboxylate in the ring formation step and the product is stabilized by Tyr97 and Tyr258 by hydrogen bonding. Ser161 interacts with the carbonyl adjacent to the aromatic ring to put the

intermediate in the right position, and takes pro-2*R* proton through a water molecule to generate the final DHNA-CoA as the final product.

Inhibition studies of DeCOOH-OSB-CoA

Since compound **16-18** are designed as MenB substrate analogues, they might also serve as inhibitors against the enzyme. Inhibition test was performed base on the coupled assay against *mtMenB* and the result is summarized in **Table 2.1**. From the table, three compounds inhibit *mtMenB* activity in micromolar scale. The CoA moiety contributes most of the binding affinity because their corresponding free acid compound **13-15** have no inhibition against the enzyme at a concentration as high as 200 μ M.

Compounds were also sent to Dr. Richard A. Slayden's group in Colorado State University for cell based inhibition study against *M. tuberculosis*. However, due to their high hydrophilicity, they cannot penetrate the waxy *M. tuberculosis* cell wall, thus they showed no inhibition activity against the growth of the bacteria.

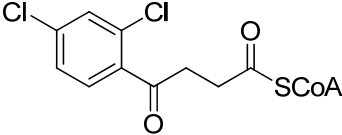
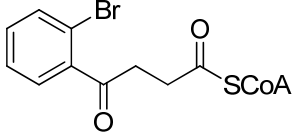
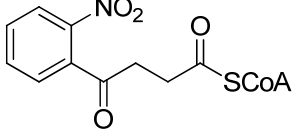
Compound	Structure	IC ₅₀ ^(a) (μM)
16		2.2±0.2
17		1.1±0.1
18		32.1±3.0

Table 2.1 DeCOOH-OSB-CoA analogues inhibition against *mtMenB*

(a) *mtMenB* concentration is fixed at 150nM.

Conclusion

MenB, a crotonase superfamily member, catalyzes the formation of a carbon-carbon bond formation through an intramolecular Claisen condensation. The MenB substrate, OSB-CoA, is not stable, which can form the OSB spirodilactone in pH 7.0 buffer spontaneously in minutes.

In order to reveal the MenB reaction mechanism, substrate analogues were designed and synthesized. The analogues can be divided into two individual groups. OSB-N-CoA, a single-atom substitution of a nitrogen for a sulfur, is expected to have minimal effect on the geometry of the ligand. However, it stabilizes the molecule by preventing the abstraction of α -proton and hydrolysis of thioester. The stabilized compound was used to cocrystallize with *ecMenB*. The cocrystallization structure first

revealed an ordered loop, formed by Q88 – L106, which was always invisible due to its flexibility. More importantly, tyrosine 97 in the ordered loop, which is adjacent to the active site, is proved to serve as a catalytic residue.

The other group of substrate analogues is the DeCOOH-OSB-CoA (3 compounds). It prevents the formation of OSB spirodilactone by blocking the first step of the degradation reaction. Compounds were also sent for cocrystallography study. However, it is difficult to get complete electron density for the binding ligand especially the aromatic part (OSB part) of the molecule due to its flexibility in the active site. Inhibition studies against *mtMenB* were performed. These compounds inhibit the enzyme activity in micromolar scale. Due to their hydrophilic property, these compounds have no inhibition against the *M. tuberculosis* growth *in vitro*.

Experimental section

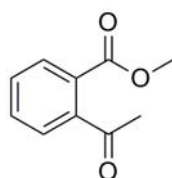
General

All chemicals were purchased from commercial suppliers (Sigma-Aldrich, Acros Organics, Alfa Aesar, Fisher Scientific, and TCI America) with the highest purity and used without further purification. All solvents were purchased from Fisher Scientific. ¹H-NMR spectral data were recorded on Varian Gemini-2300 or Varian Inova-400 NMR spectrometers. Mass spectral data were obtained using an Agilent 1100 LS-MS electrospray ionization single quadrupole mass spectrometer.

HPLC separations were performed on a Shimadzu LC-10AVP with Phenomenex Luna 5 μ C18(2) 250 \times 10.00 mm reverse phase semi-preparative column or a GraceVydac 5 μ C18 100 \times 10.00 mm reverse phase semi-preparative column with a linear gradient of 0-40% solvent B (acetonitrile) in solvent A (20 mM ammonium acetate in water) in 40 minutes, and 40-100% in the next 10 minutes, and a flow rate of 4 mL/min. The aromatic compounds were monitored by UV absorbance at 254 nm and non-aromatic compounds were monitored by UV absorbance at 220 nm.

Synthesis of OSB-N-CoA

Synthesis of Compound 1



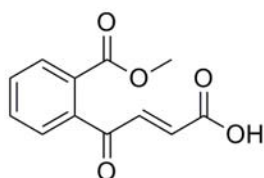
Method 1: 2-Acetyl benzoic acid (1.0 mmol), 4-dimethylaminopyridine (DMAP) (0.1 mmol), and methanol (1.2 mmol) were first dissolved in anhydrous CH₂Cl₂ (20 mL) at room temperature under N₂. The mixture was cooled to 0°C on ice bath and subsequently *N,N'*-dicyclohexylcarbodiimide (DCC) (1.1 mmol) was added into the mixture and continuously stirred for 3 hours. The resulting precipitate was filtered and the filtrate was washed with saturated NaHCO₃ solution (20 mL), brine (20 mL), and deionized water (20 mL), respectively. The organic phase was dried with anhydrous

MgSO₄ and concentrated under reduced pressure. The crude product was purified by silica-gel chromatography (EtOAc/Petroleum ether = 1/3), giving the product as a clear oil.

Method 2: 2-Acetyl benzoic acid (1.0 mmol) and sodium carbonate (1.2 mmol) were first suspended in anhydrous dimethylformamide (DMF) (10 mL) at room temperature under N₂. The mixture was then cooled to 0°C with an ice bath. Methyl iodide (1.2 mmol) was then added into the resulting suspension drop-wise, and the mixture was continuously stirred at room temperature for 3 hours. After quenching the reaction with deionized H₂O (10 mL), the mixture was washed with saturated NaHCO₃ solution (10 mL), brine (10 mL), and deionized water (10 mL). The organic phase was dried with anhydrous MgSO₄, and the crude product was purified with silica-gel chromatography (EtOAc/Petroleum ether = 1/3), giving the product as a clear oil.

Characterization: ¹H-NMR (300 MHz, chloroform-*d*₁) δ 7.84 (1H, d, *J*=1.5 Hz), 7.58-7.50 (2H, m), 7.43 (1H, d, *J*=1.5 Hz), 3.90 (3H, s), 2.55 (3H, s). ESI-MS (Pos): found 179.1 [M+H]⁺; calculated for C₁₀H₁₀O₃: 178.0.

Synthesis of compound 2

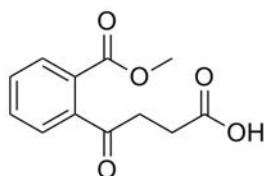


Method: Compound 1 (1.0 mmol) and glyoxylic acid monohydrate (1.3 mmol) were first dissolved in acetic acid (10 mL) at room temperature under N₂. The resulting mixture was heated to 110°C and continuously stirred for 18 hours at reflux. After

cooling to room temperature, the acetic acid was removed under reduced pressure and the crude product was purified by silica-gel chromatography (EtOAc/Hexanes = 25/75), giving the product as a white solid.

Characterization: $^1\text{H-NMR}$ (300 MHz, acetone- d_6) δ 8.00 (1H, d, $J=8.0$ Hz), 7.80-7.65 (2H, m), 7.55 (1H, d, $J=8.0$ Hz), 7.26 (1H, d, $J=15.9$ Hz), 6.30 (1H, d, $J=15.9$ Hz), 3.86 (3H, s). ESI-MS (Neg): found 233.0 [M-H] $^-$; calculated for $\text{C}_{12}\text{H}_{10}\text{O}_5$: 234.1.

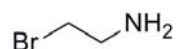
Synthesis of compound 3



Method: Compound **2** (1.0 mmol) and Pd/C (15 mg) were first dissolved in ethyl acetate (10 mL) with a hydrogen balloon at room temperature. The resulting mixture was continuously stirred at room temperature for 1 hour. The Pd/C was subsequently removed by filtration and the solvent was evaporated under reduced pressure. The product was obtained as a white solid and was directly used without further purification.

Characterization: ESI-MS (Neg): found 235.0 [M-H] $^-$; calculated for $\text{C}_{12}\text{H}_{12}\text{O}_5$: 236.1.

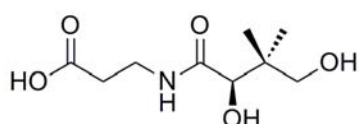
Synthesis of compound 4



Method: 2-Bromoethanamine hydrochloride (1.0 mmol) and sodium azide (2.2 mmol) were first dissolved in the deionized H₂O (10 mL) at room temperature under N₂. The mixture was subsequently heated to 75-80°C and stirred continuously for 18 hours. After cooling to room temperature, sodium hydroxide (2.0 mmol) was added and the product was extracted with CH₂Cl₂ (3×20 mL). The organic phase was collected, combined, and dried with anhydrous MgSO₄. The solvent was removed under reduced pressure, giving the product as a clear oil and was directly used without further purification.

Characterization: ¹H-NMR (300 MHz, chloroform-*d*₁) δ 3.37 (2H, t, *J*=5.4 Hz), 2.88 (2H, q, *J*=5.4 Hz). ESI-MS (Pos): found 87.1 [M+H]⁺; calculated for C₂H₆N₄: 86.1.

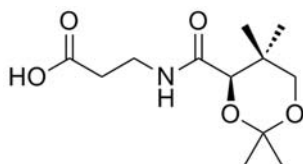
Synthesis of compound 5



Method: Calcium pantothenate (1.0 g) was first dissolved in distilled deionized water (10 mL) and the resulting solution was loaded on a cation-exchange column filled with Dowex[®] 50WX2 hydrogen form resin. The elute with pH between 1.0-5.0 was collected. After lyophilization, the product was obtained as a clear oil and was directly used without further purification.

Characterization: $^1\text{H-NMR}$ (300 MHz, $\text{DMSO-}d_6$): 3.63 (1H, s), 3.40-3.10 (4H, m), 2.39 (2H, t, $J=6.0$ Hz), 0.89 (3H, s), 0.85(3H, s). ESI-MS (Neg): found 218.1 $[\text{M-H}]^-$; calculated for $\text{C}_9\text{H}_{17}\text{NO}_5$: 219.1.

Synthesis of compound 6:

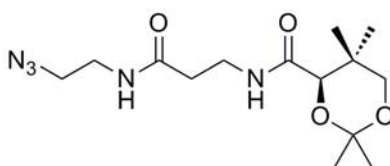


Method 1: compound **5** (1.0 mmol) and TsOH (0.1 mmol) were first dissolved in acetone (10 mL) at room temperature under N_2 . The resulting mixture was continuously stirred at room temperature for 18 hours. The reaction was subsequently quenched with 30 mL deionized water, and the product was extracted by ethyl acetate (3×20 mL). The organic phase was collected, combined, and dried with anhydrous MgSO_4 . After the solvent was removed under reduced pressure, the resulting product was obtained as a clear oil and was directly used without further purification.

Method 2: Calcium pantothenate (1.0 mmol), TsOH (1.0 mmol), and 2,2-dimethoxypropane (50 mmol) were first suspended in anhydrous DMF (20 mL) at room temperature under N_2 . The resulting suspension was continuously stirred for 15 hours. The solvent was subsequently removed under reduced pressure. The residue was washed with CH_2Cl_2 (3×20 mL) and the resulting precipitation was filtered. The filtrate was combined and concentrated under reduced pressure, giving the product as a clear oil and was directly used without further purification.

Characterization: $^1\text{H-NMR}$ (300 MHz, acetone- d_6): 4.06 (1H, s), 3.61 (1H, s), 3.40-3.20 (4H, m), 2.39 (2H, t, $J=6.3$ Hz), 1.40 (3H, s), 1.36 (3H, s), 0.99 (3H, s), 0.94 (3H, s). ESI-MS (Neg): found 258.1 $[\text{M-H}]^-$; calculated for $\text{C}_{12}\text{H}_{21}\text{NO}_5$: 259.1.

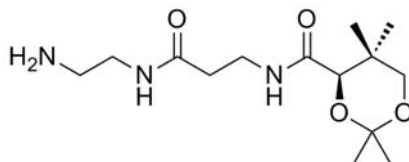
Synthesis of compound **7**



Method: Compound **6** (1.0 mmol), compound **4** (1.1 mmol), and diisopropylethylamine (DIPEA) (2.0 mmol) were first dissolved in anhydrous CH_2Cl_2 (20 mL) at room temperature under N_2 . 1-Ethyl-3-(3-dimethylaminopropyl)carbodiimide hydrochloride (EDC·HCl) (1.05 mmol) was subsequently added into the resulting solution and the mixture was continuously stirred at room temperature for 18 hours. The reaction was then quenched by deionized water (20 mL). The product was extracted with CH_2Cl_2 (3×20 mL), and the organic phase was collected, combined and dried by anhydrous MgSO_4 . After removal of the solvent under reduced pressure, the crude product was purified by silica-gel chromatography (EtOAc/Hexanes = 70/30), giving the product as a white solid.

Characterization: $^1\text{H-NMR}$ (300 MHz, chloroform- d_1) δ 7.01 (1H, br), 6.30 (1H, br), 4.06 (1H, s), 3.64 (1H, d, $J=11.7$ Hz), 3.60-3.50 (3H, m), 3.50-3.40 (3H, m), 3.24 (1H, d, $J=11.7$ Hz), 2.45 (2H, t, $J=6.3$ Hz), 1.44 (3H, s), 1.40 (3H, s), 1.01 (3H, s), 0.94 (3H, s). ESI-MS (Pos): found 328.2 $[\text{M+H}]^+$; calculated for $\text{C}_{14}\text{H}_{25}\text{N}_5\text{O}_4$: 327.2.

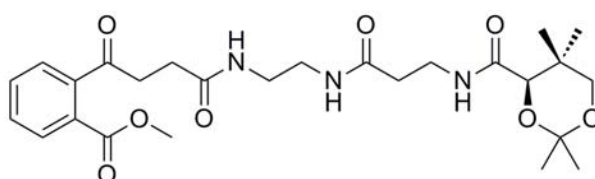
Synthesis of compound **8**



Method: Compound **7** (1.0 mmol) and Pd/C (50 mg) were first suspended in ethyl acetate (10 mL) with a hydrogen balloon at room temperature. The suspension was continuously stirred at room temperature for 1 hour. The Pd/C was removed by filtration and the solvent was removed under reduced pressure. The product was obtained as a clear oil and was used without further purification.

Characterization: ¹H-NMR (300 MHz, chloroform-*d*₁) δ 7.05 (1H, br), 6.28 (1H, br), 4.05 (1H, s), 3.65 (1H, d, *J*=12.0 Hz), 3.62-3.40 (2H, m), 3.38-3.20 (3H, m), 2.80 (2H, t, *J*=6.0 Hz), 2.44 (2H, t, *J*=6.0 Hz), 1.44 (3H, s), 1.40 (3H, s), 1.01 (3H, s), 0.95 (3H, s). ESI-MS (Pos): found 302.2 [M+H]⁺; calculated for C₁₄H₂₇N₃O₄: 301.2.

Synthesis of compound **9**

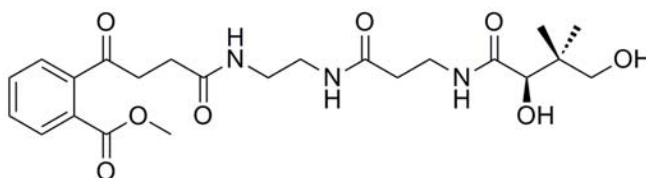


Method: Compound **3** (1.0 mmol), compound **8** (1.1 mmol), and diisopropylethylamine (DIPEA) (2.0 mmol) were first dissolved in anhydrous CH₂Cl₂ (20 mL) at room temperature under N₂. 1-Ethyl-3-(3-dimethylaminopropyl)carbodiimide hydrochloride (EDC·HCl) (1.05 mmol) was subsequently added into the resulting solution and the mixture was continuously stirred at room temperature for 18 hours. The

reaction was then quenched by deionized water (20 mL). The mixture was extracted with CH₂Cl₂ (3×20 mL), and the organic phase was collected, combined and dried by anhydrous MgSO₄. After removal of the solvent under reduced pressure, the crude product was purified by silica-gel chromatography (EtOAc/Hexanes = 70/30), giving the product as a white solid.

Characterization: ¹H-NMR (300 MHz, chloroform-*d*₁) δ 7.90-7.30 (4H, m), 4.00 (1H, s), 3.82 (3H, s), 3.65 (1H, d, *J*=12.0 Hz), 3.60-3.40 (3H, m), 3.40-3.20 (4H, m), 3.11 (2H, d, *J*=6.0 Hz), 2.59 (2H, d, *J*=6.3 Hz), 2.37 (2H, d, *J*=6.3 Hz), 1.40 (3H, s), 1.36 (3H, s), 0.96 (3H, s), 0.90 (3H, s). ESI-MS (Pos): found 520.2 [M+H]⁺; calculated for C₂₆H₃₇N₃O₈: 519.3.

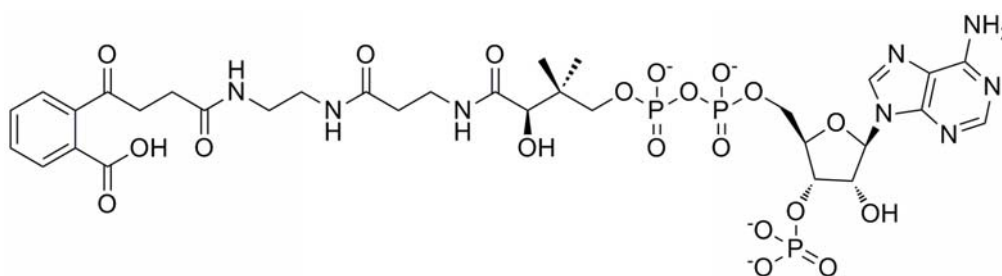
Synthesis of compound **OSB-N-Pantetheine**



Method: Compound **9** (10 mg) were first dissolved in MeOH (10 mL) at room temperature under N₂. NaOH aqueous solution (1M, 10 mL) was then added into the solution drop-wise, and the resulting mixture was continuously stirred for 1 hour until the starting material had been consumed as shown by TLC. The pH was then adjusted to 1.0 with slow addition of 10% HCl while cooling in an ice bath. The mixture was continually stirred at room temperature for another hour, after which the product was purified by HPLC. Lyophilization yields the product as a white powder.

Characterization: $^1\text{H-NMR}$ (300 MHz, water- d_2) δ 7.50-7.30 (4H, m), 3.77 (1H, s), 3.40-3.20 (4H, m), 3.20-3.00 (6H, m), 2.42 (2H, t, $J=6.0$ Hz), 2.28 (2H, t, $J=6.0$ Hz). ESI-MS (Neg): found 464.1 $[\text{M-H}]^-$; calculated for $\text{C}_{22}\text{H}_{31}\text{N}_3\text{O}_8$: 465.2. Retention time: 19.0 minutes.

Synthesis of **OSB-N-CoA**



OSB-*N*-Pantetheine can be converted to OSB-*N*-OSB by pantothenate kinase (PanK), phosphopantetheine adenylyltransferase (PPAT), and 3'-dephosphoCoA kinase (DPCK) by a single step (132). However, the major obstacle of this enzymatic synthesis is low overall yield.

Enzyme expression: The plasmids (from Dr. Yuguo Feng) containing the gene, encoding pantothenate kinase (PanK), phosphopantetheine adenylyltransferase (PPAT), and 3'-dephosphoCoA kinase (DPCK) were transformed into BL21(DE3) cells. Cells were grown in 800 mL LB media in 4 L flask containing specific antibiotics (PanK: ampicillin at 200 mg/L, PPAT and DPCK: kanamycin at 30 mg/L) at 37°C until the OD_{600} value reached between 0.8-1.0. Isopropyl-1-thio- β -D-galactopyranoside (1 mM) (IPTG) was then added to induce protein expression for 12 hours. Cells were subsequently harvested by centrifugation at 5,000 rpm for 15 minutes at 4°C.

PanK purification: Cells were resuspended in 50 mL of His-binding buffer (5 mM imidazole, 20 mM Tris-HCl, 0.5 M NaCl, pH 7.9) and lysed by 3 passages through a French Press. Cell debris was removed by centrifugation at 33,000 rpm for 90 minutes at 4°C. The clarified supernatant was passed through a 1×3 cm His-bind resin column, which was pre-equilibrated by 30 mL His-binding buffer. The column was first washed with 50 mL His-binding buffer and 50 mL His-washing buffer (60 mM imidazole, 20 mM Tris-HCl, 0.5 M NaCl, pH 7.9). The protein was subsequently eluted with 30 mL His-eluting buffer (500 mM imidazole, 20 mM Tris-HCl, 0.5 M NaCl, pH 7.9). The high concentration of imidazole was immediately removed by passing the fractions containing the protein through a 2.5×60 cm G-25 resin column, using 20 mM Tris-HCl, 0.1 M NaCl, pH 8.0 as the elution buffer. The fractions containing PanK were collected, combined, and concentrated and the concentration of PanK was determined by measuring the absorption at 280 nm using an extinction coefficient of 43,810 M⁻¹cm⁻¹. The enzyme was stored at -80°C.

PPAT purification: Cells were resuspended in 50 mL of His-binding buffer (5 mM imidazole, 20 mM Tris-HCl, 0.5 M NaCl, pH 7.9) and lysed by 3 passages through a French Press. Cell debris was removed by centrifugation at 33,000 rpm for 90 minutes at 4°C. The clarified supernatant was passed through a 1×3 cm His-bind resin column, which was pre-equilibrated by 30 mL His-binding buffer. The column was first washed with 50 mL His-binding buffer and 50 mL His-washing buffer (60 mM imidazole, 20 mM Tris-HCl, 0.5 M NaCl, pH 7.9). The protein was subsequently eluted with 30 mL His-eluting buffer (500 mM imidazole, 20 mM Tris-HCl, 0.5 M NaCl, pH 7.9). The high concentration of imidazole was immediately removed by passing the fractions

containing the protein through a 2.5×60 cm G-25 resin column, using 20 mM Tris·HCl, 0.1 M NaCl, pH 8.0 as the elution buffer. The fractions containing PPAT were collected, combined, and concentrated and the concentration of PPAT was determined by measuring the absorption at 280 nm using an extinction coefficient of $2,680 \text{ M}^{-1}\text{cm}^{-1}$. The enzyme was stored at -80°C .

DPCCK purification: Cells were resuspended in 20 mM Tris·HCl, pH 8.0 buffer and lysed by 3 passages through a French Press. Cell debris was removed by centrifugation at 33,000 rpm for 90 minutes at 4°C . The clarified supernatant was dialyzed against 4 L buffer containing 20 mM Tris·HCl, pH 8.0 overnight. The dialyzed solution was loaded onto a 2.5×15 cm DEAE sepharose column. The proteins were eluted from the column using 500 mL linear NaCl gradient 0-0.4 M in 20 mM Tris·HCl buffer. Fractions containing DPCCK were collected and dialyzed against 4 L 20 mM Tris·HCl buffer again. The dialyzed protein solution was loaded on to a 2.5×15 cm Q-sepharose column. The protein was eluted from the column using 500 mL linear NaCl gradient 0-0.2 M in 20 mM Tris·HCl buffer. The fractions containing DPCCK were collected, combined, and concentrated and the concentration of DPCCK was determined by measuring the absorption at 280 nm using an extinction coefficient of $16,500 \text{ M}^{-1}\text{cm}^{-1}$. The enzyme was stored at -80°C .

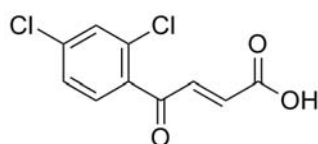
OSB-N-Pantetheine (1.0 μmol), ATP (3.5 μmol), PanK (0.1 μmol), PPAT (0.1 μmol), DPCCK (0.1 μmol), and 10mL Tris buffer (containing 20 mM Tris, 50 mM MgCl_2 , and 100 mM NaCl at pH 7.5) were mixed and incubated under room temperature for 4 hours. The product was then purified by HPLC and the product was obtained as a white powder after the lyophilization.

Characterization: ESI-MS (Neg): found 953.2 [M-H]⁻; calculated for C₃₂H₄₅N₈O₂₀P₃: 954.2. Retention time: 16.0 minutes.

General method for the synthesis of compounds 10-12

Commercially available substituted acetophenone (1.0 mmol) and glyoxylic acid monohydrate (1.3 mmol) were first dissolved in glacial acetic acid (10 mL) at room temperature under N₂. The resulting mixture was then heated to 130°C on an oil bath and continuously stirred for 18 hours. After cooling to room temperature, the acetic acid was subsequently removed under reduced pressure and the crude product was purified by silica-gel chromatography (EtOAc/Hexanes = 25/75).

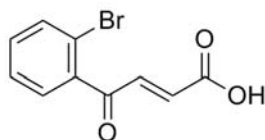
Synthesis of compound 10



Method: Compound **10** was prepared according to the general procedure from 2',4'-dichloroacetophenone and the product was obtained as a yellow solid.

Characterization: ¹H-NMR (300 MHz, Acetone-*d*₆) δ 8.12-8.00 (1H, m), 7.77 (1H, d, *J*=15.6 Hz), 7.38-7.24 (2H, m), 6.821 (1H, d, *J*=15.6 Hz). ESI-MS (Neg): found 243.0 [M-H]⁻; calculated for C₁₀H₆Cl₂O₃: 244.0.

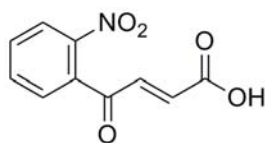
Synthesis of compound 11



Method: Compound **11** was prepared according to the general procedure from 2'-bromoacetophenone and the product was obtained as a light yellow solid.

Characterization: $^1\text{H-NMR}$ (300 MHz, acetone- d_6) δ 7.78-7.73 (1H, m), 7.63-7.48 (3H, m), 7.39 (1H, d, $J=15.6$ Hz), 6.53 (1H, d, $J=15.6$ Hz). ESI-MS (Neg): 252.9 [M-H] $^-$; calculated for $\text{C}_{10}\text{H}_7\text{BrO}_3$: 254.0.

Synthesis of compound 12



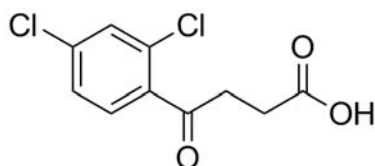
Method: Compound **12** was prepared according to the general procedure from 2'-nitroacetophenone and the product was obtained as a light yellow solid.

Characterization: $^1\text{H-NMR}$ (300 MHz, Acetone- d_6) δ 8.25 (1H, d, $J=9.0$ Hz), 8.00-7.92 (2H, m), 7.70 (1H, d, $J=9.0$ Hz), 7.30 (1H, d, $J=16.2$ Hz), 6.47 ((1H, d, $J=16.2$ Hz). ESI-MS (Neg): found 220.0 [M-H] $^-$; calculated for $\text{C}_{10}\text{H}_7\text{NO}_5$: 221.0.

General method for the synthesis of compounds 13-15

Compound **10-12** (1.0 mmol) and Pd/C (15 mg) were first suspended in ethyl acetate (10 mL) with a hydrogen balloon at room temperature. The resulting suspension was continuously stirred at room temperature for 1 hour. The Pd/C was subsequently removed by filtration and the solvent was removed under reduced pressure, giving the product which can be directly used without further purification.

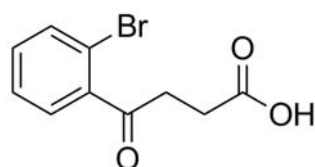
Synthesis of compound 13



Method: Compound **13** was prepared according to the general procedure from compound **10** and the product was obtained as a white solid.

Characterization: (¹H-NMR (300 MHz, chloroform-*d*) δ 7.52 (1H, d, *J*=8.1 Hz), 7.43 (1H, d, *J*=1.8 Hz), 7.31 (1H, d, *J*=1.8 Hz), 3.23 (2H, t, *J*=6.3 Hz), 2.79 (2H, t, *J*=6.3 Hz). ESI-MS (Neg): 245.0 [M-H]⁻; calculated for C₁₀H₈Cl₂O₃: 246.0.

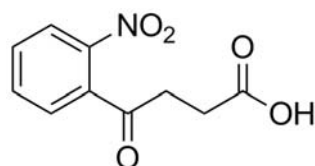
Synthesis of compound 14



Method: Compound **14** was prepared according to the general procedure from compound **11** and the product was obtained as a white solid.

Characterization: ($^1\text{H-NMR}$ (300 MHz, chloroform- d_1) δ 7.63 (1H, d, $J=1.8$ Hz), 7.59 (1H, d, $J=7.5$ Hz), 7.46 (1H, t, $J=1.8$ Hz), 7.33 (1H, m), 3.25 (2H, t, $J=6.6$ Hz), 2.83 (2H, t, $J=6.6$ Hz). ESI-MS (Neg): 254.9 $[\text{M-H}]^-$; calculated for $\text{C}_{10}\text{H}_9\text{BrO}_3$: 256.0.

Synthesis of compound 15



Method: Compound **15** was prepared according to the general procedure from compound **12** and the product was obtained as a white solid.

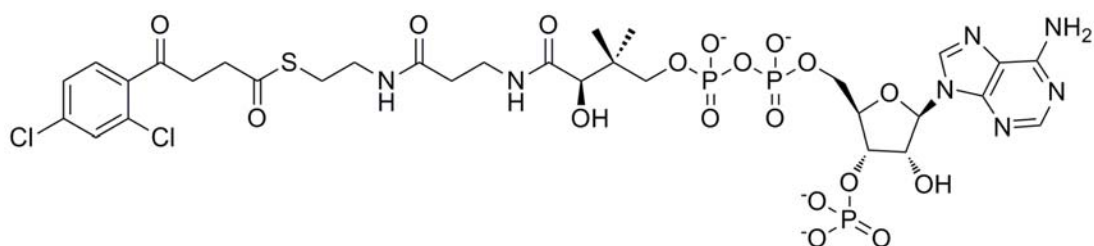
Characterization: $^1\text{H-NMR}$ (300 MHz, Acetone- d_6) δ 8.12 (1H, dd, $J=0.9$ Hz, 7.2 Hz), 7.73 (1H, t, $J=6.3$ Hz), 7.61 (2H, t, $J=6.3$ Hz), 7.46 (1H, dd, $J=0.9$ Hz, 6.3 Hz), 3.12 (2H, t, $J=6.3$ Hz), 2.88 (2H, t, $J=6.3$ Hz). ESI-MS (Neg): found 222.0 $[\text{M-H}]^-$; calculated for $\text{C}_{10}\text{H}_9\text{NO}_5$: 223.0.

General method for the synthesis of compound 16-18

Compound **13-15** (1.0 mmol) and TEA (1.1 mmol) were first dissolved in anhydrous THF (10 mL) at room temperature under N_2 . The resulting solution was subsequently cooled to 0°C on an ice bath before ECF (1.1 mmol) was added into the solution drop-wise. The mixture was continuously stirred at room temperature for 1 hour and the resulting precipitate was removed by filtration and the filtrate was then added

into 10mg CoASH aqueous solution (10 mL). The mixture was further stirred at room temperature for another 45 minutes. The crude product was separated by HPLC.

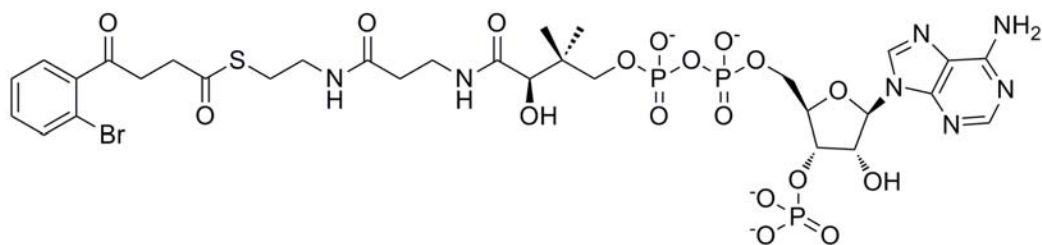
Synthesis of compound 16



Method: Compound **16** was prepared according to the general procedure from compound **13**. Lyophilization of the solvent gives the product as a white powder.

Characterization: $^1\text{H-NMR}$ (300 MHz, in D_2O) δ 8.33 (1H, s), 8.00 (1H, s), 7.50-7.15 (3H, m), 5.94 (1H, d, $J=6.3$ Hz), 4.42 (1H, s), 4.06 (2H, s), 3.86 (1H, s), 3.72-64 (1H, m), 3.51-3.45 (1H, m), 3.41-3.35 (2H, m), 3.26 (2H, t, $J=6.0$ Hz), 3.18-3.10 (2H, m), 3.06 (2H, t, $J=6.6$ Hz), 2.92-2.80 (2H, m), 2.40 (4H, m), 2.24 (2H, t, $J=6.6$ Hz), 0.72 (3H, s), 0.57 (3H, s). ESI-MS (Neg): 994.1 $[\text{M-H}]^-$; calculated for $\text{C}_{31}\text{H}_{42}\text{Cl}_2\text{N}_7\text{O}_{18}\text{P}_3\text{S}$: 995.1. Retention time: 27.6 minutes.

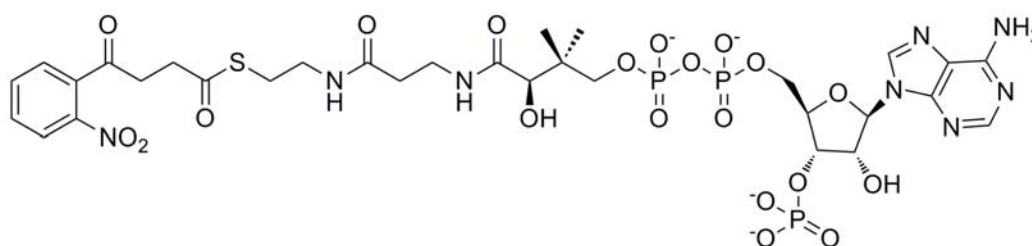
Synthesis of compound 17



Method: Compound **17** was prepared according to the general procedure from compound **14**. Lyophilization of the solvent gives the product as a white powder.

Characterization: $^1\text{H-NMR}$ (300 MHz, in D_2O) δ 8.38 (1H, s), 8.03 (1H, s), 7.60-7.25 (4H, m), 5.94 (1H, d, $J=6.3$ Hz), 4.45 (1H, s), 4.08 (2H, bs), 3.85 (1H, s), 3.74-66 (1H, m), 3.56-3.48 (1H, m), 3.44-3.37 (2H, m), 3.28 (2H, t, $J=6.0$ Hz), 3.18-3.10 (2H, m), 3.06 (2H, t, $J=6.6$ Hz), 2.92-2.80 (2H, m), 2.40 (2H, t, $J=6.6$ Hz), 2.24 (2H, t, $J=6.6$ Hz), 0.69 (3H, s), 0.57 (3H, s). ESI-MS (Neg): 1004.0 $[\text{M-H}]^-$; calculated for $\text{C}_{31}\text{H}_{43}\text{BrN}_7\text{O}_{18}\text{P}_3\text{S}$: 1005.1. Retention time: 28.0 minutes.

Synthesis of compound **18**



Method: Compound **18** was prepared according to the general procedure from compound **15**. Lyophilization of the solvent gives the product as a white powder.

Characterization: $^1\text{H-NMR}$ (300 MHz, in D_2O) δ 8.31 (1H, s), 7.98 (1H, s), 7.88 (1H, d, $J=8.4$ Hz), 7.58 (1H, t, $J=8.4$ Hz), 7.45 (1H, t, $J=8.4$ Hz), 7.31 (1H, d, $J=7.2$ Hz), 5.91 (1H, d, $J=6.6$ Hz), 4.38 (1H, bs), 4.04-4.01 (2H, m), 3.81 (1H, s), 3.66-3.58 (1H, m), 3.46-3.40 (1H, m), 3.38-3.28 (2H, m), 3.26-3.18 (2H, m), 3.14 (2H, d, $J=6.0$ Hz), 3.06 (2H, d, $J=6.0$ Hz), 2.84 (4H, m), 2.20 (2H, d, 5.7 Hz), 0.63 (3H, s), 0.55 (3H, s). ESI-MS (Neg): 971.0 $[\text{M-H}]^-$; calculated for $\text{C}_{31}\text{H}_{43}\text{N}_8\text{O}_{20}\text{P}_3\text{S}$: 972.1. Retention time: 27.9 minutes.

Expression and purification of mtMenB

The plasmids (from Dr. Huaning Zhang) containing the *menb* gene were transformed into BL21(DE3) cells. Cells were grown in 800 mL LB media in 4 L flask containing 200 mg/L ampicillin at 37°C until OD₆₀₀ value reached between 0.8-1.0. IPTG (1 mM) was then added to induct protein expression for 12 hours. Cells were subsequently harvested by centrifugation at 5,000 rpm for 15 minutes at 4°C.

mtMenB was purified by His-Tag column. Cells were first resuspended in 30 mL of His-binding buffer, which contained 20 mM Tris·HCl, 5 mM imidazole, and 500 mM NaCl at pH 7.90. Cells were lysed by 4-5 passage through French Press. Cell debris was removed by centrifuging at 8,600 rpm for 2 h at 4°C. The resulting supernatant was filtrated and passed through a 1×3 cm His-bind resin column, which was pre-equilibrated with 30 mL His-binding buffer. The column was first washed with 30 mL His-binding buffer, and then with 50 mL His-washing buffer, which contained 20 mM Tris·HCl, 60 mM imidazole, and 500mM NaCl at pH 7.90. Proteins were eluted by washing the column with His-eluting buffer, containing 20 mM Tris·HCl, 500 mM imidazole, 500 mM NaCl at pH 7.90. Fractions containing *mtMenB* were collected and the high concentration of imidazole was immediately removed by passing through a 2.5cm×60cm G-25 resin column, using 20 mM Na₂HPO₄ and 100 mM NaCl at pH 7.0 as elution buffer. The fractions containing *mtMenB* were collected, combined, and concentrated and the concentration of *mtMenB* was determined by measuring the absorbance at 280 nm using coeffiency of 41,370 M⁻¹cm⁻¹. The enzyme was stored at -80°C.

Expression and purification of ecMenB

The plasmids (from Dr. Huaning Zhang) containing the *menb* gene were transformed into BL21(DE3) cells. Cells were grown in 800 mL LB media in 4 L flask containing 200 mg/L ampicillin at 37°C until the OD₆₀₀ value reached between 0.8-1.0. IPTG (1 mM) was then added to induct protein expression for 12 hours. Cells were subsequently harvested by centrifugation at 5,000 rpm for 15 minutes at 4°C.

ecMenB was purified by His-Tag column. Cells were first resuspended in 30 mL of His-binding buffer, which contained 20 mM NaH₂PO₄, 10 mM imidazole, and 300 mM NaCl at pH 7.90. Cells were lysed by 4-5 passage through French Press. Cell debris was removed by centrifuging at 8,600 rpm for 2 h at 4°C. The resulting supernatant was filtrated and passed through a 1×3 cm His-bind resin column, which was pre-equilibrated with 30 mL His-binding buffer. The column was first washed with 30 mL His-binding buffer, and then with 50 mL His-washing buffer, which contained 20 mM NaH₂PO₄, 20 mM imidazole, and 300 mM NaCl at pH 7.90. Proteins were eluted by washing the column with His-eluting buffer, containing 20 mM NaH₂PO₄, 250 mM imidazole, 300 mM NaCl at pH 7.90. Fractions containing *ecMenB* were collected and the high concentration of imidazole was immediately removed by passing through a 2.5cm×60cm G-25 resin column, using 20 mM Na₂HPO₄ and 100 mM NaCl at pH 7.0 as elution buffer. The fractions containing *ecMenB* were collected, combined, and concentrated and the concentration of *ecMenB* was determined by measuring the absorbance at 280 nm using coefficient of 36,040 M⁻¹cm⁻¹. The enzyme was stored at -80°C.

Expression and purification of ecMenE

The plasmids (from Dr. Huaning Zhang) containing the *mene* gene were transformed into BL21(DE3) cells. Cells were grown in 800 mL LB media in 4 L flask containing 200 mg/L ampicillin at 37°C until the OD₆₀₀ value reached between 0.8-1.0. IPTG (1 mM) was then added to induct the protein expression for 12 hours. Cells were subsequently harvested by centrifugation at 5,000 rpm for 15 minutes at 4°C. The enzyme was stored at -80°C.

ecMenE was purified by His-Tag column. Cells were first resuspended in 30 mL of His-binding buffer, which contained 20 mM Tris·HCl, 5 mM imidazole, and 500 mM NaCl at pH 7.90. Cells were lysed by 4-5 passage through French Press. Cell debris was removed by centrifuging at 8,600 rpm for 2 h at 4 °C. The resulting supernatant was filtrated and passed through a 1×3 cm His-bind resin column, which was pre-equilibrated with 30 mL His-binding buffer. The column was washed with 30 mL His-binding buffer, and then with 50 mL His-washing buffer, which contained 20 mM Tris·HCl, 60 mM imidazole, and 500 mM NaCl at pH 7.90. Proteins were eluted by washing the column with His-eluting buffer, containing 20 mM Tris·HCl, 500 mM imidazole, 500 mM NaCl at pH 7.90. Fractions containing ecMenE were collected and the high concentration of imidazole was immediately removed by passing through a 2.5cm×60cm G-25 resin column, using 20 mM Na₂HPO₄ and 100 mM NaCl at pH 7.0 as elution buffer. The fractions containing ecMenE were collected, combined, and concentrated and the concentration of ecMenE was determined by measuring the absorbance at 280 nm using coeffiency of 104,770 M⁻¹cm⁻¹. The enzyme was stored at -80°C.

Expression and purification of ecMenB Y97F mutant

ecMenB Y97F mutant plasmid was prepared by site-directed mutagenesis (133) with the following primers:

Forward: 5'-GTGATTACGGCGGAAAGATGATTCCG-3'

Reverse: 5'-CGGAATCATCTTTCCGCCGTAATCAC-3'

The plasmids containing mutant gene were transformed into BL21(DE3) cells. Cells were grown in 800 mL LB media containing 200 mg/L ampicillin at 37°C until the OD₆₀₀ value reached between 0.8-1.0. IPTG (1 mM) was then added into the medium to induct the protein expression for 12 hours at 25°C. Cells were harvested by centrifugation at 5,000 rpm for 15 minutes at 4°C.

Cells were resuspended in 50 mL of His-binding buffer (10 mM imidazole, 20 mM NaH₂PO₄, 0.3 M NaCl, pH 8.0) and lysed by 3 passages through a French Press. Cell debris was removed by centrifugation at 33,000 rpm for 90 minutes at 4°C. The clarified supernatant was passed through a 1×3cm His-bind resin column which was pre-equilibrated with 30 mL His-binding buffer. The column was first washed with 50mL His-binding buffer and then 50mL His-washing buffer (20 mM imidazole, 20 mM NaH₂PO₄, 0.3 M NaCl, pH 8.0). The protein was subsequently eluted using 30 mL His-eluting buffer (250 mM imidazole, 20 mM NaH₂PO₄, 0.3 M NaCl, pH 8.0). The high concentration of imidazole was immediately removed by passing through a 2.5×60 cm G-25 resin column, using 20 mM NaH₂PO₄, 0.1 M NaCl, pH 7.0 as the elution buffer. The fractions containing Y97F ecMenB were collected, combined, and concentrated.

The concentration of protein was determined by measuring the absorption at 280 nm using an extinction coefficient of 34,760 M⁻¹cm⁻¹. The enzyme was stored at -80°C.

IC₅₀ measurement of mtMenB

OSB (30 μM), ATP (30 μM), CoA (30 μM), and *mtMenB* (150 nM) were first mixed in 20 mM NaH₂PO₄, 150 mM NaCl, 1 mM MgCl₂, and pH 7.0 buffer solution. Inhibitors were first dissolved in deionized water, which were then added into the reaction buffer at various concentrations (0-200 μM). After the reaction was initiated by adding *ecMenE* (3 μM), the formation of DHNA-CoA was monitored by UV at 392 nm. The initial velocities were converted from the slope measured using an extinction coefficient of 4,000 M⁻¹cm⁻¹. IC₅₀ values were calculated by fitting the data into **Equation 2.1**, where v_i is the initial velocity in the presence of certain concentration of inhibitor, v_0 is the initial velocity in the absence of inhibitor, and $[I]$ is the inhibitor concentration.

$$\frac{v_i}{v_0} = \frac{100\%}{1 + [I]/IC_{50}}$$

Equation 2.1

Chapter 3 : Identification of *mtMenB* inhibitors by high-throughput screen and structure-activity relationship studies on 4-aryl-2-CoA-4-oxo-butanoic Acid

High-throughput screens (HTS) are widely used in drug discovery projects. Through this process, researchers can rapidly identify active compounds, antibodies, or genes that can modulate a particular pathway. In this chapter, HTS was applied to identify novel chemical scaffolds that can inhibit the *mtMenB* enzyme. A series of 2-amino-4-aryl-4-oxo-butanoic acids were first identified as promising hits. However, these compounds were found unstable in screening aqueous buffers and decomposed through *retro*-Michael addition. The product formed by the reaction, (*E*)-4-aryl-4-oxo-but-2-enoic acid, subsequently reacted with coenzyme A in the aqueous solution and generated the 4-aryl-2-CoA-4-oxo-butanoic acid adduct *in situ*, which behaved as the authentic inhibitor. SAR studies were subsequently performed on this scaffold, which lead to more potent inhibitors. Target validation experiments also demonstrated that these compounds can interfere with the menaquinone biosynthesis in *S. aureus*.

Introduction

Tuberculosis is a global health threat and efforts to combat the spread of this disease are hindered by the emergence of drug resistance, coupled with the ability of *M. tuberculosis* to survive in a latent, non-replicating state for many years (1, 5, 134). Since latent mycobacteria are thought to consume ATP in order to remain viable (135), compounds that interfere with bacterial respiration hold the promise of targeting both replicating as well as non-replicating bacterial populations. For example, a diarylquinoline, R207910, potently inhibits the *M. tuberculosis* ATP synthase activity, which has been successfully applied in a phase II efficacy study (91).

The lipid-soluble electron carrier menaquinone occupies a central and essential role in the electron transport chain coupled ATP synthesis (136). There is a debate about whether menaquinone biosynthesis pathway is a potential drug target. It is reported that most of the Gram-positive bacteria, including *M. tuberculosis*, utilize only menaquinone in their electron transport system (67). Moreover, humans use ubiquinone (coenzyme Q) instead in the electron transport chain (67). Although menaquinone plays an important role in blood clotting, humans lack the biosynthetic pathway which must be obtained in diet (137) or from intestinal bacteria (138). Consequently, enzymes in the bacterial menaquinone biosynthetic pathway are promising targets for antibacterial drug development. However, the major concern about targeting the menaquinone biosynthesis pathway is that menaquinone is found widely distributed in different organs in the host (139). Although menaquinone biosynthesis is impaired in the bacteria, bacteria can uptake menaquinone from the environment in its host. Therefore, drugs targeting menaquinone biosynthesis might do not have satisfactory *in vivo* efficacy. In

my personal opinion, although auxotrophy can be recovered by supplementation the key metabolites *in vitro*, it still remains questionable that whether the auxotrophy can be recovered *in vivo*. For example, small colony variants of *S. aureus* can be generated by mutations in *menD* or *hemB*, yielding menadione and hemin auxotrophs and resulting slow growth and resistant to several antibiotics (140-142). It is also reported that SCV phenotype could restore normal growth by appropriate medium supplements, such as hemin and menadione, or by complementation with the wild-type allele of the mutant gene *in vitro* (143-144). However, current work performed in our lab by a Ph.D. student Yang Lu demonstrates that after the *menD*-deficient SCV of *S. aureus* strain was injected into the mouse via the thigh-infection model, there is no active infection found in the host and no bacterial counting was found in different organs. This experiment supported that the menadione-deficiency cannot be recovered by menaquinone components *in vivo* in mouse. After weighing the previous work, we believe that menaquinone biosynthesis pathway is still an attracting target for drug discovery.

Recently, inhibitors targeting against MenE (98-99), MenA (96-97), and MenD (100) are identified and developed. MenB might also be a potential drug target. First, MenB-deficient mutants of *B. subtilis* can only regain normal growth by 1,4-dihydroxy-2-naphthoic acid supplementation (105-106). Second, it is recently reported that if the bacteria incubated under oxygen limiting conditions of unagitated liquid culture, a systematic increase in the expression of the *menb* gene product was observed over the incubation period with an 85.8-fold increase at week 15 relative to day 0 (145). Third, it is also discovered that *menb* gene was mutated in the menadione-auxotrophic SCV in *S. aureus* isolates, resulting slow growth and menadione auxotrophy (146). However, it

is also reported that *menb*, unlike *menc*, *mend*, *mene*, and *ubie*, was identified as a non-essential gene for optimal growth of *M. tuberculosis* by transposon site hybridization (TraSH) method (147). TraSH still has its limitations. It is noticed the genes identified by this method are for *in vitro* optimal growth. However, the *in vivo* system is completely different from *in vitro* medium. In order to prove that MenB is a potential drug target, chemical knockout can be performed.

Based on the hypothesis that MenB is a potential drug target, HTS was performed at Harvard Medical School in Boston, MA. In the following chapter, we will discuss the inhibition studies of *mtMenB*, including hit identification, SAR studies, and lead optimization.

Result and discussion

Pilot screen

A pilot screen was performed to identify the most appropriate conditions for the HTS. The MenE/MenB coupled assay (**Scheme 2.4**) was performed using a substrate concentration ranging from 200-300 μM with incubation times from 20-60 minutes to optimize the Z'-factor. The plate design is shown as **Figure 3A**. The Z'-factor is a statistical parameter, which is used for quantitative evaluation of assay conditions (148). An assay can be considered validated for high-throughput screen as long as it shows reproducible and suitable Z'-factor values.

To quantitatively rank assay conditions, Z'-factor is calculated based on **Equation 3.1**. If the Z'-factor is greater than 0.7, the assay is considered as an excellent assay for HTS. This requires the standard deviation in each control as low as possible and the average difference in each control as significant as possible.

$$Z' = 1 - \frac{3(SD_+ + SD_-)}{|Ave_+ - Ave_-|}$$

Equation 3.1

SD₊: positive control standard deviation SD₋: negative control standard deviation

Ave₊: positive control average Ave₋: negative control average

After careful evaluation, the concentrations of OSB, ATP, and CoA were fixed at 250 μM, and *mtMenB* concentration was fixed at 150 nM, and *ecMenE* concentration was fixed at 3.0 μM. We also noticed that the Z'-value increased as the incubation time increased, and it reached a maximum value of 0.63 at a 60 minutes time point, and it decreased due to the DHNA-CoA decomposition.

After we figured out the optimized HTS condition, 2,630 compounds (**Table 3.1**) were first used to the HTS. The plate design was shown in **Figure 3.1B**. The assay was performed in duplicate to reduce the inherent variability and error.

Category	Library Name	Number of compounds
Known bioactive collections	Biomol ICCB Known Bioactives	480
	Ninds Custom Collection 2	1,040
	Prestwick 1 Collection	1,120

Table 3.1 Compounds information for pilot screen

%inhibition is defined by the **Equation 3.2**:

$$\%inhibition = \frac{Ave_- - Abs}{|Ave_- - Ave_+|} \times 100\%$$

Equation 3.2

Ave_+ and Ave_- are the average absorbance values for the positive and negative control respectively, and Abs is the absorbance in each different compound well at 405 nm. When the absorbance approaches the negative control, the %inhibition is low, indicating the compound is not a good inhibitor against the enzyme. On the contrast, when the absorbance approaches the positive control, the %inhibition is near 100%, indicating the compound is a good inhibitor.

According to the %inhibition, compounds were divided into 4 major groups: strong inhibition ($I > 70\%$), medium inhibition ($50\% < I < 70\%$), weak inhibition ($30\% < I < 50\%$), and no inhibition ($I < 30\%$).

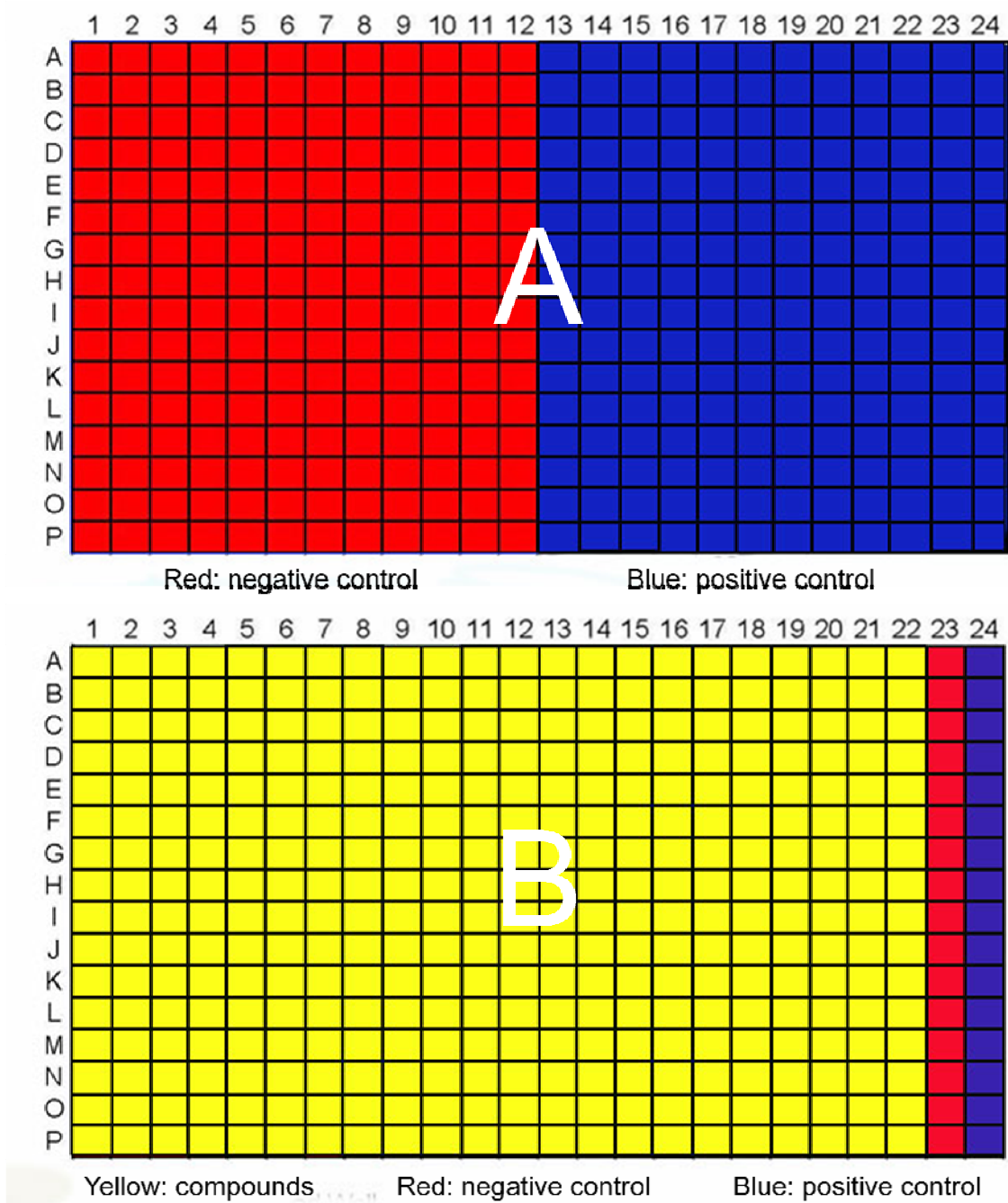


Figure 3.1 Plate design in the high-throughput screen

A: plate design for Z'-factor determination; B: plate design for compound screening

The most potent compound from the pilot screen was hexachlorophene (**Figure 3.2**), which is used as a topical anti-infective, anti-bacterial agent, often used in soaps

and toothpastes (149-150). In the enzymatic assay, hexachlorophene is a competitive inhibitor of *mtMenB* with an IC_{50} value of $9.3 \pm 0.9 \mu\text{M}$, K_i value of $7.4 \pm 0.8 \mu\text{M}$, and K_d value of $17.2 \pm 0.5 \mu\text{M}$. The studies in *Bacillus megaterium* showed that the primary lethal action of hexachlorophene is related to respiratory inhibition at a site within the membrane-bound part of the electron transport chain (151). It is also pointed out that menadione, a structural analogue of menaquinone that lacks the 35-carbon side chain, partially restore the oxygen uptake. Combined with our research, hexachlorophene may target menB in the living bacteria.

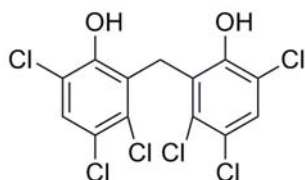


Figure 3.2 Chemical structure of hexachlorophene

High-throughput Screen

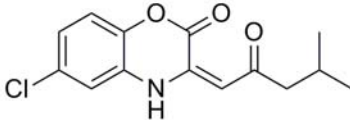
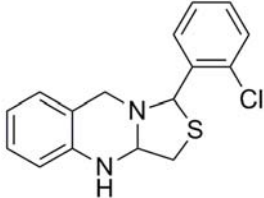
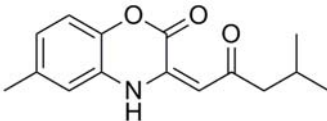
After validating the assay conditions for the high-throughput screen by the pilot screen, HTS was performed on 102,451 different small drug-like molecules that represented a large variety of chemical structures. The detailed information of the libraries was summarized in **Table 3.2**.

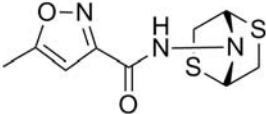
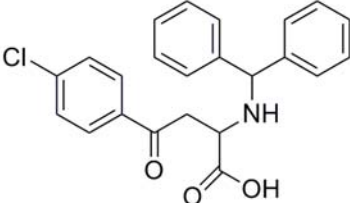
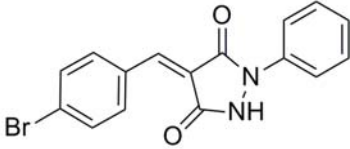
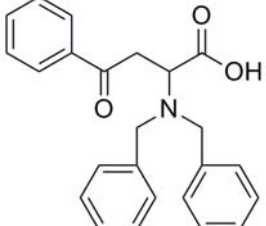
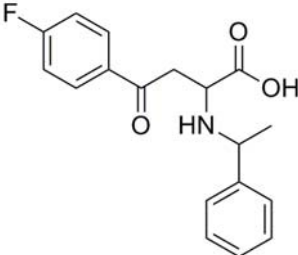
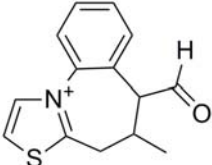
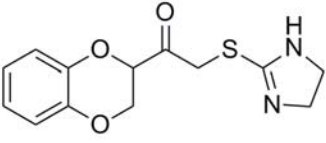
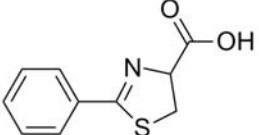
In the screen, 455 compounds were identified as inhibitors with at least weak inhibition against the enzymatic activity at the concentration of $10 \mu\text{g/mL}$. The chemical

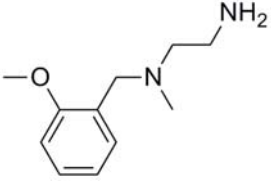
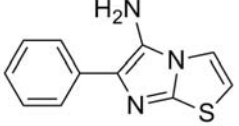
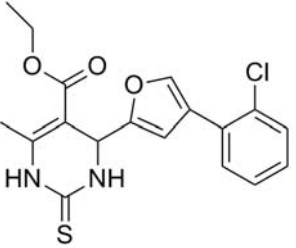
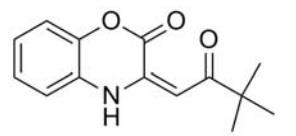
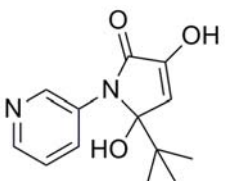
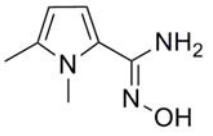
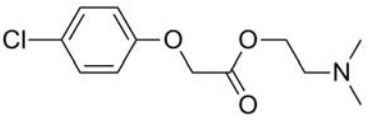
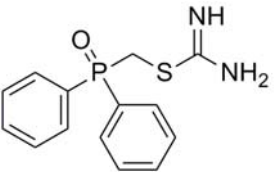
structures and information of strong (14 compounds) and medium (21 compounds) inhibitors are shown in **Table 3.3**.

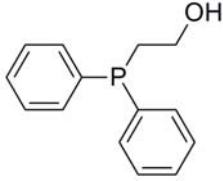
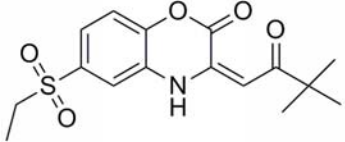
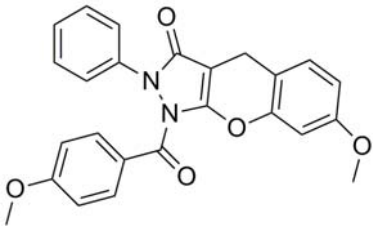
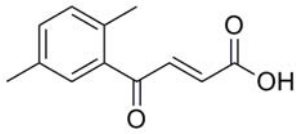
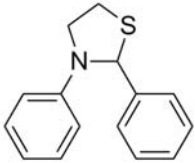
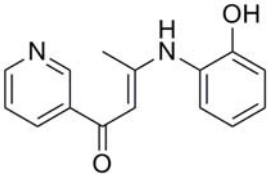
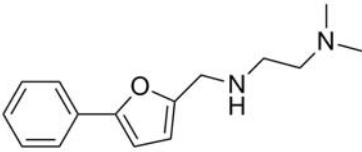
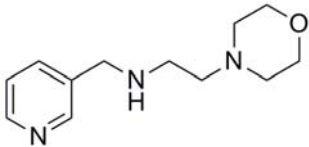
Category	Library Name	Number of compounds
Most recently plated commercial compounds (Plated Summer/Fall 2006 & Summer 2007)	Asinex 1	12,378
	ChemBridge 3	10,560
	ChemDiv 4	14,677
	Enamine 2	26,576
	Life Chemicals 1	3,893
	Maybridge 5	3,212
	ChemDiv 3	16,544
Recent plated commercial compounds (Plated May 2005)	ChemDiv 5	1,249
	MixCommercial 5	268
	Maybridge 4	4,576
	Biomol-TimTec 1	8,518

Table 3.2 Compound library information for the high-throughput screen

Compound	Plate No.	Well No.	Mw.	%Inhibition
	1486	C16	279.07	89.9%
	1504	L09	302.06	71.7%
	1515	O10	259.12	70.0%

	1533	D13	257.03	87.7%
	1535	P15	393.11	70.7%
	1546	C13	342.00	80.0%
	1548	J21	373.17	84.9%
	1548	L21	315.13	81.8
	1552	E13	244.08	97.7%
	1671	E18	278.07	94.6%
	1697	A04	207.04	88.9%

	1704	G20	194.14	76.0%
	1727	B01	215.05	81.5%
	1474	D06	376.06	60.6%
	1482	I15	245.11	62.0%
	1538	N21	248.12	54.8%
	1540	P05	153.09	52.2%
	1570	I08	257.08	69.4%
	1577	B21	290.06	56.8%

	1578	I09	230.09	60.0%
	1615	I20	337.10	54.7%
	1622	I10	428.14	55.3%
	1670	O07	204.08	67.6%
	1671	O16	241.09	53.4%
	1684	C02	254.11	61.7%
	1701	M18	244.16	66.7%
	1703	F20	221.15	58.7%

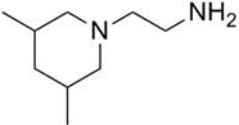
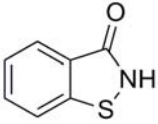
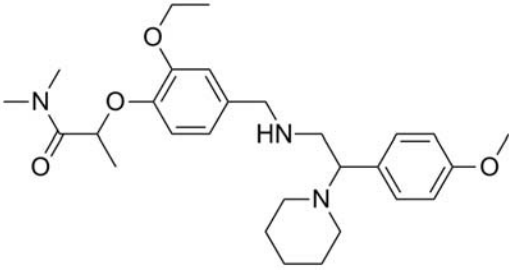
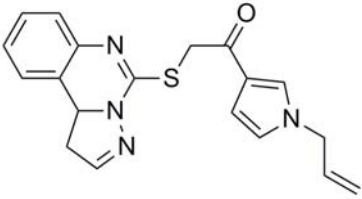
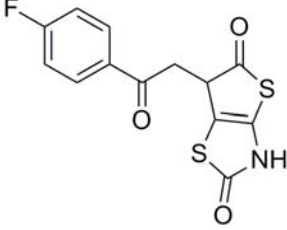
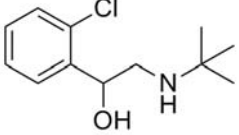
	1704	M18	156.16	54.0%
	1755	P21	151.01	53.8%
	1759	E18	483.31	50.0%
	1759	I10	350.12	55.8%
	1772	J21	308.99	60.0%
	1922	O06	227.11	54.7%

Table 3.3 Hits with strong and medium inhibition against *mtMenB* activity

A key problem caused by HTS is the generation of nonspecific or “promiscuous” inhibitors, which form aggregates and thereby inhibit enzyme activity (152-153). In order to exclude these unrelated chemicals, hits from strong and medium inhibition groups were subject to a secondary screen, which is called “cherry picks”. In the secondary screening, inhibition was measured in the present or absence of 0.1% Triton X-100

according to the method described by Dr. Shoichet (154). Compounds that only showed inhibition in the absence of detergent are considered as the promiscuous aggregators, which were not potential hits for further investigation.

2-Amino-4-aryl-4-oxo-butanoic acid as a potent scaffold to inhibit mtMenB

In the 455 hit compounds, 7 compounds were identified, which all shared a common structure containing OSB backbone (Figure 3.3). We hypothesized that these molecules could bind to the active site of either MenE or MenB. Compound 1548L21 was first randomly picked to evaluate for its inhibitory ability against ecMenE directly by monitoring the formation of pyrophosphate in the presence of MenE alone (155). Using this assay, it was found that 1548L21 did not inhibit ecMenE (100 nM) up to a concentration of 300 μ M.

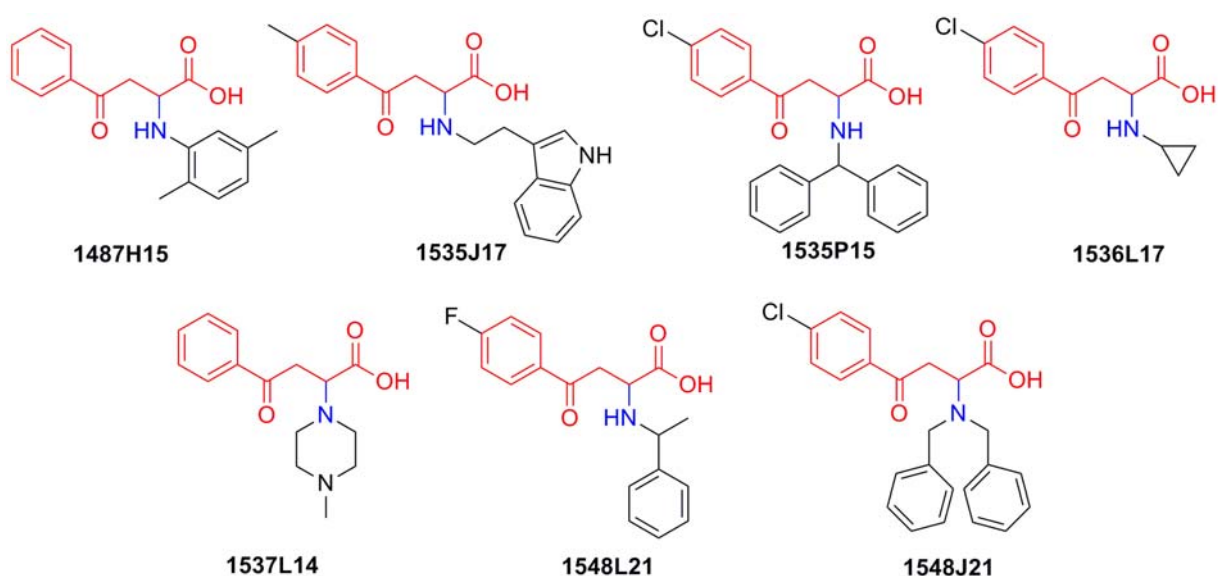
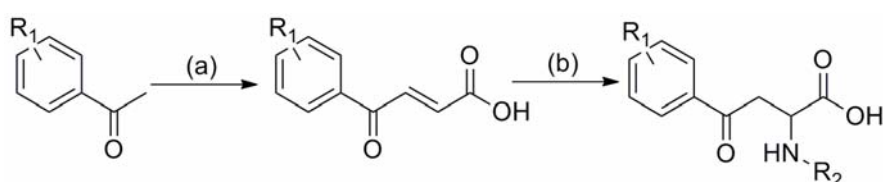


Figure 3.3 HTS hits containing OSB backbone

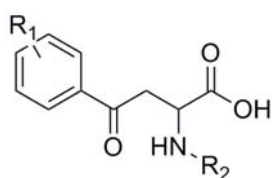
Synthesis of 2-amino-4-aryl-4-oxo-butanoic acids

Analogues of 1548L21 were synthesized using the protocol shown in **Scheme 3.1**. In the first step, the commercially available substituted acetophenone was converted to (*E*)-benzoylacrylic acid by reflux with glyoxylic acid monohydrate in glacial acetic acid (156). Subsequently, the unsaturated acid underwent Michael addition with a variety of amines to generate the final product (157). Using this method we synthesized 32 compounds which were evaluated for their ability to inhibit bacterial growth as well as the reaction catalyzed by MenB (**Table 3.4**).

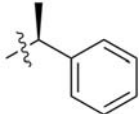
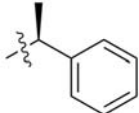
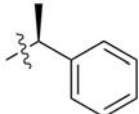
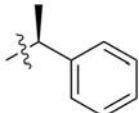
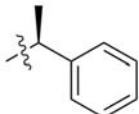
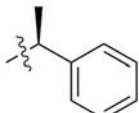
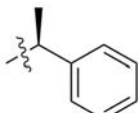
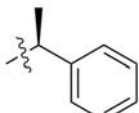
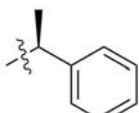
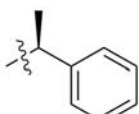
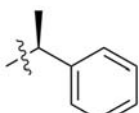


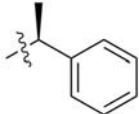
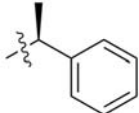
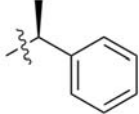
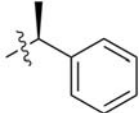
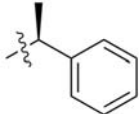
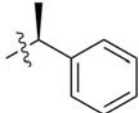
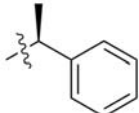
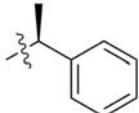
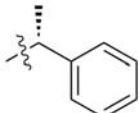
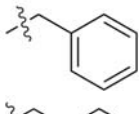
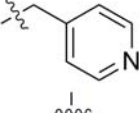
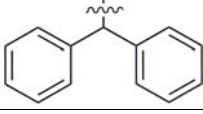
Scheme 3.1 Synthesis of 2-amino-4-aryl-4-oxo-butanoic acid

Reagents and conditions: (a) glyoxylic acid monohydrate, acetic acid, 110°C, 18 hours; (b), primary amine, anhydrous ethanol, 40°C, 3 hours.



Compound	R ₁	R ₂	IC ₅₀ (μM) ^(a)	MIC _{mt} (μg/mL)
38	H		112.1±10.6	6.25
39	4-F		13.2±0.75	12.5
40	4-Cl		8.54±0.80	50.0

41	4-Br		105.4±15.0	12.5
42	4-NO ₂		>150	100
43	4-OMe		>150	12.5
44	2-F		8.70±0.80	25.0
45	2-Cl		8.50±0.80	50.0
46	2-Br		0.60±0.07	12.5
47	2-I		0.63±0.03	6.25
48	2-NO ₂		2.10±0.22	12.5
49	2-CF ₃		2.10±0.19	25.0
50	2-COOMe		>150	>300
51	2-OMe		>150	>200

52	3-Cl		>150	12.5
53	3-NO ₂		>150	100
54	2,4-diF		1.40±0.18	6.25
55	2-Cl, 4-F		1.10±0.08	12.5
56	2-Br, 4-F		0.43±0.32	12.5
57	2-CF ₃ , 4-F		0.82±0.09	12.5
58	2,4-diCl		0.26±0.02	25.0
59	2,6-diCl		7.11±0.11	1.56
60	4-Cl		41.9±3.4	12.5
61	4-Cl		17.2±2.7	25.0
62	4-Cl		>200	12.5
63	4-Cl		18.1±2.2	12.5

64	4-Cl		3.25±0.33	12.5
65	4-Cl		10.0±0.9	125
66	4-Cl		7.25±0.60	100
67	4-Cl		15.1±1.6	12.5
68	4-Cl		12.4±1.1	50
69	4-Cl		NT ^(b)	50
70			>150	50
71			>150	50
72			>150	NT ^(b)

Table 3.4 2-Amino-4-aryl-4-oxo-butanoic acid as *m*MenB inhibitor and whole cell inhibition

(a) pre-treated with 0.5% NaOH; (b) Not tested.

In general, addition of a bulky substituent at either *meta* (compounds **52** and **53**) or *para* (compounds **41** and **42**) position of the phenyl group resulted in significant reduction in enzyme inhibition as well as a reduction in antibacterial activity.

Additionally, incorporation of electron-donating substituents at either *ortho* (compound **51**) or *para* (compound **43**) positions of the aromatic ring also decreased inhibitor potency. In contrast, introduction of an electron-withdrawing substituent into the aromatic ring resulted in an increase in both enzyme inhibition and antibacterial activity (compounds **44-49**). It is worth noting that introducing electron-withdrawing groups into both the *ortho* and *para* positions (compounds **54-58**) resulted in significant increase in activity. The SAR data also demonstrate that the amino group adjacent to the carboxylate is essential for the high affinity for enzyme binding, since replacement of amine with either thioether (compound **70**) or methylene (compounds **71** and **72**) group results in a decreased inhibition activity. Finally, alteration of the amine next to the carboxylate had only minor effects on activity (compounds **60-69**).

Inhibitors were broken down by retro-Michael addition

Although several compounds showed promising inhibitory activity against *mtMenB* with IC₅₀ values of less than 1 μM (**46, 47, 56-58**), there was generally a poor correlation between enzyme inhibition and antibacterial activity (**Figure 3.4**). For example, compound **59** is at least 10-fold more active in the antibacterial assay than compounds **56-58** (MIC 1.56 μg/ml compared to 12.5-25 μg/ml), but is a significantly poorer inhibitor of MenB (IC₅₀ 7.11 μM). Subsequent studies revealed that the inhibitors undergo *retro*-Michael addition (**158**), which leads to regeneration of the (*E*)-benzoylacrylic acid and the amine in solution (**Scheme 3.2**). The 2-aminobutanoates

have half-lives of ~10 minutes to 12 hr in pH 7.4 phosphate buffer (0.2 M) (Table 3.5), which is significant since the MIC measurements take at least 24-48 hour to complete.

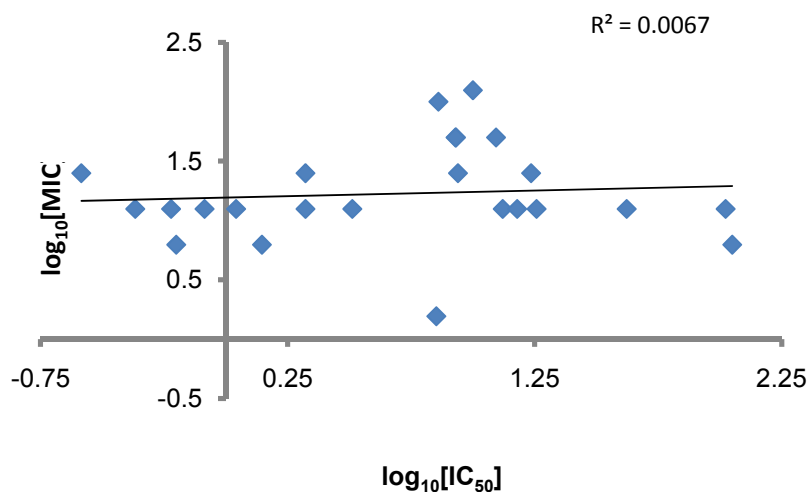
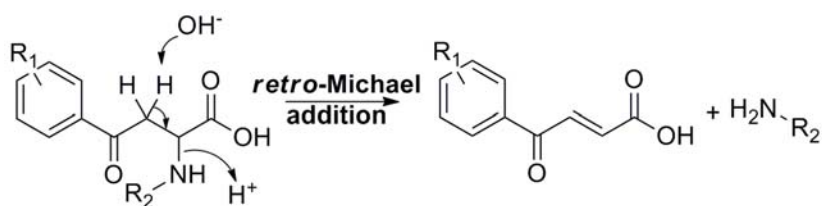


Figure 3.4 Correlation between enzymatic and bacterial growth inhibition



Scheme 3.2 *retro*-Michael addition

Compound	Structure	R	$t_{1/2}$ (hours) ^(a)
38		H	11.6
39		4-F	12.2
40		4-Cl	6.8
45		2-Cl	0.4
49		2-CF ₃	0.2
51		2-OMe	11.6

Table 3.5 Stability test on randomly selected compounds

(a) Stability at pH 7.4 and 25°C.

Stable 2-amino-4-aryl-4-oxo-butanoic acid analogues

From **Scheme 3.2**, the acidity of the proton adjacent to the ketone is the determinant of the rate of *retro*-Michael addition. **Table 3.5** also revealed that the more acidic the proton is, the less stable the compounds are. Based on the mechanism how these compounds degrade and the commercially available starting materials, several stable 2-amino-4-aryl-4-oxo-butanoic acid analogues were designed and synthesized (**Figure 3.5**).

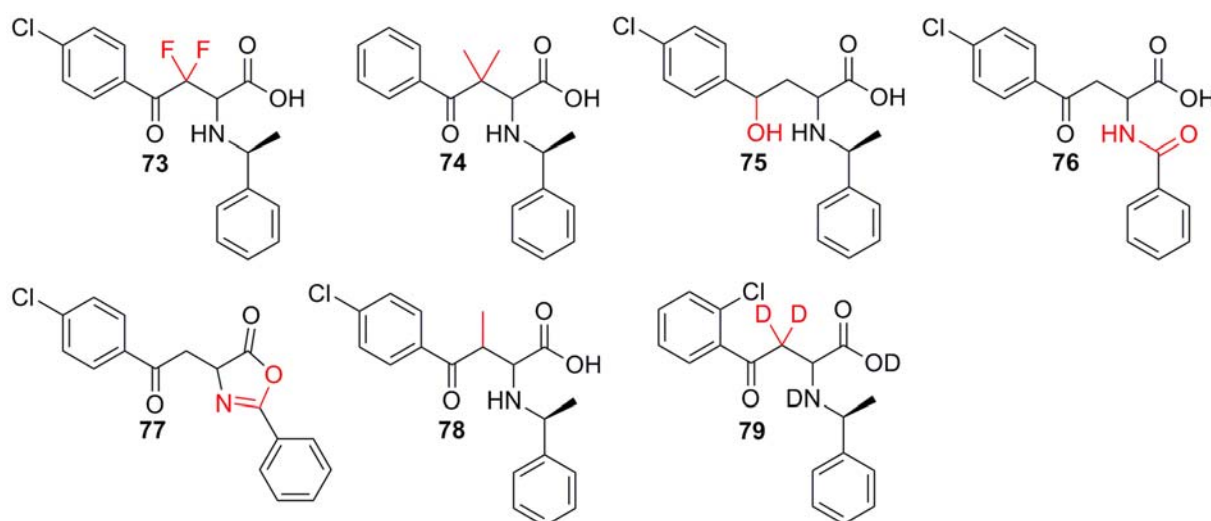
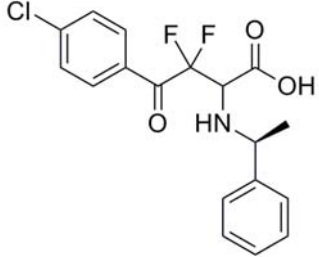
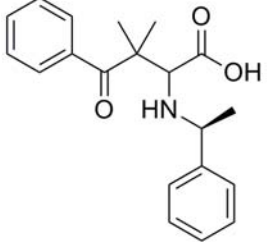
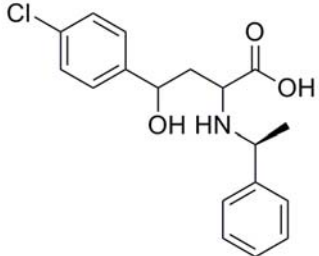
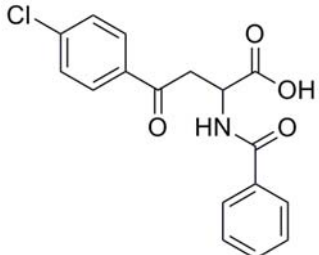
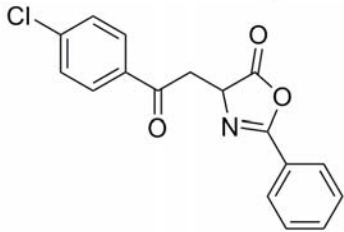


Figure 3.5 Stable 2-amino-4-aryl-4-oxo-butanoic acid analogues

In compounds **73** and **74**, the acidic hydrogens are replaced with fluorine or methyl group, which cannot be taken by base in the solution. The ketone group is replaced with hydroxyl, which can decrease the acidity of the α -proton in compound **75**. In compound **76**, amine group is replaced by amide which has lower tendency to break down. Compound **77** has similar structure with 2-amino-4-aryl-4-oxo-butanoic acid with a heterocyclic ring. Introducing one methyl group at the alpha position may increase the steric hindrance in compound **78**. Deuterium is designed to increase the stability by

isotope effect in compound **79** (159). Their stability and inhibitory properties are summarized in **Table 3.6**.

Compound	Structure	IC ₅₀ ^(a) (μM)	MIC _{mt} (μg/mL)	h _{1/2} (hour) ^(b)
73		>100	100	>12
74		>100	>100	>12
75		>100	NT ^(c)	>12
76		>100	NT	>12
77		>100	NT	>12

78		5.4±0.6	NT	6.1
79		2.1±0.2	NT	7.0

Table 3.6 Inhibition and stability test of 2-amino-4-aryl-4-oxo-butanoic acid analogues

(a) *mtMenB* concentration was fixed at 150 nM; (b) Stability at pH 7.4 and 25°C; (c) Not tested.

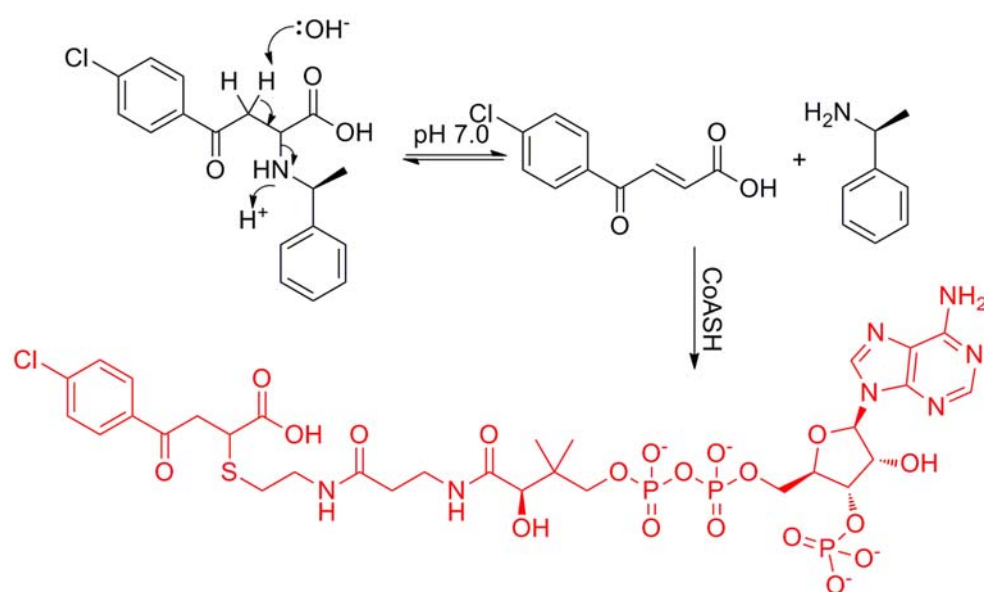
From **Table 3.6**, it is found that the strategies applied to the molecules help compounds **73-77** become stabilized (half life is longer than 12 hours), and simultaneously the inhibition activity was impaired (IC_{50} is higher than 100 μ M). Compounds **78** and **79** were still active inhibitors against *mtMenB*, while these two compounds still can undergo *retro*-Michael addition. These relationships indicate that the stability and inhibition cannot exist synchronously.

***In situ* formation of CoA adduct inhibitors**

It is spontaneously to hypothesize that the inhibition is related with the product from the degradation, thus inhibition test was subsequently applied to the degraded product, (*E*)-4-(4'-chlorophenyl)-4-oxo-but-2-enoic acid and (*S*)-phenylethylamine. It is surprising that the result showed that (*E*)-4-(4'-chlorophenyl)-4-oxo-but-2-enoic acid is

an inhibitor of *mtMenB* with IC_{50} of 8.1 μ M. Further research also found out that the inhibition is time-dependable and the inhibition activity increases with longer incubation time. HPLC analysis identified a new peak is generated, which indicates (*E*)-4-(4'-chlorophenyl)-4-oxo-but-2-enoic acid turned into another product during the incubation. Combined the information gained from NMR and LC-MS, the structure of the product was solved, which is shown in **Scheme 3.3**. It is also noticed that the compound cannot undergo *retro*-Michael addition.

Subsequent analysis also demonstrates that the 2-amino-4-aryl-4-oxo-butanoic acid is not a good scaffold for the *mtMenB* inhibitor design. Previous improper conclusion was lead by the pre-treatment of these molecules in 0.5% NaOH aqueous water, which facilitated the degradation of these compounds. If these molecules were first dissolved in 0.1% HCl in acetone solution, in which compounds would be stable, no inhibition was found against *mtMenB* if IC_{50} was tested immediately. However, the inhibition can be regained by incubating these compounds in the reaction buffer (**Table 3.7**) due to the degradation.



Scheme 3.3 CoA adduct formation in situ

Compound	Structure	R	IC ₅₀ (μM) ^(a)	IC ₅₀ (μM) ^(b)	IC ₅₀ (μM) ^(c)
38		H	112±10.6	>120	52.7±6.1
39		4-F	13.2±0.8	>120	14.4±2.3
40		4-Cl	8.54±0.80	>120	11.7±1.8
45		2-Cl	8.50±0.80	>120	8.40±0.80
49		2-CF ₃	2.10±0.19	>120	3.20±0.50
51		2-OMe	>120	>120	>120

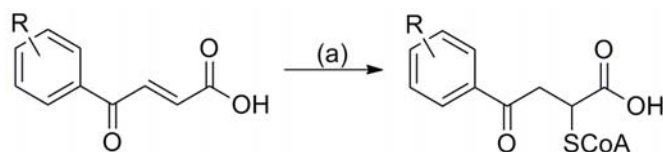
Table 3.7 Analysis of 2-amino-4-aryl-4-oxo-butanoic acid enzyme inhibition

(a) Compounds were dissolved by 0.5% NaOH aqueous solution and *mtMenB* concentration was fixed at 150 nM; (b) Compounds were dissolved by 0.1% HCl acetone solution, and the inhibition test was performed without incubation; (c) Compounds were dissolved by 0.1% HCl acetone solution, and the inhibition test was performed with incubation the compounds in pH 7.0 buffer.

SAR of CoA adduct inhibitors

CoA adduct was successfully identified as a *mtMenB* inhibitor. In order to generate SAR data for the new inhibitors, a series of compounds were synthesized and their inhibitory properties were evaluated using the coupled assay (Table 3.8).

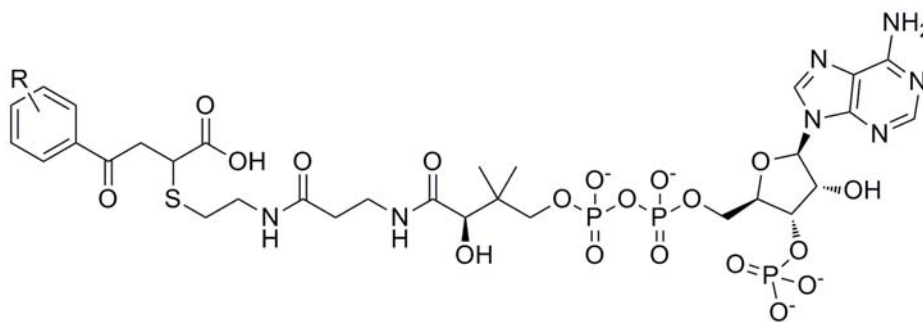
The (*E*)-4-aryl-4-oxo-but-2-enoic acid (1.0 mmol) was first dissolved in anhydrous DMSO (1 mL) at room temperature under N₂. Subsequently the solution was added into a 10 mL pH 7.0 phosphate buffer containing CoASH (0.1 mmol). The resulting mixture was continuously stirred for 4 hours at room temperature (**Scheme 3.4**). The product was then purified by HPLC.



Scheme 3.4 Synthesis of 4-aryl-2-CoA-4-oxo-butanoic acids

Reagents and conditions: (a) CoASH, pH 7.0 phosphate buffer, 25°C, 4 hours.

In general, addition of a bulky substituent at the *meta* position (compound **88**) of the phenyl group resulted in significant reduction in enzyme inhibition. Additionally, incorporation of electron-donating substituents at either the *ortho* (compound **87**) or *para* (compound **81**) positions of the aromatic ring also decreased inhibitor potency. In contrast, introduction of an electron-withdrawing substituent into the aromatic ring resulted in an increase in enzyme inhibition (compounds **80**, **82-86**, **89**). In order to gain further mechanistic insight into the functioning of these compounds, we used steady state kinetic methods to study the inhibition of *mtMenB* by **89**. These studies revealed that compound **89** is a noncompetitive inhibitor with respect to the substrate OSB-CoA, with K_i and K_i' values of 49 and 286 nM, respectively. In order to account for noncompetitive inhibition, we are currently exploring the possibility that binding of inhibitor to one subunit in the MenB homohexamer can modulate the activity of adjacent subunits.



Compound	R	IC ₅₀ (μM) ^(a)	K _i (nM) and K _i ' (nM)	<i>h</i> _{1/2} (hr) ^(b)
80	4-Cl	0.468±0.062	350±50 and 1630±280	>100
81	4-OMe	33.5±2.6		36.5
82	2-F	0.204±0.037		53.3
83	2-Cl	0.103±0.023		>100
84	2-Br	0.135±0.022		99.0
85	2-I	0.421±0.057		43.3
86	2-NO ₂	0.154±0.024		86.6
87	2-OMe	12.1±1.0		38.5
88	3-Cl	14.1±1.5		18.7
89	2,4-diCl	0.106±0.026	49±6 and 286±7	11.4

Table 3.8 SAR of CoA adducts

(a) *mtMenB* concentration was fixed as 150 nM; (b) Stability at pH 7.4 and 25°C.

Analysis of the *mtMenB* reaction suggests an explanation for the potent inhibition of *mtMenB* by the CoA adducts. A mechanism for the *mtMenB* catalyzed reaction has been proposed in which an intramolecular proton abstraction by the OSB carboxylate leads to the formation of a resonance stabilized carbanion (70). Model building suggests that the CoA adducts can adopt a bound structure that resembles the intermediate required for α-proton abstraction (**Figure 3.6A**), which may account for the high affinity of these compounds for MenB. Of key importance in this model is the location of the free carboxylate of the adduct. Consequently we synthesized compound **90** (**Scheme 3.17**) which have similar structures to the CoA adducts but lack a free carboxylate group in order to provide additional SAR data. Compared with the CoA adducts, the CoA thioester (**16-18**) in Chapter 2 has a significantly lower affinity for MenB (**Table 2.1**) with

an IC_{50} value in micromolar range compared to nanomolar for the corresponding adduct (**89**, **84**, and **86**). In addition, compound **90** displayed no significant inhibition up to a concentration of 400 μ M. Compound **89** was also utilized to gain crystal structure with *ecMenB* and *mtMenB*. **Figure 3.6B** reveals that the free carboxylate in compound **89** contacts with the oxyanion hole residues G86 and G133 in *ecMenB* by hydrogen bond formation. Similar binding pattern was also found in *mtMenB* and compound **70** by docking experiments. These four compounds thus support the importance of the free carboxylate for CoA adduct binding.

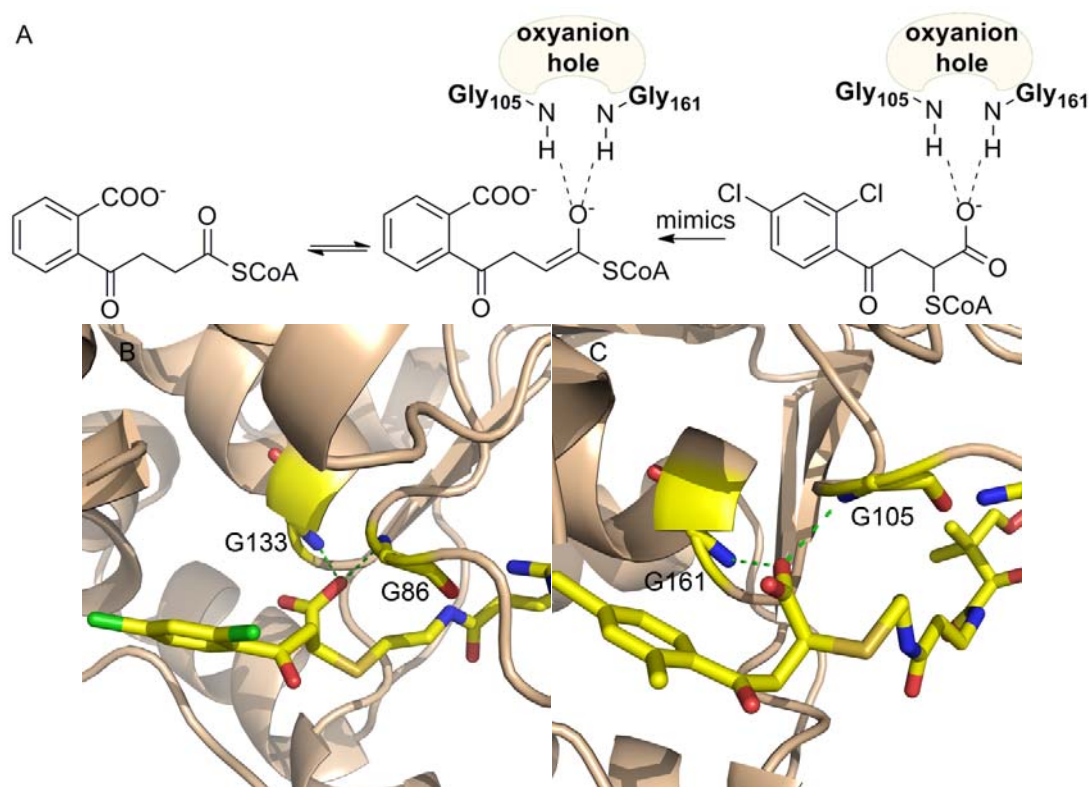
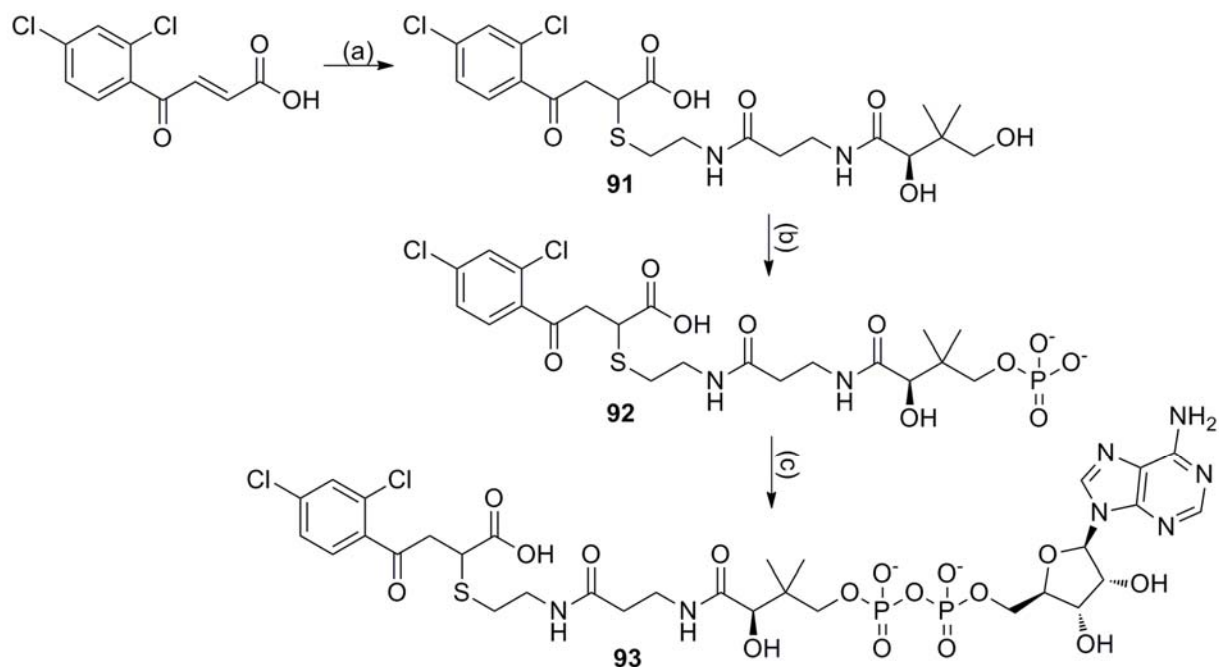


Figure 3.6 CoA adduct binding mode

A. *mtMenB* oxyanion hole formed by G105 and G161 stabilizes the reaction intermediate by forming hydrogen bonding; B. The crystallographic structure of *ecMenB* bound with compound **89** reveals that the carboxylate interacts with oxyanion hole residues; C. *mtMenB* and compound **89** docking structure showed the interaction between the carboxylate and oxyanion hole residues.

Compounds **91-93** were synthesized (**Scheme 3.5**) to study the binding affinity contributed by the CoA moiety. The inhibition result is summarized in **Table 3.9**.



Scheme 3.5 Synthesis of compound 91-93

Reagents and conditions: (a) pantetheine, pH 7.0 buffer, 25°C, 5 hours; (b) PanK, ATP, pH 8.0 buffer, 25°C, 3 hours; (c) PPAT, ATP, pH 8.0 buffer, 25°C, 3 hours.

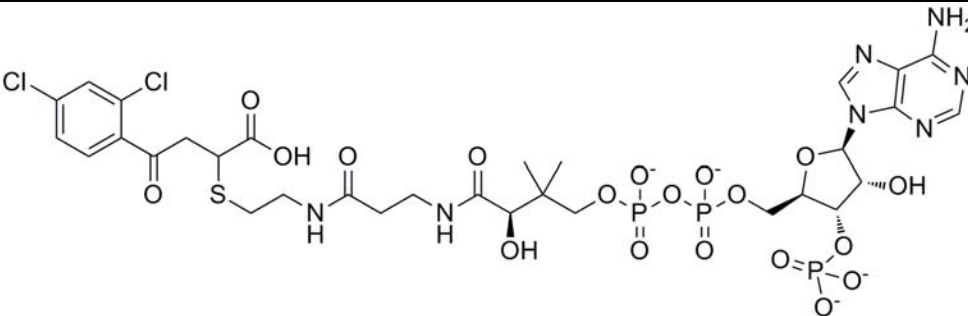
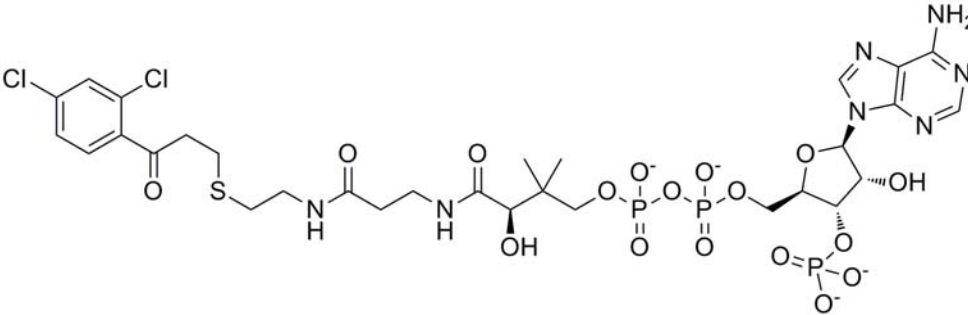
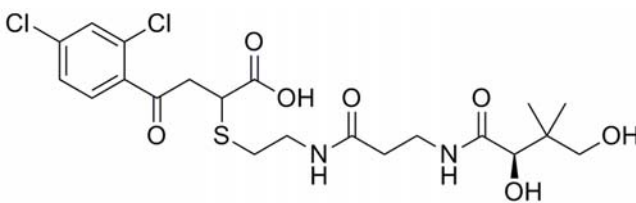
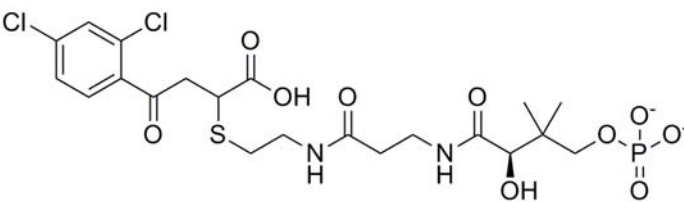
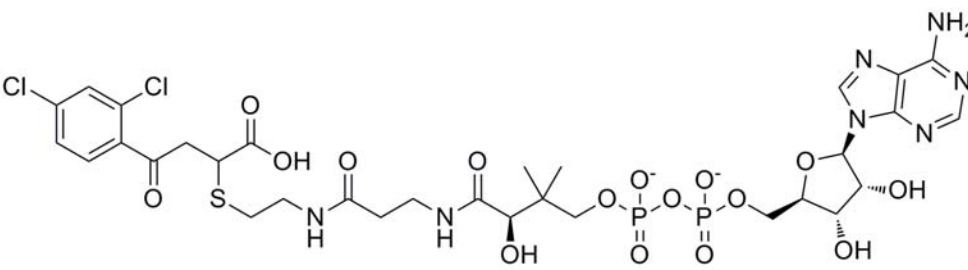
cpd	Structure	IC ₅₀ (μM)
89		0.106± 0.026
90		>400
91		28.5 ±0.6
92		170
93		0.506 ±0.060

Table 3.9 Inhibition comparison among compound 89-93

Compared with the parent compound **89**, compound **91** utilized pantetheine instead of CoA moiety. The inhibition activity decreased significantly by about 300-fold. In compound **92**, 4'-phosphopantothenate further compromises the binding affinity. However, utilization of dephospho-CoA in **93** significantly increased the binding affinity compared with compound **91** and **92**. However, the inhibition activity is still 5-fold lower than the parent compound. These results indicate that the 4-aryl-4-oxo-butanoic acid moiety functioned as an anchor to specifically bind within the active site and CoA moiety increased the enzyme recognition. The AcAc-CoA:*mtMenB* cocrystallography structure clearly elucidates the hydrogen bond network between enzyme residues and phosphates in CoA moiety (**Figure 3.7**). R58 contacts with the phosphate in the pantetheine and K95 and K'302 in another subunit interact with the phosphate on the ribose ring. G105 and Q107 form hydrogen bonds with the adenine. This figure demonstrated that the importance of CoA moiety and replacement of CoA in the inhibitor would result in significant decrease in binding affinity.

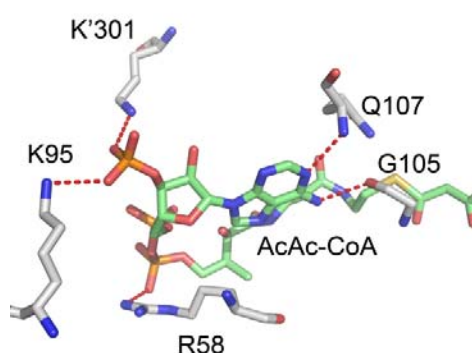
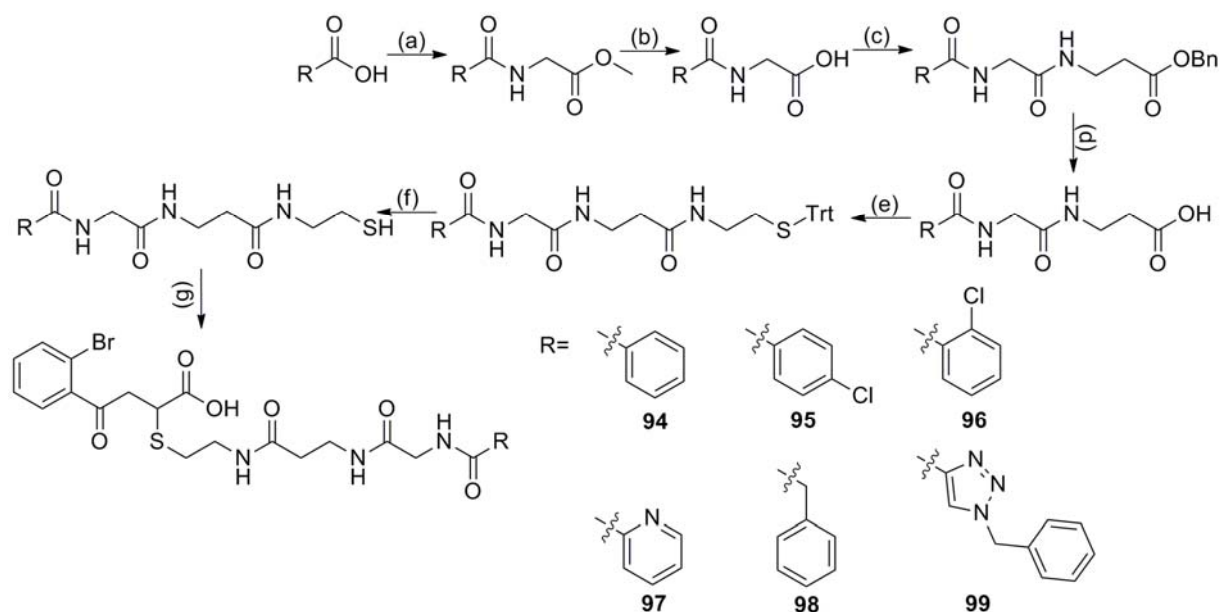


Figure 3.7 Potential hydrogen bond interactions between *mtMenB* and AcAc-CoA

Preliminary CoA surrogates library synthesis

Compound **84** and **89**, with high binding affinity towards the enzyme target, were selected to test their inhibition against the growth of *M. tuberculosis*. However, no inhibition was found at a concentration as high as 100 µg/mL. This can be explained by the hydrophilic property of these compounds and the unique cell wall structure of *M. tuberculosis*. *M. tuberculosis* cell wall is rich in high molecular weight lipids and it forms a protective barrier similar as the outer membrane of Gram-negative bacteria (160). The lipid-rich mycobacterial cell wall allows relatively hydrophobic antibiotics to penetrate by diffusion through the hydrophobic mycolic acids and glycolipids bilayer (17, 161). However, hydrophilic antibiotics and nutrients are difficult to penetrate through diffusion and they are believed to use porin channels to reach the inner cell (162-163). Due to the size of the porin channel and abundance on the cell membrane, it only uptake small hydrophilic antibiotics and nutrients, such as isoniazid, to pass through the cell wall with a limited rate (164). ClogP value of CoA is -0.2 and the molecular weight is 767.53, calculated by ChemBioDraw 12 (165). Although compound **80-89** have adequate binding affinity against the target *in vitro*, they cannot penetrate the cell wall and reach a sufficient concentration in the cell to inhibit the target activity. In order to improve the antibacterial property of the compounds, compound **94-99** were designed and synthesized (**Scheme 3.6**).



Scheme 3.6 Synthesis of CoA surrogates 94-99

Reagents and conditions: (a) glycine methyl ester hydrochloride, EDC·HCl, DIPEA, anhydrous CH_2Cl_2 , 25°C , 18 hours; (b) 1M NaOH aqueous solution, 25°C , 1 hour; (c) β -alanine benzyl ester *p*-toluenesulfonate, EDC·HCl, DIPEA, anhydrous CH_2Cl_2 , 25°C , 18 hours; (d) H_2 , Pd/C, EtOAc, 25°C , 1 hour; (e) Trt-protected cysteamine, EDC·HCl, DIPEA, anhydrous CH_2Cl_2 , 25°C , 18 hours; (f) triisopropylsilane, TFA, anhydrous CH_2Cl_2 , 25°C , 18 hours; (g) (*E*)-4-(2-bromophenyl)-4-oxo-but-2-enoic acid, pH 7.0 phosphate buffer, 25°C , 5 hours.

In general, commercially available carboxylic acid was first coupled with methylated glycine ester with a standard EDC·HCl coupling procedure (166) and the protecting methyl group was subsequently removed by 1M NaOH aqueous solution. The exposed free carboxylic acid was then coupled with β -alanine benzyl ester *p*-toluenesulfonate and the benzyl group was removed by H_2 with catalytical amount of Pd/C. The new released carboxylic acid was further react with Trt-protected cysteamine (167) and the Trt group was removed by triisopropylsilane and TFA condition (168). The Michael addition between the (*E*)-4-(2-bromophenyl)-4-oxo-but-2-enoic acid and the free thiol at pH 7.0 buffer generates the final product, which was subsequently purified by HPLC.

Inhibition data was summarized in **Table 3.10**. In general, CoA surrogates activity against *mtMenB* was less potent than the CoA adducts. This also supports the conclusion that CoA moiety is essential for the tight binding affinity. The disruption of hydrogen bonding with the enzyme compromises the inhibition significantly. However, this method provides a combinational solution to generate a molecular library, which can be used to synthesize more CoA mimics and to screen more potent inhibitors against the enzyme.

Compound	Structure	R	IC ₅₀ (μM)
94			14±1
95			19±3
96			18±4
97			23±4
98			75±4
99			77±17

Table 3.10 CoA surrogates inhibition against *mtMenB*

Antibacterial activity of (E)-4-aryl-4-oxo-but-2-enoic acid as a prodrug

Coenzyme A is biosynthesized from pantothenic acid, cysteine, and ATP in a five-step process in bacteria. Since CoA plays its essential role in biosynthesis and oxidation of fatty acid and the oxidation of pyruvate, the concentration of CoA in the live bacteria can reach as high as 2-5 g/L medium (169-170). As discussed above, the 4-aryl-2-CoA-4-oxo-butanoic acid scaffold possesses a hydrophilic core, which leads to the low permeability through bacteria cell wall. In this study, (E)-4-aryl-4-oxo-but-2-enoic acid and its methyl ester were used as a prodrug to inhibit the bacterial growth. The unsaturated acids were first selected to treat the bacteria and the hypothesis is that these compounds can react with free CoA in the live bacteria and form the 4-aryl-2-CoA-4-oxo-butanoic acid scaffold, and subsequently inhibit the bacteria growth by targeting MenB and hampering the menaquinone production. To demonstrate and prove the mechanism, their influence on the menaquinone production in *S. aureus* was also monitored.

Compared with the *M. tuberculosis*, *S. aureus* is a fast replicating bacterium, whose growth can be evaluated in one day. Moreover, *S. aureus* is a BSL-2 bacterium, which is more easily to get access. It is also demonstrated in our laboratory that menadione can be uptaken by *S. aureus* to synthesize its required menaquinone components (data not published) by a Ph. D. student Yang Lu. A subsequent experiment was performed to discover that whether the menadione supplementation can recover the bacterial growth inhibited by the 1,4-benzoxazines.

The antibacterial experiment results demonstrated that the (*E*)-4-aryl-4-oxo-but-2-enoic acids (compounds **24**, **36**, **102**, and **104**) and their esters (compounds **100** and **101**) are all active against the bacteria. The comparison between the methyl ester (compound **101**) and free acid (compound **102**) revealed that the hydrophobic property can significantly influence the antibacterial property, since the ester is at least 25-fold and 40-fold stronger than its free acid by inhibiting the growth of *M. tuberculosis* and *S. aureus*, respectively. This can be explained by the compound permeability. Free acid is more hydrophilic than its methyl ester, thus it is more difficult to penetrate the waxy bacterial cell wall. However, its methyl ester is more hydrophobic, which can penetrate the bacterial cell wall through diffusion.

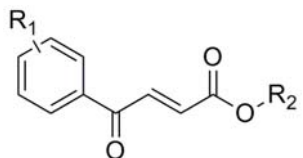
Compound	Structure	R ₁	R ₂	MIC _{mt} ^(a) (µg/mL)	MIC _{sa} ^(b) (µg/mL)
102		4-Cl	H	25	10
24		2-Br	H	50	NT ^(c)
36		2,4-diCl	H	NT	5
104		4-OMe	H	NT	100
100		4-F	Me	<1	NT
101		4-Cl	Me	<1	0.25

Table 3.11 Antibacterial activities of (*E*)-4-aryl-4-oxo-but-2-enoic acid and its methyl esters

(a): MIC against *M. tuberculosis* H37Rv; (b) MIC against *S. aureus* RN4220; (c) not tested.

In order to study the mechanism of the inhibition, menadione, a precursor of menaquinone that can be utilized by the bacteria to synthesize menaquinone (**171**), was artificially supplemented into the bacteria medium to study its influence on the growth recovery (**Table 3.12**). For compounds **36**, **101**, and **102**, MIC increased 2.5 to 5-fold after menadione was added into the medium as supplementation, indicating menadione

can partially recover the *S. aureus* growth by replenishing menaquinone concentration. Compound **104** has only minor inhibition against the bacteria and the MIC is not influenced by menadione is because its CoA adduct (compound **87**) behaves as a weak inhibitor against *mtMenB*. The correlation between the (*E*)-4-aryl-4-oxo-but-2-enoic acids MIC and the IC₅₀ of their corresponding CoA adduct derivatives indicates the (*E*)-4-aryl-4-oxo-but-2-enoic acid scaffold behaves as a prodrug and inhibit the menaquinone biosynthesis in bacteria. However, it is also noticed that the bacterial growth is not completely recovered after the menadione supplementation. It may suggest that this (*E*)-4-aryl-4-oxo-but-2-enoic acid scaffold's activity against the bacteria under the supplementation condition is due to an off-target effect. The MIC(with supplement)/MIC(without supplement) is defined as the inhibitor selectivity (172), and in our case, the best selective inhibitor is compound **36**, with a selectivity of 5. The low selectivity may come from the reactive Michael acceptor scaffold, which can react with many nucleophile, such as thio group in cysteine, thus the (*E*)-4-aryl-4-oxo-but-2-enoic acid scaffold might act as an irreversible inhibitor against many enzymes in other essential metabolic pathway (173-174). Moreover, it is reported that around 4% of the enzyme substrate involves with a CoA moiety, thus there is high possibility that the 4-aryl-2-CoA-4-oxo-butanoic acid scaffold targets other CoA-dependent enzymes.

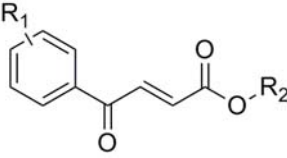
Compound	Structure	R ₁	R ₂	MIC _{sa} w/o menadione (µg/mL)	MIC _{sa} w/ menadione (0.5 µg/mL) (µg/mL)
102		4-Cl	H	10	25
36		2,4- diCl	H	5	25
104		4- OMe	H	100	100
101		4-Cl	Me	0.25	1

Table 3.12 Menadione supplementary MIC testing

Further experiment was also conducted to monitor the menaquinone production in *S. aureus*. In wild-type, menaquinone-8 is the most abundant component in the bacteria. The menaquinone production in a menD-disrupted strain (175) is significantly impaired, as the menaquinone concentration decreases at least 100 folds. Instead, after treatment of the wild-type bacteria with compounds **36**, **40**, and **101**, the menaquinone production is also hampered. For example, compounds **36** and **40** lead a 10-fold decrease in the menaquinone production, while compound 100 is a more efficient suppressor, causing around 100-fold decrease. This offers direct evidence that the (*E*)-4-aryl-4-oxo-but-2-enoic acids and their methyl ester can penetrate the bacterial cell wall and interfere with the menaquinone biosynthesis (**Figure 3.8**).

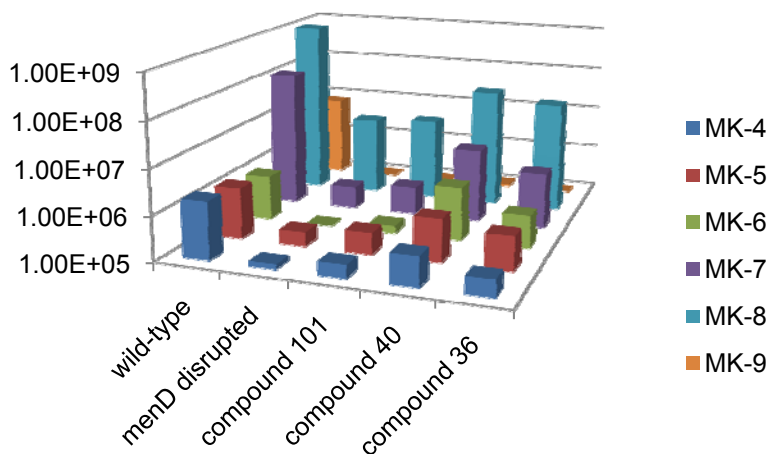


Figure 3.8 Menaquinone production in *S. aureus*

Non-replicating M. tuberculosis inhibition evaluation

Finally, compound **101** was selected for a LORA inhibition test for non-replicating *M. tuberculosis* (176) and it was found that it effectively inhibited the bacteria growth under low oxygen conditions with a MIC value as low as 1.5 $\mu\text{g/mL}$. Although this suggests a 10-fold increase in MIC under aerobic cultures, it still indicates that the compound **101** targets essential cellular events in the non-replicating *M. tuberculosis* (177). It is reported that the rifampin, have MIC values as low as 0.4 $\mu\text{g/mL}$ and it is the only first-line drug can sterilize latent infection (176). The methyl (*E*)-4-aryl-4-oxo-but-2-enoate scaffold has a comparable activity with rifampin, and it has a more superior activity against the latent tuberculosis than other compounds evaluated by the LORA assay (176). The result also supports that menaquinone is an essential component for

the survival of *M. tuberculosis* under non-replicating condition and it might offer a potential scaffold for non-replicating *M. tuberculosis*.

Conclusion

MenB inhibitor discovery starts with the high-throughput screen, in which several 2-amino-4-aryl-4-oxo-butanoic acids were identified as hit molecules. Further stability test revealed that these compounds were relatively unstable and *retro*-Michael addition broke the compounds into (*E*)-4-aryl-4-oxo-but-2-enoic acids, which subsequently reacted with CoA in the MenB reaction buffer and generated 4-aryl-2-CoA-4-oxo-butanoic acids *in situ*. Several stable 2-amino-4-aryl-4-oxo-butanoic acid analogues were also designed and synthesized. These analogues were not efficient MenB inhibitors, indicating that the 2-amino-4-aryl-4-oxo-butanoic acid scaffold was not a potential chemical entity for MenB inhibitor development.

Further SAR studies on the 4-aryl-2-CoA-4-oxo-butanoic acid scaffold generated more potent noncompetitive inhibitors against *mtMenB*, with a K_i and K_i' values as low as 49 and 286 nM, respectively. SAR data, supplemented with crystallography structure, offered an explanation on the high binding affinity towards the enzyme: the free carboxylic acid at the end formed hydrogen bonds with the oxyanion hole residues.

4-Aryl-2-CoA-4-oxo-butanoic acid scaffold had no/low antibacterial activity due to its hydrophilic property, which makes it almost impossible to penetrate the bacterial cell

wall to reach the effective concentration in the bacteria. Several CoA surrogate analogues were randomly designed and synthesized. Although these molecules did not efficiently inhibit the enzyme activity, it still offered a feasible method to develop a more sophisticated library.

Several (*E*)-4-aryl-4-oxo-but-2-enoic acids and their methyl esters were utilized to eliminate the bacteria, acting as a prodrug. These compounds can penetrate the high lipid content cell wall, react with CoA in the cell, and impair the menaquinone biosynthesis by targeting MenB.

In this chapter, we first identified a group of unique molecules that can inhibit the *mtMenB* activity and compromise the menaquinone production in live cells. Further research will be addressed on the improvement of the pharmacological issues to make these molecules more drug-like.

Experimental section

General

All chemicals were purchased from commercial suppliers (Sigma-Aldrich, Acros Organics, Alfa Aesar, Fisher Scientific, and TCI America) with the highest purity and used without further purification. (*E*)-4-Oxo-4-phenyl-but-2-enoic acid, (*E*)-4-(4'-chlorophenyl)-4-oxo-but-2-enoic acid, and (*E*)-4-(4'-methoxyphenyl)-4-oxo-but-2-enoic acid were commercially available from Aldrich. All solvents were purchased from Fisher

Scientific. ¹H-NMR spectral data were recorded on Varian Gemini-2300 or Varian Inova-400 NMR spectrometers. Mass spectral data were obtained using an Agilent 1100 LS-MS electrospray ionization single quadrupole mass spectrometer.

HPLC separations were performed on a Shimadzu LC-10AVP with Phenomenex Luna 5 μ C18(2) 250 \times 10.00 mm reverse phase semi-preparative column or a GraceVydac 5 μ C18 100 \times 10.00 mm reverse phase semi-preparative column with a linear gradient of 0-40% solvent B (acetonitrile) in solvent A (20 mM ammonium acetate in water) in 40 minutes, and 40-100% in the next 10 minutes, and a flow rate of 4 mL/min. The aromatic compounds were monitored by UV absorbance at 254 nm and non-aromatic compounds were monitored by UV absorbance at 220 nm.

***Z'*-factor determination**

In the *Z'*-factor determination experiment, a 384-well plate was divided into two parts (**Figure 3A**). Half of the wells were used as negative control (DHNA-CoA generation was not inhibited), which contained 40 μ L reaction buffer (20 mM NaH₂PO₄, 1 mM MgCl₂, 150 mM NaCl, pH 7.0) including OSB, ATP, and CoA, and *mtMenB*. *mtMenB* mutant Y287F, which was inactive, was utilized in the positive control (DHNA-CoA generation was inhibited). Subsequently, *ecMenE* was added into the system at the last step, which initiated the reaction. The concentration of OSB, ATP and CoA ranged from 100-250 μ M. The concentration of *mtMenB* ranged from 100-200 nM, and the concentration of *ecMenE* ranged from 1-3 μ M. After the 384-well plate was

incubated under room temperature for a certain time (20-60 minutes), the absorbance in each well was collected by an automatic plate reader. The Z'-factor was calculated by **Equation 3.1** at different conditions.

High-throughput screen

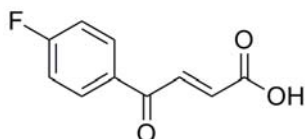
In a 384-well plate, from Column **1** to Column **23**, 24.9 μL buffer solution containing 250 μM OSB, 250 μM CoA, 250 μM ATP, and 150 nM *mtMenB* was sequentially added into each well. In Column **24**, which is used as positive control, 24.9 μL buffer solution containing 250 μM OSB, 250 μM CoA, 250 μM ATP, and 150 nM *mtMenB* mutant Y287F were added. The Epsom compound transfer robot precisely transfers 0.1 μL stock compound solution into Column **1** to Column **22**, and the final compound concentration is between 20-100 μM , which is depended on the compound's molecular weight. Finally, 15 μL of 3 μM *ecMenE* was added to initiate the reaction. The plate was incubated at room temperature for 1 hour and the absorbance at 405 nm in each well was detected by an Envison plate reader.

General procedure for the synthesis of (E)-4-aryl-4-oxo-but-2-enoic acids 19-37

The commercially available substituted acetophenone (1.0 mmol) and glyoxylic acid monohydrate (1.3 mmol) were first dissolved in glacier acetic acid (20 mL) at room

temperature under N₂. The reaction temperature was subsequently increased to 130 °C and the resulting mixture was continuously stirred under reflux for 18 hours. After cooling to room temperature, the acetic acid was removed under reduced pressure. The product was then purified by silica-gel chromatography (EtOAc/Petroleum ether = 1:1).

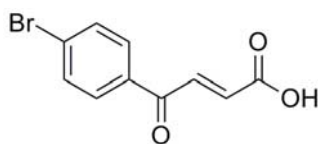
Synthesis of compound 19



Method: compound **19** was prepared according to the general procedure from 4'-fluoroacetophenone and the product was obtained as light yellow liquid.

Characterization: ¹H-NMR (300 MHz, acetone-*d*₆) δ 8.22-8.17 (2H, m), 7.96 (1H, d, *J*=15.6 Hz), 7.40-7.36 (2H, m), 6.79 (1H, d, *J*=15.6 Hz). ESI-MS (Neg): found 193.0 [M-H]⁻; calculated for C₁₀H₇FO₃: 194.0.

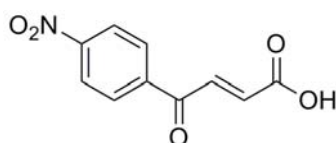
Synthesis of compound 20



Method: compound **20** was prepared according to the general procedure from 4'-bromoacetophenone and the product was obtained as a yellow solid.

Characterization: ¹H-NMR (300 MHz, DMSO-*d*₆) δ 7.96 (2H, d, *J*=9.0 Hz), 7.83 (1H, d, *J*=15.6 Hz), 7.78 (2H, d, *J*=9.0 Hz), 6.67 (1H, d, *J*=15.6 Hz). ESI-MS (Neg): found 252.9 [M-H]⁻; calculated for C₁₀H₇BrO₃: 254.0.

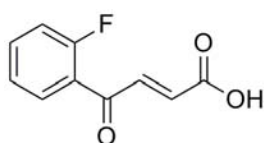
Synthesis of compound **21**



Method: compound **21** was prepared according to the general procedure from 4'-nitroacetophenone and the product was obtained as a yellow solid.

Characterization: $^1\text{H-NMR}$ (300 MHz, chloroform- d_1) δ 8.38 (2H, d, $J=9.0$ Hz), 8.16 (2H, d, $J=9.0$ Hz), 7.95 (1H, d, $J=15.3$ Hz), 6.96 (1H, d, $J=15.3$ Hz). ESI-MS (Neg): found 220.0 $[\text{M-H}]^-$; calculated for $\text{C}_{10}\text{H}_7\text{NO}_5$: 221.0.

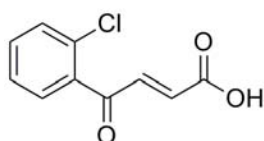
Synthesis of compound **22**



Method: compound **22** was prepared according to the general procedure from 2'-fluoroacetophenone and the product was obtained as a yellow solid.

Characterization: $^1\text{H-NMR}$ (300 MHz, acetone- d_6) δ 7.92-7.80 (1H, m), 7.80-7.62 (2H, m), 6.73 (1H, d, $J=15.6$ Hz). ESI-MS (Neg): found 193.0 $[\text{M-H}]^-$; calculated for $\text{C}_{10}\text{H}_7\text{FO}_3$: 194.0.

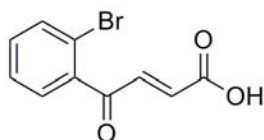
Synthesis of compound **23**



Method: compound **23** was prepared according to the general procedure from 2'-chloroacetophenone and the product was obtained as a light yellow solid.

Characterization: $^1\text{H-NMR}$ (400 MHz, chloroform- d_1) δ 7.65 (1H, d, $J=16.0$ Hz), 7.56-7.52 (1H, m), 7.50-7.46 (1H, m), 7.43-7.37 (2H, m), 6.79 (1H, d, $J=16.0$ Hz). ESI-MS (Neg): found 208.9 $[\text{M-H}]^-$; calculated for $\text{C}_{10}\text{H}_7\text{ClO}_3$: 211.0.

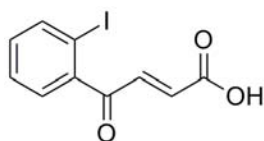
Synthesis of compound 24



Method: compound **24** was prepared according to the general procedure from 2'-bromoacetophenone and the product was obtained as a yellow solid.

Characterization: $^1\text{H-NMR}$ (300 MHz, acetone- d_6) δ 7.78-7.73 (1H, m), 7.63-7.48 (3H, m), 7.39 (1H, d, $J=15.6$ Hz), 6.53 (1H, d, $J=15.6$ Hz). ESI-MS (Neg): 252.9 $[\text{M-H}]^-$; calculated for $\text{C}_{10}\text{H}_7\text{BrO}_3$: 254.0.

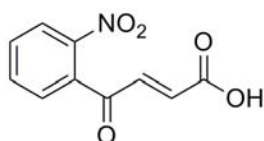
Synthesis of compound 25



Method: compound **25** was prepared according to the general procedure from 2'-iodoacetophenone and the product was obtained as a yellow solid.

Characterization: $^1\text{H-NMR}$ (300 MHz, acetone- d_6) δ 8.02 (1H, d, $J=9.0$ Hz), 7.62-7.52 (2H, m), 7.42-7.28 (2H, m), 6.52 (1H, d, $J=15.9$). ESI-MS (Neg): found 300.9 [M-H] $^-$, calculated for $\text{C}_{10}\text{H}_7\text{O}_3$: 301.9.

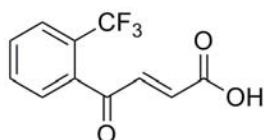
Synthesis of compound **26**



Method: compound **26** was prepared according to the general procedure from 2'-nitroacetophenone and the product was obtained as a yellow solid.

Characterization: $^1\text{H-NMR}$ (300 MHz, acetone- d_6) δ 8.25 (1H, d, $J=9.0$ Hz), 8.00-7.92 (2H, m), 7.70 (1H, d, $J=9.0$ Hz), 7.30 (1H, d, $J=16.2$ Hz), 6.47 ((1H, d, $J=16.2$ Hz). ESI-MS (Neg): found 220.0 [M-H] $^-$; calculated for $\text{C}_{10}\text{H}_7\text{NO}_5$: 221.0.

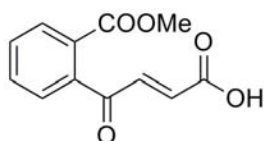
Synthesis of compound **27**



Method: compound **27** was prepared according to the general procedure from 2'-trifluoromethylacetophenone and the product was obtained as a yellow oil.

Characterization: $^1\text{H-NMR}$ (300 MHz, acetone- d_6) δ 7.92-7.66 (4H, m), 7.31 (1H, d, $J=16.2$ Hz), 6.47 (1H, d, $J=16.2$ Hz). ESI-MS (Neg): found 243.0 [M-H] $^-$; calculated for $\text{C}_{11}\text{H}_7\text{F}_3\text{O}_3$: 244.0.

Synthesis of compound **28**

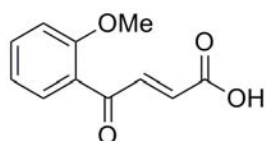


Method: compound **28** was prepared according to the general procedure from methyl 2-acetylbenzoate and the product was obtained as a yellow solid.

Characterization: $^1\text{H-NMR}$ (300 MHz, acetone- d_6) δ 8.01 (1H, d, $J=6.3$ Hz), 7.80-7.63 (2H, m), 7.52 (1H, d, $J=6.3$ Hz), 7.25 (1H, d, $J=15.9$ Hz), 6.30 (1H, d, $J=15.9$ Hz). ESI-MS (Neg): found 233.0 $[\text{M-H}]^-$; calculated for $\text{C}_{12}\text{H}_{10}\text{O}_5$: 234.0.

Methyl 2-acetylbenzoate was prepared as described in the following procedure. 2-Acetylbenzoic acid (1.0 mmol), DMAP (1.2 mmol), and anhydrous MeOH (2.0 mmol) were first dissolved in anhydrous CH_2Cl_2 (20 mL) i at room temperature under N_2 . DCC (1.2 mmol) was subsequently added into the resulting solution and the mixture was continuously for 18 hours. The precipitate was then removed by filtration and the filtrate was sequentially washed with saturated NaHCO_3 solution (20 mL), brine (20 mL), and deionized water (20 mL). The combined organic phase was dried by anhydrous MgSO_4 and the solvent was removed under reduced pressure. The crude product was purified by silica-gel chromatography (EtOAc:Petroleum ether = 1:19), giving the product a clear oil. $^1\text{H-NMR}$ (300 MHz, Chloroform- d_1) δ 7.82 (1H, d, $J=6.0$ Hz), 7.58-7.43 (2H, m), 7.40 (1H, d, $J=6.0$ Hz), 3.88 (3H, s), 2.53 (3H, s). ESI-MS (Pos): found 179.1 $[\text{M+H}]^+$; calculated for $\text{C}_{10}\text{H}_{10}\text{O}_3$: 178.1.

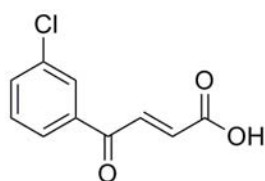
Synthesis of compound **29**



Method: compound **29** was prepared according to the general procedure from 2'-methoxyacetophenone and the product was obtained as a yellow solid.

Characterization: $^1\text{H-NMR}$ (300 MHz, acetone- d_6) δ 7.74 (1H, d, $J=15.3$ Hz), 7.65-7.57 (2H, m), 7.22 (1H, d, $J=9.0$ Hz), 7.07 (1H, t, $J=7.5$ Hz), 6.62 (1H, d, $J=15.9$ Hz), 3.96 (3H, s). ESI-MS (Neg): found 205.0 $[\text{M-H}]^-$; calculated for $\text{C}_{11}\text{H}_{10}\text{O}_4$: 206.1.

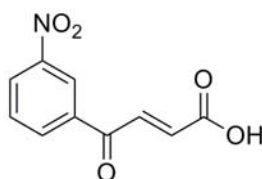
Synthesis of compound **30**



Method: compound **30** was prepared according to the general procedure from 3'-chloroacetophenone and the product was obtained as a yellow solid.

Characterization: $^1\text{H-NMR}$ (400 MHz, acetone- d_6) δ 8.06-8.03 (2H, m), 7.92 (1H, d, $J=15.6$ Hz), 7.75-7.73 (1H, m), 7.66-7.64 (1H, m), 6.80 (1H, d, $J=15.6$ Hz). ESI-MS (Neg): found 209.0 $[\text{M-H}]^-$; calculated for $\text{C}_{10}\text{H}_7\text{ClO}_3$: 210.0.

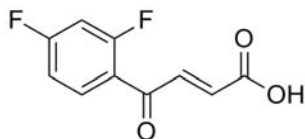
Synthesis of compound **31**



Method: compound **31** was prepared according to the general procedure from 3'-nitroacetophenone and the product was obtained as a yellow solid.

Characterization: $^1\text{H-NMR}$ (300 MHz, acetone- d_6) δ 8.83-8.79 (1H, m), 8.60-8.50 (2H, m), 7.99 (1H, d, $J=15.3$ Hz), 7.96-7.99 (1H, m), 6.86 (1H, d, $J=15.3$ Hz). ESI-MS (Neg): found 220.0 [M-H] $^-$; calculated for $\text{C}_{10}\text{H}_7\text{NO}_5$: 221.0.

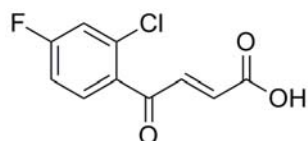
Synthesis of compound **32**



Method: compound **32** was prepared according to the general procedure from 2',4'-difluoroacetophenone and the product was obtained as a yellow solid.

Characterization: $^1\text{H-NMR}$ (300 MHz, acetone- d_6) δ 8.12-8.00 (1H, m), 7.77 (1H, d, $J=15.6$ Hz), 7.38-7.24 (2H, m), 6.821 (1H, d, $J=15.6$ Hz). ESI-MS (Neg): found 211.0 [M-H] $^-$; calculated for $\text{C}_{10}\text{H}_6\text{F}_2\text{O}_3$: 212.0.

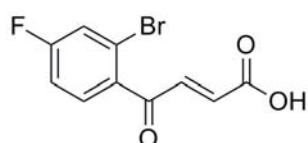
Synthesis of compound **33**



Method: compound **33** was prepared according to the general procedure from 2'-chloro-4'-fluoroacetophenone and the product was obtained as a yellow solid.

Characterization: $^1\text{H-NMR}$ (300 MHz, acetone- d_6) δ 7.79-7.72 (1H, m), 7.50-7.28 (3H, m), 6.60 (1H, d, $J=15.6$ Hz). ESI-MS (Neg): found 226.9 [M-H] $^-$; calculated for $\text{C}_{10}\text{H}_6\text{ClFO}_3$: 228.0.

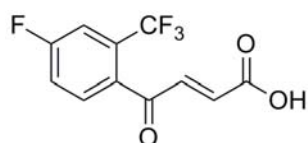
Synthesis of compound **34**



Method: compound **34** was prepared according to the general procedure from 2'-bromo-4'-fluoroacetophenone and the product was obtained as a yellow solid.

Characterization: $^1\text{H-NMR}$ (300 MHz, acetone- d_6) δ 7.76-7.66 (1H, m), 7.66-7.57 (1H, m), 7.47-7.33 (2H, m), 6.57 (1H, d, $J=15.9$ Hz). ESI-MS (Neg): found 270.9 [M-H] $^-$; calculated for $\text{C}_{10}\text{H}_6\text{BrFO}_3$: 271.9.

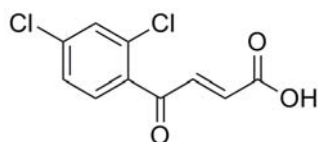
Synthesis of compound **35**



Method: compound **35** was prepared according to the general procedure from 4'-fluoro-2'-trifluoromethylacetophenone and the product was obtained as a yellow solid.

Characterization: $^1\text{H-NMR}$ (300 MHz, acetone- d_6) δ 7.90-7.80 (1H, m), 7.70-7.60 (2H, m), 7.32 (1H, d, $J=15.9$ Hz), 6.53 (1H, 1H, d, $J=15.9$ Hz). ESI-MS (Neg): found 261.0 [M-H] $^-$; calculated for $\text{C}_{11}\text{H}_6\text{F}_4\text{O}_3$: 262.0.

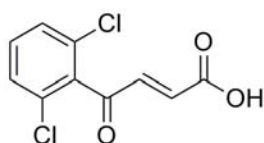
Synthesis of compound 36



Method: compound **36** was prepared according to the general procedure from 2',4'-dichloroacetophenone and the product was obtained as a yellow solid.

Characterization: $^1\text{H-NMR}$ (300 MHz, DMSO- d_6) δ 7.79 (1H, d, $J=2.1$ Hz), 7.67 (1H, d, $J=8.1$ Hz), 7.62-7.56 (1H, m), 7.30 (1H, d, $J=15.9$ Hz), 6.48 (1H, d, $J=15.9$ Hz). ESI-MS (Neg): found 242.9 [M-H] $^-$; calculated for $\text{C}_{10}\text{H}_6\text{Cl}_2\text{O}_3$: 244.0.

Synthesis of compound 37



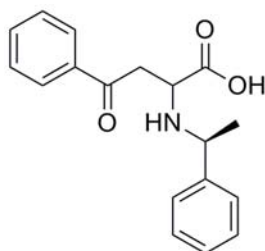
Method: compound **37** was prepared according to the general procedure from 2',6'-dichloroacetophenone and the product was obtained as a yellow solid.

Characterization: $^1\text{H-NMR}$ (300 MHz, acetone- d_6) δ 7.60-7.50 (3H, m), 7.16 (1H, d, $J=16.2$ Hz), 6.49 (1H, d, $J=16.2$ Hz). ESI-MS (Neg): found 242.9 [M-H] $^-$; calculated for $\text{C}_{10}\text{H}_6\text{Cl}_2\text{O}_3$: 244.0.

General procedure for the synthesis of the 2-amino-4-aryl-4-oxo-butanoic acids (38-69)

The (*E*)-4-aryl-4-oxo-but-2-enoic acid (1.0 mmol) was first dissolved in anhydrous ethanol (5 mL) at room temperature under N_2 . Primary amines (1.1 mmol) in anhydrous ethanol (5 mL) were then added to the solution and the temperature was increased to 40-50°C by an oil bath. The resulting mixture was continuously stirred for 4 hours and the formed precipitate was obtained by filtration. The crude product was resuspended in 1:1 acetonitrile/ H_2O (pH 1.0) and purified by recrystallization.

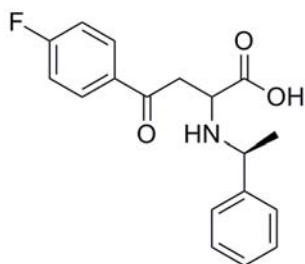
Synthesis of compound 38



Method: compound **38** was prepared according to the general procedure from commercially available (*E*)-4-oxo-4-phenylbut-2-enoic acid and (*S*)-1-phenylethylamine. The product was obtained as a white solid.

Characterization: $^1\text{H-NMR}$ (300 MHz, 1% DCl in acetone- d_6) δ 7.99 (2H, d, $J=9.0$ Hz), 7.70 (2H, d, $J=9.0$ Hz), 7.63 (1H, t, $J=7.5$ Hz), 7.55-7.42 (5H, m), 4.97 (1H, q, $J=7.2$ Hz), 4.16 (1H, t, $J=5.0$ Hz), 4.10-3.96 (2H, m), 1.92 (3H, d, $J=7.2$ Hz). ESI-MS (Pos): found 298.1 $[\text{M}+\text{H}]^+$; calculated for $\text{C}_{18}\text{H}_{19}\text{NO}_3$: 297.1.

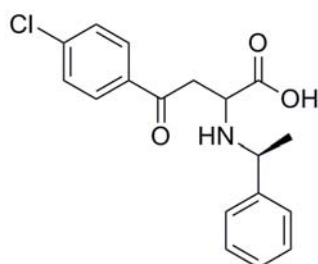
Synthesis of compound **39**



Method: compound **39** was prepared according to the general procedure from (*E*)-4-(4'-fluorophenyl)-4-oxo-but-2-enoic acid (**19**) and (*S*)-1-phenylethylamine. The product was obtained as a white solid.

Characterization: $^1\text{H-NMR}$ (300 MHz, 1% DCl in acetone- d_6) δ 8.22-8.12 (2H,m), 7.87-7.77 (2H, m), 7.54-7.42 (3H, m), 7.32-7.22 (2H, m), 4.94 (1H, q, $J=6.8$ Hz), 4.20-3.98 (3H, m), 1.90 (3H, d, $J=6.9$ Hz). ESI-MS (Pos): found 316.1 $[\text{M}+\text{H}]^+$; calculated for $\text{C}_{18}\text{H}_{18}\text{FNO}_3$: 315.1.

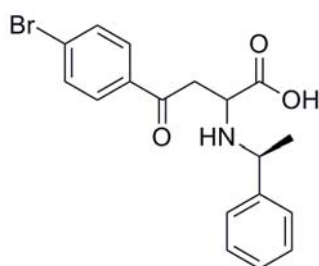
Synthesis of compound **40**



Method: compound **40** was prepared according to the general procedure from commercially available (*E*)-4-(4'-chlorophenyl)-4-oxo-but-2-enoic acid and (*S*)-1-phenylethylamine. The product was obtained as a white solid.

Characterization: ¹H-NMR (300 MHz, 1% DCI in acetonitrile-*d*₃) δ 7.96 (2H, d, *J*=7.2 Hz), 7.50-7.35 (5H, m), 7.08 (2H, d, *J*=7.2 Hz), 4.78 (1H, q, *J*=7.2 Hz), 4.13 (1H, t, *J*=6.0 Hz), 3.82 (2H, d, *J*=6.9 Hz), 1.87 (3H, d, 7.2 Hz). ESI-MS (Pos): found 332.0 [M+H]⁺; calculated for C₁₈H₁₈ClNO₃: 331.1.

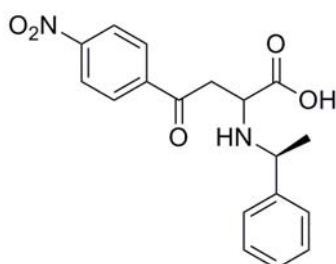
Synthesis of compound **41**



Method: compound **41** was prepared according to the general procedure from (*E*)-4-(4'-bromophenyl)-4-oxo-but-2-enoic acid (**20**) and (*S*)-1-phenylethylamine. The product was obtained as a white solid.

Characterization: ¹H-NMR (300 MHz, 1% DCI in acetone-*d*₆) δ 7.92 (2H, d, *J*=7.5 Hz), 7.85-7.75 (2H, m), 7.70 (2H, d, *J*=7.5 Hz), 4.95 (1H, q, *J*=6.9 Hz), 4.20-3.95 (3H, m), 1.90 (3H, d, *J*=6.9 Hz). ESI-MS (Pos): found 376.0 [M+H]⁺; calculated for C₁₈H₁₈BrNO₃: 375.0.

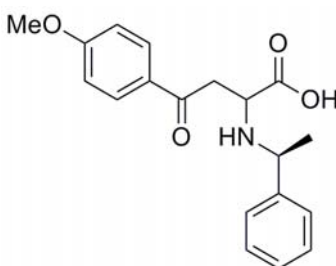
Synthesis of compound **42**



Method: compound **42** was prepared according to the general procedure from (*E*)-4-(4'-nitrophenyl)-4-oxo-but-2-enoic acid (**21**) and (*S*)-1-phenylethylamine. The product was obtained as a white solid.

Characterization: $^1\text{H-NMR}$ (300 MHz, 1% DCl in acetone- d_6) δ 8.41-8.31 (2H, m), 8.37-8.31 (2H, m), 7.94-7.91 (2H, m), 7.56-7.53 (3H, m), 5.01 (1H, q, $J=6.9$ Hz), 4.42-4.30 (1H, m), 4.24-4.16 (2H, m), 1.97 (3H, d, $J=6.9$ Hz). ESI-MS (Pos): found 343.1 $[\text{M}+\text{H}]^+$; calculated for $\text{C}_{18}\text{H}_{18}\text{N}_2\text{O}_5$: 342.1.

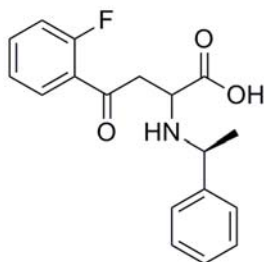
Synthesis of compound **43**



Method: compound **43** was prepared according to the general procedure from commercially available (*E*)-4-(4'-methoxyphenyl)-4-oxo-but-2-enoic acid and (*S*)-1-phenylethylamine. The product was obtained as a white solid.

Characterization: $^1\text{H-NMR}$ (300 MHz, 1% DCl in acetone- d_6) δ 7.99-7.95 (2H, m), 7.95-7.78 (2H, m), 7.52-7.45 (3H, m), 7.05-7.01 (2H, m), 4.95 (1H, q, $J=6.9$ Hz), 4.14-4.09 (1H, m), 4.03-3.91 (2H, m), 3.88 (3H, s), 1.90 (3H, d, $J=6.6$ Hz). ESI-MS (Pos): found 328.1 $[\text{M}+\text{H}]^+$; calculated for $\text{C}_{19}\text{H}_{21}\text{NO}_4$: 327.1.

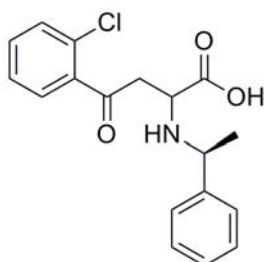
Synthesis of compound **44**



Method: compound **44** was prepared according to the general procedure from (*E*)-4-(2'-fluorophenyl)-4-oxo-but-2-enoic acid (**22**) and (*S*)-1-phenylethylamine. The product was obtained as a white solid.

Characterization: $^1\text{H-NMR}$ (300 MHz, 1% DCl in acetone- d_6) δ 7.95-7.82 (1H, m), 7.82-7.72 (2H, m), 7.72-7.62 (1H, m), 7.52-7.40 (3H, m), 7.36-7.20 (2H, m), 4.94 (1H, q, $J=6.9$ Hz), 4.18 (1H, t, $J=6.0$ Hz), 4.00-3.92 (2H, m), 1.89 (3H, d, $J=6.9$ Hz). ESI-MS (Pos): found 316.1 $[\text{M}+\text{H}]^+$; calculated for $\text{C}_{18}\text{H}_{18}\text{FNO}_3$: 315.1.

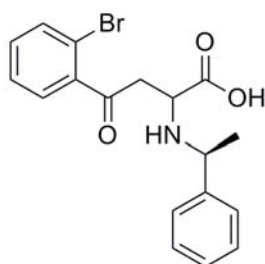
Synthesis of compound **45**



Method: compound **45** was prepared according to the general procedure from (*E*)-4-(2'-chlorophenyl)-4-oxo-but-2-enoic acid (**23**) and (*S*)-1-phenylethylamine. The product was obtained as a white solid.

Characterization: ¹H-NMR (400 MHz, 1% DCl in acetone-*d*₆) δ 7.91-7.89 (1H, m), 7.83-7.81 (2H, m), 7.58-7.40 (6H, m), 4.93 (1H, q, *J*=7.2 Hz), 4.12 (1H, t, *J*=5.2 Hz), 4.00 (2H, d, *J*=5.6 Hz), 1.91 (3H, d, *J*=6.8 Hz). ESI-MS (Pos): found 332.0 [M+H]⁺; calculated for C₁₈H₁₈ClNO₃: 331.1.

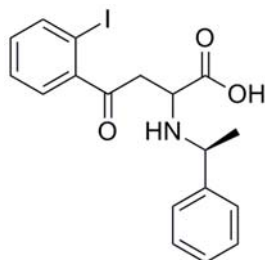
Synthesis of compound **46**



Method: compound **46** was prepared according to the general procedure from (*E*)-4-(2'-bromophenyl)-4-oxo-but-2-enoic acid (**24**) and (*S*)-1-phenylethylamine. The product was obtained as a white solid.

Characterization: ¹H-NMR (300 MHz, 1% DCl in acetone-*d*₆) δ 7.98-7.92 (1H, m), 7.88-7.82 (2H, m), 7.68-7.62 (1H, m), 7.53-7.35 (5H, m), 4.93 (1H, q, *J*=6.9 Hz), 4.16-3.90 (3H, m), 1.94 (3H, d, *J*=6.9 Hz). ESI-MS (Pos): found 376.0 [M+H]⁺; calculated for C₁₈H₁₈BrNO₃: 375.0.

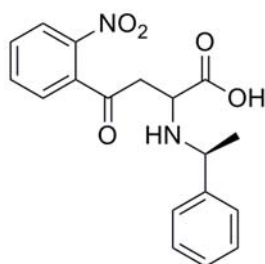
Synthesis of compound **47**



Method: compound **47** was prepared according to the general procedure from (*E*)-4-(2'-iodophenyl)-4-oxo-but-2-enoic acid (**25**) and (*S*)-1-phenylethylamine. The product was obtained as a white solid.

Characterization: $^1\text{H-NMR}$ (300 MHz, 1% DCl in acetone- d_6) δ 8.02-7.94 (2H, m), 7.88-7.80 (2H, m), 7.58-7.42 (4H, m), 7.28-7.20 (1H, m), 4.93 (1H, q, $J=7.2$ Hz), 4.16-3.88 (3H, m), 1.92 (3H, d, $J=7.2$ Hz). ESI-MS (Pos): found 424.0 $[\text{M}+\text{H}]^+$; calculated for $\text{C}_{18}\text{H}_{18}\text{INO}_3$: 423.0.

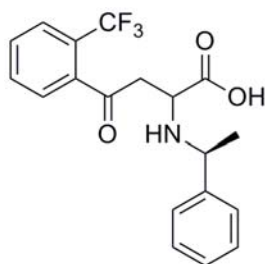
Synthesis of compound **48**



Method: compound **48** was prepared according to the general procedure from (*E*)-4-(2'-nitrophenyl)-4-oxo-but-2-enoic acid (**26**) and (*S*)-1-phenylethylamine. The product was obtained as a white solid.

Characterization: $^1\text{H-NMR}$ (300 MHz, 1% DCI in acetone- d_6) δ 8.25-8.20 (1H, m), 8.12-8.08 (1H, m), 7.92-7.76 (4H, m), 7.52-7.40 (3H, m), 4.91 (1H, q, $J=6.9$ Hz), 4.21-4.05 (2H, m), 3.98-3.88 (1H, m), 1.94 (3H, d, $J=7.2$ Hz). ESI-MS (Pos): found 343.1 $[\text{M}+\text{H}]^+$; calculated for $\text{C}_{18}\text{H}_{18}\text{N}_2\text{O}_5$: 342.1.

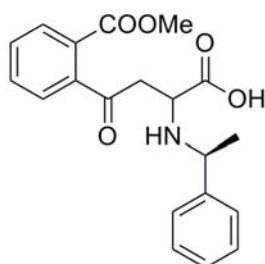
Synthesis of compound **49**



Method: compound **49** was prepared according to the general procedure from (*E*)-4-oxo-4-(2'-trifluoromethylphenyl)-but-2-enoic acid (**27**) and (*S*)-1-phenylethylamine. The product was obtained as a white solid.

Characterization: $^1\text{H-NMR}$ (300 MHz, 1% DCI in acetone- d_6) δ 8.25 (1H, d, $J=7.5$ Hz), 7.92-7.68 (5H, m), 7.56-7.40 (3H, m), 4.97 (1H, q, $J=7.2$ Hz), 4.20 (1H, dd, $J=4.5$, 9.0 Hz), 4.17 (1H, t, $J=2.7$ Hz), 3.90 (1H, dd, $J=4.5$, 9.0 Hz), 1.93 (3H, d, $J=7.5$ Hz). ESI-MS (Pos): found 366.1 $[\text{M}+\text{H}]^+$; calculated for $\text{C}_{19}\text{H}_{18}\text{F}_3\text{NO}_3$: 365.1.

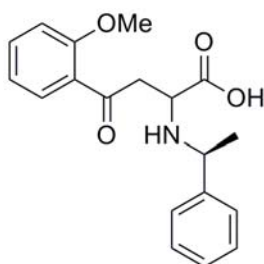
Synthesis of compound **50**



Method: compound **50** was prepared according to the general procedure from (*E*)-4-(2-(methoxycarbonyl)phenyl)-4-oxo-but-2-enoic acid (**28**) and (*S*)-1-phenylethylamine. The product was obtained as a white solid.

Characterization: ¹H-NMR (300 MHz, 1% DCl in acetone-*d*₆) δ 7.90-7.80 (4H, m), 7.65-7.55 (2H, m), 7.50-7.40 (3H, m), 4.94 (1H, q, *J*=6.6 Hz), 4.16 (1H, t, *J*=6.3 Hz), 3.95-3.85 (2H, m), 3.80 (3H, s), 1.97 (3H, d, *J*=6.6 Hz). ESI-MS (Pos): found 356.1 [M+H]⁺; calculated for C₂₀H₂₁NO₅: 355.1.

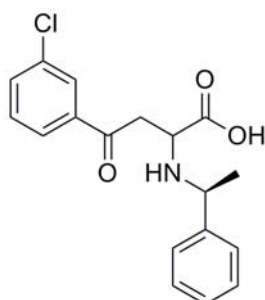
Synthesis of compound **51**



Method: compound **51** was prepared according to the general procedure from (*E*)-4-(2'-methoxyphenyl)-4-oxo-but-2-enoic acid (**29**) and (*S*)-1-phenylethylamine. The product was obtained as a white solid.

Characterization: ¹H-NMR (300 MHz, 1% DCl in acetone-*d*₆) δ 7.85-7.74 (3H, m), 7.60-7.40 (4H, m), 7.17 (1H, d, *J*=7.8 Hz), 7.02 (1H, t, *J*=7.5 Hz), 4.94 (1H, q, 6.9 Hz), 4.13 (1H, t, *J*=6.3 Hz), 4.03-3.98 (2H, m), 3.95 (3H, s), 1.92 (3H, d, *J*=7.2 Hz). ESI-MS (Pos): found 328.1 [M+H]⁺; calculated for C₁₉H₂₁NO₄: 327.1.

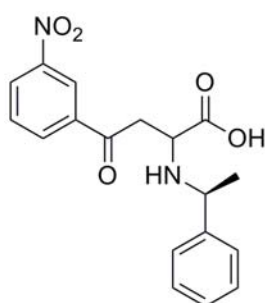
Synthesis of compound **52**



Method: compound **52** was prepared according to the general procedure from (*E*)-4-(3'-chlorophenyl)-4-oxo-but-2-enoic acid (**30**) and (*S*)-1-phenylethylamine. The product was obtained as a white solid.

Characterization: $^1\text{H-NMR}$ (300 MHz, 1% DCl in acetone- d_6) δ 7.98-7.90 (2H, m), 7.84-7.76 (2H, m), 7.70-7.64 (1H, m), 7.60-7.40 (4H, m), 4.97 (1H, q, $J=6.9$ Hz), 4.20-3.98 (3H, m), 1.90 (3H, d, $J=6.9$ Hz). ESI-MS (Pos): found 332.0 $[\text{M}+\text{H}]^+$; calculated for $\text{C}_{18}\text{H}_{18}\text{ClNO}_3$: 331.1.

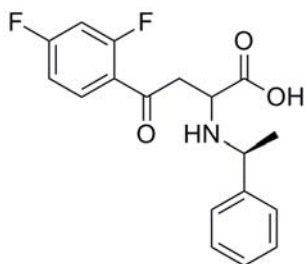
Synthesis of compound **53**



Method: compound **53** was prepared according to the general procedure from (*E*)-4-(3'-nitrophenyl)-4-oxo-but-2-enoic acid (**31**) and (*S*)-1-phenylethylamine. The product was obtained as a white solid.

Characterization: $^1\text{H-NMR}$ (300 MHz, 1% DCl in acetone- d_6) δ 8.74-8.70 (1H, m), 8.54-8.40 (2H, m), 7.90-7.80 (3H, m), 7.55-7.45 (3H, m), 4.95 (1H, q, $J=7.2$), 4.30-4.10 (3H, m), 1.79 (3H, d, $J=7.2$ Hz). ESI-MS (Pos): found 343.1 $[\text{M}+\text{H}]^+$; calculated for $\text{C}_{18}\text{H}_{18}\text{N}_2\text{O}_5$: 342.1.

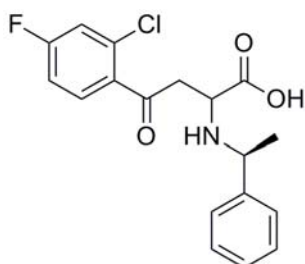
Synthesis of compound **54**



Method: compound **54** was prepared according to the general procedure from (*E*)-4-(2',4'-difluorophenyl)-4-oxo-but-2-enoic acid (**32**) and (*S*)-1-phenylethylamine. The product was obtained as a white solid.

Characterization: $^1\text{H-NMR}$ (300 MHz, 1% DCl in acetone- d_6) δ 8.15-8.05 (1H, m), 7.92-7.80 (2H, m), 7.55-7.40 (4H, m), 7.30-7.20 (1H, m), 4.92 (1H, q, $J=6.9$ Hz), 4.20-3.90 (3H, m), 1.93 (3H, d, $J=7.2$ Hz). ESI-MS (Pos): found 334.0 $[\text{M}+\text{H}]^+$; calculated for $\text{C}_{18}\text{H}_{17}\text{F}_2\text{NO}_3$: 333.1.

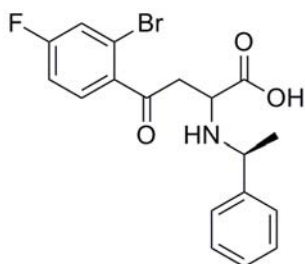
Synthesis of compound **55**



Method: compound **55** was prepared according to the general procedure from (*E*)-4-(2'-chloro-4'-fluorophenyl)-4-oxo-but-2-enoic acid (**32**) and (*S*)-1-phenylethylamine. The product was obtained as a white solid.

Characterization: $^1\text{H-NMR}$ (300 MHz, 1% DCI in acetone- d_6) δ 8.10-8.00 (1H, m), 7.83-7.78 (2H, m), 7.52-7.20 (5H, m), 4.93 (1H, q, $J=6.9$ Hz), 4.12 (1H, t, $J=6.3$ Hz), 4.00 (2H, d, $J=6.3$ Hz), 1.92 (3H, d, $J=7.2$ Hz). ESI-MS (Pos): found 350.0 $[\text{M}+\text{H}]^+$; calculated for $\text{C}_{18}\text{H}_{17}\text{ClFNO}_3$: 349.1.

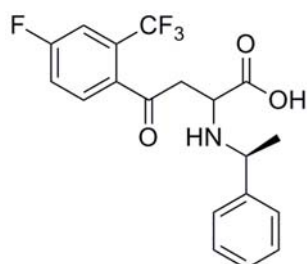
Synthesis of compound **56**



Method: compound **56** was prepared according to the general procedure from (*E*)-4-(2'-bromo-4'-fluorophenyl)-4-oxo-but-2-enoic acid (**34**) and (*S*)-1-phenylethylamine. The product was obtained as a white solid.

Characterization: $^1\text{H-NMR}$ (300 MHz, 1% DCI in acetone- d_6) δ 8.15-8.05 (1H, m), 7.92-7.82 (2H, m), 7.54-7.40 (4H, m), 7.35-7.25 (1H, m), 4.95 (1H, q, $J=7.2$ Hz), 4.15-3.90 (3H, m), 1.92 (3H, d, $J=7.2$ Hz). ESI-MS (Pos): found 394.0 $[\text{M}+\text{H}]^+$; calculated for $\text{C}_{18}\text{H}_{17}\text{BrFNO}_3$: 393.0.

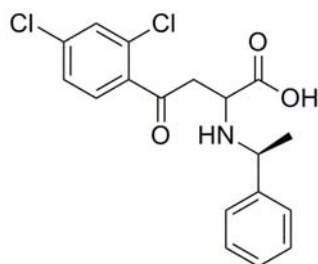
Synthesis of compound **57**



Method: compound **57** was prepared according to the general procedure from (*E*)-4-(4'-fluoro-2'-trifluoromethylphenyl)-4-oxo-but-2-enoic acid (**35**) and (*S*)-1-phenylethylamine. The product was obtained as a white solid.

Characterization: $^1\text{H-NMR}$ (300 MHz, 1% DCl in acetone- d_6) δ 8.42-8.32 (1H, m), 7.90-7.80 (2H, m), 7.65-7.40 (5H, m), 4.95 (1H, q, $J=7.2$ Hz), 4.20-4.00 (2H, m), 3.95-3.85 (1H, dd, $J=6.3, 15.0$ Hz). 1.94 (3H, d, $J=7.2$ Hz). ESI-MS (Pos): found 384.1 $[\text{M}+\text{H}]^+$; calculated for $\text{C}_{19}\text{H}_{17}\text{F}_4\text{NO}_3$: 383.1.

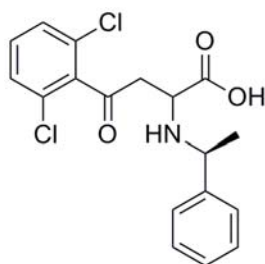
Synthesis of compound **58**



Method: compound **58** was prepared according to the general procedure from (*E*)-4-(2',4'-dichlorophenyl)-4-oxo-but-2-enoic acid (**36**) and (*S*)-1-phenylethylamine. The product was obtained as a white solid.

Characterization: $^1\text{H-NMR}$ (300 MHz, 1% DCl in acetone- d_6) δ 8.00 (1H, d, $J=7.5$ Hz), 7.86-7.80 (2H, m), 7.60-7.40 (5H, m), 4.92 (1H, q, $J=6.9$ Hz), 4.15-3.95 (3H, m), 1.92 (3H, d, $J=6.9$ Hz). ESI-MS (Pos): found 366.0 $[\text{M}+\text{H}]^+$; calculated for $\text{C}_{18}\text{H}_{17}\text{Cl}_2\text{NO}_3$: 365.1.

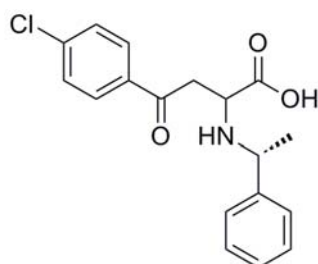
Synthesis of compound **59**



Method: compound **59** was prepared according to the general procedure from (*E*)-4-(2',6'-dichlorophenyl)-4-oxo-but-2-enoic acid (**37**) and (*S*)-1-phenylethylamine. The product was obtained as a white solid.

Characterization: $^1\text{H-NMR}$ (300 MHz, 1% DCl in acetone- d_6) δ 7.90-7.80 (2H, m), 7.55-7.40 (6H, m), 4.86 (1H, q, $J=6.9$ Hz), 4.25-4.10 (2H, m), 4.02-3.88 (1H, m), 1.88 (3H, d, $J=7.2$ Hz). ESI-MS (Pos): found 366.0 $[\text{M}+\text{H}]^+$; calculated for $\text{C}_{18}\text{H}_{17}\text{Cl}_2\text{NO}_3$: 365.0.

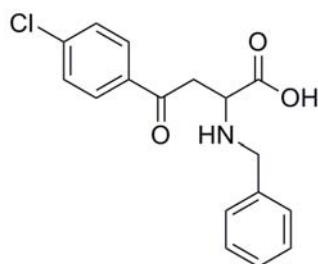
Synthesis of compound **60**



Method: compound **60** was prepared according to the general procedure from commercially available (*E*)-4-(4'-chlorophenyl)-4-oxo-but-2-enoic acid and (*R*)-1-phenylethylamine. The product was obtained as a white solid.

Characterization: $^1\text{H-NMR}$ (300 MHz, 1% DCI in acetone- d_6) δ 8.00 (2H, d, $J=7.2$ Hz), 7.82-7.75 (2H, m), 7.58 (2H, d, $J=7.2$ Hz) 7.52-7.42 (3H, m), 4.86 (1H, q, $J=7.2$ Hz), 4.20-4.10 (1H, m), 4.10-4.00 (2H, m), 1.90 (3H, d, 7.2 Hz). ESI-MS (Pos): found 332.0 $[\text{M}+\text{H}]^+$; calculated for $\text{C}_{18}\text{H}_{18}\text{ClNO}_3$: 331.1.

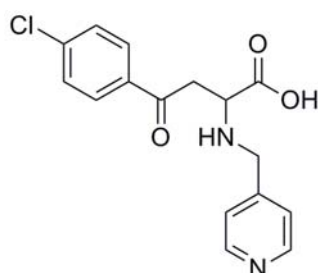
Synthesis of compound **61**



Method: compound **61** was prepared according to the general procedure from commercially available (*E*)-4-(4'-chlorophenyl)-4-oxo-but-2-enoic acid and benzylamine. The product was obtained as a white solid.

Characterization: $^1\text{H-NMR}$ (300 MHz, 1% DCI in acetone- d_6) δ 8.06 (2H, dd, $J=2.1$ Hz, 4.5 Hz), 7.76-7.73 (2H, m), 7.58 (2H, dd, $J=2.1$ Hz, 8.7 Hz), 7.45-6.43 (3H, m), 4.63 (1H, t, $J=4.8$ Hz), 4.60 (2H, s), 4.22 (1H, dd, $J=5.1$ Hz, 18.0 Hz), 4.10 (2H, dd, $J=2.1$ Hz, 8.7 Hz). ESI-MS (Pos): found 318.0 $[\text{M}+\text{H}]^+$; calculated for $\text{C}_{17}\text{H}_{16}\text{ClNO}_3$: 317.1.

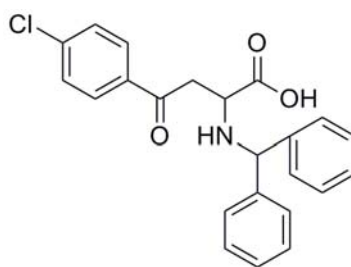
Synthesis of compound **62**



Method: compound **62** was prepared according to the general procedure from commercially available (*E*)-4-(4'-chlorophenyl)-4-oxo-but-2-enoic acid and pyridin-4-ylmethanamine. The product was obtained as a white solid.

Characterization: $^1\text{H-NMR}$ (300 MHz, 1% DCl in acetone- d_6) δ 9.13 (2H, d, $J=6.0$ Hz), 8.62 (2H, d, $J=6.0$ Hz), 8.08 (2H, d, $J=7.2$ Hz), 7.56 (2H, d, $J=7.2$ Hz), 5.08 (2H, s), 4.92 (1H, t, $J=4.8$ Hz), 4.31 (1H, dd, $J=4.8$ Hz, 18.0 Hz) 4.12 (1H, dd, $J=4.8$ Hz, 18.0 Hz). ESI-MS (Pos): found 319.0 $[\text{M}+\text{H}]^+$; calculated for $\text{C}_{16}\text{H}_{15}\text{ClN}_2\text{O}_3$: 318.1.

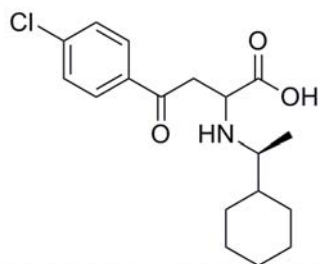
Synthesis of compound **63**



Method: compound **63** was prepared according to the general procedure from commercially available (*E*)-4-(4'-chlorophenyl)-4-oxo-but-2-enoic acid and diphenylmethanamine. The product was obtained as a white solid.

Characterization: $^1\text{H-NMR}$ (300 MHz, 1% DCl in acetone- d_6) δ 8.04-8.01 (2H, m), 7.58-7.53 (2H, m), 7.48-7.41 (4H, m), 7.30-7.19 (6H, m), 5.14 (1H, s), 3.67 (1H, t, $J=5.7$ Hz), 3.56-3.48 (2H, m). ESI-MS (Pos): found 394.0 $[\text{M}+\text{H}]^+$; calculated for $\text{C}_{23}\text{H}_{20}\text{ClNO}_3$: 393.1.

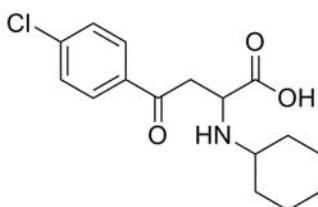
Synthesis of compound **64**



Method: compound **64** was prepared according to the general procedure from commercially available (*E*)-4-(4'-chlorophenyl)-4-oxo-but-2-enoic acid and (*S*)-1-cyclohexylethanamine. The product was obtained as a white solid.

Characterization: $^1\text{H-NMR}$ (300 MHz, 1% DCl in acetone- d_6) δ 8.08 (2H, d, $J=7.5$ Hz), 7.58 (2H, d, $J=7.5$ Hz), 4.80 (1H, m), 4.22 (1H, t, $J=5.7$ Hz), 4.17 (1H, d, $J=6.0$ Hz), 3.60-3.40 (1H, m), 2.00-1.60 (6H, m), 1.47 (3H, dd, $J=6.0, 12.0$), 1.40-1.10 (5H, m). ESI-MS (Pos): found 338.2 $[\text{M}+\text{H}]^+$; calculated for $\text{C}_{18}\text{H}_{24}\text{ClNO}_3$: 337.1.

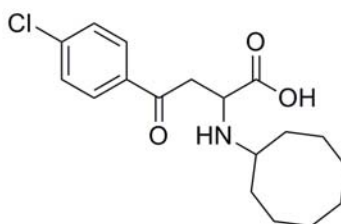
Synthesis of compound **65**



Method: compound **65** was prepared according to the general procedure from commercially available (*E*)-4-(4'-chlorophenyl)-4-oxo-but-2-enoic acid and cyclohexanamine. The product was obtained as a white solid.

Characterization: $^1\text{H-NMR}$ (300 MHz, 1% DCI in acetone- d_6) δ 8.02 (2H, d, $J=7.2$ Hz), 7.57 (2H, d, $J=7.2$ Hz), 4.78 (1H, t, $J=5.4$ Hz), 4.20-4.00 (2H, m), 3.50-3.40 (1H, m), 2.40-2.20 (2H, m), 1.90-1.60 (4H, m), 1.40-1.10 (4H, m). ESI-MS (Pos): found 310.1 $[\text{M}+\text{H}]^+$; calculated for $\text{C}_{16}\text{H}_{20}\text{ClNO}_3$: 309.1.

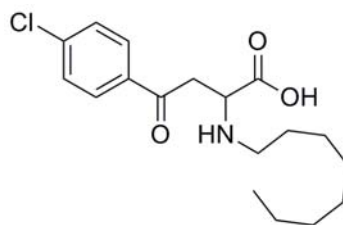
Synthesis of compound **66**



Method: compound **66** was prepared according to the general procedure from commercially available (*E*)-4-(4'-chlorophenyl)-4-oxo-but-2-enoic acid and cyclooctylamine. The product was obtained as a white solid.

Characterization: $^1\text{H-NMR}$ (300 MHz, 1% DCI in acetone- d_6) δ 8.05 (2H, d, $J=7.2$ Hz), 7.56 (2H, d, $J=7.2$ Hz), 4.78 (1H, t, $J=5.1$ Hz), 4.10-4.06 (2H, m), 3.73-3.63 (1H, m), 2.30-2.10 (4H, m), 1.90-1.40 (10H, m). ESI-MS (Pos): found 338.2 $[\text{M}+\text{H}]^+$; calculated for $\text{C}_{18}\text{H}_{24}\text{ClNO}_3$: 337.1.

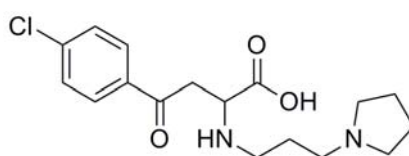
Synthesis of compound **67**



Method: compound **67** was prepared according to the general procedure from commercially available (*E*)-4-(4'-chlorophenyl)-4-oxo-but-2-enoic acid and *n*-octylamine. The product was obtained as a white solid.

Characterization: $^1\text{H-NMR}$ (300 MHz, 1% DCl in acetone- d_6) δ 8.03 (2H, d, $J=7.2$ Hz), 7.57 (2H, d, $J=7.2$ Hz), 4.58 (1H, t, $J=4.8$ Hz), 4.23 (1H, dd, $J=4.8$ Hz, 10.8 Hz), 4.08 (1H, dd, $J=4.8$ Hz, 10.8 Hz), 3.40-3.26 (2H, m), 2.00-1.90 (2H, m), 1.50-1.20 (10H, m), 0.85 (3H, t, $J=6.0$ Hz). ESI-MS (Pos): found 340.2 $[\text{M}+\text{H}]^+$; calculated for $\text{C}_{18}\text{H}_{26}\text{ClNO}_3$: 339.2.

Synthesis of compound **68**

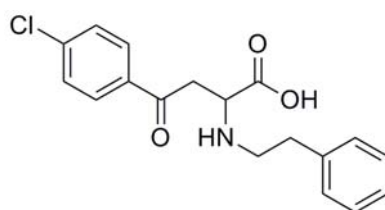


Method: compound **68** was prepared according to the general procedure from commercially available (*E*)-4-(4'-chlorophenyl)-4-oxo-but-2-enoic acid and 3-(pyrrolidin-1-yl)propan-1-amine. The product was obtained as a white solid.

Characterization: $^1\text{H-NMR}$ (300 MHz, 1% DCl in acetone- d_6) δ 8.05 (2H, d, $J=7.5$ Hz), 7.58 (2H, d, $J=7.2$ Hz), 4.76 (1H, t, $J=5.1$ Hz), 4.23 (1H, dd, $J=5.1$ Hz, 12.0 Hz),

4.10-4.00 (2H, m), 3.80-3.70 (2H, m), 3.65-3.50 (4H, m), 3.30-3.20 (2H, m), 2.60-2.50 (2H, m), 2.20-2.10 (2H, m). ESI-MS (Pos): found 339.1 [M+H]⁺; calculated for C₁₇H₂₃ClN₂O₃: 338.1.

Synthesis of compound **69**



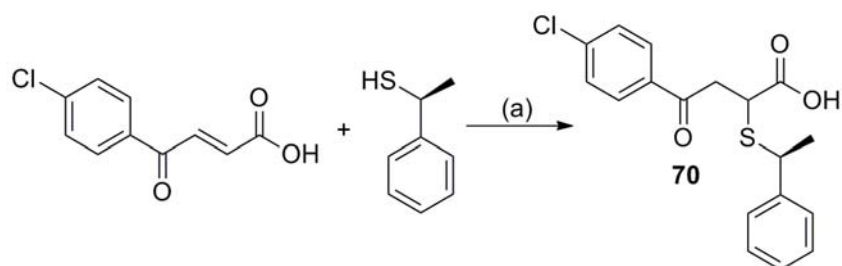
Method: compound **69** was prepared according to the general procedure from commercially available (*E*)-4-(4'-chlorophenyl)-4-oxo-but-2-enoic acid and 2-phenylethanamine. The product was obtained as a white solid.

Characterization: ¹H-NMR (300 MHz, 1% DCl in acetone-*d*₆) δ 8.04 (2H, d, *J*=7.2 Hz), 7.59 (2H, d, *J*=7.2 Hz), 4.75 (1H, t, *J*=5.1 Hz), 4.23 (1H, dd, *J*=4.8 Hz, 12.0 Hz), 4.10 (1H, dd, *J*=5.1 Hz, 12.0 Hz), 3.65-3.55 (2H, m), 3.30 (2H, t, *J*=6.6 Hz). ESI-MS (Pos): 332.0 [M+H]⁺; calculated for C₁₈H₁₈ClNO₃: 331.1.

Synthesis of compound **70**

Method: compound **70** was prepared according to **Scheme 3.7** (178). Commercially available (*E*)-4-(4'-chlorophenyl)-4-oxo-but-2-enoic acid (1.0 mmol) was first dissolved in anhydrous methanol (20 mL) at room temperature under N₂. (*S*)-1-

phenylethanethiol (1.5 mmol) was subsequently added into the solution and the resulting mixture was continuously stirred at room temperature for 4 hours before the solvent was removed under reduced pressure. Product precipitated out by adding deionized water to the oily residue and was separated by filtration. The product was purified by recrystallization from benzene.



Scheme 3.7 Synthesis of compound 70

Reagents and conditions: (a) MeOH, 25°C, 5 hours.

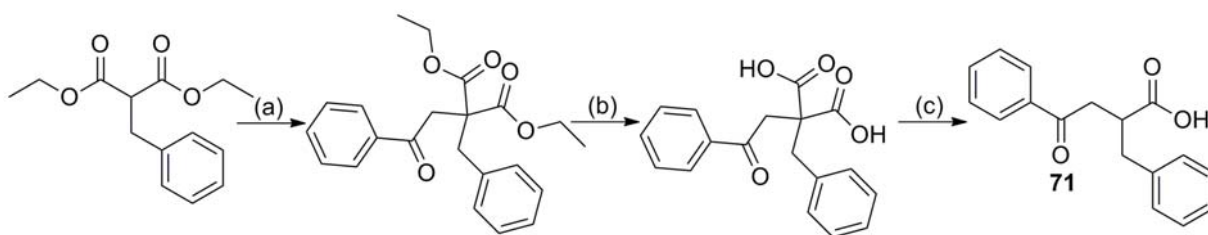
Characterization: $^1\text{H-NMR}$ (300 MHz, 1% DCl in acetone- d_6) δ 8.03-7.97 (2H, m), 7.65-7.27 (7H, m), 4.53-4.40 (1H, m), 3.96-3.50 (2H, m), 3.40-3.10 (1H, m), 1.65 (3H, dd, $J=7.5$ Hz, 15.0 Hz). ESI-MS (Pos): 349.0 $[\text{M}+\text{H}]^+$; calculated for $\text{C}_{18}\text{H}_{17}\text{ClO}_3\text{S}$: 348.1.

Synthesis of compound 71

Method: compound 71 was prepared according to **Scheme 3.8** (179). Magnesium (pre-treated with HCl solution) (0.1 mmol), anhydrous CCl_4 (0.25 mL), and diethyl benzylmalonate (0.1 mmol) were first suspended in anhydrous ethanol (12.5 mL) at room temperature under N_2 . After heating at reflux for 2 hours, the solvent was

removed under reduced pressure and subsequently a solution of phenacyl bromide (0.1 mmol) in anhydrous benzene (150 mL) was added at once. The resulting mixture was allowed to continuously stir at room temperature for 2 days before it was quenched by adding 10% HCl aqueous solution (75 mL). The organic phase was then collected, dried over anhydrous MgSO_4 , concentrated, and the diethyl benzylphenacilmalonate was recrystallized from petroleum ether, which was then resuspended into KOH aqueous/ethanol (1:1) solution. Within a few minutes, precipitates were formed, filtered, and subsequently redissolved in water. The pH was adjusted by concentrated HCl solution to 1.0, and the benzylphenacilmalonic acid was precipitated from the aqueous solution, which was directly used for the next thermal decarboxylation without further purification. Compound **71** was purified by recrystallization from an acetic acid/ H_2O (3:2) solution.

Characterization: $^1\text{H-NMR}$ (300 MHz, acetone- d_6) δ 7.97 (2H, d, $J=7.5$ Hz), 7.63-7.43 (2H, m), 7.35-7.15 (5H, m), 3.55-3.40 (1H, m), 3.40-3.27 (1H, m), 3.18-3.00 (2H, m), 2.97-2.85 (1H, m). ESI-MS (Neg): 267.1 $[\text{M-H}]^-$; calculated for $\text{C}_{17}\text{H}_{16}\text{O}_3$: 268.1.

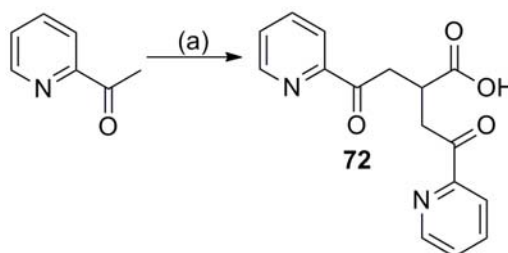


Scheme 3.8 Synthesis of compound **71**

Reagents and conditions: (a) Mg, CCl_4 , phenacyl bromide, anhydrous ethanol, 25°C , 48 hours; (b) KOH/ H_2O solution, 25°C , 2 hours; (c) water, reflux, 3 hours.

Synthesis of compound 72

Method: compound **72** was synthesized as a side product according to **Scheme 3.9**. 2-Acetyl pyridine (1.0mmol), glyoxylic acid monohydrate (1.2mmol), methanol (1.0 mL), and 2.0M KOH aqueous solution (20mL) were mixed at room temperature under N₂. The resulting mixture was continuously stirred at 50°C for 5 hours before the reaction was quenched by adding 10% HCl solution drop-wise and the final pH was controlled to 5.0. The aqueous solution was extracted with CH₂Cl₂ (3×30 mL), and the organic phase was collected, combined, dried over anhydrous MgSO₄. The solvent was then removed under reduced pressure. The crude product was purified by silica-gel chromatography (EtOAc:Petroleum ether = 3:1).



Scheme 3.9 Synthesis of compound 72

Reagents and conditions: glyoxylic acid monohydrate, KOH aqueous solution, 50°C, 5 hours.

Characterization: ¹H-NMR (300 MHz, acetone-*d*₆) δ 8.70-8.66 (2H, m), 8.03-7.95 (4H, m), 7.62-7.58 (2H, m), 3.80 (2H, dd, *J*=4.8 Hz, 12.0 Hz), 3.65 (1H, quint), 3.48 (2H, dd, *J*=4.8 Hz, 12.0 Hz). ESI-MS (Pos): 299.1 [M+H]⁺; calculated for C₁₆H₁₄N₂O₄: 298.1.

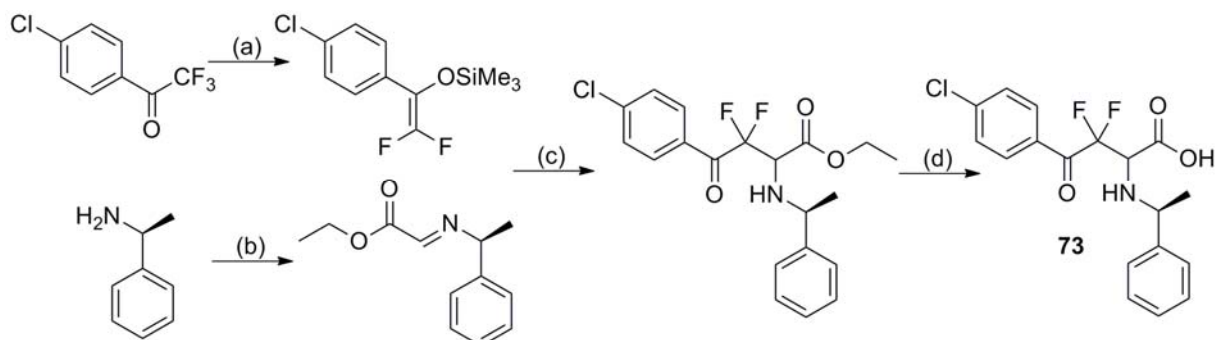
Synthesis of Stable 2-amino-4-aryl-4-oxo-butanoic acid analogues

Synthesis of compound 73

Compound **73** was synthesized according to **Scheme 3.10**.

Method: Commercial available 1-(4-chlorophenyl)-2,2,2-trifluoroethanone (1.0 mmol), trimethylsilyl chloride (2.0mmol), and Mg metal (pre-treated with HCl solution) (2.0 mmol) were first suspended in anhydrous THF (10 mL) at room temperature under N₂. The resulting suspension was cooled to 0°C on an ice bath. The mixture was stirred for 30 minutes and the resulting precipitate was removed by filtration. The filtrate was collected and the solvent was removed under reduced pressure, resulting the product difluoro enol silyl ether as a yellow oil (180-181) without further purification. The Schiff base was prepared by mixing ethyl glyoxylate (1.0 mmol), (S)-1-phenylethylamine (1.1mmol), and anhydrous ethanol (20 mL) at room temperature under N₂ for 1 hour. The solvent was removed under reduced pressure and the Schiff base was purified by silica-gel chromatography (182). Subsequently, the Schiff base (0.4 mmol) and difluoro enol silyl ether (0.4 mmol) were first dissolved in anhydrous CH₂Cl₂ (10 mL) and the solution was cooled to -78°C. TiCl₄ CH₂Cl₂ solution (0.44 mmol) was then added into the solution drop-wise and the resulting mixture was stirred for 1 hour before it was quenched by deionized water (10 mL). The mixture was extracted by CH₂Cl₂ (3×20 mL), which was combined, dried over anhydrous MgSO₄, and the solvent was removed under reduced pressure. The product was separated by silica-gel chromatography, which was then hydrolyzed by 1M NaOH aqueous solution (20 mL) for 1 hour. Crude product forms precipitation when the pH was adjusted to 1.0 by adding 10% HCl

aqueous solution. The product was filtrated and dried in the oven. Compound **73** was obtained as a white solid without further purification.



Scheme 3.10 Synthesis of compound **73**

Reagents and conditions: (a) Mg, TMS-Cl, THF, 0°C, 30 minutes; (b) ethyl glyoxylate, anhydrous ethanol, 25°C, 1 hour; (c) TiCl₄, CH₂Cl₂, -78°C, 1 hour; (d) 1M NaOH aqueous solution, 25°C, 1 hour.

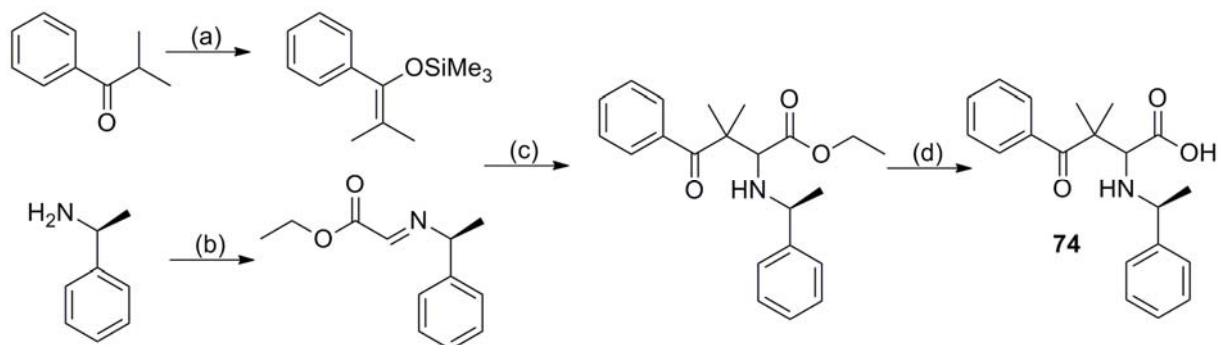
Characterization: ¹H-NMR (300 MHz, acetone-*d*₆) δ 7.87-7.45 (9H, m), 5.38 (1H, dd, *J*=3.0 Hz, 18.0 Hz), 5.23 (1H, q, *J*=6.9 Hz), 2.04-2.00 (3H, m). ESI-MS (Pos): 368.0 [M+H]⁺, calculated for C₁₈H₁₆ClF₂NO₃: 367.1.

Synthesis of compound **74**

Compound **74** was synthesized according to **Scheme 3.11**.

Method: The synthetic method is similar with compound **73**. The only difference is the formation of dimethyl enol silyl ether (**183**). *N*-methyl-*N*-(TMS)acetamide (1.5 mmol) was added to a suspended of isobutylacetophenone (1.0 mmol) and NaH (0.05 mmol) in anhydrous DMF (10 mL) at room temperature under N₂. The resulting mixture was continuously stirred at 60-65 °C for 1 hour. Hexane was then added to the mixture, which was used to generate the hexane phase and DMF phase. DMF phase was continuously extracted with hexane (3×20 mL) and the hexane was combined and washed with brine (20 mL) and deionized water (20 mL) sequentially. The organic phase was subsequently dried by anhydrous MgSO₄ and the solvent was removed

under reduced pressure, giving the desired dimethyl enol silyl ether without further purification.



Scheme 3.11 Synthesis of compound 74

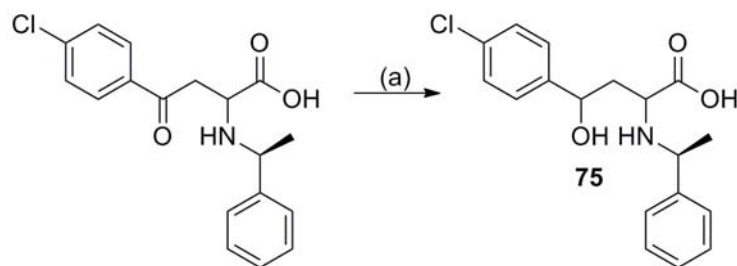
Reagents and conditions: Reaction condition: (a) *N*-methyl-*N*-trimethylsilylacetylamide, DMF, 60°C, 1 hour; (b) ethyl glyoxylate, anhydrous ethanol, 25°C, 1 hour; (c) TiCl₄, CH₂Cl₂, -78°C, 1 hour; (d) 1M NaOH aqueous solution, 25°C, 1 hour.

Characterization: ESI-MS (Pos): 326.2 [M+H]⁺, calculated for C₂₀H₂₃NO₃: 325.2.

Synthesis of compound 75

Compound 75 was synthesized according to **Scheme 3.12** (184).

Method: compound 40 (1.0 mmol) was first suspended in anhydrous methanol (20 mL) at room temperature under N₂. The resulting suspension was cooled to 0°C on ice bath and subsequently sodium borohydride NaBH₄ (8.0 mmol) was added into the suspension at once. The reaction temperature was then allowed to raise to room temperature the mixture was continuously stirred for 4 hours before the solvent was removed under reduced pressure. The reaction was quenched by adding deionized water (20 mL) and the pH was adjusted to 6.0 by 10% HCl aqueous solution. The precipitate was obtained by filtration and washed with ether, giving the crude product as a white solid without further purification.



Scheme 3.12 Synthesis of compound 75

Reagents and conditions: (a) sodium borohydride, methanol, 25°C, 4 hours.

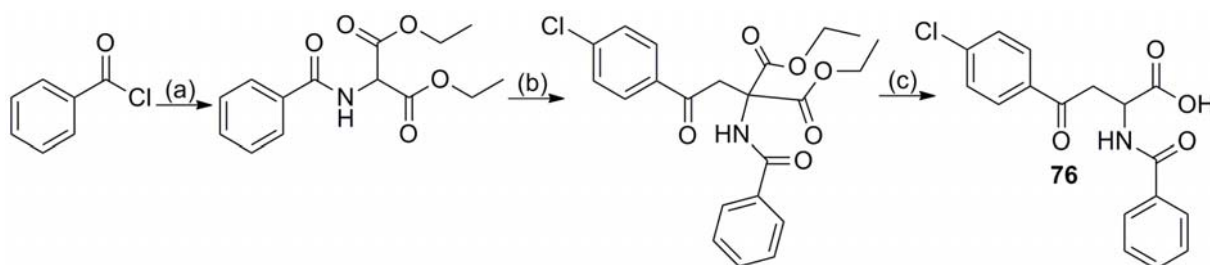
Characterization: $^1\text{H-NMR}$ (300 MHz, $\text{D}_2\text{O-d}_2$) δ 7.30-7.20 (7H, m), 7.05-7.00 (2H, m), 4.71-4.54 (1H, t, $J=6.0$ Hz), 3.54 (1H, q, $J=6.6$ Hz), 2.64-2.57 (1H, m), 1.78 (1H, t, $J=6.9$ Hz), 1.28-1.23 (3H, m). ESI-MS (Pos): 334.1 $[\text{M}+\text{H}]^+$; ESI-MS (Neg): 332.1 $[\text{M}-\text{H}]^-$; calculated for $\text{C}_{18}\text{H}_{20}\text{ClNO}_3$: 333.1.

Synthesis of compound 76

Compound **76** was synthesized according to **Scheme 3.13**.

Method: 2-Aminodiethylmalonate (1.1 mmol) and TEA (1.2 mmol) were first dissolved in anhydrous CH_2Cl_2 (20 mL) at room temperature under N_2 . The solution was cooled to 0°C on an ice bath. Benzoyl chloride (1.0 mmol) was then added into the resulting solution and the mixture was continuously stirred for 3 hours. The reaction was then quenched by 20 mL deionized water. The organic phase was separated, dried by anhydrous MgSO_4 , and the solvent was removed under reduced pressure. The crude diethyl amidomalonate was purified by silica-gel chromatography (185). Sodium hydride (1.1 mmol) was added to a solution of diethyl amidomalonate (1.0 mmol) in anhydrous DMF (15 mL) at room temperature under N_2 . The resulting suspension was continuously stirred for 5 hours, after which a solution of 2-bromo-4'-chloroacetophenone (1.0 mmol) in anhydrous DMF (15 mL) was added into the mixture drop-wise. The solution was

continuously stirred for another 15 hours before the reaction was quenched by deionized water (20 mL). The product was obtained by extraction with ethyl acetate (3×20 mL) and purified by silica-gel chromatography. The resulting 2-substituted amidomalonic acid diethyl esters were then stirred with 10 mL 1M NaOH at room temperature for 2 hours. Glacial acetic acid was added, and the solution was reflux for 1 hour. The cooled solution was then extracted with ethyl acetate and the combined organic phase was concentrated. The crude residue was separated by silica-gel chromatography, giving compound **76** as a white powder (186).



Scheme 3.13 Synthesis of compound 76

Reagents and conditions: (a) 2-aminodiethylmalonate, TEA, anhydrous CH_2Cl_2 , 25°C, 3 hours; (b) 2-bromo-4'-chloroacetophenone, NaH, anhydrous DMF, 25°C, 20 hours; (c) 1M NaOH aqueous solution, then HCl reflux, 2 hours.

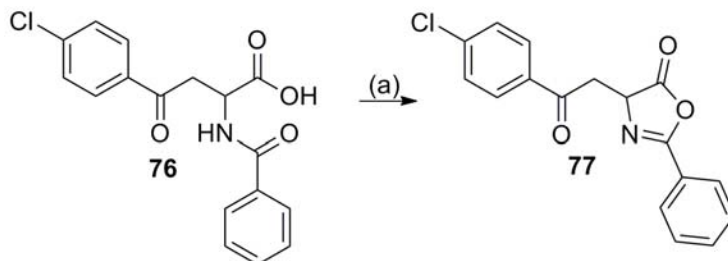
Characterization: $^1\text{H-NMR}$ (300 MHz, methanol- d_4) δ 8.00 (2H, d, $J=6.9$ Hz), 7.81 (2H, m), 7.53-7.41 (5H, m), 5.12 (1H, t, $J=6.3$ Hz), 3.66 (2H, q, $J=6.3$ Hz). ESI-MS (Neg): 330.1 [M-H] $^-$, calculated for $\text{C}_{17}\text{H}_{14}\text{ClNO}_4$: 331.1.

Synthesis of compound 77

Compound **77** was synthesized according to **Scheme 3.14**.

Method: Compound **76** (1.0 mmol) and TEA (1.1 mmol) were first dissolved in 10 anhydrous CH_2Cl_2 (10 mL) at room temperature N_2 . EDC·HCl (1.1 mmol) was then added into the solution and the resulting mixture was continuously stirred for a further 30 minutes. The solvent was then removed under reduced pressure and the crude

product was purified by silica-gel chromatography, giving the product as a white powder (187).



Scheme 3.14 Synthesis of compound 77

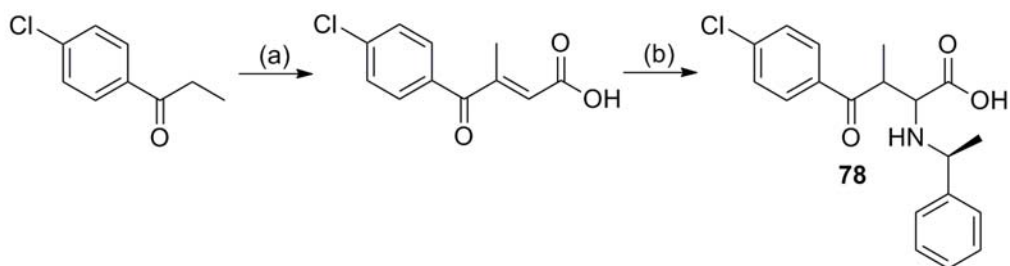
Reaction condition: EDC·HCl, TEA, anhydrous CH₂Cl₂, 25°C, 30 minutes.

Characterization: ¹H-NMR (300 MHz, chloroform-*d*₁) δ 7.97 (2H, d, *J*=7.8 Hz), 7.85 (2H, m), 7.54-7.40 (5H, m), 4.73 (1H, t, *J*=5.4 Hz), 3.89 (1H, dd, *J*=3.6 Hz, 14.4 Hz), 3.58 (1H, dd, *J*=5.4 Hz, 12.6 Hz).

Synthesis of compound 78

Compound **78** was synthesized according to **Scheme 3.15**.

Method: 4'-Chloropropiophenone (1.0 mmol) and glyoxylic acid monohydrate (1.5 mmol) were first dissolved in anhydrous 1,4-dioxane (20 mL) at room temperature under N₂. Concentrated H₂SO₄ (96%) (0.4 mL) was then added into the solution drop-wise. The resulting mixture was continuously stirred at reflux for 90 minutes. The mixture was cooled to room temperature and the solvent was then removed under reduced pressure. The crude product was separated by silica-gel chromatography. The product (1.0 mmol) was suspended into deionized water (10 mL) and (*S*)-phenylethylamine (1.1 mmol) was added into the suspension. The resulting mixture was allowed to stir at 40°C for 3 days. The precipitate was removed by filtration and washed with diethyl ether, giving the product as a white powder without further purification (188).



Scheme 3.15 Synthesis of compound 78

Reagents and conditions: (a) glyoxylic acid monohydrate, concentrated H_2SO_4 (cat.), 1,4-dioxane, reflux, 2 hours; (b) (S)-phenylethylamine, methanol, 40°C , 3 days.

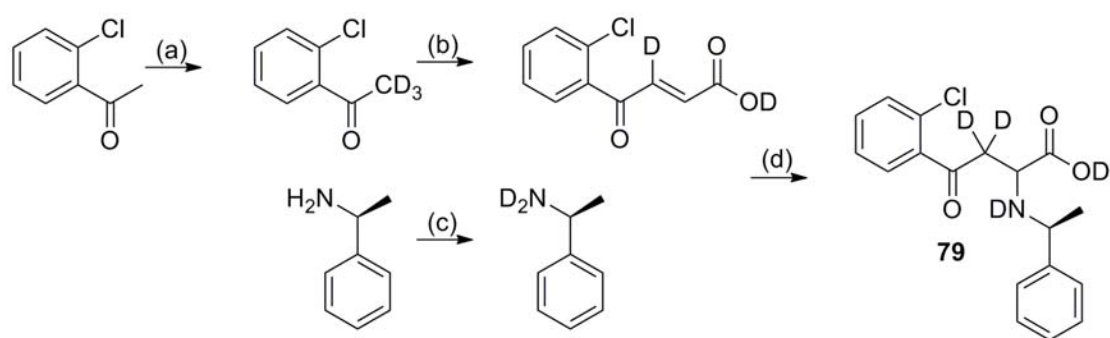
Characterization: $^1\text{H-NMR}$ (300 MHz, acetonitrile- d_3) δ 7.75 (2H, d, $J=7.2$ Hz), 7.60 (2H, d, $J=7.2$ Hz), 7.50-7.40 (5H, m), 4.50-4.40 (2H, m), 3.79 (1H, d, $J=6.3$ Hz), 1.82 (3H, d, $J=6.3$ Hz), 1.18 (3H, d, $J=6.7$ Hz). ESI-MS (Pos): 346.1 $[\text{M}+\text{H}]^+$, calculated for $\text{C}_{19}\text{H}_{20}\text{ClNO}_3$: 345.1.

Synthesis of compound 79

Compound **79** was synthesized according to **Scheme 3.16**.

Method: 2'-chloroacetophenone (12 mmol), NaOD (1 mmol), and D_2O (10 mL) were mixed at room temperature under N_2 . The resulting mixture was continuously stirred for 18 hours before the product was extracted by anhydrous diethyl ether. The combined organic phase is concentrated, giving the deuterated acetophenone as a clear oil (**189**). Similar procedure was also applied to the deuteration of (S)-phenylethylamine (**190**). The deuterated 2'-chloroacetophenone (1.0 mmol) and glyoxylic acid monohydrate (1.5 mmol) were first dissolved in the deuterated acetic acid (10 mL) at room temperature under N_2 . The temperature then increased to 120°C and the resulting solution was continuously stirred for 18 hours. The mixture was cooled to room temperature and the solvent was removed under reduced pressure. The crude deuterated (*E*)-4-(2-chlorophenyl)-4-oxo-but-2-enoic acid was purified by silica-gel

chromatography. Subsequently, the deuterated (*E*)-4-(2-chlorophenyl)-4-oxo-but-2-enoic acid (1.0 mmol) and deuterated (*S*)-phenylethylamine (1.1 mmol) were then dissolved in MeOD (10 mL) at room temperature under N₂. The resulting solution was heated to 40°C and continuously stirred for 3 hours. The precipitation was then removed by filtration and washed by diethyl ether. The crude product was recrystallized from D₂O: CD₃CN (1:1) solution, giving the product as a white powder.



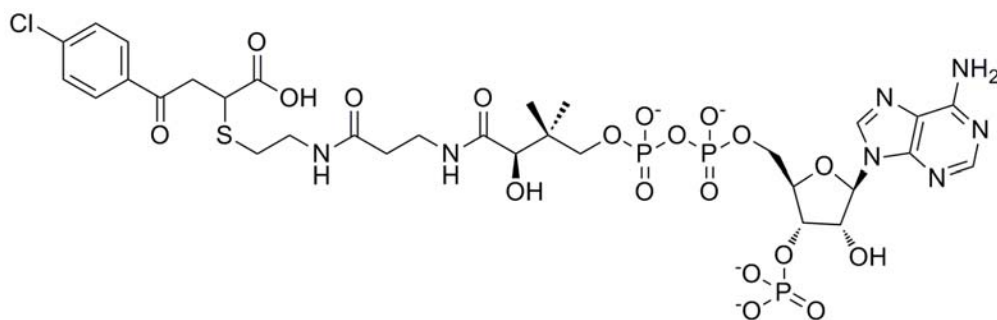
Scheme 3.16 Synthesis of compound 79

Reagents and conditions: (a) NaOD, D₂O, 25°C, 18 hours; (b) NaOD, D₂O, 25°C, 1 hour; (c) glyoxylic acid monohydrate, CD₃COOD, reflux, 18 hours; (d) MeOD, 40°C, 4 hours.

Characterization: ¹H-NMR (300 MHz, 0.1% DCl in Acetone-*d*₆) δ 7.95-7.84 (3H, m), 7.49-7.39 (6H, m), 4.93 (1H, q, *J*=6.9 Hz), 4.08 (1H, s), 1.91 (3H, d, *J*=6.9 Hz).

Synthesis of the 4-aryl-2-CoA-4-oxo-butanoic acids (80-89)

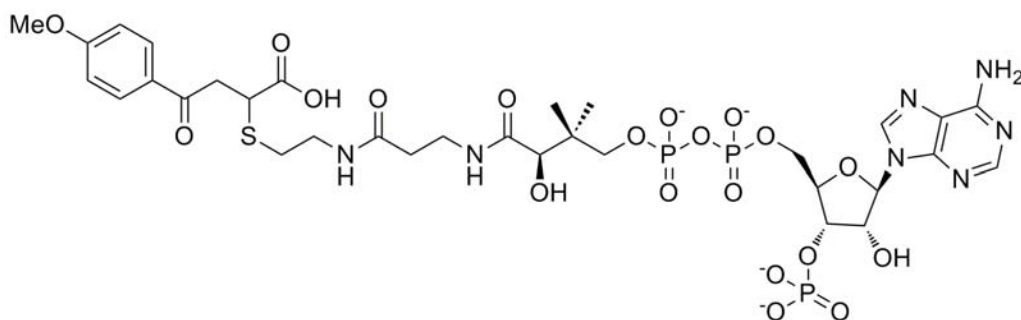
Synthesis of compound 80



Method: compound **80** was prepared according to the general procedure from commercially available (*E*)-4-(4'-chlorophenyl)-4-oxo-but-2-enoic acid and the product was obtained as a white solid.

Characterization: $^1\text{H-NMR}$ (300 MHz, in $\text{D}_2\text{O-d}_2$) δ 8.36 (1H, s), 8.09 (1H, s), 7.96 (2H, d, $J=7.2$ Hz), 7.08 (2H, d, $J=7.2$ Hz), 6.01 (1H, d, $J=6.0$ Hz), 4.42-4.40 (1H, m), 4.11-4.09 (2H, m), 3.88 (1H, s), 3.74-3.62 (1H, m), 3.56-3.50 (1H, m), 3.47-3.04 (9H, m), 2.75-2.50 (2H, m), 2.35 (2H, t, $J=6.9$ Hz), 0.74 (3H, s), 0.62 (3H, s). ESI-MS (Neg): 976.2 $[\text{M-H}]^-$; calculated for $\text{C}_{31}\text{H}_{43}\text{ClN}_7\text{O}_{19}\text{P}_3\text{S}$: 977.1.

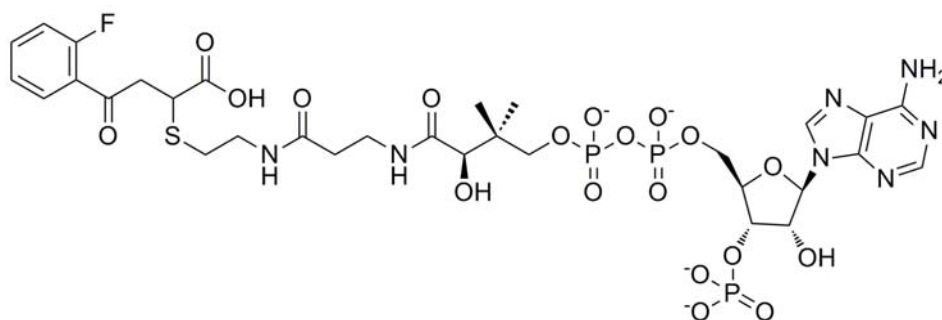
Synthesis of compound 81



Method: Compound **81** was prepared according to the general procedure from commercially available (*E*)-4-(4'-methoxyphenyl)-4-oxo-but-2-enoic acid and the product was obtained as a white solid.

Characterization: ¹H-NMR (300 MHz, in D₂O-*d*₂) δ 8.30 (s, 1H), 7.98 (s, 1H), 7.67 (2H, d, *J*=8.1 Hz), 6.75 (2H, d, *J*=8.1 Hz), 5.91 (1H, d, *J*=6.0 Hz), 4.40 (1H, s), 4.07 (2H, s), 3.82 (1H, s), 3.68 (3H, s), 3.67-3.62 (1H, m), 3.53 (1H, t, *J*=6.6 Hz), 3.42-3.04 (9H, m), 2.64-2.54 (2H, m), 2.25 (2H, t, *J*=6.0 Hz), 0.69 (3H, s), 0.56 (3H, s). ESI-MS (Neg): 972.2 [M-H]⁻; calculated for C₃₂H₄₆N₇O₂₀P₃S: 973.1.

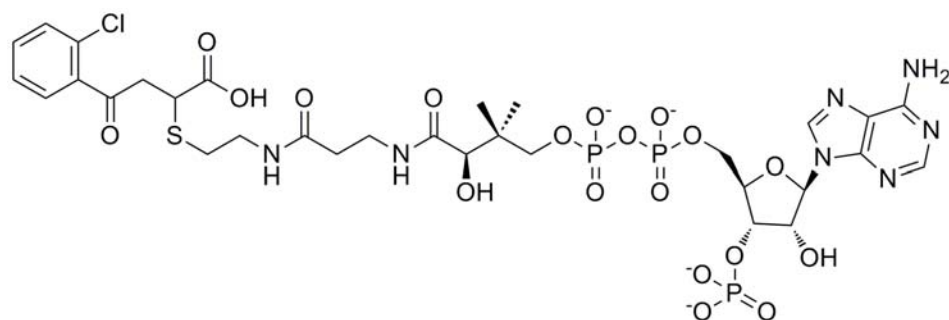
Synthesis of compound **82**



Method: compound **82** was prepared according to the general procedure from (*E*)-4-(2'-fluorophenyl)-4-oxo-but-2-enoic acid (**22**) and the product was obtained as a white solid.

Characterization: ¹H-NMR (300 MHz, in D₂O-*d*₂) δ 8.33 (1H, s), 8.02 (1H, s), 7.70-7.40 (2H, m), 7.20-7.00 (2H, m), 5.95 (1H, q, *J*=3.0 Hz), 4.44-4.38 (1H, m), 4.10-4.02 (2H, m), 3.83 (1H, s), 3.70-3.60 (1H, m), 3.58-3.50 (1H, m), 3.44-3.06 (9H, m), 2.64-2.56 (2H, m), 2.27 (2H, d, *J*=6.6 Hz), 0.71 (3H, s), 0.57 (3H, s). ESI-MS (Neg): 960.1 [M-H]⁻; calculated for C₃₁H₄₃FN₇O₁₉P₃S: 961.1.

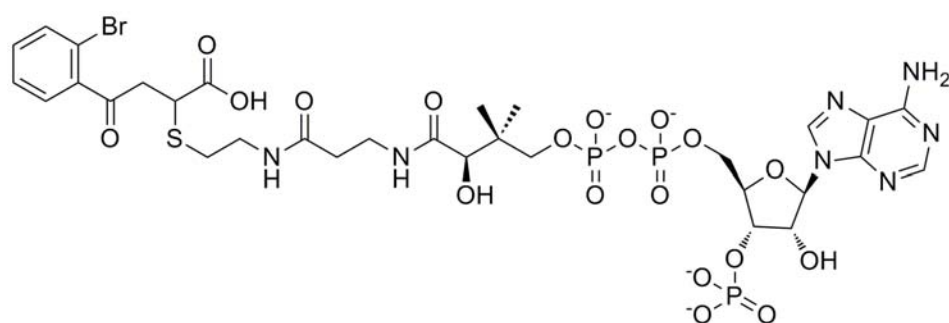
Synthesis of compound **83**



Method: compound **83** was prepared according to the general procedure from (*E*)-4-(2'-chlorophenyl)-4-oxo-but-2-enoic acid (**23**) and the product was obtained as a white solid.

Characterization: $^1\text{H-NMR}$ (300 MHz, in $\text{D}_2\text{O-d}_2$) δ 8.38 (1H, s), 8.08 (1H, s), 7.45-7.40 (1H, m), 7.31-7.20 (3H, m), 5.99 (1H, d, $J=6.0$ Hz), 4.45-4.42 (1H, m), 4.12-4.09 (2H, m), 3.86 (1H, s), 3.69 (1H, q, $J=4.8$ Hz), 3.54 (1H, dd, $J=2.4, 6.0$ Hz), 3.40-3.10 (9H, m), 2.63-2.52 (2H, m), 2.29 (2H, d, $J=6.6$ Hz), 0.73 (3H, s), 0.59 (3H, s). ESI-MS (Neg): 976.1 $[\text{M-H}]^-$; calculated for $\text{C}_{31}\text{H}_{43}\text{ClN}_7\text{O}_{19}\text{P}_3\text{S}$: 977.1.

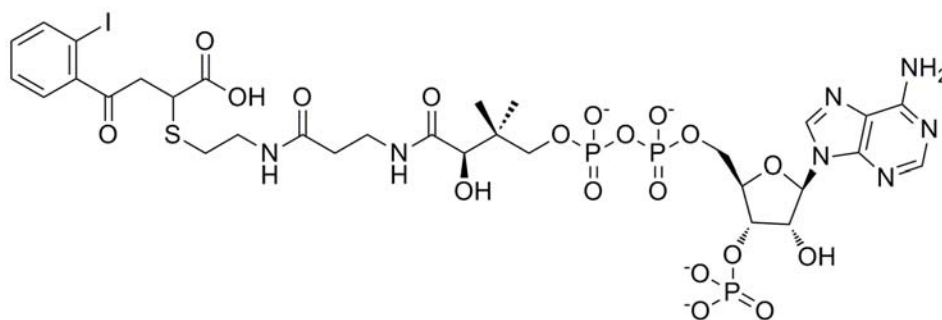
Synthesis of compound **84**



Method: compound **84** was prepared according to the general procedure from (*E*)-4-(2'-bromophenyl)-4-oxo-but-2-enoic acid (**24**) and the product was obtained as a white solid.

Characterization: $^1\text{H-NMR}$ (300 MHz, in $\text{D}_2\text{O-}d_2$) δ 8.38 (1H, s), 8.07 (1H, s), 7.46 (1H, d, $J=7.8$ Hz), 7.38 (1H, d, $J=6.0$ Hz), 7.30-7.15 (2H, m), 5.99 (1H, d, $J=5.4$ Hz), 4.44 (1H, s), 4.10 (2H, s), 3.86 (1H, s), 3.74-3.62 (1H, m), 3.58-3.48 (1H, m), 3.44-3.06 (9H, m), 2.65-2.50 (2H, m), 2.29 (2H, t, $J=6.9$ Hz), 0.73 (3H, s), 0.59 (3H, s). ESI-MS (Neg): 1020.1 $[\text{M-H}]^-$; calculated for $\text{C}_{31}\text{H}_{43}\text{BrN}_7\text{O}_{19}\text{P}_3\text{S}$: 1021.0.

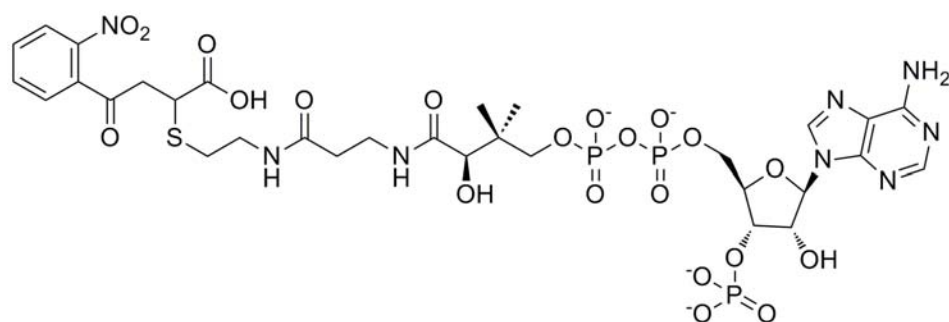
Synthesis of compound **85**



Method: Compound **85** was prepared according to the general procedure from (*E*)-4-(2'-iodophenyl)-4-oxo-but-2-enoic acid (**25**) and the product was obtained as a white solid.

Characterization: $^1\text{H-NMR}$ (300 MHz, in $\text{D}_2\text{O-}d_2$) δ 8.31 (1H, s), 7.99 (1H, s), 7.70 (1H, d, $J=7.5$ Hz), 7.38-7.32 (1H, m), 7.30-7.20 (1H, m), 7.04-6.94 (1H, m), 5.94 (1H, d, $J=6.3$ Hz), 4.40 (1H, s), 4.06 (2H, s), 3.82 (1H, s), 3.64 (1H, q, $J=4.8$ Hz), 3.48 (1H, dd, $J=2.1, 6.3$ Hz), 3.42-2.98 (9H, m), 2.62-2.50 (2H, m), 2.25 (2H, t, $J=6.3$), 0.69 (3H, s), 0.54 (3H, s). ESI-MS (Neg): 1068.0 $[\text{M-H}]^-$; calculated for $\text{C}_{31}\text{H}_{43}\text{IN}_7\text{O}_{19}\text{P}_3\text{S}$: 1069.0.

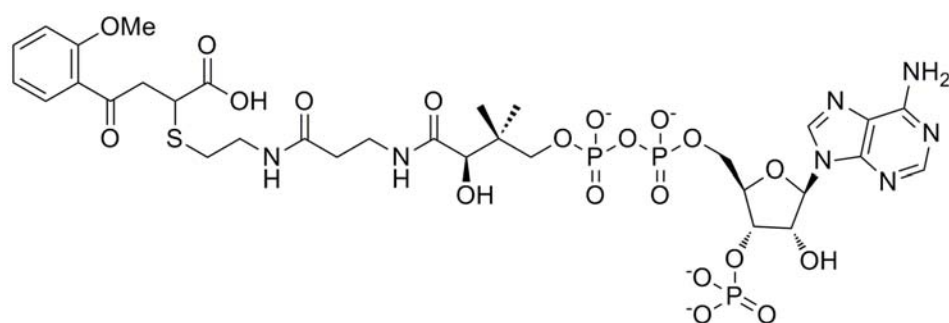
Synthesis of compound **86**



Method: Compound **86** was prepared according to the general procedure from (*E*)-4-(2'-nitrophenyl)-4-oxo-but-2-enoic acid (**26**) and the product was obtained as a brown solid.

Characterization: $^1\text{H-NMR}$ (300 MHz, in $\text{D}_2\text{O-d}_2$) δ 8.36 (1H, s), δ 8.25-8.20 (1H, m), 8.08 (1H, s), 8.00-7.92 (2H, m), 7.70-7.62 (1H, m), 6.01 (1H, d, $J=6.3$ Hz), 4.46 (1H, s), 4.10 (2H, s), 3.85 (1H, s), 3.68-3.64 (1H, m), 3.52-3.46 (1H, m), 3.42-3.06 (9H, m), 2.62-2.52 (2H, m), 2.27 (2H, d, $J=6.6$ Hz), 0.72 (3H, s), 0.60 (3H, s). ESI-MS (Neg): 987.1 $[\text{M-H}]^-$; calculated for $\text{C}_{31}\text{H}_{43}\text{N}_8\text{O}_{21}\text{P}_3\text{S}$: 988.1.

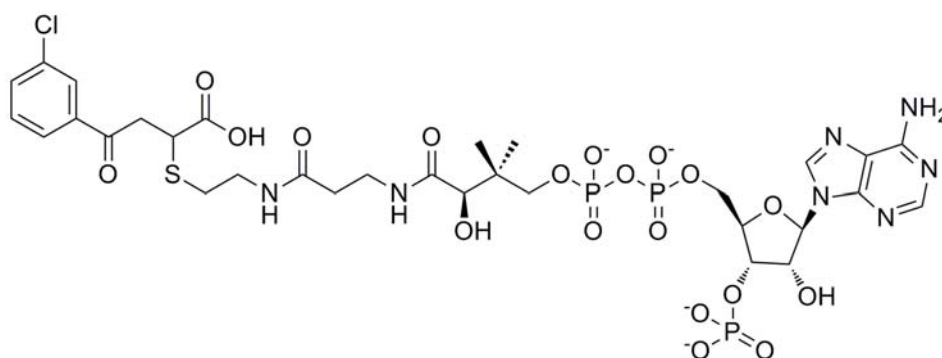
Synthesis of compound **87**



Method: compound **87** was prepared according to the general procedure from (*E*)-4-(2'-methoxyphenyl)-4-oxo-but-2-enoic acid (**29**) and the product was obtained as a white solid.

Characterization: $^1\text{H-NMR}$ (300 MHz, in $\text{D}_2\text{O}-d_2$) δ 8.36 (1H, s), 8.05 (1H, s), 7.50-7.35 (2H, m), 7.00-6.80 (2H, m), 6.97 (1H, d, $J=6.0$ Hz), 4.44 (1H, s), 4.11 (2H, s), 3.85 (1H, s), 3.72 (3H, s), 3.70-3.62 (1H, m), 3.56-3.46 (1H, m), 3.44-3.04 (9H, m), 2.70-2.50 (2H, m), 2.27 (2H, t, $J=6.6$ Hz), 0.72 (3H, s), 0.58 (3H, s). ESI-MS (Neg): 972.1 $[\text{M-H}]^-$; calculated for $\text{C}_{32}\text{H}_{46}\text{N}_7\text{O}_{20}\text{P}_3\text{S}$: 973.1.

Synthesis of compound **88**

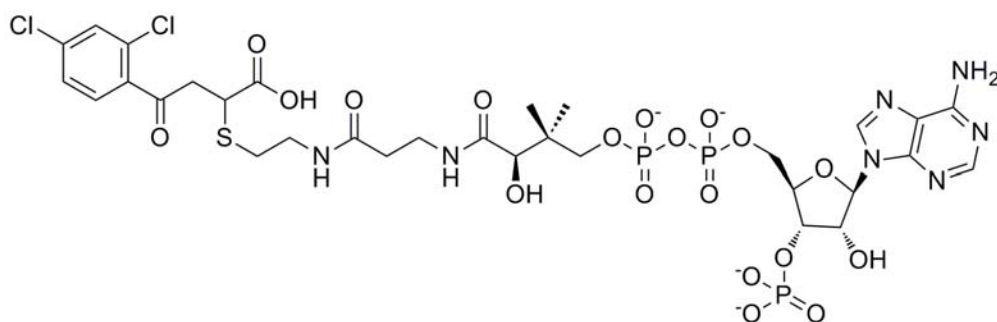


Method: compound **88** was prepared according to the general procedure from (*E*)-4-(3'-chlorophenyl)-4-oxo-but-2-enoic acid (**30**) and the product was obtained as a white solid.

Characterization: $^1\text{H-NMR}$ (300 MHz, in $\text{D}_2\text{O}-d_2$) δ 8.29 (1H, s), 7.97 (1H, s), 7.66-7.56 (2H, m), 7.40-7.33 (1H, m), 7.28-7.16 (1H, m), 5.91 (1H, d, $J=6.0$ Hz), 4.39 (1H, s), 4.06 (2H, s), 3.82 (1H, s), 3.68-3.60 (1H, m), 3.58-3.48 (1H, m), 3.44-3.06 (9H, m).

m), 2.66-2.56 (2H, m), 2.30-2.20 (2H, m), 0.68 (3H, s), 0.55 (3H, s). ESI-MS (Neg): 976.1 [M-H]⁻; calculated for C₃₁H₄₃ClN₇O₁₉P₃S: 977.1.

Synthesis of compound **89**



Method: Compound **89** was prepared according to the general procedure from (*E*)-4-(2',4'-dichlorophenyl)-4-oxo-but-2-enoic acid (**36**) and the product was obtained as a white solid.

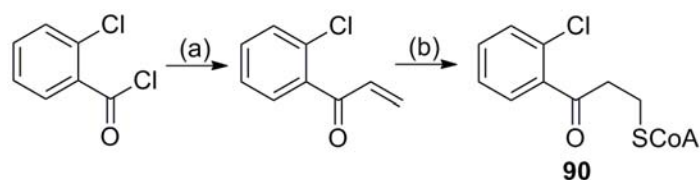
Characterization: ¹H-NMR (300 MHz, in D₂O-*d*₂) δ 8.35 (1H, s), 8.04 (1H, s), 7.41-7.38 (1H, m), 7.33-7.30 (1H, m), 7.22-7.16 (1H, m), 5.97 (1H, d, *J*=6.0 Hz), 4.43 (1H, s), 4.09 (1H, s), 3.85 (1H, s), 3.72-3.62 (1H, m), 3.56-3.47 (1H, m), 3.44-3.06 (9H, m), 2.64-2.54 (2H, m), 2.28 (2H, t, *J*=6.6 Hz), 0.72 (3H, s), 0.58 (3H, s). ESI-MS (Neg): 1010.1 [M-H]⁻; calculated for C₃₁H₄₂Cl₂N₇O₁₉P₃S: 1011.1.

Synthesis of compound **90**

Compound **90** was synthesized according to **Scheme 3.17**.

Method: 2'-Chlorobenzoyl chloride (5.0 mmol) and Pd(PPh₃)₄ (0.05 mmol) were first dissolved in anhydrous THF (10 mL) at room temperature under N₂. Subsequently vinyltributyltin (5.0 mmol) was added into the solution and the resulting mixture was

continuously stirred for another 1 hour. The solution was first diluted with ethyl acetate (10 mL) and washed with saturated NaHCO₃ aqueous solution (20 mL), brine (20 mL), and deionized water (20 mL) respectively. The organic phase was dried by anhydrous MgSO₄ and the solvent was removed under reduced pressure. The 1-(2'-chlorophenyl)prop-2-en-1-one was purified by silica-gel chromatography, giving the product as a lightly yellow oil (191). Compound **90** was prepared according to the general procedure from 1-(2'-chlorophenyl)prop-2-en-1-one and the product was obtained as a white powder.



Scheme 3.17 Synthesis of compound 90

Reagents and conditions: (a) vinyltributyltin, Pd(PPh₃)₄ (cat.), anhydrous THF, 25°C, 1 hour; (b) CoASH, pH 7.0 phosphate buffer, 25°C, 5 hours.

Characterization: ¹H-NMR (300 MHz, in D₂O-*d*₂) δ 8.35 (1H, s), 8.02 (1H, s), 7.40-7.20 (4H, m), 5.96 (2H, d, *J*=5.7 Hz), 4.42 (1H, s), 4.01 (1H, s), 3.86 (1H, s), 3.67 (1H, dd, *J*=4.8 Hz, 5.1 Hz), 3.39 (1H, dd, *J*=4.8 Hz, 4.8 Hz), 3.29 (2H, t, *J*=6.3 Hz), 3.17 (2H, t, *J*=6.6 Hz), 3.11 (2H, t, *J*=6.6 Hz), 2.69 (2H, t, *J*=6.6 Hz), 2.50 (2H, t, *J*=6.6 Hz), 2.28 (2H, t, *J*=6.6 Hz), 0.73 (3H, s), 0.59 (3H, s). ESI-MS (Neg): 966.1 [M-H]⁻; calculated for C₃₀H₄₂Cl₂N₇O₁₇P₃S: 967.1.

Synthesis of compounds 91-93

Synthesis of compound 91

Method: The (*E*)-4-(2',4'-dichlorophenyl)-4-oxo-but-2-enoic acid (0.1 mmol) was first dissolved in DMSO (1 mL) at room temperature under N₂. Pantetheine (0.11 mmol), obtained by reduction of pantethine under NaBH₄ (192), in deionized H₂O (10 mL) was then added to the solution and the resulting mixture was continuously stirred for 5 hours. Subsequently the product was purified by HPLC and the solvent was lyophilized, giving the product as white powder.

Characterization: ¹H-NMR (300 MHz, in D₂O) δ 7.49 (1H, d, *J*=8.4 Hz), 7.46 (1H, d, *J*=2.1 Hz), 7.32 (1H, dd, *J*=2.1 Hz, 6.3 Hz), 3.82 (1H, s), 3.60-3.50 (1H, m), 3.40-3.25 (4H, m), 3.25-3.15 (4H, m), 2.62 (2H, t, *J*=6.6 Hz), 2.34 (2H, t, *J*=6.3 Hz), 0.75 (3H, s), 0.71 (3H, s). ESI-MS (Neg): 521.0 [M-H]⁻; calculated for C₂₁H₂₈Cl₂N₂O₇S: 522.1. Retention time: 15.9 minutes.

Synthesis of compound 92

Method: Compound **91** (1.0 μmol), ATP (1.5 μmol), PanK (0.1 μmol), and 10 mL pH 8.0 Tris buffer (containing 20 mM Tris, 50 mM MgCl₂, and 100 mM NaCl) were mixed at room temperature and incubated for 4 hours. The product was purified by HPLC and the solvent was subsequently lyophilized, giving the product as white powder.

Characterization: ESI-MS (Neg): 601.0 [M-H]⁻; calculated for C₂₁H₂₉Cl₂N₂O₁₀PS: 602.1. Retention time: 31.0 minutes.

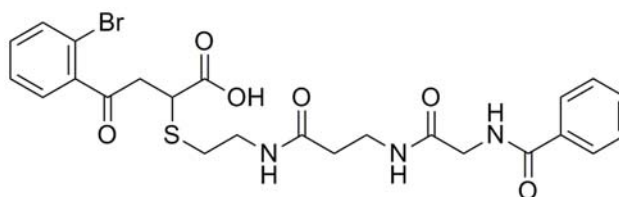
Synthesis of compound **93**

Method: Compound **91** (1.0 μmol), ATP (3.5 μmol), PanK (0.1 μmol), PPAT (0.1 μmol), and pH 8.0 Tris buffer (containing 20 mM Tris, 50 mM MgCl_2 , and 100 mM NaCl) (10 mL) were mixed under room temperature and incubated for 4 hours. The product was purified by HPLC and the solvent was subsequently lyophilized, giving the product as white powder.

Characterization: ESI-MS (Neg): 601.0 $[\text{M-H}]^-$; calculated for $\text{C}_{31}\text{H}_{41}\text{Cl}_2\text{N}_7\text{O}_{16}\text{P}_2\text{S}$: 931.1. Retention time: 27.6 minutes.

Synthesis of CoA surrogates **94-99**

Synthesis of compound **94**

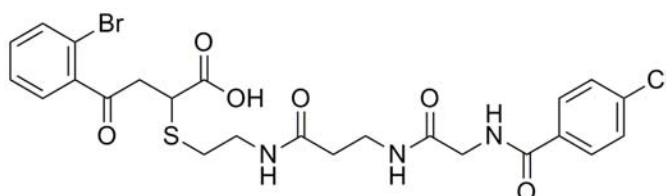


Method: compound **94** was prepared according to the general procedure from commercially available benzoic acid and the product was obtained as a white solid.

Characterization: $^1\text{H-NMR}$ (300 MHz, in chloroform- d_1) δ 7.74-7.67 (2H, m), 7.59-7.46 (2H, m), 7.30-7.16 (5H, m), 3.91 (2H, s), 3.85-3.76 (1H, m), 3.70-3.50 (3H, m),

3.30-3.19 (1H, m), 2.48-2.38 (2H, m), 2.28 (2H, t, $J=7.2$ Hz). ESI-MS (Neg): 562.0 [M-H]⁻; calculated for C₂₄H₂₅BrClN₃O₆S: 563.1. Retention time: 33.8 minutes.

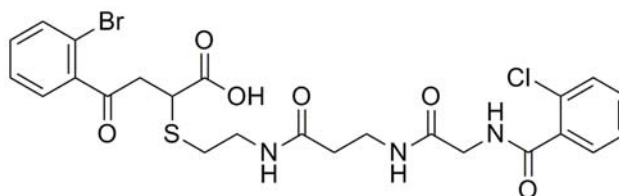
Synthesis of compound 95



Method: compound **95** was prepared according to the general procedure from commercially available 4-chlorobenzoic acid and the product was obtained as a white solid.

Characterization: ¹H-NMR (300 MHz, in DMSO-*d*₆) δ 9.40 (1H, s), 8.56 (1H, s), 8.15 (1H, s), 7.93 (2H, d, $J=8.1$ Hz), 7.67 (2H, d, $J=7.8$ Hz), 7.51-7.39 (4H, m), 3.82 (2H, t, $J=5.7$ Hz), 3.60-3.50 (1H, m), 3.40-3.20 (4H, m), 3.04-2.96 (1H, dd, $J=4.5$ Hz, 13.2 Hz), 2.80-2.60 (2H, m), 2.24 (2H, t, $J=6.9$ Hz). ESI-MS (Neg): 596.0 [M-H]⁻; calculated for C₂₄H₂₅BrClN₃O₆S: 597.0. Retention time: 38.0 minutes.

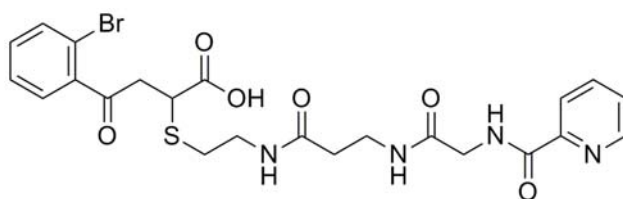
Synthesis of compound 96



Method: compound **96** was prepared according to the general procedure from commercially available 2-chlorobenzoic acid and the product was obtained as a white solid.

Characterization: $^1\text{H-NMR}$ (300 MHz, in chloroform- d_1) δ 7.54-7.44 (3H, m), 7.40-7.25 (5H, m), 4.03 (2H, s), 3.70-3.60 (1H, m), 3.55-3.35 (3H, m), 3.20-3.10 (1H, m), 2.58-2.48 (2H, m), 2.38 (2H, t, $J=6.9$ Hz). ESI-MS (Neg): 596.0 $[\text{M-H}]^-$; calculated for $\text{C}_{24}\text{H}_{25}\text{BrClN}_3\text{O}_6\text{S}$: 597.0. Retention time: 30.5 minutes.

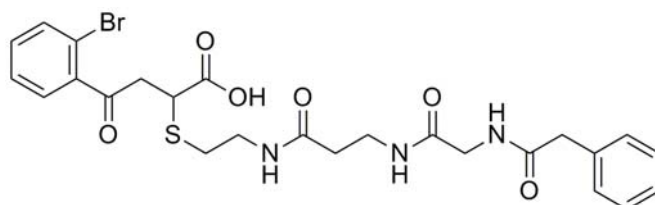
Synthesis of compound 97



Method: compound **97** was prepared according to the general procedure from commercially available picolinic acid and the product was obtained as a white solid.

Characterization: ESI-MS (Neg): 562.9 $[\text{M-H}]^-$; calculated for $\text{C}_{23}\text{H}_{25}\text{BrN}_4\text{O}_6\text{S}$: 564.1. Retention time: 30.3 minutes.

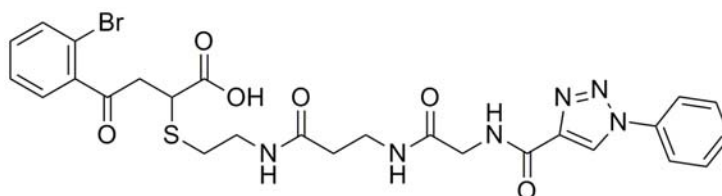
Synthesis of compound 98



Method: compound **98** was prepared according to the general procedure from commercially available 2-phenylacetic acid and the product was obtained as a white solid.

Characterization: $^1\text{H-NMR}$ (300 MHz, in acetone- d_6) δ 7.70-7.65 (2H, m), 7.49-7.29 (7H, m), 3.84 (1H, dd, $J=4.5$ Hz, 5.4 Hz), 3.81 (2H, s), 3.60 (1H, dd, $J=8.1$ Hz, 9.9 Hz), 3.59 (2H, s), 3.41 (4H, dd, $J=6.6$ Hz, 7.5 Hz), 3.25 (1H, dd, $J=4.5$ Hz, 13.2 Hz), 2.96-2.78 (2H, m), 2.34 (2H, t, $J=7.2$ Hz). ESI-MS (Neg): 576.0 [M-H] $^-$; calculated for $\text{C}_{25}\text{H}_{28}\text{BrN}_3\text{O}_6\text{S}$: 577.1. Retention time: 34.9 minutes.

Synthesis of compound **99**

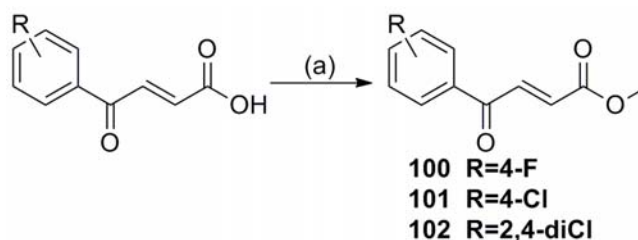


Method: compound **99** was prepared according to the general procedure from 1-benzyl-1*H*-1,2,3-triazole-4-carboxylic acid (**193**) and the product was obtained as a white solid.

Characterization: $^1\text{H-NMR}$ (300 MHz, in acetone- d_6) δ 8.45 (1H, s), 7.66 (2H, d, $J=7.8$ Hz), 7.40-7.35 (6H, m), 5.70 (2H, s), 4.02 (2H, s), 3.92-3.80 (1H, m), 3.60-3.50 (1H, m), 3.40-3.20 (5H, m), 2.90-2.80 (2H, m), 2.37 (2H, t, $J=6.6$ Hz). ESI-MS (Neg): 642.9 [M-H] $^-$; calculated for $\text{C}_{27}\text{H}_{29}\text{BrN}_6\text{O}_6\text{S}$: 644.1. Retention time: 35.2 minutes.

General procedure for the synthesis of methyl (*E*)-4-aryl-4-oxo-but-2-enoate **100, **101**, and **103****

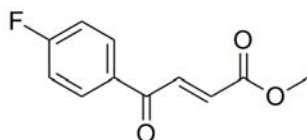
In general, the (*E*)-4-aryl-4-oxo-but-2-enoic acid (1.0 mmol) and K₂CO₃ (1.2 mmol) were first suspended in anhydrous DMF (10 mL) at room temperature under N₂. Methyl iodide (1.2 mmol) was subsequently added into the resulting suspension and the mixture was continuously stirred for 3 hours (**Scheme 3.18**). The reaction was soon quenched with deionized water (10 mL) and the solution was extracted by ethyl acetate (3×20 mL). The organic phase was then collected, combined, and dried by anhydrous MgSO₄, which was then removed under reduced pressure. The crude product was purified by silica-gel chromatography (EtOAc:Petroleum ether=1:19).



Scheme 3.18 Synthesis of methyl (*E*)-4-aryl-4-oxo-but-2-enoate

Reagents and conditions: (a) MeI, K₂CO₃, anhydrous DMF, 25°C, 3h.

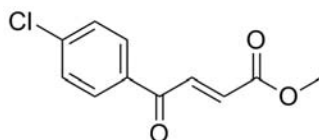
Synthesis of compound **100**



Method: compound **100** was prepared according to the general procedure from (*E*)-4-(4'-fluorophenyl)-4-oxo-but-2-enoic acid (**19**) and the product was obtained as a lightly yellow powder.

Characterization: $^1\text{H-NMR}$ (300 MHz, in chloroform- d_1) δ 8.35 (2H, d, $J=9.0$ Hz), 8.13 (2H, d, $J=9.0$ Hz), 7.87 (1H, d, $J=15.6$ Hz), 6.93 (1H, d, $J=15.6$ Hz), 3.85 (3H, s).

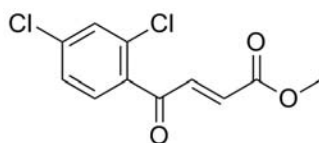
Synthesis of compound 101



Method: compound **101** was prepared according to the general procedure from commercial (*E*)-4-(4'-chlorophenyl)-4-oxo-but-2-enoic acid (**102**) and the product was obtained as a lightly yellow powder.

Characterization: $^1\text{H-NMR}$ (300 MHz, chloroform- d_1) δ 7.96 (2H, d, $J=8.4$ Hz), 7.87 (1H, d, $J=15.3$ Hz), 7.48 (2H, d, $J=8.4$ Hz), 6.90 (1H, d, $J=15.3$ Hz), 3.85 (3H, s).

Synthesis of compound 103



Method: compound **103** was prepared according to the general procedure from commercial (*E*)-4-(2',4'-dichlorophenyl)-4-oxo-but-2-enoic acid (**36**) and the product was obtained as a lightly yellow powder.

Characterization: $^1\text{H-NMR}$ (300 MHz, chloroform- d_1) δ 7.70-7.65 (2H, m), 7.58-7.50 (1H, m), 7.42 (1H, d, $J=15.9$ Hz), 6.60 (1H, d, $J=15.9$ Hz), 3.80 (3H, s).

IC₅₀ measurement of mtMenB

Enzyme IC₅₀ inhibition was performed as described in Chapter 2.

K_i and K_i' determination of compound 80

Inhibition mechanism was characterized by measuring initial velocities at a fixed concentration of 120 μM ATP, 120 μM CoA, 2 μM ecMenE and 150 nM mtMenB and at various concentrations of OSB (7.5-90 μM) and **80** (0, 380, 570 and 1275 nM). Data was analyzed in Lineweaver Burk plot. The interception of the lines occurred above the X-axis, indicating that **80** was noncompetitive inhibitor. The dissociate constant (K_i and K_i') was calculated by fitting the data in **Equation 3.3**, which described noncompetitive inhibition, where [S] is the concentration of OSB, [I] is the concentration of inhibitor added, K_m is the Michaelis-Menten constant for OSB, V_{max} is the maximum velocity, K_i and K_i' are the inhibition constants.

$$\frac{1}{v} = \frac{K_m}{v_{max}} \left(\frac{1}{[S]} \right) \left(1 + \frac{[I]}{K_i} \right) + \frac{1}{V_{max}} \left(1 + \frac{[I]}{K_i'} \right)$$

Equation 3.3

K_i and K_i' determination of compound 89

Inhibition mechanism and dissociate constants of **89** were characterized by measuring initial velocities at various concentrations of **89** (0-4350 nM) and OSB (7.5-

90 μM) in reaction mixtures containing 120 μM ATP, 120 μM CoA, 2 μM ecMenE and 150 nM *mtMenB*. K_i^{app} and $[E]$ was calculated by fitting the data in **Equation 3.4**, where v_i and v_0 are the initial velocities in the presence and absence of inhibitor and K_i^{app} is the apparent dissociation constant. Values of K_i^{app} and $[E]$ obtained from **Equation 3.4** were then fit to Equation **3.5**, **3.6** and **3.7** which describe the relationship between K_i^{app} and the inhibition constants for competitive, uncompetitive, and noncompetitive inhibition.

$$\frac{v_i}{v_0} = 1 - \frac{([E] + [I] + K_i^{\text{app}}) - \sqrt{([E] + [I] + K_i^{\text{app}})^2 - 4[E][I]}}{2[E]}$$

Equation 3.4

$$K_i^{\text{app}} = K_i \left(1 + \frac{[S]}{K_m} \right) + \frac{1}{2} [E]$$

Equation 3.5

$$K_i^{\text{app}} = K_i' \left(1 + \frac{K_m}{[S]} \right) + \frac{1}{2} [E]$$

Equation 3.6

$$K_i^{\text{app}} = \frac{[S] + K_m}{\left(\frac{K_m}{K_i} \right) + ([S]/K_i')} + \frac{1}{2} [E]$$

Equation 3.7

The dependence of K_i^{app} and $[E]$ was best described by **Equation 3.7**, indicating **89** is a noncompetitive inhibitor with K_i value of 49 nM and K_i' value of 286 nM.

MIC determination against M. tuberculosis

MIC data were acquired essentially as described previously using the microplate dilution assay (194). Briefly, bacterial cells were grown to early-mid log phase in Middlebrook 7H9 liquid medium containing 10% OADC enrichment and 0.05% Tween-80. Fifty μL of bacteria were added to the test wells and compounds were added individually to a final volume of 100 μL per well in 2 fold serial dilutions. Each drug dilution series was performed in triplicate. Plates were incubated at 37°C for 5-7 days and each well was evaluated for growth. AlamarBlue® was used as a growth indicator. The MIC was the lowest drug concentration that maintained a blue color in all replicates. A blue color in the AlamarBlue® assay indicates no bacterial growth whereas a red color in the assay was indicative of cell growth (BioSource International, Inc).

MIC determination against S. aureus

A single *S. aureus* colony was picked from Mueller-Hilton sheep blood agar plate and transferred into 20 mL tryptic soy broth (TSB) media followed by shaking at 37°C and 180 rpm overnight and the cell culture was subsequently diluted to 10^6 CFU/mL. 150 μL of the diluted cell culture was transferred into a 96-well plate, diluted with another 150 μL of fresh TSB media. Inhibitors were first dissolved in DMSO and serially diluted in each well and the final concentration of the inhibitor ranged from 1 $\mu\text{g/mL}$ to 200 $\mu\text{g/mL}$. The 96-well plate was incubated at 37°C for 24h and the minimum concentration that inhibited the bacterial growth was considered as the MIC value.

Menadione rescue

A single *S. aureus* colony was picked from Mueller-Hilton sheep blood agar plate and transferred into 20 mL tryptic soy broth (TSB) media followed by shaking at 37°C and 180 rpm overnight and the cell culture was subsequently diluted to 10⁶ CFU/mL. 150 µL of the diluted cell culture was then transferred into a 96-well plate and further diluted with another 150 µL of fresh TSB media. Inhibitors were first dissolved in DMSO and serially diluted in each well and the final concentration of the inhibitor ranged from 1 µg/mL to 200 µg/mL. Menadione (0.5 µg/mL) was subsequently added in each well. The 96-well plate was incubated at 37°C for 24h and the minimum concentration that inhibited the bacterial growth was considered as the MIC value.

Chapter 4 : Synthesis and SAR studies of 1,4-benzoxazine MenB inhibitors as novel antibacterial reagents against *M. tuberculosis*

This chapter is based on part of work that has been published in: Synthesis and SAR studies of 1,4-benzoxazine MenB inhibitors: Novel antibacterial agents against *Mycobacterium tuberculosis*. Li, X., Liu, N., Zhang, H., Knudson, S. E., Slayden, R. A., Tonge, P. J.. *Bioorg. Med. Chem. Lett.*, 2010, 20, 6306-6309.

Menaquinone is an essential component of the electron transport chain in many pathogens and consequently enzymes in the menaquinone biosynthesis pathway are potential drug targets for the development of novel antibacterial agents. In order to identify leads that target MenB, the 1,4-dihydroxy-2-naphthoyl-CoA synthase from *M. tuberculosis*, a high-throughput screen was performed. Subsequent SAR studies resulted in the discovery of compounds with excellent antibacterial activity against *M. tuberculosis* H37Rv with MIC values as low as 0.6 µg/mL. The 1,4-benzoxazine scaffold is thus a promising foundation for the development of antitubercular agents.

Introduction

1,4-Benzoxazine is a privileged ring system that has been heavily studied in the recent 10 years, and it is widely found in a broad range of biologically active molecules (**Figure 4.1**). For example, (3*S*)-9-fluoro-2,3-dihydro-3-methyl-10-(4-methyl-1-piperazinyl)-7-oxo-7*H*-pyrido[1,2,3-*de*]-1,4-benzoxazine-6-carboxylic acid (levofloxacin) analogues (195) and 6,8-dichloro-2,3-dihydro-3-hydroxymethyl-1,4-benzoxazine (196-198) target angiogenesis, which is a major therapeutic strategy for cancer drug development (199). 6-4*H*-imidazo-[5,1-*c*][1,4]benzoxazine-3-carboxamide was identified as potent 5-HT_{1A/B/D} receptor antagonists both with and without concomitant hSerT activity and one of its analogues has been developed as a clinical candidate to faster treat depression/anxiety with lowered side effect (200). (*Z*)-6-Amino-2-(3',5'-dibromo-4'-hydroxybenzylidene)-2*H*-benzo[*b*][1,4]oxazin-3(4*H*)-one analogues are also developed as GSK3, p38 MAPK, and cyclin-dependent kinase (CDKs) inhibitors and they are highly productive in tissue culture models of neurodegradation (201). Furthermore, 1,4-benzoxazine scaffold are also potent antimicrobial reagents. For example, ethyl 3,4-dihydro-3-oxo-4,6,7-trisubstituted-2*H*-1,4-benzoxazine-2-acetate derivatives are active against *S. aureus*, *B. subtilis*, *Streptococcus faecalis*, *E. coli*, and *Pseudomonas aeruginosa*, with MIC ranging from 12.5-100 µg/mL (202). Benzoxazino-rifamycin derivatives are also reported to have activity against *M. tuberculosis* both *in vitro* and *in vivo* (203-204). Finally, the 1,4-benzoxazine scaffold is also discovered to have antifungal activity (205-206).

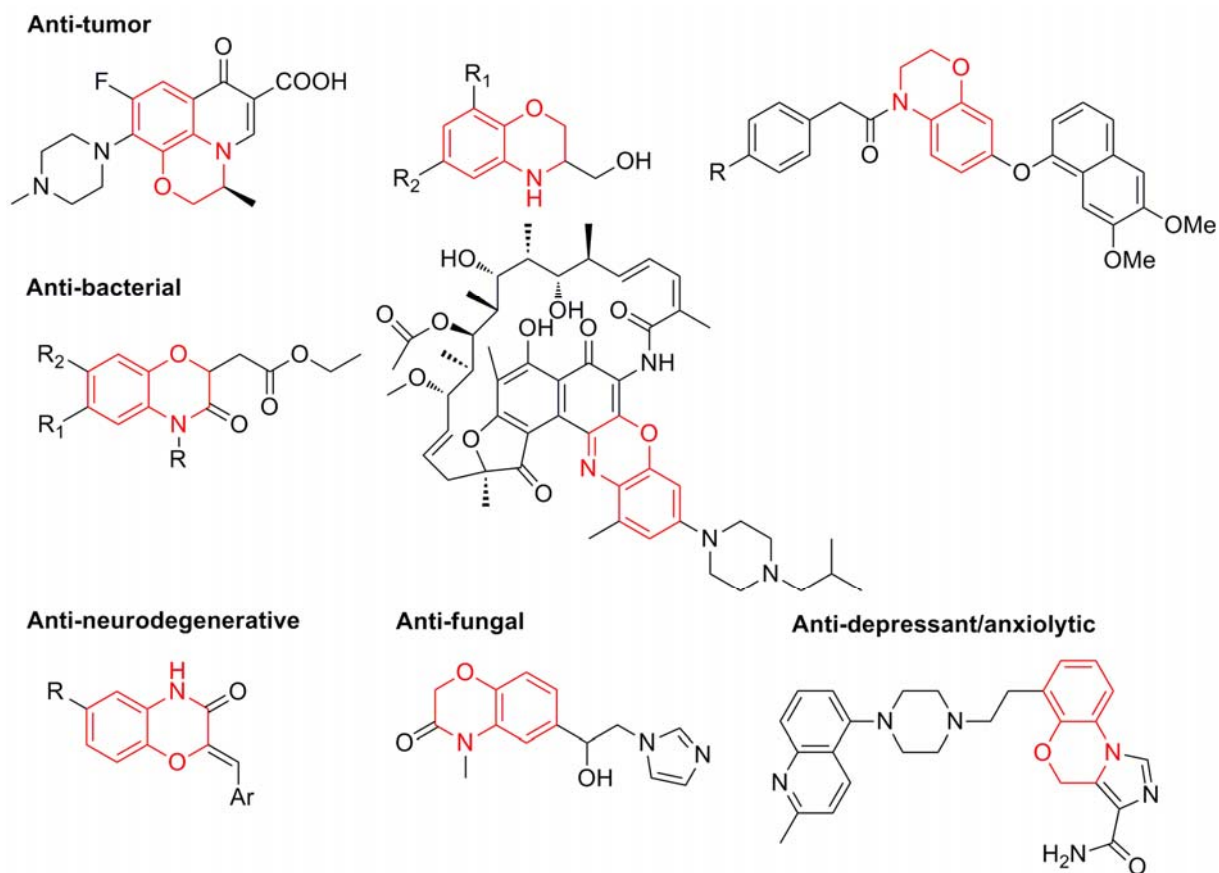


Figure 4.1 1,4-Benzoxazine scaffolds with various biological activities

Menaquinone is the sole quinone found in several Gram-positive bacteria which is used to shuttle electrons between membrane-bound protein complexes in the electron transport chain (67). The transmembrane electrochemical potential gradient resulting from the electron transport process enables ATP production, which is a major energy source for most of the living organisms. Inhibition of the menaquinone biosynthesis proteins would impair the electron transport chain and shut down the ATP supply, resulting a termination of bacterial growth. Moreover, the menaquinone biosynthesis pathway is absent in humans, thus drugs targeting the menaquinone biosynthesis enzymes will cause minor side effects. This has resulted in the proposal

that enzymes involved in the menaquinone biosynthesis may be promising targets for drug discovery.

MenB, the 1,4-dihydroxy-2-naphthoyl-CoA (DHNA-CoA) synthase, catalyzes an intramolecular Claisen condensation leading to the formation of DHNA from OSB-CoA (102). It is reported that the MenB-deficient mutant *B. subtilis* strain can only regain normal growth by 1,4-dihydroxy-2-naphthoic acid supplementation (105), and the *menb* gene is overexpressed if *M. tuberculosis* is grown under oxygen limiting conditions of unagitated liquid culture (145). To further demonstrate that MenB is an essential enzyme required by *M. tuberculosis*, a high-throughput screen was performed to identify novel chemical scaffolds as MenB inhibitors.

Result and discussion

Hits from HTS

In order to provide a foundation for the discovery of compounds that target MenB, we used a coupled assay (**Scheme 2.4**) to screen 105,091 small drug-like molecules that contained a large variety of chemical structures. Following the primary screen, in which compounds were tested at a single concentration of 100 µg/mL, we obtained 455 hits that had at least 30% enzyme inhibition relative to control (data not shown). Within these hits, we identified 4 compounds (**Figure 4.2**) that possessed the 1,4-benzoxazine scaffold. Inhibition data for these compounds is summarized in **Table 4.1**.

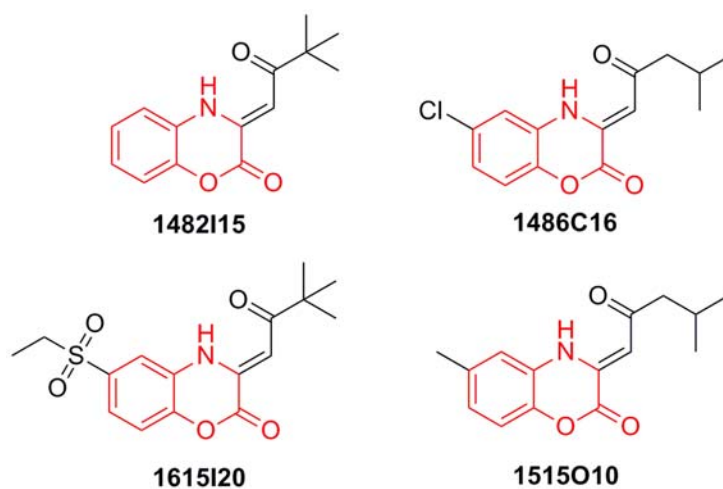


Figure 4.2 Chemical structures of hits from the HTS

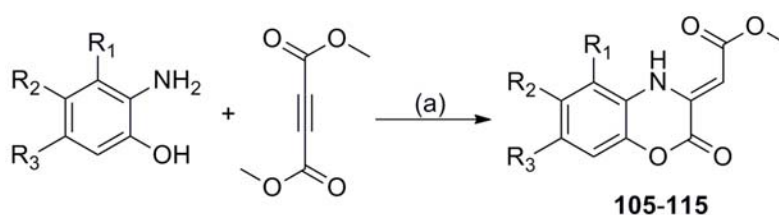
Compound	% inhibition at 100 $\mu\text{g/mL}$
1482I15	68.4
1486C16	98.0
1615I20	60.3
1515O10	77.3

Table 4.1 Inhibition data from hits of the HTS

In order to explore the utility of this ring system as a starting point for developing MenB inhibitors, we synthesized 13 compounds as shown in **Scheme 4.1**. In this procedure the ketone group is replaced by an ester for synthetic convenience.

Synthesis of (Z)-methyl 2-(2-oxo-2H-substituted benzo[b][1,4]oxazin-3(4H)ylidene)acetates 105-115

In general, commercially available substituted 2-aminophenols (1.0 mmol) and dimethyl but-2-ynedioate (1.0 mmol) were first dissolved in anhydrous methanol (10 mL) at room temperature under N₂. The temperature was then raised to 40°C and the resulting solution was continuously stirred for 3 hours. The product gradually precipitated out of the solution, which was separated by filtration. The crude product was further resuspended in MeOH/EtOAc (5:1) solution and the temperature was increased until the crude product was completely redissolved. The resulting solution was then put on ice bath for 1 hour and the product was purified by recrystallization (207).



Scheme 4.1 Synthesis of compounds 105-115

Reagents and condition: (a) methanol, 40°C, 3 hours.

In vitro inhibition of mtMenB and antibacterial activity against *M. tuberculosis* and *M. smegmatis*

The synthesized compounds were evaluated for their ability to inhibit the reaction catalyzed by MenB as well as the growth of different bacteria (**Table 4.2**). In general,

enzyme inhibition was not significantly affected by the functional groups on the benzene ring and most compounds had IC₅₀ values for MenB inhibition of ~ 20 μM. However, whole cell inhibition test against *M. tuberculosis* varied significantly with the nature of the functional group. Introduction of larger electron-withdrawing groups (compound **110**, **111**, and **115**) or electron-donating groups (compound **106**, **107**, and **112**) reduced antibacterial activity, while halogen substituents (F, Cl) increased antibacterial activity (compound **108**, **119**, **113**, and **114**). The SAR data also demonstrated that the benzoxazine core is essential for enzyme inhibition and antibacterial activity, since the benzothiazine (compound **117**) and quinoxaline-based (compound **116**) compounds had higher IC₅₀ and MIC values compared to the parent compounds. Most MIC values for *M. smegmatis* and *M. tuberculosis* (except compound **113**) agree with each other with a linear relationship, indicating that these compounds behave the same in inhibiting two different organisms. However, the inhibition for *M. smegmatis* is significantly weaker than *M. tuberculosis*, which may be explained by the differences of the cell permeability and different MenB expression level in the two organisms.

While several compounds demonstrated a good correlation between IC₅₀ and MIC values, suggesting that these compounds target MenB in the cell, there are also several examples where IC₅₀ and MICs diverge, suggesting that other factors such as altered cell permeability and/or evasion of detoxification strategies may also modulate antibacterial activity, together with the possibility that MenB might not be the only target in the cell. In order to demonstrate that menaquinone biosynthesis pathway is one of the target of these molecules, menadione rescue experiment was subsequently performed.



Compound	R ₁	R ₂	R ₃	IC ₅₀ ^(a) (μM)	MIC _{mt} ^(b) (μg/mL)	MIC _{ms} ^(c) (μg/mL)
105	H	H	H	10.0±1.0	0.64	1.0
106	Me	H	H	24.1±1.8	25	125
107	H	Me	H	23.1±1.0	>100	>500
108	H	F	H	27.0±3.0	0.63	30
109	H	Cl	H	46.3±3.5	5	250
110	H	NO ₂	H	28.2±4.4	50	500
111	H	EtSO ₂	H	17.9±3.0	>100	125
112	H	H	Me	18.2±2.8	100	30
113	H	H	F	30.0±3.7	0.63	>500
114	H	H	Cl	35.7±4.8	0.63	4
115	H	H	NO ₂	20.3±1.8	>100	125
116				>122	>100	500
117				>140	>100	16

Table 4.2 Inhibition studies for 1,4-benzoxazine analogues (compound 105-117)

(a) *mtMenB* concentration was fixed at 150 nM; (b) MIC against *M. tuberculosis* H37Rv; (c) MIC against *M. smegmatis* mc²155.

Menadione rescue experiment with S. aureus

Compounds **105**, **113**, and **114** were selected to test their inhibition properties against *S.aureus*, and they were also subsequently tested in the menadione rescue. The MIC data were summarized in **Table 4.3**. In the table, we can find that the bacterial growth was partially recovered by feeding the bacteria with menadione, since all the MIC values increased in the presence of menadione. For example, the MIC of compound **113** increased from 50 to 200 µg/mL after the incubation with menadione. However, it is assumed that MenB is not an essential protein after menadione is supplemented in the bacterial growth medium. The inhibitor selectivity is defined as MIC(with supplement)/MIC(without supplement) and the ratio should be as significant as possible to be an effective selective inhibitor. In our case, compound **113** possesses a ratio of 4, which cannot be considered as a selective inhibitor (172). The low selectivity may also come from the menadione toxicity against the bacteria. It is reported that plumbagin derivatives, analogues of menadione, have MICs against *M. tuberculosis* H37Rv and *M. smegmatis* mc²155 ranging from 10-30 µM (101). In the rescue experiment, the concentration of menadione is 3 µM, which might cause toxicity against *S. aureus*.

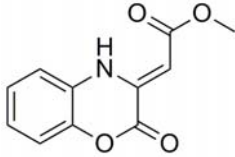
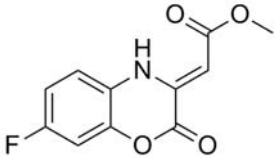
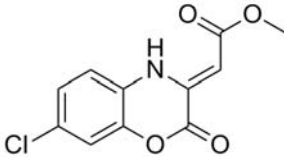
Compound	Structure	MIC w/o menadione (µg/mL)	MIC w. menadione (µg/mL)
105		100	>200
113		50	200
114		200	>200

Table 4.3 Whole-cell inhibition against *S. aureus* RN4220 with or without menadione

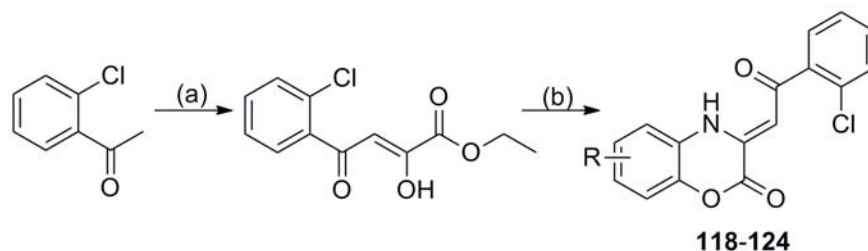
Non-replicating M. tuberculosis inhibition evaluation

Since it is reported that the *menB* gene is overexpressed under oxygen limiting conditions of unagitated liquid culture (145), it is assumed that MenB plays an essential role for its viability under the dormant condition. Compounds **105** and **108** are subsequently selected for the whole cell inhibition test for non-replicating *M. tuberculosis* and their MIC values result in 20.5 and 23.6 µg/mL, respectively. Although this suggests a 32- to 37-fold increase in MIC under aerobic cultures, it still indicates that the 1,4-benzoxazine scaffold targets essential cellular events in the non-replicating *M. tuberculosis* (177). It is reported that rifampin, have MIC values as low as 0.4 µg/mL (176) and it is the only first-line drug that can sterilize latent infection (208). The 1,4-

benzoxazine scaffold has a comparable activity with rifampin, and it has a more superior activity against the latent tuberculosis compared to other compounds evaluated by the LORA assay (176).

Synthesis of (Z)-3-(2-(2-chlorophenyl)-2-oxo-ethylidene)-3,4-dihydro-2H-substitutedbenzo[b][1,4]oxazin-2-one 118-128

To further explore the antibacterial properties of the 1,4-benzoxazines, we synthesized a second series of compounds in which the methyl ester was replaced with a substituted phenyl ring (**Scheme 4.2**). In this procedure, 2'-chloroacetophenone (1.0 mmol) and diethyl oxalate (1.0 mmol) were first dissolved in anhydrous benzene (15 mL) at room temperature under N₂. Sodium ethoxide (1.0 mmol) was subsequently added into the solution and the resulting mixture was continuously stirred for 18 hours. The solvent was then removed under reduced pressure and the resulting product, (Z)-ethyl 4-(2-chlorophenyl)-2-hydroxy-4-oxo-but-2-enoate, was purified by silica-gel chromatography (209). Subsequently, the (Z)-ethyl 4-(2-chlorophenyl)-2-hydroxy-4-oxo-but-2-enoate (1.0 mmol) and substituted 2-aminophenols (1.0 mmol) were first dissolved in acetic acid (20 mL). The resulting solution was continuously stirred at reflux for 2 hours to generate the (Z)-3-(2-(2-chlorophenyl)-2-oxo-ethylidene)-3,4-dihydro-2H substituted benzo[b][1,4]oxazin-2-ones, which were purified by recrystallization in MeOH (210).



Scheme 4.2 Synthesis of compounds 118-124

Reagents and conditions: (a) diethyl oxalate, NaOEt, benzene, 25°C, 12 hours; (b) substituted 2-aminophenol, acetic acid, 110°C, 2 hours.

***In vitro* antibacterial activity of compound 118-124**

Compounds **118-124** were first evaluated for their inhibitory activities against *mtMenB*. Interestingly, none of these compounds (**118-124**) was able to inhibit MenB up to concentrations of 100 μ M. Thus, introduction of a bulky group into the side chain significantly perturbed the ability of the 1,4-benzoxazines to inhibit *mtMenB*.

However several compounds retained their ability to inhibit bacterial growth (**Table 4.3**), suggesting that they do so by binding to targets other than MenB. MIC data showed that the antibacterial properties are mainly based on the nature of functional groups on the benzoxazine core. If minor electron-donating groups, such as a methyl group, are placed on the benzoxazine ring, the antibacterial properties are impaired (Compound **119** and **122**). This phenomenon was also noticed for compound **107** and **112** in **Table 4.4**. Compounds **118-124** have previously been shown to inhibit the growth of *E. coli* M₁₇ and *S. aureus* P-209 (211), and the SAR data presented here follows a similar trend to that reported previously in which halogen substituents lead to

an increase in antibacterial activity. The target(s) for the compounds in *E. coli* and *S. aureus* are also unknown and current studies are focused on elucidating the mode of action of the antibacterial benzoxazines.

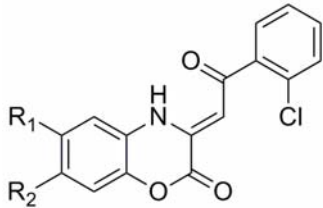
Compound	Structure	R ₁	R ₂	MIC _{mt} ^(a) µg/mL
118		H	H	3.13
119		Me	H	100
120		F	H	3.13
121		Cl	H	12.5
122		H	Me	>100
123		H	F	1.56
124		H	Cl	3.13

Table 4.4 Inhibition studies for 1,4-benzoxazine analogues (compound 118-124)

(a) MIC against *M. tuberculosis* H37Rv.

Conclusion

In summary, we have identified a group of 1,4-benzoxazines that inhibit the activity of *mtMenB* and that have promising *in vitro* antibacterial activity toward *M. tuberculosis* H37Rv, *M. smegmatis*, and *S. aureus*. These molecules are relatively simply to synthesize and the 1,4-benzoxazine scaffold provides a foundation for the development of novel antimycobacterial agents that may ultimately lead to the discovery of new therapeutics for treating patients with tuberculosis.

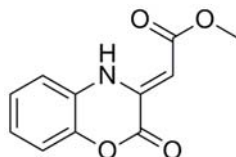
Experimental section

General

All chemicals were purchased from commercial suppliers (Sigma-Aldrich, Acros Organics, Alfa Aesar, Fisher Scientific, and TCI America) with the highest purity and used without further purification. All solvents were purchased from Fisher Scientific. ^1H -NMR spectral data were recorded on Varian Gemini-2300 or Varian Inova-400 NMR spectrometers. Mass spectral data were obtained using an Agilent 1100 LS-MS electrospray ionization single quadrupole mass spectrometer.

Synthesis of compound 105-115

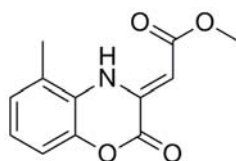
Synthesis of compound 105



Method: compound **105** was synthesized according to the general procedure from 2-aminophenol and the product was obtained as yellow needle-like crystals.

Characterization: ^1H -NMR (300 MHz, $\text{DMSO}-d_6$): δ 10.63 (s, 1H), δ 7.48-7.45 (m, 1H), δ 7.21-7.10 (m, 2H), δ 7.08-7.00 (m, 1H), δ 5.60 (s, 1H), δ 3.68 (s, 3H).

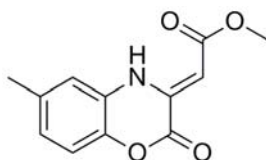
Synthesis of compound 106



Method: compound **106** was synthesized according to the general procedure from 2-amino-3-methylphenol and the product was obtained as yellow needle-like crystals.

Characterization: $^1\text{H-NMR}$ (300 MHz, chloroform- d_1): δ 10.82 (s, 1H), δ 7.04-6.90 (m, 3H), δ 5.95 (s, 1H), δ 3.80 (s, 3H), δ 2.38 (s, 3H).

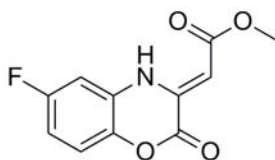
Synthesis of compound 107



Method: compound **107** was synthesized according to the general procedure from 2-amino-4-methylphenol and the product was obtained as yellow needle-like crystals.

Characterization: $^1\text{H-NMR}$ (300 MHz, chloroform- d_1): δ 10.60 (s, 1H), δ 7.02 (d, $J=6.9$ Hz, 1H), δ 7.85-7.73 (m, 2H), δ 5.92 (s, 1H), δ 3.87 (s, 3H), δ 2.33 (s, 3H).

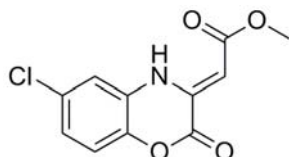
Synthesis of compound 108



Method: compound **108** was synthesized according to the general procedure from 2-amino-4-fluorophenol and the product was obtained as dark green needle-like crystals.

Characterization: ^1H -NMR (300 MHz, chloroform- d_1): δ 10.66 (s, 1H), δ 7.23-7.06 (m, 1H), δ 6.74-6.67 (m, 2H), δ 5.96 (s, 1H), δ 3.78 (s, 3H).

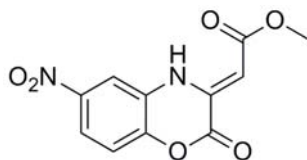
Synthesis of compound 109



Method: compound **109** was synthesized according to the general procedure from 2-amino-4-chlorophenol and the product was obtained as yellow needle-like crystals.

Characterization: ^1H -NMR (300 MHz, chloroform- d_1): δ 10.70 (s, 1H), δ 7.60-7.50 (m, 1H), δ 7.38-7.30 (m, 1H), δ 7.24-7.16 (m, 1H), δ 5.62 (s, 1H), δ 3.69 (s, 3H).

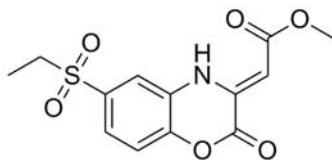
Synthesis of compound 110



Method: compound **110** was synthesized according to the general procedure from 2-amino-4-nitrophenol and the product was obtained as yellow needle-like crystals.

Characterization: ^1H -NMR (300 MHz, chloroform- d_1): δ 10.95 (s, 1H), δ 8.13-8.04 (m, 2H), δ 7.06 (d, $J=9.0$ Hz, 1H), δ 6.12 (s, 1H), δ 3.83 (s, 3H).

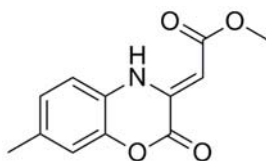
Synthesis of compound **111**



Method: compound **111** was synthesized according to the general procedure from 2-amino-4-(ethylsulfonyl)phenol and the product was obtained as a yellow powder.

Characterization: $^1\text{H-NMR}$ (300 MHz, chloroform- d_1): δ 10.82 (s, 1H), δ 7.55-7.51 (m, 2H), δ 7.31 (d, $J=9.0$ Hz, 1H), δ 6.02 (s, 1H), δ 3.81(s, 1H), 3.13 (q, $J=7.5$ Hz, 2H), 1.29 (t, $J=7.5$ Hz, 3H).

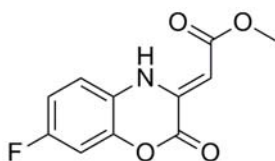
Synthesis of compound **112**



Method: compound **112** was synthesized according to the general procedure from 2-amino-5-methylphenol and the product was obtained as yellow needle-like crystals.

Characterization: $^1\text{H-NMR}$ (300 MHz, chloroform- d_1): δ 10.62 (s, 1H), δ 6.96-6.90 (m, 2H), δ 6.88-6.90 (m, 1H), 5.89 (s, 1H), 3.77 (s, 3H), 2.32 (s, 3H).

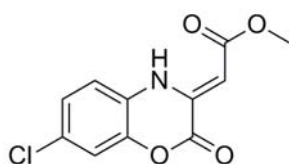
Synthesis of compound **113**



Method: compound **113** was synthesized according to the general procedure from 2-amino-5-fluorophenol and the product was obtained as a yellow powder.

Characterization: $^1\text{H-NMR}$ (300 MHz, chloroform- d_1): δ 10.63 (s, 1H), δ 7.15-7.10 (m, 1H), 6.98-6.85 (m, 2H), δ 5.91 (s, 1H), δ 3.78 (s, 3H).

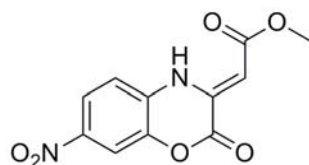
Synthesis of compound 114



Method: Method: compound **114** was synthesized according to the general procedure from 2-amino-5-chlorophenol and the product was obtained as a yellow powder.

Characterization: $^1\text{H-NMR}$ (300 MHz, DMSO- d_6): δ 10.64 (s, 1H), δ 7.79-7.70 (m, 1H), δ 7.22-7.17 (m, 1H), 7.07- 7.00 (m, 1H), 5.63 (s, 1H), 3.72 (s, 3H).

Synthesis of compound 115

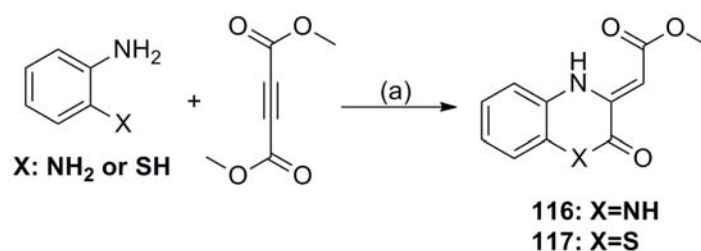


Method: compound **115** was synthesized according to the general procedure from 2-amino-5-nitrophenol and the product was obtained as a yellow powder.

Characterization: $^1\text{H-NMR}$ (300 MHz, CDCl_3 - d_1): δ 10.82 (s, 1H), δ 7.95-7.68 (m, 2H), δ 7.29 (s, 1H), 6.06 (s, 1H), 3.82 (s, 3H).

Synthesis of compound 116

Method: Benzene-1,2-diamine (1.0 mmol) and dimethyl but-2-ynedioate (1.0 mmol) were first dissolved in anhydrous methanol (10 mL) at room temperature and under N₂. The reaction temperature was raised to 40°C, and the resulting solution was continuously stirred for 3 hours. The product gradually precipitated out of the solution and the crude product was separated by filtration. The crude product was further resuspended in MeOH/EtOAc (5:1) solution and the temperature was increased until it was completely redissolved in the solution. The crude product solution was cooled on ice bath for 1 hour and the product was purified by recrystallization (**Scheme 4.2**) (212).



Scheme 4.3 Synthesis of compounds 116 and 117

Reagents and conditions: (a) anhydrous methanol, 40°C, 3 hours.

Characterization: ¹H-NMR (300 MHz, chloroform-*d*₁): δ 11.08 (s, 1H), δ 9.62 (s, 1H), 7.18-6.95 (m, 4H), 5.85 (s, 1H), 3.78 (s, 3H).

Synthesis of compound 117

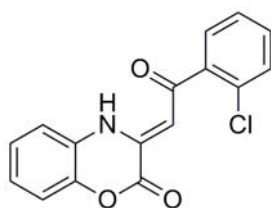
Method: 2-aminobenzenethiol (1.0 mmol) and dimethyl but-2-ynedioate (1.0 mmol) were first dissolved in anhydrous methanol (10 mL) at room temperature under

N₂. The reaction temperature was increased to 40°C and the resulting solution was continuously stirred for 3 hours. The product gradually precipitated out of the solution and the crude product was separated by filtration. The crude product was further resuspended in MeOH/EtOAc (5:1) solution and the temperature was increased until it was completely redissolved in the solution. The crude product solution was put back on ice bath for 1h and the product was purified by recrystallization (**Scheme 4.3**) (213).

Characterization: ¹H-NMR (300 MHz, chloroform-*d*₁): δ 9.18 (s, 1H), δ 7.32-7.07 (m, 4H), δ 6.93 (d, *J*=7.8 Hz, 1H), 3.84 (s, 3H).

Synthesis of (Z)-3-(2-(2-chlorophenyl)-2-oxo-ethylidene)-3,4-dihydro-2H-substitutedbenzo[b][1,4]oxazin-2-one compound 118-128

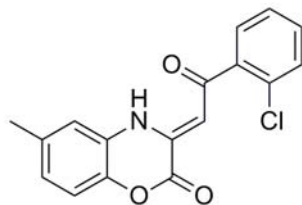
Synthesis of compound 118



Method: compound **118** was synthesized according to the general procedure from 2-aminophenol. The product was obtained as a yellow powder.

Characterization: ¹H-NMR (300 MHz, DMSO-*d*₆): δ 12.50 (s, 1H), δ 7.70-7.43 (m, 5H), δ 7.28-7.10 (m, 3H), 6.46 (s, 1H).

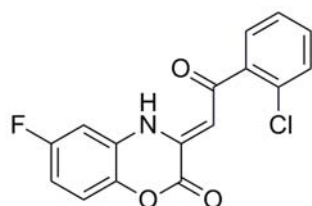
Synthesis of compound **119**



Method: compound **119** was synthesized according to the general procedure from 2-amino-4-methylphenol. The product was obtained as a dark green powder.

Characterization: $^1\text{H-NMR}$ (300 MHz, $\text{DMSO-}d_6$): δ 12.42 (s, 1H), δ 7.62-7.40 (m, 5H), 7.12-7.00 (m, 2H), 6.43 (s, 1H), 2.31 (s, 3H).

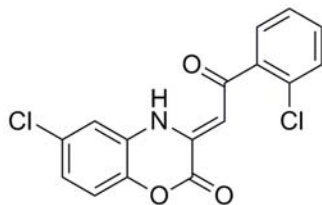
Synthesis of compound **120**



Method: compound **120** was synthesized according to the general procedure from 2-amino-4-fluorophenol. The product was obtained as a dark yellow powder.

Characterization: $^1\text{H-NMR}$ (300 MHz, $\text{DMSO-}d_6$): δ 12.37 (s, 1H), δ 7.77-7.65 (m, 1H), δ 7.58-7.40 (m, 4H), δ 7.32-7.20 (m, 1H), δ 7.02-6.92 (m, 1H), δ 6.50 (s, 1H).

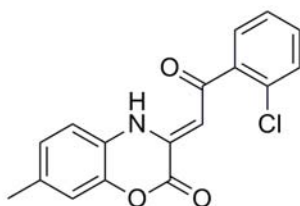
Synthesis of compound **121**



Method: compound **121** was synthesized according to the general procedure from 2-amino-4-chlorophenol. The product was obtained as a yellow powder.

Characterization: $^1\text{H-NMR}$ (300 MHz, $\text{DMSO-}d_6$): δ 12.31 (s, 1H), δ 7.91 (s, 1H), δ 7.70-7.40 (m, 4H), δ 7.26 (d, $J=9.0$ Hz, 1H), δ 7.20-7.10 (m, 1H), δ 6.51 (s, 1H).

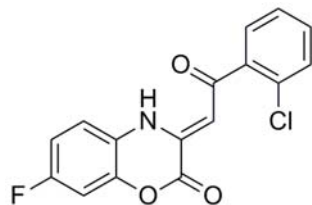
Synthesis of compound **122**



Method: compound **122** was synthesized according to the general procedure from 2-amino-5-methylphenol. The product was obtained as a yellow powder.

Characterization: $^1\text{H-NMR}$ (300 MHz, $\text{DMSO-}d_6$): δ 12.35 (s, 1H), δ 7.62-7.40 (m, 5H), δ 7.15 (d, $J=8.1$ Hz, 1H), δ 7.00-7.92 (m, 1H), δ 6.45 (s, 1H), δ 2.30 (s, 3H).

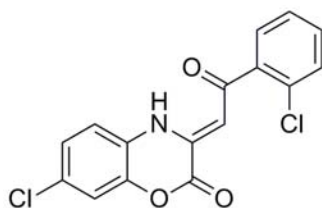
Synthesis of compound **123**



Method: compound **123** was synthesized according to the general procedure from 2-amino-5-fluorolphenol. The product was obtained as a yellow powder.

Characterization: $^1\text{H-NMR}$ (300 MHz, $\text{DMSO-}d_6$): δ 12.36 (s, 1H), δ 7.80-7.72 (m, 1H), δ 7.65-7.40 (m, 4H), δ 7.35-7.24 (m, 1H), δ 7.17-7.06 (m, 1H), δ 6.44 (s, 1H).

Synthesis of compound **124**



Method: compound **124** was synthesized according to the general procedure from 2-amino-5-chlorolphenol. The product was obtained as a yellow powder.

Characterization: $^1\text{H-NMR}$ (300 MHz, $\text{DMSO-}d_6$): δ 12.43 (s, 1H), δ 7.75 (d, $J=8.7$ Hz, 1H), δ 7.62-7.40 (m, 4H), δ 7.27 (dd, $J=2.4$ Hz, 4.5 Hz, 1H), δ 6.47 (s, 1H).

MIC determination against M. tuberculosis

Antibacterial activity against *M. tuberculosis* was performed as described in Chapter 3.

MIC determination against S. aureus

Antibacterial activity against *S. aureus* was performed as described in Chapter 3.

MIC determination against M. Smegmatis

Whole-cell antibacterial activity was determined by a standard broth microdilution susceptibility procedure (214). Bacterial cells were first grown in Middlebrook 7H9 medium to early-mid log phase, and sequentially aliquoted into a 96-well plate (10 μ L). Inhibitors were first dissolved in DMSO and serially diluted in each well and the final concentration of the inhibitor ranged from 1 μ g/mL to 500 μ g/mL. Plates were incubated at 37°C for 1-2 days and each well was evaluated for bacterial growth by reading the absorbance at 600 nm (OD₆₀₀), and the minimum concentration that inhibit the bacterial growth was considered as MIC value.

Bibliography

1. Bloom, B. R., and Murray, C. J. L. (1992) Tuberculosis - commentary on a reemergent killer, *Science* 257, 1055-1064.
2. Fletcher, H. A., Donoghue, H. D., Holton, J., Pap, I., and Spigelman, M. (2003) Widespread occurrence of *Mycobacterium tuberculosis* DNA from 18th-19th century Hungarians, *Am. J. Phys. Anthropol.* 120, 144-152.
3. Mackowiak, P. A., Blos, V. T., Aguilar, M., and Buikstra, J. E. (2005) On the origin of American tuberculosis, *Clin. Infect. Dis.* 41, 515-518.
4. Daniel, T. M. (2006) The history of tuberculosis, *Resp. Med.* 100, 1862-1870.
5. Dye, C., Scheele, S., Dolin, P., Pathania, V., Raviglione, R. C., and Project, W. H. O. G. S. M. (1999) Global burden of tuberculosis - Estimated incidence, prevalence, and mortality by country, *JAMA-J. Am. Med. Assoc.* 282, 677-686.
6. Shafer, R. W., Kim, D. S., Weiss, J. P., and Quale, J. M. (1991) Extrapulmonary tuberculosis in patients with human immunodeficiency virus infection, *Medicine* 70, 384-397.
7. Alvarez, S., and McCabe, W. R. (1984) Extrapulmonary tuberculosis revisited: a review of experience at Boston city and other hospitals, *Medicine* 63, 25-55.
8. Frieden, T. R., Sterling, T. R., Munsiff, S. S., Watt, C. J., and Dye, C. (2003) Tuberculosis, *Lancet* 362, 887-899.
9. Parrish, N. M., Dick, J. D., and Bishai, W. R. (1998) Mechanisms of latency in *Mycobacterium tuberculosis*, *Trends Microbiol.* 6, 107-112.
10. Manabe, Y. C., and Bishai, W. R. (2000) Latent *Mycobacterium tuberculosis* - persistence, patience, and winning by waiting, *Nat. Med.* 6, 1327-1329.

11. Corbett, E. L., Watt, C. J., Walker, N., Maher, D., Williams, B. G., Raviglione, M. C., and Dye, C. (2003) The growing burden of tuberculosis - global trends and interactions with the HIV epidemic, *Arch. Intern. Med.* 163, 1009-1021.
12. Barnes, P. F., Bloch, A. B., Davidson, P. T., and Snider, D. E. (1991) Tuberculosis in patients with human-immunodeficiency-virus infection, *New Engl. J. Med.* 324, 1644-1650.
13. vanSoolingen, D., Hoogenboezem, T., deHaas, P. E. W., Hermans, P. W. M., Koedam, M. A., Teppema, K. S., Brennan, P. J., Besra, G. S., Portaels, F., Top, J., Schouls, L. M., and vanEmbden, J. D. A. (1997) A novel pathogenic taxon of the *Mycobacterium tuberculosis* complex, Canetti: Characterization of an exceptional isolate from Africa, *Int. J. Syst. Bacteriol.* 47, 1236-1245.
14. Cox, R. A. (2004) Quantitative relationships for specific growth rates and macromolecular compositions of *Mycobacterium tuberculosis*, *Streptomyces coelicolor* A3(2) and *Escherichia coli* B/r: an integrative theoretical approach, *Microbiol.* 150, 1413-1426.
15. Madison, B. (2001) Application of stains in clinical microbiology, *Biotech. Histochem.* 76, 119-125.
16. Cole, S. T., Brosch, R., Parkhill, J., Garnier, T., Churcher, C., Harris, D., Gordon, S. V., Eiglmeier, K., Gas, S., Barry, C. E., Tekaiia, F., Badcock, K., Basham, D., Brown, D., Chillingworth, T., Connor, R., Davies, R., Devlin, K., Feltwell, T., Gentles, S., Hamlin, N., Holroyd, S., Hornby, T., Jagels, K., Krogh, A., McLean, J., Moule, S., Murphy, L., Oliver, K., Osborne, J., Quail, M. A., Rajandream, M. A., Rogers, J., Rutter, S., Seeger, K., Skelton, J., Squares, R., Squares, S.,

- Sulston, J. E., Taylor, K., Whitehead, S., and Barrell, B. G. (1998) Deciphering the biology of *Mycobacterium tuberculosis* from the complete genome sequence, *Nature* 393, 537-544.
17. Brennan, P. J., and Nikaido, H. (1995) The envelope of mycobacteria, *Annu. Rev. Biochem* 64, 29-63.
 18. Means, T. K., Wang, S. Y., Lien, E., Yoshimura, A., Golenbock, D. T., and Fenton, M. J. (1999) Human toll-like receptors mediate cellular activation by *Mycobacterium tuberculosis*, *J. Immunol.* 163, 3920-3927.
 19. Via, L. E., Lin, L., Ray, S. M., Carrillo, J., Allen, S. S., Eum, S. Y., Taylor, K., Klein, E., Manjunatha, U., Gonzales, J., Lee, E. G., Park, S. K., Raleigh, J. A., Cho, S. N., McMurray, D. N., Flynn, J. L., and Barry, C. E. (2008) Tuberculous granulomas are hypoxic in guinea pigs, rabbits, and nonhuman primates, *Infect. immun.* 76, 2333-2340.
 20. Russell, D. G., Barry, C. E., and Flynn, J. L. (2010) Tuberculosis: What We Don't Know Can, and Does, Hurt Us, *Science* 328, 852-856.
 21. Choudhry, V. P., Singh, M. M., and Verma, I. C. (1974) BCG and Mantoux intradermal tests in diagnosis of tuberculosis, *Indian Pediatr.* 11, 535-538.
 22. Mahomed, H., Hughes, E. J., Hawkrigde, T., Minnies, D., Simon, E., Little, F., Hanekom, W. A., Geiter, L., and Hussey, G. D. (2006) Comparison of Mantoux skin test with three generations of a whole blood IFN-gamma assay for tuberculosis infection, *Int. J. Tuberc. Lung D.* 10, 310-316.

23. Pottumarthy, S., Morris, A. J., Harrison, A. C., and Wells, V. C. (1999) Evaluation of the tuberculin gamma interferon assay: potential to replace the Mantoux skin test, *J. Clin. Microbiol.* 37, 3229-3232.
24. Behr, M. A., Wilson, M. A., Gill, W. P., Salamon, H., Schoolnik, G. K., Rane, S., and Small, P. M. (1999) Comparative genomics of BCG vaccines by whole-genome DNA microarray, *Science* 284, 1520-1523.
25. Stover, C. K., Delacruz, V. F., Fuerst, T. R., Burlein, J. E., Benson, L. A., Bennett, L. T., Bansal, G. P., Young, J. F., Lee, M. H., Hatfull, G. F., Snapper, S. B., Barletta, R. G., Jacobs, W. R., and Bloom, B. R. (1991) New use of BCG for recombinant vaccines, *Nature* 351, 456-460.
26. Banerjee, A., Dubnau, E., Quemard, A., Balasubramanian, V., Um, K. S., Wilson, T., Collins, D., Delisle, G., and Jacobs, W. R. (1994) InhA, a gene encoding a target for isoniazid and ethionamide in *Mycobacterium tuberculosis*, *Science* 263, 227-230.
27. Zhang, Y., Heym, B., Allen, B., Young, D., and Cole, S. (1992) The catalase peroxidase gene and isoniazid resistance of *Mycobacterium tuberculosis*, *Nature* 358, 591-593.
28. Heifets, L., and Lindholmlevy, P. (1992) Pyrazinamide sterilizing activity *in vitro* against semidormant *Mycobacterium tuberculosis* bacterial populations, *Am. Rev. Respir. Dis.* 145, 1223-1225.
29. Heifets, L. B., and Lindholmlevy, P. J. (1990) Is pyrazinamide bactericidal against *Mycobacterium tuberculosis*?, *Am. Rev. Respir. Dis.* 141, 250-252.

30. Zimhony, O., Cox, J. S., Welch, J. T., Vilcheze, C., and Jacobs, W. R. (2000) Pyrazinamide inhibits the eukaryotic-like fatty acid synthetase I (FASI) of *Mycobacterium tuberculosis*, *Nat. Med.* 6, 1043-1047.
31. Boshoff, H. I., Mizrahi, V., and Barry, C. E. (2002) Effects of pyrazinamide on fatty acid synthesis by whole mycobacterial cells and purified fatty acid synthase I, *J. Bacteriol.* 184, 2167-2172.
32. Zhang, Y., Wade, M. M., Scorpio, A., Zhang, H., and Sun, Z. H. (2003) Mode of action of pyrazinamide: disruption of *Mycobacterium tuberculosis* membrane transport and energetics by pyrazinoic acid, *J. Antimicrob. Chemoth.* 52, 790-795.
33. Zhang, Y., and Mitchison, D. (2003) The curious characteristics of pyrazinamide: a review, *Int. J. Tuberc. Lung D.* 7, 6-21.
34. Scorpio, A., and Zhang, Y. (1996) Mutations in *pncA*, a gene encoding pyrazinamidase/nicotinamidase, cause resistance to the antituberculous drug pyrazinamide in tubercle bacillus, *Nat. Med.* 2, 662-667.
35. Belanger, A. E., Besra, G. S., Ford, M. E., Mikusova, K., Belisle, J. T., Brennan, P. J., and Inamine, J. M. (1996) The *embAB* genes of *Mycobacterium avium* encode an arabinosyl transferase involved in cell wall arabinan biosynthesis that is the target for the antimycobacterial drug ethambutol, *P. Natl. Acad. Sci. USA* 93, 11919-11924.
36. Lee, R. E., Mikusova, K., Brennan, P. J., and Besra, G. S. (1995) Synthesis of the mycobacterial arabinose donor beta-D-arabinofuranosyl-1-monophosphoryldecaprenol, development of a basic arabinosyl-transferase

- assay, and identification of ethambutol as an arabinosyl transferase inhibitor, *J. Am. Chem. Soc.* **117**, 11829-11832.
37. Telenti, A., Philipp, W. J., Sreevatsan, S., Bernasconi, C., Stockbauer, K. E., Wieles, B., Musser, J. M., and Jacobs, W. R. (1997) The *emb* operon, a gene cluster of *Mycobacterium tuberculosis* involved in resistance to ethambutol, *Nat. Med.* **3**, 567-570.
 38. Campbell, E. A., Korzheva, N., Mustaev, A., Murakami, K., Nair, S., Goldfarb, A., and Darst, S. A. (2001) Structural mechanism for rifampicin inhibition of bacterial RNA polymerase, *Cell* **104**, 901-912.
 39. Telenti, A., Imboden, P., Marchesi, F., Lowrie, D., Cole, S., Colston, M. J., Matter, L., Schopfer, K., and Bodmer, T. (1993) Detection of rifampicin-resistance mutations in *Mycobacterium tuberculosis*, *Lancet* **341**, 647-650.
 40. Lambert, M. P., and Neuhaus, F. C. (1972) Mechanism of D-cycloserine action: alanine racemase from *Escherichia coli* W, *J. Bacteriol.* **110**, 978-987.
 41. Bruning, J. B., Murillo, A. C., Chacon, O., Barletta, R. G., and Sacchettini, J. C. (2011) Structure of the *Mycobacterium tuberculosis* D-alanine:D-alanine ligase, a target of the antituberculosis drug D-cycloserine, *Antimicrob. Agents Chemother.* **55**, 291-301.
 42. Oliva, B., Comanducci, A., and Chopra, I. (1998) Antibacterial spectra of drugs used for chemotherapy of mycobacterial infections, *Tuber. Lung Dis.* **79**, 107-109.

43. Shaila, M. S., Ramakris.T, and Gopinath.Kp. (1972) Protein synthesis in *Mycobacterium tuberculosis* H37Rv and effect of streptomycin, *Biochem. J.* 128, 47.
44. Heifets, L., and Lindholmlevy, P. (1989) Comparison of bactericidal activities of streptomycin, amikacin, kanamycin, and capreomycin against *Mycobacterium avium* and *Mycobacterium tuberculosis*, *Antimicrob. Agents Chemother.* 33, 1298-1301.
45. van den Boogaard, J., Kibiki, G. S., Kisanga, E. R., Boeree, M. J., and Aarnoutse, R. E. (2009) New Drugs against Tuberculosis: Problems, Progress, and Evaluation of Agents in Clinical Development, *Antimicrob. Agents Chemother.* 53, 849-862.
46. Koul, A., Arnoult, E., Lounis, N., Guillemont, J., and Andries, K. (2011) The challenge of new drug discovery for tuberculosis, *Nature* 469, 483-490.
47. Boshoff, H. I. M., and Barry, C. E. (2005) Tuberculosis - Metabolism and respiration in the absence of growth, *Nat. Rev. Microbiol.* 3, 70-80.
48. Cosma, C. L., Sherman, D. R., and Ramakrishnan, L. (2003) The secret lives of the pathogenic mycobacteria, *Annu. Rev. Microbiol.* 57, 641-676.
49. Wayne, L. G., and Sramek, H. A. (1994) Metronidazole is bactericidal to dormant cells of *Mycobacterium tuberculosis*, *Antimicrob. Agents Chemother.* 38, 2054-2058.
50. Iona, E., Giannoni, F., Pardini, M., Brunori, L., Orefici, G., and Fattorini, L. (2007) Metronidazole plus rifampin sterilizes long-term dormant *Mycobacterium tuberculosis*, *Antimicrob. Agents Chemother.* 51, 1537-1540.

51. Klinkenberg, L. G., Sutherland, L. A., Bishai, W. R., and Karakousis, P. C. (2008) Metronidazole lacks activity against Mycobacterium tuberculosis in an in vivo hypoxic granuloma model of latency, *J. Infect. Dis.* *198*, 275-283.
52. Hoff, D. R., Caraway, M. L., Brooks, E. J., Driver, E. R., Ryan, G. J., Peloquin, C. A., Orme, I. M., Basaraba, R. J., and Lenaerts, A. J. (2008) Metronidazole Lacks Antibacterial Activity in Guinea Pigs Infected with Mycobacterium tuberculosis, *Antimicrob. Agents Chemother.* *52*, 4137-4140.
53. Manjunatha, U. H., Boshoff, H., Dowd, C. S., Zhang, L., Albert, T. J., Norton, J. E., Daniels, L., Dickl, T., Pang, S. S., and Barry, C. E. (2006) Identification of a nitroimidazo-oxazine-specific protein involved in PA-824 resistance in Mycobacterium tuberculosis, *Proc. Natl. Acad. Sci. U. S. A.* *103*, 431-436.
54. Stover, C. K., Warrener, P., VanDevanter, D. R., Sherman, D. R., Arain, T. M., Langhorne, M. H., Anderson, S. W., Towell, J. A., Yuan, Y., McMurray, D. N., Kreiswirth, B. N., Barry, C. E., and Baker, W. R. (2000) A small-molecule nitroimidazopyran drug candidate for the treatment of tuberculosis, *Nature* *405*, 962-966.
55. de Carvalho, L. P. S., Lin, G., Jiang, X. J., and Nathan, C. (2009) Nitazoxanide Kills Replicating and Nonreplicating Mycobacterium tuberculosis and Evades Resistance, *J. Med. Chem.* *52*, 5789-5792.
56. Hoffman, P. S., Sisson, G., Croxen, M. A., Welch, K., Harman, W. D., CremadeS, N., and Morash, M. G. (2007) Antiparasitic drug nitazoxanide inhibits the pyruvate oxidoreductases of Helicobacter pylori, selected anaerobic bacteria and

- parasites, and *Campylobacter jejuni*, *Antimicrob. Agents Chemother.* 51, 868-876.
57. Sisson, G., Goodwin, A., Raudonikiene, A., Hughes, N. J., Mukhopadhyay, A. K., Berg, D. E., and Hoffman, P. S. (2002) Enzymes associated with reductive activation and action of nitazoxanide, nitrofurans, and metronidazole in *Helicobacter pylori*, *Antimicrob. Agents Chemother.* 46, 2116-2123.
58. Muller, J., Wastling, J., Sanderson, S., Muller, N., and Hemphill, A. (2007) A novel *Giardia lamblia* nitroreductase, GINR1, interacts with nitazoxanide and other thiazolides, *Antimicrob. Agents and Chemother.* 51, 1979-1986.
59. Muller, J., Naguleswaran, A., Muller, N., and Hemphill, A. (2008) Neospora caninum: Functional inhibition of protein disulfide isomerase by the broad-spectrum anti-parasitic drug nitazoxanide and other thiazolides, *Exp. Parasitol.* 118, 80-88.
60. Bryk, R., Gold, B., Venugopal, A., Singh, J., Samy, R., Pupek, K., Cao, H., Popescu, C., Gurney, M., Hotha, S., Cherian, J., Rhee, K., Ly, L., Converse, P. J., Ehrt, S., Vandal, O., Jiang, X. J., Schneider, J., Lin, G., and Nathan, C. (2008) Selective killing of nonreplicating mycobacteria, *Cell Host Microbe* 3, 137-145.
61. Mitchison, D. A. (2008) A new antituberculosis drug that selectively kills nonmultiplying *Mycobacterium tuberculosis*, *Cell Host Microbe* 3, 122-124.
62. Koul, A., Vranckx, L., Dendouga, N., Balemans, W., Van den Wyngaert, I., Vergauwen, K., Goehlmann, H. W. H., Willebrords, R., Poncelet, A., Guillemont, J., Bald, D., and Andries, K. (2008) Diarylquinolines are bactericidal for dormant

- mycobacteria as a result of disturbed ATP homeostasis, *J. Biol. Chem.* **283**, 25273-25280.
63. Koul, A., Dendouga, N., Vergauwen, K., Molenberghs, B., Vranckx, L., Willebrords, R., Ristic, Z., Lill, H., Dorange, I., Guillemont, J., Bald, D., and Andries, K. (2007) Diarylquinolines target subunit c of mycobacterial ATP synthase, *Nat. Chem. Biol.* **3**, 323-324.
64. Diacon, A. H., Pym, A., Grobusch, M., Patientia, R., Rustomjee, R., Page-Shipp, L., Pistorius, C., Krause, R., Bogoshi, M., Churchyard, G., Venter, A., Allen, J., Palomino, J. C., De Marez, T., van Heeswijk, R. P. G., Lounis, N., Meyvisch, P., Verbeeck, J., Parys, W., de Beule, K., Andries, K., and Mc Neeley, D. F. (2009) The diarylquinoline TMC207 for multidrug-resistant tuberculosis, *New Engl. J. Med.* **360**, 2397-2405.
65. Weinstein, E. A., Yano, T., Li, L. S., Avarbock, D., Avarbock, A., Helm, D., McColm, A. A., Duncan, K., Lonsdale, J. T., and Rubin, H. (2005) Inhibitors of type II NADH :menaquinone oxidoreductase represent a class of antitubercular drugs, *P. Natl. Acad. Sci. USA* **102**, 4548-4553.
66. Lester, R. L., and Crane, F. L. (1959) Natural occurrence of coenzyme-Q and related compounds, *J. Biol. Chem.* **234**, 2169-2175.
67. Bishop, D. H. L., Pandya, K. P., and King, H. K. (1962) Ubiquinone and vitamin K in bacteria, *Biochem. J.* **83**, 606.
68. Begley, T. P., Kinsland, C., Taylor, S., Tandon, M., Nicewonger, R., Wu, M., Chiu, H. J., Kelleher, N., Campobasso, N., and Zhang, Y. (1998) Cofactor biosynthesis: A mechanistic perspective, In *Biosynthesis - Polyketides and*

- Vitamins. Topics in Current Chemistry* (Leeper, F. J., and Vederas, J. C., Eds.), pp 93-142, Springer-Verlag, Berlin.
69. Meganathan, R. (2001) Biosynthesis of menaquinone (vitamin K-2) and ubiquinone (coenzyme Q): A perspective on enzymatic mechanisms, *Vitam. Horm.* **61**, 173-218.
 70. Truglio, J. J., Theis, K., Feng, Y., Gajda, R., Machutta, C., Tonge, P. J., and Kisker, C. (2003) Crystal structure of *Mycobacterium tuberculosis* MenB, a key enzyme in vitamin K-2 biosynthesis, *J. Biol. Chem.* **278**, 42352-42360.
 71. Bentley, R. (1990) The shikimate pathway - a metabolic tree with many branches, *Crit. Rev. Biochem. Mol.* **25**, 307-384.
 72. Kolappan, S., Zwahlen, J., Zhou, R., Truglio, J. J., Tonge, P. J., and Kisker, C. (2007) Lysine 190 is the catalytic base in MenF, the menaquinone-specific isochorismate synthase from *Escherichia coli*: Implications for an enzyme family, *Biochemistry* **46**, 946-953.
 73. Jiang, M., Cao, Y., Guo, Z. F., Chen, M. J., Chen, X. L., and Guo, Z. H. (2007) Menaquinone biosynthesis in *Escherichia coli*: Identification of 2-succinyl-5-enolpyruvyl-6-hydroxy-3-cyclohexene-1-carboxylate as a novel intermediate and re-evaluation of MenD activity, *Biochemistry* **46**, 10979-10989.
 74. Jiang, M., Chen, M. J., Cao, Y., Yang, Y. H., Sze, K. H., Chen, X. L., and Guo, Z. H. (2007) Determination of the stereochemistry of 2-succinyl-5-enolpyruvyl-6-hydroxy-3-cyclohexene-1-carboxylate, a key intermediate in menaquinone biosynthesis, *Org. Lett.* **9**, 4765-4767.

75. Jiang, M., Chen, X. L., Wu, X. H., Chen, M. J., Wo, Y. D., and Guo, Z. H. (2009) Catalytic mechanism of SHCHC synthase in the menaquinone biosynthesis of *Escherichia coli*: identification and mutational analysis of the active site residues, *Biochemistry* 48, 6921-6931.
76. Sharma, V., Meganathan, R., and Hudspeth, M. E. S. (1993) Menaquinone (Vitamin K2) biosynthesis - Cloning, nucleotide-sequence, and expression of the *menC* gene from *Escherichia Coli*, *J. Bacteriol.* 175, 4917-4921.
77. Glasner, M. E., Fayazmanesh, N., Chiang, R. A., Sakai, A., Jacobson, M. P., Gerlt, J. A., and Babbitt, P. C. (2006) Evolution of structure and function in the o-succinylbenzoate synthase/N-acylamino acid racemase family of the enolase superfamily, *J. Mol. Biol.* 360, 228-250.
78. Sharma, V., Hudspeth, M. E. S., and Meganathan, R. (1996) Menaquinone (vitamin K-2) biosynthesis: Localization and characterization of the *menE* gene from *Escherichia coli*, *Gene* 168, 43-48.
79. Young, I. G. (1975) Biosynthesis of bacterial menaquinones - menaquinone mutants of *Escherichia coli*, *Biochemistry* 14, 399-406.
80. Lee, P. T., Hsu, A. Y., Ha, H. T., and Clarke, C. F. (1997) A C-methyltransferase involved in both ubiquinone and menaquinone biosynthesis: Isolation and identification of the *Escherichia coli* *ubiE* gene, *J. Bacteriol.* 179, 1748-1754.
81. Seto, H., Jinnai, Y., Hiratsuka, T., Fukawa, M., Furihata, K., Itoh, N., and Dairi, T. (2008) Studies on a new biosynthetic pathway for menaquinone, *J. Am. Chem. Soc.* 130, 5614-5615.

82. Dairi, T. (2009) An alternative menaquinone biosynthetic pathway operating in microorganisms: an attractive target for drug discovery to pathogenic *Helicobacter* and *Chlamydia* strains, *J. Antibiot.* 62, 347-352.
83. Hiratsuka, T., Furihata, K., Ishikawa, J., Yamashita, H., Itoh, N., Seto, H., and Dairi, T. (2008) An alternative menaquinone biosynthetic pathway operating in microorganisms, *Science* 321, 1670-1673.
84. Rodrigues, T., Lopes, F., and Moreira, R. (2010) Inhibitors of the mitochondrial electron transport chain and *de novo* pyrimidine biosynthesis as antimalarials: the present status, *Curr. Med. Chem.* 17, 929-956.
85. Biagini, G. A., Viriyavejakul, P., O'Neill, P. M., Bray, P. G., and Ward, S. A. (2006) Functional characterization and target validation of alternative complex I of *Plasmodium falciparum* mitochondria, *Antimicrob. Agents Chemother.* 50, 1841-1851.
86. Dong, C. K., Patel, V., Yang, J. C., Dvorin, J. D., Duraisingh, M. T., Clardy, J., and Wirth, D. F. (2009) Type II NADH dehydrogenase of the respiratory chain of *Plasmodium falciparum* and its inhibitors, *Bioorg. Med. Chem. Lett.* 19, 972-975.
87. Suraveratum, N., Krungkrai, S. R., Leangaramgul, P., Prapunwattana, P., and Krungkrai, J. (2000) Purification and characterization of *Plasmodium falciparum* succinate dehydrogenase, *Mol. Biochem. Parasit.* 105, 215-222.
88. Aponte, J. C., Verastegui, M., Malaga, E., Zimic, M., Quiliano, M., Vaisberg, A. J., Gilman, R. H., and Hammond, G. B. (2008) Synthesis, cytotoxicity, and anti-*Trypanosoma cruzi* activity of new chalcones, *J. Med. Chem.* 51, 6230-6234.

89. Dominguez, J. N., Charris, J. E., Lobo, G., de Dominguez, N. G., Moreno, M. M., Riggione, F., Sanchez, E., Olson, J., and Rosenthal, P. J. (2001) Synthesis of quinoliny chalcones and evaluation of their antimalarial activity, *Eur. J. Med. Chem.* 36, 555-560.
90. Mather, M. W., Darrouzet, E., Valkova-Valchanova, M., Cooley, J. W., McIntosh, M. T., Daldal, F., and Vaidya, A. B. (2005) Uncovering the molecular mode of action of the antimalarial drug atovaquone using a bacterial system, *J. Biol. Chem.* 280, 27458-27465.
91. Andries, K., Verhasselt, P., Guillemont, J., Gohlmann, H. W. H., Neefs, J. M., Winkler, H., Van Gestel, J., Timmerman, P., Zhu, M., Lee, E., Williams, P., de Chaffoy, D., Huitric, E., Hoffner, S., Cambau, E., Truffot-Pernot, C., Lounis, N., and Jarlier, V. (2005) A diarylquinoline drug active on the ATP synthase of *Mycobacterium tuberculosis*, *Science* 307, 223-227.
92. Newman, D. K., and Kolter, R. (2000) A role for excreted quinones in extracellular electron transfer, *Nature* 405, 94-97.
93. Bott, M., and Niebisch, A. (2003) The respiratory chain of *Corynebacterium glutamicum*, *J. Biotechnol.* 104, 129-153.
94. Miller, P., Rabinowitz, A., and Taber, H. (1988) Molecular cloning and preliminary genetic analysis of the *men* gene cluster of *Bacillus subtilis*, *J. Bacteriol.* 170, 2735-2741.
95. Dhiman, R. K., Mahapatra, S., Slayden, R. A., Boyne, M. E., Lenaerts, A., Hinshaw, J. C., Angala, S. K., Chatterjee, D., Biswas, K., Narayanasamy, P., Kurosu, M., and Crick, D. C. (2009) Menaquinone synthesis is critical for

- maintaining mycobacterial viability during exponential growth and recovery from non-replicating persistence, *Mol. Microbiol.* 72, 85-97.
96. Kurosu, M., Narayanasamy, P., Biswas, K., Dhiman, R., and Crick, D. C. (2007) Discovery of 1,4-dihydroxy-2-naphthoate prenyltransferase inhibitors: New drug leads for multidrug-resistant gram-positive pathogens, *J. Med. Chem.* 50, 3973-3975.
 97. Kurosu, M., and Crick, D. C. (2009) MenA is a promising drug target for developing novel lead molecules to combat *Mycobacterium tuberculosis*, *Med. Chem.* 5, 197-207.
 98. Lu, X. Q., Zhang, H. N., Tonge, P. J., and Tan, D. S. (2008) Mechanism-based inhibitors of MenE, an acyl-CoA synthetase involved in bacterial menaquinone biosynthesis, *Bioorg. Med. Chem. Lett.* 18, 5963-5966.
 99. Tian, Y., Suk, D. H., Cai, F., Crich, D., and Mesecar, A. D. (2008) *Bacillus anthracis* o-succinylbenzoyl-CoA synthetase: Reaction kinetics and a novel inhibitor mimicking its reaction intermediate, *Biochemistry* 47, 12434-12447.
 100. Fang, M. H., Toogood, R. D., Macova, A., Ho, K., Franzblau, S. G., McNeil, M. R., Sanders, D. A. R., and Palmer, D. R. J. (2010) Succinylphosphonate esters are competitive inhibitors of MenD that show active-site discrimination between homologous *alpha*-ketoglutarate-decarboxylating enzymes, *Biochemistry* 49, 2672-2679.
 101. Mathew, R., Kruthiventi, A. K., Prasad, J. V., Kumar, S. P., Srinu, G., and Chatterji, D. (2010) Inhibition of mycobacterial growth by plumbagin derivatives, *Chem. Biol. Drug Des.* 76, 34-42.

102. Truglio, J. J., Theis, K., Feng, Y. G., Gajda, R., Machutta, C., Tonge, P. J., and Kisker, C. (2003) Crystal structure of *Mycobacterium tuberculosis* MenB, a key enzyme in vitamin K-2 biosynthesis, *J. Biol. Chem.* 278, 42352-42360.
103. Ulaganathan, V., Agacan, M. F., Buetow, L., Tulloch, L. B., and Hunter, W. N. (2007) Structure of *Staphylococcus aureus* 1,4-dihydroxy-2-naphthoyl-CoA synthase (MenB) in complex with acetoacetyl-CoA, *Acta Crystallogr. F* 63, 908-913.
104. Kanaujia, S. P., Ranjani, C. V., Jeyakanthan, J., Baba, S., Kuroishi, C., Ebihara, A., Shinkai, A., Kuramitsu, S., Shiro, Y., Sekar, K., and Yokoyama, S. (2007) Cloning, expression, purification, crystallization and preliminary X-ray crystallographic study of DHNA synthetase from *Geobacillus kaustophilus*, *Acta Crystallogr. F* 63, 103-105.
105. Meganathan, R., Bentley, R., and Taber, H. (1981) Identification of *Bacillus subtilis* *men* mutants which lack *ortho*-succinylbenzoyl-Coenzyme A synthase and dihydroxynaphthoate synthase, *J. Bacteriol.* 145, 328-332.
106. Taber, H. W., Dellers, E. A., and Lombardo, L. R. (1981) Menaquinone biosynthesis in *Bacillus subtilis* - Isolation of *men* mutants and evidence for clustering of *men* genes, *J. Bacteriol.* 145, 321-327.
107. Shaw, D. J., Guest, J. R., Meganathan, R., and Bentley, R. (1982) Characterization of *Escherichia coli* *men* mutants defective in conversion of *ortho*-succinylbenzoate to 1,4-dihydroxy-2-naphthoate, *J. Bacteriol.* 152, 1132-1137.

108. Engel, C. K., Mathieu, M., Zeelen, J. P., Hiltunen, J. K., and Wierenga, R. K. (1996) Crystal structure of enoyl-coenzyme A (CoA) hydratase at 2.5 angstrom resolution: A spiral fold defines the CoA-binding pocket, *EMBO J.* 15, 5135-5145.
109. Benning, M. M., Haller, T., Gerlt, J. A., and Holden, H. M. (2000) New reactions in the crotonase superfamily: Structure of methylmalonyl CoA decarboxylase from *Escherichia coli*, *Biochemistry* 39, 4630-4639.
110. Modis, Y., Filppula, S. A., Novikov, D. K., Norledge, B., Hiltunen, J. K., and Wierenga, R. K. (1998) The crystal structure of dienoyl-CoA isomerase at 1.5 angstrom resolution reveals the importance of aspartate and glutamate sidechains for catalysis, *Structure* 6, 957-970.
111. Mursula, A. M., van Aalten, D. M. F., Hiltunen, J. K., and Wierenga, R. K. (2001) The crystal structure of Delta(3)-Delta(2)-enoyl-CoA isomerase, *J. Mol. Biol.* 309, 845-853.
112. Benning, M. M., Taylor, K. L., Liu, R. Q., Yang, G., Xiang, H., Wesenberg, G., DunawayMariano, D., and Holden, H. M. (1996) Structure of 4-chlorobenzoyl coenzyme A dehalogenase determined to 1.8 angstrom resolution: An enzyme catalyst generated via adaptive mutation, *Biochemistry* 35, 8103-8109.
113. Whittingham, J. L., Turkenburg, J. P., Verma, C. S., Walsh, M. A., and Grogan, G. (2003) The 2-Å crystal structure of 6-oxo camphor hydrolase - New structural diversity in the crotonase superfamily, *J. Biol. Chem.* 278, 1744-1750.
114. Kurimoto, K., Fukai, S., Nureki, O., Muto, Y., and Yokoyama, S. (2001) Crystal structure of human AUH protein, a single-stranded RNA binding homolog of enoyl-CoA hydratase, *Structure* 9, 1253-1263.

115. Holden, H. M., Benning, M. M., Haller, T., and Gerlt, J. A. (2001) The crotonase superfamily: Divergently related enzymes that catalyze different reactions involving acyl coenzyme A thioesters, *Acc. Chem. Res.* **34**, 145-157.
116. Mishra, P. K., and Drueckhammer, D. G. (2000) Coenzyme A analogues and derivatives: Synthesis and applications as mechanistic probes of coenzyme A ester-utilizing enzymes, *Chem. Rev.* **100**, 3283-3309.
117. Paige, L. A., Zheng, G. Q., Defrees, S. A., Cassady, J. M., and Geahlen, R. L. (1989) S-(2-Oxopentadecyl)-CoA, a nonhydrolyzable analogue of myristoyl-CoA, is a potent inhibitor of myristoyl-CoA: protein N-myristoyltransferase, *J. Med. Chem.* **32**, 1665-1667.
118. Karl, R. M., Hupperich, M., Thomer, A., and Eggerer, H. (1995) Inhibition of 3-hydroxy-3-methylglutaryl-CoA reductase and citrate synthase by sulfoxides and sulfones of substrate-analogue CoA-thioether derivatives, *Eur. J. Biochem.* **227**, 292-295.
119. Dai, M., Feng, Y. G., and Tonge, P. J. (2001) Synthesis of crotonyl-OxyCoA: A mechanistic probe of the reaction catalyzed by enoyl-CoA hydratase, *J. Am. Chem. Soc.* **123**, 506-507.
120. Tosin, M., Spiteller, D., and Spencer, J. B. (2009) Malonyl carba(dethia)- and malonyl oxa(dethia)-coenzyme A as tools for trapping polyketide intermediates, *ChemBioChem* **10**, 1714-1723.
121. Richard, J. P., Williams, G., O'Donoghue, A. C., and Amyes, T. L. (2002) Formation and stability of enolates of acetamide and acetate anion: An eigen plot for proton transfer at alpha-carbonyl carbon, *J. Am. Chem. Soc.* **124**, 2957-2968.

122. Meganathan, R., Folger, T., and Bentley, R. (1980) Conversion of *o*-succinylbenzoate to dihydroxynaphthoate by extracts of *Micrococcus luteus*, *Biochemistry* 19, 785-789.
123. Hur, G. H., Meier, J. L., Baskin, J., Codelli, J. A., Bertozzi, C. R., Marahiel, M. A., and Burkart, M. D. (2009) Crosslinking studies of protein-protein interactions in nonribosomal peptide biosynthesis, *Chem. Biol.* 16, 372-381.
124. Zhang, Z. X., Yin, Z. W., Meanwell, N. A., Kadow, J. F., and Wang, T. (2003) Selective monoacylation of symmetrical diamines via prior complexation with boron, *Org. Lett.* 5, 3399-3402.
125. Kolkmann, R., and Leistner, E. (1987) Synthesis, analysis and characterization of the coenzyme A esters *o*-succinylbenzoic acid, an intermediate in vitamin K2 (menaquinone) biosynthesis, *Z. Naturforsch. C* 42, 542-552.
126. Walkowiak, A., Wakiec, R., Bontemps-Gracz, M. M., and Andruszkiewicz, R. (2005) Glutamine analogues containing a keto function - novel inhibitors of fungal glucosamine-6-phosphate synthase, *J. Enzym. Inhib. Med. Chem.* 20, 439-447.
127. Hanessian, S., Claridge, S., and Johnstone, S. (2002) The power of visual imagery in synthesis planning. Stereocontrolled approaches to CGP-60536B, a potent renin inhibitor, *J. Org. Chem.* 67, 4261-4274.
128. Worthington, A. S., Hur, G. H., Meier, J. L., Cheng, Q., Moore, B. S., and Burkart, M. D. (2008) Probing the compatibility of type II ketosynthase-carrier protein partners, *ChemBioChem* 9, 2096-2103.

129. Worthington, A. S., Rivera, H., Torpey, J. W., Alexander, M. D., and Burkart, M. D. (2006) Mechanism-based protein cross-linking probes to investigate carrier protein-mediated biosynthesis, *ACS Chem. Biol.* **1**, 687-691.
130. Hahn, F. E., Langenhahn, V., and Pape, T. (2005) Template synthesis of tungsten complexes with saturated N-heterocyclic carbene ligands, *Chem. Comm.*, 5390-5392.
131. Trabocchi, A., Rolla, M., Menchi, G., and Guarna, A. (2005) Synthesis of a constrained tricyclic scaffold based on trans-4-hydroxy-L-proline, *Tetrahedron Lett.* **46**, 7813-7816.
132. van Wyk, M., and Strauss, E. (2007) One-pot preparation of coenzyme A analogues via an improved chemoenzymatic synthesis of pre-CoA thioester synthons, *Chem. Comm.*, 398-400.
133. Ho, S. N., Hunt, H. D., Horton, R. M., Pullen, J. K., and Pease, L. R. (1989) Site-directed mutagenesis by overlap extension using the polymerase chain reaction, *Gene* **77**, 51-59.
134. Corper, H. J., and Cohn, M. L. (1951) The viability and virulence of old cultures of tubercle bacilli: (Studies on 30-year-old broth cultures maintained at 37° C.) *Tubercle* **32**, 232-237.
135. Gengenbacher, M., Rao, S. P., Pethe, K., and Dick, T. (2010) Nutrient-starved, non-replicating *Mycobacterium tuberculosis* requires respiration, ATP synthase and isocitrate lyase for maintenance of ATP homeostasis and viability, *Microbiology* **156**, 81-87.

136. Kurosu, M., and Begari, E. (2010) Vitamin K-2 in electron transport system: Are enzymes involved in Vitamin K-2 biosynthesis promising drug targets?, *Molecules* **15**, 1531-1553.
137. Booth, S. L., and Suttie, J. W. (1998) Dietary intake and adequacy of vitamin K, *J. Nutr.* **128**, 785-788.
138. Ramotar, K., Conly, J. M., Chubb, H., and Louie, T. J. (1984) Production of menaquinone by intestinal anaerobes, *J. Infect Dis.* **150**, 213-218.
139. Thijssen, H. H. W., DrittijReijnders, M. J., and Fischer, M. (1996) Phylloquinone and menaquinone-4 distribution in rats: Synthesis rather than uptake determines menaquinone-4 organ concentrations, *J. Nutr.* **126**, 537-543.
140. vonEiff, C., Heilmann, C., Proctor, R. A., Woltz, C., Peters, G., and Gotz, F. (1997) A site-directed *Staphylococcus aureus hemB* mutant is a small-colony variant which persists intracellularly, *J. Bacteriol.* **179**, 4706-4712.
141. Proctor, R. A., von Eiff, C., Kahl, B. C., Becker, K., McNamara, P., Herrmann, M., and Peters, G. (2006) Small colony variants: a pathogenic form of bacteria that facilitates persistent and recurrent infections, *Nat. Rev. Microbiol.* **4**, 295-305.
142. von Eiff, C., McNamara, P., Becker, K., Bates, D., Lei, X. H., Ziman, M., Bochner, B. R., Peters, G., and Proctor, R. A. (2006) Phenotype microarray profiling of *Staphylococcus aureus menD* and *hemB* mutants with the small-colony-variant phenotype, *J. Bacteriol.* **188**, 687-693.
143. Bates, D. M., von Eiff, C., McNamara, P. J., Peters, G., Yeaman, M. R., Bayer, A. S., and Proctor, R. A. (2003) *Staphylococcus aureus menD* and *hemB* mutants

- are as infective as the parent strains, but the menadione biosynthetic mutant persists within the kidney, *J. Infect. Dis.* 187, 1654-1661.
144. vonEiff, C., Bettin, D., Proctor, R. A., Rolauffs, B., Lindner, N., Winkelmann, W., and Peters, G. (1997) Recovery of small colony variants of *Staphylococcus aureus* following gentamicin bead placement for osteomyelitis, *Clin. Infect. Dis.* 25, 1250-1251.
 145. Ramchandra, P., and Sturm, A. W. (2010) Expression of the naphthoate synthase gene in *Mycobacterium tuberculosis* in a self-generated oxygen depleted liquid culture system, *Anaerobe* 16, 610-613.
 146. Lannergard, J., von Eiff, C., Sander, G., Cordes, T., Seggewiss, J., Peters, G., Proctor, R. A., Becker, K., and Hughes, D. (2008) Identification of the genetic basis for clinical Menadione-auxotrophic small-colony variant isolates of *Staphylococcus aureus*, *Antimicrob. Agents Chemother.* 52, 4017-4022.
 147. Sassetti, C. M., Boyd, D. H., and Rubin, E. J. (2003) Genes required for mycobacterial growth defined by high density mutagenesis, *Mol. Microbiol.* 48, 77-84.
 148. Zhang, J. H., Chung, T. D. Y., and Oldenburg, K. R. (1999) A simple statistical parameter for use in evaluation and validation of high throughput screening assays, *J. Biomol. Screen.* 4, 67-73.
 149. Forfar, J. O., Gould, J. C., and Maccabe, A. F. (1968) Effect of hexachlorophane on incidence of Staphylococcal and gram-negative infection in newborn, *Lancet* 2, 177-&.

150. Sprunt, K., Redman, W., and Leidy, G. (1973) Antibacterial effectiveness of routine hand washing, *Pediatrics* 52, 264-271.
151. Frederick, J. J., Corner, T. R., and Gerhardt, P. (1974) Antimicrobial actions of hexachlorophene - inhibition of respiration in *Bacillus megaterium*, *Antimicrob. Agents Chemother.* 6, 712-721.
152. McGovern, S. L., Caselli, E., Grigorieff, N., and Shoichet, B. K. (2002) A common mechanism underlying promiscuous inhibitors from virtual and high-throughput screening, *J. Med. Chem.* 45, 1712-1722.
153. Seidler, J., McGovern, S. L., Doman, T. N., and Shoichet, B. K. (2003) Identification and prediction of promiscuous aggregating inhibitors among known drugs, *J. Med. Chem.* 46, 4477-4486.
154. Feng, B. Y., Shelat, A., Doman, T. N., Guy, R. K., and Shoichet, B. K. (2005) High-throughput assays for promiscuous inhibitors, *Nat. Chem. Biol.* 1, 146-148.
155. O'Brien, W. E. (1976) Continuous spectrophotometric assay for argininosuccinate synthetase based on pyrophosphate formation, *Anal. Biochem.* 76, 423-430.
156. Bianchi, M., Butti, A., Christidis, Y., Perronnet, J., Barzaghi, F., Cesana, R., and Nencioni, A. (1988) Gastric anti-secretory, anti-ulcer and cytoprotective properties of substituted (*E*)-4-phenyl-and heteroaryl-4-oxo-2-butenoic acids, *Eur. J. Med. Chem.* 23, 45-52.
157. Yamada, M., Nagashima, N., Hasegawa, J., and Takahashi, S. (1998) A highly efficient asymmetric synthesis of methoxyhomophenylalanine using Michael addition of phenethylamine, *Tetrahedron Lett.* 39, 9019-9022.

158. Jenner, G. (1996) Comparative study of physical and chemical activation modes. The case of the synthesis of beta-amino derivatives, *Tetrahedron* 52, 13557-13568.
159. Jumaa, M., Carlson, B., Chimilio, L., Silchenko, S., and Stella, V. J. (2004) Kinetics and mechanism of degradation of epothilone-D: An experimental anticancer agent, *J. Pharm. Sci.* 93, 2953-2961.
160. Jarlier, V., and Nikaido, H. (1994) Mycobacterial cell wall: structure and role in natural resistance to antibiotics, *FEMS Microbiol. Lett.* 123, 11-18.
161. McDonnell, G., and Russell, A. D. (1999) Antiseptics and disinfectants: Activity, action, and resistance, *Clin. Microbiol. Rev.* 12, 147-+.
162. Stephan, J., Bender, J., Wolschendorf, F., Hoffmann, C., Roth, E., Mailander, C., Engelhardt, H., and Niederweis, M. (2005) The growth rate of *Mycobacterium smegmatis* depends on sufficient porin-mediated influx of nutrients, *Mol. Microbiol.* 58, 714-730.
163. Niederweis, M. (2003) Mycobacterial porins - new channel proteins in unique outer membranes, *Mol. Microbiol.* 49, 1167-1177.
164. Lambert, P. A. (2002) Cellular impermeability and uptake of biocides and antibiotics in Gram-positive bacteria and mycobacteria, *J. Appl. Microbiol.* 92, 46S-54S.
165. Milne, G. W. A. (2010) ChemBioDraw 12.0, *J. Chem. Inf. Model.* 50, 2053-2053.
166. Thomson, S. A., Josey, J. A., Cadilla, R., Gaul, M. D., Hassman, C. F., Luzzio, M. J., Pipe, A. J., Reed, K. L., Ricca, D. J., Wiethe, R. W., and Noble, S. A.

- (1995) Fmoc mediated synthesis of peptide nucleic acids, *Tetrahedron* 51, 6179-6194.
167. Halkes, K. M., de Souza, A. C., Maljaars, C. E. P., Gerwig, G. J., and Kamerling, J. P. (2005) A facile method for the preparation of gold glyconanoparticles from free oligosaccharides and their applicability in carbohydrate-protein interaction studies, *Eur. J. Org. Chem.*, 3650-3659.
168. Zhao, H. Y., and Liu, G. (2007) Solution-phase parallel synthesis of 2,3-Dihydro-1,5-benzothiazepin-4(5H)-ones, *J. Comb. Chem.* 9, 756-772.
169. Shimizu, S., Komaki, R., Tani, Y., and Yamada, H. (1983) A high yield method for the preparative synthesis of Coenzyme A by combination of chemical and enzymic reactions, *FEBS Lett.* 151, 303-306.
170. Shimizu, S., Esumi, A., Komaki, R., and Yamada, H. (1984) Production of Coenzyme A by a mutant of *Brevibacterium ammoniagenes* resistant to oxyphantetheine, *Appl. Environ. Microbiol.* 48, 1118-1122.
171. McNamara, P. J., and Proctor, R. A. (2000) *Staphylococcus aureus* small colony variants, electron transport and persistent infections, *Int. J. Antimicrob. Agents* 14, 117-122.
172. Qiao, C. H., Gupte, A., Boshoff, H. I., Wilson, D. J., Bennett, E. M., Somu, R. V., Barry, C. E., and Aldrich, C. C. (2007) 5'-O-(N-Acyl)sulfamoyl adenosines as antitubercular agents that inhibit MbtA: An adenylation enzyme required for siderophore biosynthesis of the mycobactins, *J. Med. Chem.* 50, 6080-6094.
173. Ekici, O. D., Li, Z. Z., Campbell, A. J., James, K. E., Asgian, J. L., Mikołajczyk, J., Salvesen, G. S., Ganesan, R., Jelakovic, S., Grutter, M. G., and Powers, J. C.

- (2006) Design, synthesis, and evaluation of aza-peptide Michael acceptors as selective and potent inhibitors of caspases-2, -3, -6, -7, -8, -9, and -10, *J. Med. Chem.* **49**, 5728-5749.
174. Tsou, H. R., Overbeek-Klumpers, E. G., Hallett, W. A., Reich, M. F., Floyd, M. B., Johnson, B. D., Michalak, R. S., Nilakantan, R., Discafani, C., Golas, J., Rabindran, S. K., Shen, R., Shi, X. Q., Wang, Y. F., Upeslakis, J., and Wissner, A. (2005) Optimization of 6,7-disubstituted-4-(arylamino)quinoline-3-carbonitriles as orally active, irreversible inhibitors of human epidermal growth factor receptor-2 kinase activity, *J. Med. Chem.* **48**, 1107-1131.
175. von Eiff, C. (2008) *Staphylococcus aureus* small colony variants: a challenge to microbiologists and clinicians, *Int. J. Antimicrob. Agents* **31**, 507-510.
176. Cho, S. H., Warit, S., Wan, B. J., Hwang, C. H., Pauli, G. F., and Franzblau, S. G. (2007) Low-oxygen-recovery assay for high-throughput screening of compounds against nonreplicating *Mycobacterium tuberculosis*, *Antimicrob. Agents Chemother.* **51**, 1380-1385.
177. Hurdle, J. G., Lee, R. B., Budha, N. R., Carson, E. I., Qi, J. J., Scherman, M. S., Cho, S. H., McNeil, M. R., Lenaerts, A. J., Franzblau, S. G., Meibohm, B., and Lee, R. E. (2008) A microbiological assessment of novel nitrofuranylamides as anti-tuberculosis agents, *J. Antimicrob. Chemother.* **62**, 1037-1045.
178. Drakulic, B. J., Juranic, Z. D., Stanojkovic, T. P., and Juranic, I. O. (2005) 2-[(Carboxymethyl)sulfanyl]-4-oxo-4-arylbutanoic acids selectively suppressed proliferation of neoplastic human HeLa cells. A SAR/QSAR study, *J. Med. Chem.* **48**, 5600-5603.

179. Drake, N. L., and Tuemmler, W. B. (1955) Podophyllotoxin and picropodophyllin. II. the synthesis of an open-chain analog, *J. Am. Chem. Soc.* 77, 1204-1209.
180. Prakash, G. K. S., Hu, J. B., Alauddin, M. M., Conti, P. S., and Olah, G. A. (2003) A general method of halogenation for synthesis of alpha-halodifluoromethyl ketones and F-18 -labeled trifluoromethyl ketones, *J. Fluorine Chem.* 121, 239-243.
181. Amii, H., Kobayashi, T., Hatamoto, Y., and Uneyama, K. (1999) Mg⁰-promoted selective C-F bond cleavage of trifluoromethyl ketones: a convenient method for the synthesis of 2,2-difluoro enol silanes, *Chem. Comm.*, 1323-1324.
182. Wojaczynska, E., and Skarzewski, J. (2008) Chelating 2-azanorbornyl derivatives as effective nitrogen-nitrogen and nitrogen-chalcogen donating ligands in palladium-catalyzed asymmetric allylic alkylation, *Tetrahedron - Asymmetr.* 19, 2252-2257.
183. Iida, A., Osada, J., Nagase, R., Misaki, T., and Tanabe, Y. (2007) Mild and efficient pentafluorophenylammonium triflate (PFPAT)-catalyzed C-acylations of enol silyl ethers or ketene silyl (thio)acetals with acid chlorides, *Org. Lett.* 9, 1859-1862.
184. Berkes, D., Kolarovic, A., Manduch, R., Baran, P., and Povaanec, F. (2005) Crystallization-induced asymmetric transformations (CIAT): stereoconvergent acid-catalyzed lactonization of substituted 2-amino-4-aryl-4-hydroxybutanoic acids, *Tetrahedron - Asymmetr.* 16, 1927-1934.

185. Im, I., Lee, E. S., Choi, S. J., Lee, J. Y., and Kim, Y. C. (2009) Structure-activity relationships of heteroaromatic esters as human rhinovirus 3C protease inhibitors, *Bioorg. Med. Chem. Lett.* **19**, 3632-3636.
186. Camacho, E., Leon, J., Carrion, A., Entrena, A., Escames, G., Khaldy, H., Acuna-Castroviejo, D., Gallo, M. A., and Espinosa, A. (2002) Inhibition of nNOS activity in rat brain by synthetic kynurenines: Structure-activity dependence, *J. Med. Chem.* **45**, 263-274.
187. Uruguchi, D., Asai, Y., and Ooi, T. (2009) Site-directed asymmetric quaternization of a peptide backbone at a C-terminal azlactone, *Angew. Chem. Inter. Edit.* **48**, 733-737.
188. Berkes, D., Jakubec, P., Winklerova, D., Povazanec, F., and Daich, A. (2007) CIAT with simultaneous epimerization at two stereocenters. Synthesis of substituted beta-methyl-alpha-homophenylalanines, *Org. Biomol. Chem.* **5**, 121-124.
189. Zhao, X., Jing, J., Lu, K., Zhang, Y., and Wang, J. B. (2010) Pd-catalyzed oxidative cross-coupling of N-tosylhydrazones with arylboronic acids, *Chem. Comm.* **46**, 1724-1726.
190. Hardick, D. J., Blagbrough, I. S., and Potter, B. V. L. (1996) Isotopic enrichment by asymmetric deuteration. An investigation of the synthesis of deuterated (S)-(-)-methylsuccinic acids from itaconic acid, *J. Am. Chem. Soc.* **118**, 5897-5903.
191. Aranha, R. M., Bowser, A. M., and Madalengoitia, J. S. (2009) Facile 1,3-diazacyclization and Claisen rearrangements of tertiary allylic amines bearing an electron-deficient alkene, *Org. Lett.* **11**, 575-578.

192. Tran, L., Tosin, M., Spencer, J. B., Leadlay, P. F., and Weissman, K. J. (2008) Covalent linkage mediates communication between ACP and TE domains in modular polyketide synthases, *ChemBioChem* 9, 905-915.
193. Campbell-Verduyn, L. S., Mirfeizi, L., Dierckx, R. A., Elsinga, P. H., and Feringa, B. L. (2009) Phosphoramidite accelerated copper(I)-catalyzed 3+2 cycloadditions of azides and alkynes, *Chem. Comm.*, 2139-2141.
194. Boyne, M. E., Sullivan, T. J., amEnde, C. W., Lu, H., Gruppo, V., Heaslip, D., Amin, A. G., Chatterjee, D., Lenaerts, A., Tonge, P. J., and Slayden, R. A. (2007) Targeting fatty acid biosynthesis for the development of novel chemotherapeutics against Mycobacterium tuberculosis: evaluation of A-ring-modified diphenyl ethers as high-affinity InhA inhibitors, *Antimicrob. Agents Chemother.* 51, 3562-3567.
195. Korolyov, A., Dorbes, S., Azema, J., Guidetti, B., Danel, M., Lamoral-Theys, D., Gras, T., Dubois, J., Kiss, R., Martino, R., and Malet-Martino, M. (2010) Novel lipophilic 7H-pyrido[1,2,3-de] -1,4-benzoxazine-6-carboxylic acid derivatives as potential antitumor agents: Improved synthesis and in vitro evaluation, *Bioorg. Med. Chem.* 18, 8537-8548.
196. Zhao, J., He, Q. X., Cheng, Y. Z., Zhao, B. X., Zhang, Y., Zhang, S. L., and Miao, J. Y. (2009) A benzoxazine derivative induces vascular endothelial cell apoptosis in the presence of fibroblast growth factor-2 by elevating NADPH oxidase activity and reactive oxygen species levels, *Toxicol. in Vitro* 23, 1039-1046.
197. La, D. S., Belzile, J., Bready, J. V., Coxon, A., DeMelfi, T., Doerr, N., Estrada, J., Flynn, J. C., Flynn, S. R., Graceffa, R. F., Harriman, S. P., Larrow, J. F., Long, A.

- M., Martin, M. W., Morrison, M. J., Patel, V. F., Roveto, P. M., Wang, L., Weiss, M. M., Whittington, D. A., Teffera, Y., Zhao, Z. Y., Polverino, A. J., and Harmannet, J. C. (2008) Novel 2,3-dihydro-1,4-benzoxazines as potent and orally bioavailable inhibitors of tumor-driven angiogenesis, *J. Med. Chem.* 51, 1695-1705.
198. Jiao, P. F., Zhao, B. X., Wang, W. W., Shin, D. S., He, Q. X., Wan, M. S., and Miao, J. Y. (2006) Design, synthesis, and preliminary biological evaluation of 2,3-dihydro-3-hydroxymethyl-1,4-benzoxazine derivatives, *Bioorg. Med. Chem. Lett.* 16, 2862-2867.
199. Folkman, J. (1995) Angiogenesis in cancer, vascular, rheumatoid and other disease, *Nat. Med.* 1, 27-31.
200. Bromidge, S. M., Arban, R., Bertani, B., Bison, S., Borriello, M., Cavanni, P., Dal Forno, G., Di-Fabio, R., Donati, D., Fontana, S., Gianotti, M., Gordon, L. J., Granci, E., Leslie, C. P., Moccia, L., Pasquarello, A., Sartori, I., Sava, A., Watson, J. M., Worby, A., Zonzini, L., and Zucchelli, V. (2010) Design and Synthesis of Novel Tricyclic Benzoxazines as Potent 5-HT_{1A/B/D} Receptor Antagonists Leading to the Discovery of 6-{2-[4-(2-methyl-5-quinolinyl)-1-piperazinyl]ethyl}-4*H*-imidazo-[5,1-*c*][1,4]benzoxazine-3-carboxamide (GSK588045), *J. Med. Chem.* 53, 5827-5843.
201. Wang, L. L., Ankati, H., Akubathini, S. K., Balderamos, M., Storey, C. A., Patel, A. V., Price, V., Kretschmar, D., Bieh, E. R., and D'Mello, S. R. (2010) Identification of novel 1,4-benzoxazine compounds that are protective in tissue

- culture and *in vivo* models of neurodegeneration, *J. Neurosci. Res.* **88**, 1970-1984.
202. Alper-Hayta, S., Aki-Sener, E., Tekiner-Gulbas, B., Yildiz, I., Temiz-Arpaci, O., Yalcin, I., and Altanlar, N. (2006) Synthesis, antimicrobial activity and QSARs of new benzoxazine-3-ones, *Eur. J. Med. Chem.* **41**, 1398-1404.
203. Yamane, T., Hashizume, T., Yamashita, K., Konishi, E., Hosoe, K., Hidaka, T., Watanabe, K., Kawaharada, H., Yamamoto, T., and Kuze, F. (1993) Synthesis and biological activity of 3'-hydroxy-5'-aminobenzoxazinorifamycin derivatives, *Chem. Pharm. Bull.* **41**, 148-155.
204. Hirata, T., Saito, H., Tomioka, H., Sato, K., Jidoi, J., Hosoe, K., and Hidaka, T. (1995) *In vitro* and *in vivo* activities of the benzoxazinorifamycin KRM-1648 against *Mycobacterium tuberculosis*, *Antimicrob. Agents Chemother.* **39**, 2295-2303.
205. Macchiarulo, A., Costantino, G., Fringuelli, D., Vecchiarelli, A., Schiaffella, F., and Fringuelli, R. (2002) 1,4-benzothiazine and 1,4-benzoxazine imidazole derivatives with antifungal activity: A docking study, *Bioorg. Med. Chem.* **10**, 3415-3423.
206. Fringuelli, R., Pietrella, D., Schiaffella, F., Guarraci, A., Perito, S., Bistoni, F., and Vecchiarelli, A. (2002) Anti-*Candida albicans* properties of novel benzoxazine analogues, *Bioorg. Med. Chem.* **10**, 1681-1686.
207. Yavari, I., Souri, S., Sirouspour, M., and Bayat, M. J. (2009) An efficient synthesis of functionalized 6,10-dioxo-6,10-dihydro-5H-pyrido[1,2-*a*]quinoxalines and 6,10-Dioxo-6,10-dihydropyrido[2,1-*c*]1,4 benzoxazines, *Synlett*, 1921-1922.

208. Mitchison, D. A. (2004) The search for new sterilizing anti-tuberculosis drugs, *Front. Biosci.* **9**, 1059-1072.
209. Pommery, N., Taverne, T., Telliez, A., Goossens, L., Charlier, C., Pommery, J., Goossens, J. F., Houssin, R., Durant, F., and Henichart, J. P. (2004) New COX-2/5-LOX inhibitors: Apoptosis-inducing agents potentially useful in prostate cancer chemotherapy, *J. Med. Chem.* **47**, 6195-6206.
210. Gein, V., Rassudikhina, N., Shepelina, N., Vakhrin, M., Babushkina, E., and Voronina, E. (2008) Reaction of substituted *o*-aminophenols with acylpyruvic acid esters and α -ketoglutaric acid. Antibacterial activity of the products, *Pharm. Chem. J.* **42**, 529-532.
211. Babenysheva, A., Lisovskaya, N., Belevich, I., and Lisovenko, N. (2006) Synthesis and antimicrobial activity of substituted benzoxazines and quinoxalines, *Pharm. Chem. J.* **40**, 611-613.
212. Kushnir, O. V., and Vovk, M. V. (2010) Heterocyclizations of functionalized heterocumulenes with C,N-, C,O-, and C,S-binucleophiles: XII. Synthesis of alkyl 3-aryl-1,5-dioxo-2,3,5,6-tetrahydro-1*H*-pyrimido-[1,6-*a*] quinoxaline-4-carboxylates, *Russ. J. Org. Chem.* **46**, 890-893.
213. Acheson, R. M., Foxton, M. W., and Miller, G. R. (1965) Addition reactions of heterocyclic compounds. XXIV. Adducts from thiazoles, benzoxazole, and 2-methylbenzoselenazole with dimethyl acetylenedicarboxylate, *J. Chem. Soc.*, 3200-3206.

214. Thornsberry, C., and McDougal, L. K. (1983) Successful use of broth microdilution in susceptibility tests for methicillin-resistant (heteroresistant) Staphylococci, *J. Clin. Microbiol.* 18, 1084-1091.